

**Synthesis and Biological Evaluation of a Novel HPMA
Copolymer Conjugate-Based Combination Therapy
Designed for the Treatment of Breast Cancer**

Signed Francesca Greco (candidate)
Date 3 MAR 2006

Francesca Greco

A thesis submitted to Cardiff University in accordance with the
requirements for the degree of Doctor of Philosophy

Signed Francesca Greco (candidate)
Date 3 MAR 2006



Centre for Polymer Therapeutics and Tenovus Centre for Cancer Research
Welsh School of Pharmacy
Cardiff University

UMI Number: U584027

All rights reserved

INFORMATION TO ALL USERS

The quality of this reproduction is dependent upon the quality of the copy submitted.

In the unlikely event that the author did not send a complete manuscript and there are missing pages, these will be noted. Also, if material had to be removed, a note will indicate the deletion.



UMI U584027

Published by ProQuest LLC 2013. Copyright in the Dissertation held by the Author.
Microform Edition © ProQuest LLC.

All rights reserved. This work is protected against
unauthorized copying under Title 17, United States Code.



ProQuest LLC
789 East Eisenhower Parkway
P.O. Box 1346
Ann Arbor, MI 48106-1346

DECLARATION

This work has not previously been accepted in substance for any degree and is not being concurrently submitted in candidature for any degree.

Signed.....*Tralena Gulo*.....(candidate)
Date.....*3. MAR. 2006*.....

STATEMENT 1

This thesis is the result of my own investigations, except where otherwise stated.
Other sources are acknowledged by footnotes giving explicit references. A bibliography is appended.

Signed.....*Tralena Gulo*.....(candidate)
Date.....*3. MAR. 2006*.....

STATEMENT 2

I hereby give consent for my thesis, if accepted, to be available for photocopying and for inter-library loan, and for the title and summary to be made available to outside organisations.

Signed.....*Tralena Gulo*.....(candidate)
Date.....*3. MAR. 2006*.....

Ai miei genitori

Acknowledgements

First, I would like to thank my supervisor Prof. Ruth Duncan for her guidance, support and for her very precious advice through these years. I also extend my gratitude to Prof. Rob Nicholson for his guidance. A special thanks goes to Dr. Maria Vicent, not only for the help with the chemistry, but also for her energy, contagious enthusiasm and for some really good laughs. I want to thank Prof. Ringsdorf for transmitting to me his joyful passion for science.

Thanks are due to the Centre for Polymer Therapeutics (CPT) and Tenovus Centre for Cancer Research for funding this study, to Dr. Simons and Sook Wah Yee for their help with the aromatase enzyme studies, to Neal Penning for his technical support and to Siobhan Gee for her invaluable help in the trafficking studies.

I am also grateful to the members of Tenovus Centre for Cancer Research, in particular to Carol for teaching me tissue culture, Jan and Iain for helping me with Western blotting and to Julia, Pauline, little Sue and Michelle for their priceless advice for the immunocytochemical studies.

So many people helped me in so many ways in these 3 years in CPT, and I really feel I have to mention each of them individually. Among the “old members” thanks to super-efficient Myrto, always smiling Vivian, the tissue culture queen Michelle, sweet Lorella, Frazia, Jacopo, KaWai and Rosy. Of the present members, thanks to Jan for the smooth running of the lab and to Wendy for her precious help and for proof reading this thesis. I would also like to thank Maria Manunta (supplier of Italian magazines), Arwyn (for teaching me what is a beer), Dirk (co-founder of the cinema club), Helena, Sam, Jing and Alison. A super-special thanks goes to Karen, Tom and Zeena for sharing this experience with me from day 1 through sad and happy days and for being good friends. I would also like to thank Philipp for his daily help in the lab but most of all for his friendship and support (both in Cardiff and from Germany). A big thank also to Lucile for the endless chats and pleasant dinners and to two new personal friends: Elaine and Kerri.

Finally, I would like to thank my family back in Italy, in particular my mother for being so close to me while so far. Last but not least, I thank my boyfriend Gianluigi for coping with my stress much better than I did and for always being there.

Abstract

Polymer-anticancer drug conjugates display passive tumour targeting by the enhanced permeability and retention effect. Several conjugates containing traditional chemotherapy (doxorubicin (Dox), paclitaxel and platinates) have entered clinical trials. N-(2-hydroxypropyl)methacrylamide (HPMA) copolymer-Dox (PK1) has shown activity in anthracycline-resistant breast cancer patients and was ~ 5 times less toxic than Dox. The use of polymer conjugates to deliver endocrine agents is largely unexplored, therefore, the aim of this study was to design a novel HPMA copolymer conjugate carrying a combination of endocrine therapy (the aromatase inhibitor aminoglutethimide (AGM)) and chemotherapy (Dox) on the same polymer backbone. As patients with advanced metastatic breast cancer have a relatively poor prognosis (< 20 % survival at 5 years), it was hoped that this conjugate would elicit increased antitumour activity.

A library of conjugates was synthesised to contain Dox, AGM, or both drugs attached to the same polymer chain. First, the conjugates were prepared by aminolysis of polymeric intermediates ($M_w \sim 20,000\text{-}25,000$ g/mol; $M_w/M_n = 1.3\text{-}1.5$) where the C-terminus of the peptide side-chains were esterified with *p*-nitrophenol. The lower reactivity of the aromatic amine of AGM, however, favoured use of 1,3-dicyclohexylcarbodiimide (DCC)-mediated coupling, leading to improved yield of conjugation. NMR confirmed product identity and nuclear Overhauser effect (NOE) measurements verified the covalent binding of AGM. Total and free Dox were measured by HPLC and AGM content using an indirect method. Overall, the drug content of the conjugates was in the range 2.8 – 8.6 % w/w (free drug content < 1.4 % w/w total).

Cytotoxicity of the conjugates was determined using the human oestrogen-dependent breast cancer cell line (MCF-7) and the aromatase-transfected derivative MCF-7ca combined with the MTT assay (72 h). Although HPMA copolymer-Dox was much less active than free Dox, and neither the HPMA copolymer-AGM nor mixtures of drug conjugates bearing AGM or Dox caused an elevation in cytotoxicity in either cell line, when AGM and DOX were covalently linked to the same polymeric backbone, cytotoxicity was significantly enhanced (more evident for MCF-7ca cells).

To better understand the precise mechanism of action, the ability to inhibit aromatase was evaluated in 3 different *in vitro* systems. Free AGM and HPMA copolymer-AGM inhibited aromatase, but drug release was probably essential for the activity of the HPMA copolymer-AGM. To establish whether the rate or mechanism of uptake of HPMA copolymer-Dox (\pm AGM) were responsible for the different cytotoxicity, the uptake of the conjugates was evaluated by FACS. Internalisation and marked membrane binding were seen for both conjugates suggesting that the different cytotoxicity could not be attributed to differences in the uptake. Finally, immunocytochemistry studies showed that the HPMA copolymer-AGM-Dox reduced the level of the anti-apoptotic protein Bcl-2 in MCF-7, while the HPMA copolymer-Dox had no effect on this cellular marker.

To conclude, the HPMA copolymer-AGM-Dox conjugate is the first polymer therapeutic to combine chemotherapy and endocrine therapy. The fact that AGM and Dox can act synergistically to produce markedly enhanced cytotoxicity *in vitro* compared to the HPMA copolymer-Dox conjugate, that has already shown activity in breast cancer patients clinically, underlines the potential importance of this polymer-drug combination.

Index

Chapter 1: General Introduction	Page
1.1. Introduction	2
1.2. Breast cancer as hormone-dependent cancer	4
1.2.1. The oestrogen receptor (ER)	4
1.2.2. How does the ER work?	7
1.2.3. The ER β	8
1.3. Therapy of breast cancer	8
1.3.1. Endocrine therapy	11
1.3.2. Chemotherapy	24
1.4. Polymer conjugates	27
1.5. EPR effect: a useful tool for passive targeting	31
1.6. Aim of the project	32
Chapter 2: Materials and General Methods	
2.1. Equipment	35
2.1.1. Analytical	35
2.1.2. Cell culture	36
2.2. Materials	36
2.2.1. Chemical reagents	36
2.2.2. HPMA copolymers	37
2.2.3. Cell culture	37
2.2.4. Western blots	37
2.2.5. Immunocytochemistry	38
2.3. General methods	38
2.3.1. Synthesis of HPMA copolymer-Dox conjugate by aminolysis	40
2.3.2. Purification of HPMA copolymer-Dox	40
2.3.3. Synthesis of HPMA copolymers-aminopropanol	40
2.3.4. Determination of total and free Dox by HPLC	42
2.3.5. Characterisation of HPMA copolymers by GPC	45
2.3.6. General cell culture	45
2.3.6.1. Defrosting cells	45

2.3.6.2. Cell maintenance and passaging	45
2.3.6.3. Counting and seeding cells	47
2.3.6.4. Freezing cells	47
2.3.6.5. Preparation of SFBS	49
2.3.7. Counting cells with the Coulter counter: growth curve for MCF-7	49
2.3.8. MTT assay as means to assess cell viability: growth curve	51
2.3.9. Evaluation of cytotoxicity using the MTT assay	51
2.3.10. Determination of the effect of androstenedione/testosterone on the growth of MCF-7 and MCF-7ca	54
2.3.11. Effect of AGM (free and polymer-bound) on the mitogenic properties of androstenedione	55
2.3.12. Radiometric evaluation of isolated aromatase activity using placental microsomes	55
2.3.13. Radiometric assay of aromatase activity in cells	56
2.3.14. Cell lysis for protein extraction	57
2.3.15. Quantification of the protein content: Lowry assay	57
2.3.16. Detection of aromatase enzyme in MCF-7 and MCF-7ca by Western blot	58
2.3.17. Determination of the cellular uptake of polymer conjugates by flow cytometry	59
2.3.18. Analysis of flow cytometry data	59
2.4. Statistical analysis	60

Chapter 3: Synthesis and Characterisation of HPMA copolymer-AGM \pm Dox

3.1. Introduction	63
3.2. Methods	70
3.2.1. Synthesis and purification of HPMA copolymer-AGM \pm Dox conjugates	70
3.2.2. Characterisation of HPMA copolymer-AGM \pm Dox conjugates	75
3.3. Results	78
3.3.1. Content of total and free drug in HPMA copolymer conjugates	80
3.3.3. Characterisation of the conjugates by GPC.	86
3.3.4. Summary of the conjugates synthesised and their characteristics	86

3.4. Discussion	88
-----------------	----

Chapter 4: Preliminary evaluation of the biological activity of HPMA copolymers-Dox \pm AGM and assessment of aromatase inhibition.

4.1. Introduction	99
4.2. Methods	105
4.2.1. Evaluation of interferences between HPMA copolymers and MTT assay	107
4.3. Results	107
4.4. Discussion	123
4.5. Conclusions	127

Chapter 5: Comparison of the cellular uptake of HPMA-copolymer Dox and HPMA copolymer-Dox-AGM.

5.1. Introduction	130
5.2. Methods	137
5.2.1. Characterisation of Dox, HPMA copolymer-Dox and HPMA copolymer-Dox-AGM fluorescence	137
5.2.2. Fluorescence microscopy. Live-cell imaging	137
5.2.3. Cytotoxicity of the inhibitors	138
5.2.4. Effect of inhibitors on the endocytic uptake of HPMA copolymer conjugates	139
5.3. Results	139
5.3.1. Characterisation of the fluorescent probes	139
5.3.2. Uptake of HPMA copolymer-Dox and HPMA copolymer-AGM-Dox by MCF-7 and MCF-7ca using flow cytometry or fluorescence microscopy	141
5.3.3. Evaluation of the toxicity of the endocytosis inhibitors and the effect of inhibitors on the uptake of HPMA copolymer-Dox and HPMA copolymer- AGM-Dox	146
5.4. Discussion	152
5.5. Conclusions	158

Chapter 6: Using immunocytochemistry to look at the effect of the HPMA copolymer-Dox and the HPMA copolymer-AGM-Dox on the cellular markers ER, PR, pS-2, Ki67 and Bcl-2

6.1. Introduction	160
6.2. Methods	162
6.2.1. Immunocytochemistry	162
6.2.1.1. Cells preparation	165
6.2.1.2. The fixation protocol: “Oestrogen receptor immunocytochemical assay” (ERICA) fixation	170
6.2.1.3. Staining of ER, PR, pS-2, Bcl-2 and Ki67	170
6.3. Results	175
6.3.1. Optimisation of the ER staining and experimental set-up.	175
6.3.2. Characterisation of ER, PgR and pS-2 expression in MCF-7 and MCF-7ca cells in presence and absence of AGM.	180
6.3.3. Effect of HPMA copolymer-Dox and HPMA copolymer-AGM-Dox on the expression of the proliferation marker Ki67.	191
6.3.4. Effect of HPMA copolymer-Dox and HPMA copolymer-AGM-Dox on the Bcl-2 expression	191
6.4. Discussion	191
6.5. Conclusions	203

Chapter 7: General Discussion

7.1. General comments and historical perspective	205
7.2. Critical review of the underlying strategies	207
7.3. Recent developments in the field: this work in the context of other polymer-drug conjugates and other breast cancer treatments	208
7.4. Summary of the main findings of this work and possible future developments	209

References	216
-------------------	-----

Appendix I (List of publications)

Appendix II (publications)

List of Figures

Chapter 1

Fig. 1.1.	Incidence of breast cancer in the UK	3
Fig. 1.2.	Rate of survival from breast cancer in relation with tumour stage	3
Fig. 1.3.	Schematic representation of ER α	6
Fig. 1.4.	Mechanism of action of ER	6
Fig. 1.5.	Decision algorithm for patients with metastatic breast cancer	9
Fig. 1.6.	Endocrine system interactions and main drugs sites of action	12
Fig. 1.7.	Mechanism of action of drugs used for breast cancer	13
Fig. 1.8.	Chemical structures of selective oestrogen receptor modulators	14
Fig. 1.9.	Steroidogenesis pathway	16
Fig. 1.10.	Chemical structures of aromatase inhibitors	16
Fig. 1.11.	Design of the clinical trials of aromatase inhibitors	18
Fig. 1.12.	Chemical structure of some anthracyclines	25
Fig. 1.13.	Ringsdorf model of polymer conjugate	28
Fig. 1.14.	Tumour passive targeting	30

Chapter 2

Fig. 2.1.	Aminolysis reaction	41
Fig. 2.2.	Monitoring the aminolysis reaction by UV	41
Fig. 2.3.	Determination of free and total Dox by HPLC	43
Fig. 2.4.	Quantification of free and total Dox by HPLC.	44
Fig. 2.5.	Typical GPC calibration curve for polysaccharide standards	46
Fig. 2.6.	The Coulter counter	50
Fig. 2.7.	Growth curves of B16F10 and MCF-7 cells	52
Fig. 2.8.	Mechanism of action of MTT assay	53
Fig. 2.9.	Interpretation of the flow cytometry data	61

Chapter 3

Fig. 3.1.	Examples of chemical structure of the polymer conjugates	64
Fig. 3.2.	Preparation of HPMA copolymer-drug conjugates	68

Fig. 3.3.	Chemical structures of the library of target compounds	71
Fig. 3.4.	Synthesis of HPMA copolymer-AGM by DCC coupling	72
Fig. 3.5.	Purification of HPMA copolymer-AGM conjugates	74
Fig. 3.6.	Synthesis of HPMA copolymer-Dox-AGM conjugate by DCC coupling	76
Fig. 3.7.	UV scan of the hydrolysis reaction of HPMA-copolymer-ONp	79
Fig. 3.8.	HPLC analysis of Dox aglycone	81
Fig. 3.9.	HPLC analysis of free Dox	82
Fig.3.10.	HPLC analysis of free and total AGM	83
Fig. 3.11.	UV scan of free AGM in MeOH	84
Fig. 3.12.	UV spectrum of Gly-AGM in MeOH	85
Fig. 3.13.	UV spectrum of HPMA copolymer GFLG (5 mol%)-AGM	87
Fig. 3.14.	GPC profiles of HPMA copolymer conjugates	88
Fig. 3.15.	Mechanism of the DCC coupling reaction	91
Fig. 3.16.	NOE ¹ H-NMR spectra of HPMA copolymer GFLG-AGM	92
Fig. 3.17.	Rationale for the HPLC method used for Dox	94
Fig. 3.18.	Schematic representation of the potential explanation of the results obtained by GPC	96

Chapter 4

Fig. 4.1.	Cellular pharmacokinetics of free and polymer-bound drug	100
Fig. 4.2.	Parameters that can be measured to evaluate the enzymatic activity	102
Fig. 4.3.	The three model systems used to evaluate inhibition of aromatase	106
Fig. 4.4.	Morphology of MCF-7ca and MCF-7	108
Fig. 4.5.	Aromatase expression in MCF-7 and MCF-7ca by western blot	109
Fig. 4.6.	<i>In vitro</i> cytotoxicity	112
Fig. 4.7.	Interference of HPMA copolymer conjugates with the MTT assay	117
Fig. 4.8.	Effect of testosterone on MCF-7 and MCF-7ca cell growth	119
Fig. 4.9.	Effect of androstenedione on MCF-7 and MCF-7ca cell growth	120
Fig. 4.10.	Inhibition of the mitogenic effect of androstenedione by free and bound AGM	121
Fig. 4.11.	Effect of free and polymer-bound AGM on aromatase activity in MCF-7ca cells	122
Fig. 4.12.	Effect of free and polymer-bound AGM on aromatase activity in	

isolated human placental microsomal extract	124
---	-----

Chapter 5

Fig. 5.1.	Possible routes of uptake of the conjugates	133
Fig.5.2.	Fluorescence emission scan of Dox, HPMA copolymer-Dox and HPMA copolymer-Dox-AGM	140
Fig.5.3.	Effect of concentration and pH on fluorescence	142
Fig.5.4.	Ratio between the fluorescence output of HPMA copolymer-Dox and HPMA copolymer-AGM-Dox	143
Fig.5.5.	Uptake of HPMA copolymer Dox conjugates by MCF-7ca cells	144
Fig.5.6.	Uptake of HPMA copolymer-Dox (\pm AGM) by MCF-7 and MCF-7ca cells	145
Fig.5.7.	Fluorescence microscopy pictures of MCF-7ca cells after incubation with HPMA copolymer-Dox	147
Fig.5.8.	Fluorescence microscopy pictures of MCF-7 and MCF-7ca cells after 30 min incubation with HPMA copolymer-Dox (\pm AGM)	148
Fig. 5.9.	Example of photo-bleaching in MCF-7ca cells	149
Fig. 5.10.	Cytotoxicity of the inhibitors of endocytic pathways against MCF-7 cells	150
Fig. 5.11.	Cytotoxicity of the inhibitors of endocytic pathways against MCF-7ca cells	151
Fig. 5.12.	Effect of the inhibitors of endocytic pathways on the uptake of polymer conjugates by MCF-7 cells	153
Fig. 5.13.	Effect of the inhibitors of endocytic pathways on the uptake of polymer conjugates by MCF-7ca cells	154

Chapter 6

Fig. 6.1.	Possible mechanisms of action of the HPMA copolymer-Dox-AGM at cellular level	163
Fig. 6.2.	The Bcl-2 family of proteins	164
Fig. 6.3.	The three systems tested for growing cells prior to ICC staining	166
Fig. 6.4.	Cell preparation prior to immunocytochemical analysis	167
Fig. 6.5.	The different experimental protocols used for MCF-7 and MCF-7ca prior to immunocytochemical analysis	168

Fig. 6.6.	Schematic representation of the fixation procedure followed	171
Fig. 6.7.	Schematic representation of the ICC staining procedure followed for ER, PgR, pS2, Bcl-2 and Ki67	172
Fig. 6.8.	ER staining in MCF-7 cells using the primary antibody at 4 different dilutions	176
Fig.6.9.	ER staining in MCF-7 cells visualised following incubation with different concentrations of GAM	178
Fig. 6.10.	Comparison of ER staining in MCF-7 cells grown using three different techniques	181
Fig. 6.11.	ER expression in MCF-7 cells	183
Fig. 6.12.	ER expression in MCF-7ca cells	184
Fig. 6.13.	PgR expression in MCF7 cells	185
Fig. 6.14.	PgR expression in MCF-7ca cells	187
Fig. 6.15.	pS2 expression in MCF-7 cells	188
Fig. 6.16.	pS2 expression in MCF-7ca cells	189
Fig. 6.17.	Effect of androstenedione, free AGM and HPMA copolymer-AGM on PgR expression in MCF-7ca cells	190
Fig. 6.18.	Effect of HPMA copolymer-Dox conjugates on Ki67 expression in absence of steroids in MCF-7 cells	192
Fig. 6.19.	Effect of HPMA copolymer-Dox conjugates on Ki67 expression in presence of oestradiol in MCF-7 cells	193
Fig. 6.20.	Effect of HPMA copolymer-Dox conjugates on Ki67 expression in absence of steroids in MCF-7ca cells	194
Fig. 6.21.	Effect of HPMA copolymer-Dox conjugates on Ki67 expression in presence of oestradiol in MCF-7ca cells	195
Fig. 6.22.	Effect of HPMA copolymer-Dox conjugates on Bcl-2 expression in absence of steroids in MCF-7 cells	196
Fig. 6.23.	Effect of HPMA copolymer-Dox conjugates on Bcl-2 expression in presence of oestradiol in MCF-7 cells	197
Fig. 6.24.	Effect of HPMA copolymer-Dox conjugates on Bcl-2 expression in absence of steroids in MCF-7ca cells	198
Fig. 6.25.	Effect of HPMA copolymer-Dox conjugates on Bcl-2 expression in presence of oestradiol in MCF-7ca cells	199

Chapter 7

Fig. 7.1.	Milestones in the history of polymer anticancer drug conjugates and breast cancer treatment	206
Fig. 7.2.	Assessment of HPMA copolymer-AGM (\pm Dox) conjugates	211
Fig. 7.3.	Some of the possible synthetic approaches for novel polymer-aromatase inhibitor conjugates	213

List of Tables

Chapter 1

Table 1.1.	Response to endocrine therapy by hormone receptor status	10
Table 1.2.	Drugs acting on growth factor signalling pathway	20
Table 1.3.	Polymer conjugates in clinical trials	28

Chapter 2

Table 2.1.	Composition of the lysis buffer and protease inhibitors.	39
Table 2.2.	Buffers and solutions used for SDS page and Western blot	39
Table 2.3.	Cell culture conditions	48

Chapter 3

Table 3.1	HPMA copolymer conjugates synthesized	90
-----------	---------------------------------------	----

Chapter 4

Table 4.1.	Experimental models used to assess aromatase activity	104
Table 4.2.	IC ₅₀ values of free and polymer-bound AGM and Dox and their combinations (with 10 ⁻⁹ M oestradiol)	111
Table 4.3.	IC ₅₀ values of free and polymer-bound AGM and Dox and their combinations (without oestradiol)	111

Chapter 5

Table 5.1.	Inhibitors of specific routes of endocytic uptake	135
------------	---	-----

ABBREVIATIONS

AF-1:	activating function 1
AF-2:	activating function 2
AGM:	aminoglutethimide
ANOVA:	analysis of variance
APS:	ammonium persulfate
CPT:	camptothecin
ddH ₂ O:	double distilled water
DAB:	diaminobenzidine
DBD:	DNA binding domain
DCC:	1,3-dicyclohexylcarbodiimide
DES:	diethylstilbestrol
DMF:	dimethylformamide
DMSO:	dimethylsulphoxide
Dox:	doxorubicin
DTT:	dithiothreitol
EDTA:	ethylenediaminetetraacetic acid
EGF:	epidermal growth factor
EGFR:	epidermal growth factor receptor
EGTA:	ethylene glycol-bis(beta-aminoethyl ether)-N,N,N',N'-tetraacetic acid
EPR:	enhanced permeability and retention
ET:	endocrine therapy
ER:	oestrogen receptor
ERICA:	oestrogen receptor immunocytochemical assay

F:	phenylalanine
FBS:	foetal bovine serum
G:	glycine
GAM:	goat anti mouse
GPC:	gel permeation chromatography
HOBt:	1-hydroxy benzotriazol
HPLC:	high performance liquid chromatography
HPMA:	N-(2-hydroxypropyl)methacrylamide
i.v.:	intra-venous
L:	leucine
LBD:	ligand binding domain
M β CD:	methyl- β -cyclodextrin
MTD:	maximum tolerated dose
MTT:	3-(4,5-dimethylthiazol-2-yl)-2,5-diphenyl-2H-tetrazolium bromide
NHS:	normal human serum
NOE:	nuclear Overhauser effect
n.s.:	non significant
ONp:	p-nitrophenol
PAP:	peroxidase anti peroxidase
PBS:	phosphate buffered saline
PEG:	polyethylenglycol
PgR:	progesterone receptor
PGA:	polyglutamic acid

PI3:	phosphatidylinositol 3
PMSF:	phenylmethanesulfonyl fluoride
R.I.:	refractive index
S.D.:	standard deviation
SDS:	sodium dodecyl sulfate
SEC:	size exclusion chromatography
S.E.M.:	standard error of the mean
SFCS:	stripped foetal calf serum
TBS:	tris-buffered saline
TEMED:	tetramethylethylenediamine
TLC:	thin-layer chromatography
t _r :	retention time
WRPMI:	RPMI medium without phenol red

Chapter 1:

General Introduction

1.1 INTRODUCTION

The terms “nanomedicines” and “nanotechnologies” are becoming very popular both in scientific and non-scientific press (reviewed in Duncan 2004; Moghimi et al., 2005). If from one side they might be perceived as a threat by the general public, they have, undoubtedly, an enormous therapeutic potential. Despite the current increase in attention the design and use of nanosized medicines is not exactly “new”. Indeed, the concept of polymer-drug conjugates dates from the 1970s, (Ringsdorf, 1975). During the 1970’s and 1980’s, Duncan and collaborators began to systematically design the first polymer anticancer conjugate that would eventually enter clinical trials. This was an HPMA copolymer-doxorubicin (Dox) conjugate called PK1 or FCE 28068 (Vasey et al., 1999; reviewed in Duncan 2003a). Many polymer-drug conjugates carrying established anticancer agents such as paclitaxel, camptothecin and platinates have now followed into clinical trials and several are showing considerable promise (Meerum Terwogt et al., 2001; Schoemaker et al., 2002; reviewed in Duncan 2003b). This has paved the way for design of second generation conjugates containing experimental drugs directed towards new molecular targets. For example, the first HPMA copolymer carrying the antiangiogenic drug TNP470 (Satchi-Fainaro et al., 2004), and the first HPMA copolymer carrying the phosphatidylinositol-3 (PI3) kinase wortmannin (Varticovski L. et al., 2001). Also, the use of HPMA copolymers to deliver a combination of photo and chemotherapy has been suggested (Shiah et al., 2001). Although the term nanomedicines includes a variety of delivery systems, namely, polymer therapeutics, nanoparticles, nanosized liposomes and micelles, this study focuses on the development of a novel polymer-drug combination specifically for use as a potential therapy for breast cancer.

Nowadays cancer, together with cardiovascular diseases, is the major cause of death. Despite improved diagnosis and therapy achieved in the area, breast cancer is still a frightening issue. According to statistics (Fig. 1.1) (Cancer Research UK, 2003), breast cancer accounts for 28 % of tumours diagnosed in women. Various approaches have been used to treat breast cancer, nevertheless, the survival rates remain low particularly if metastases are present at the time of diagnosis (Fig. 1.2). In several cases, hormone therapy fails as tumours become eventually resistant

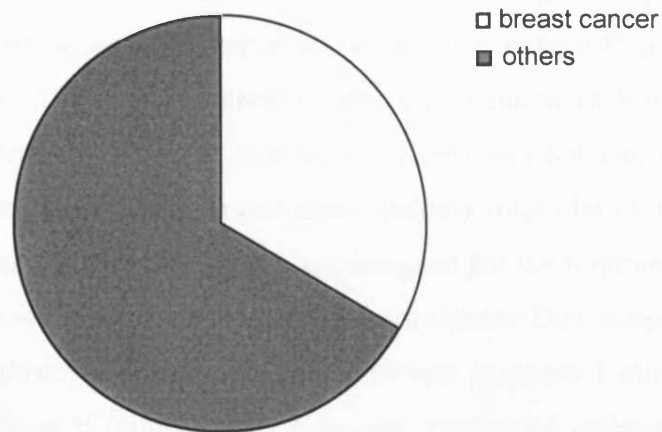


Fig. 1.1. Incidence of breast cancer in women in the UK (taken from Cancer Research UK, 2003)

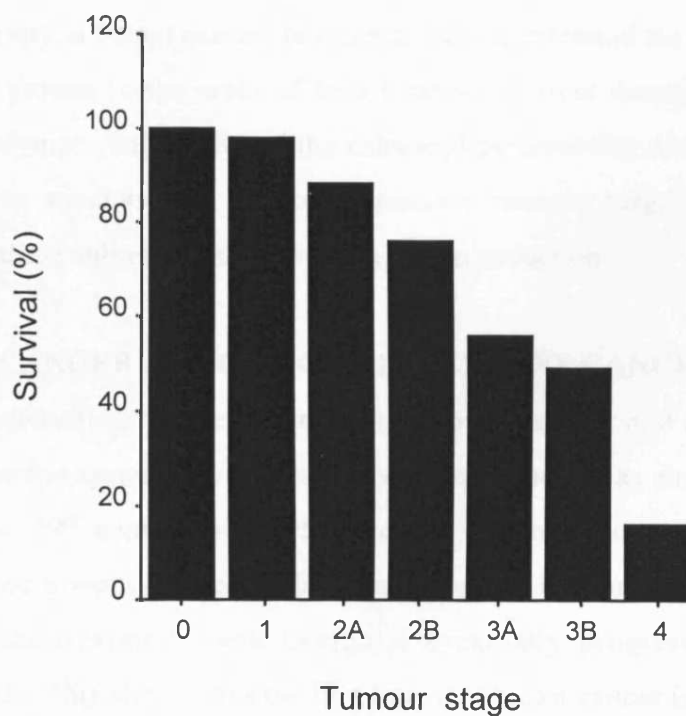


Fig. 1.2. Rate of survival from breast cancer in relation with tumour stage after 5 years from diagnosis. (Data taken from American Cancer Society)

(Dorssers et al., 2001; Osborne and Fuqua, 1994). On the other hand, chemotherapy has limitations because it is not selectively toxic (resulting in unpleasant or lifethreatening side effects), and because many agents can induce P-gp mediated resistance (Rang et al., 1995). Consequently, an improvement in hormone and chemotherapy in the context of breast cancer is urgently needed and the use of polymer conjugates combining hormone and chemotherapy might be useful for this purpose. Polymer anticancer drug conjugates are designed for the treatment of solid tumours (including breast cancer) and the HPMA copolymer-Dox conjugate PK1 showed activity in anthracycline-resistant breast cancer in phase I clinical trials (Vasey et al., 1999). Phase II clinical trials have also confirmed activity in breast cancer (Cassidy, 2000; reviewed in Duncan 2005). This study is building on these observations to design for the first time a conjugate *specifically* for the treatment of breast cancer.

The aim of this project was to synthesise a polymer carrying endocrine and chemotherapy on the same backbone with the hope of eliciting a potentiated antitumour activity in breast cancer. In order to fully understand the rationale for this project, a background in the areas of breast cancer, current therapies available for this disease, polymer conjugates and the enhanced permeability and retention effect (EPR effect) as mechanisms to obtain passive tumour targeting is required. Consequently, these subjects are reviewed in this introduction.

1.2. BREAST CANCER AS HORMONE-DEPENDENT CANCER

The strict connection between hormones and breast cancer and the possibility to act on the endocrine system to achieve a therapeutic benefit was elegantly proved at the end of the 19th century when Sir George Thomas Beatson performed an oophorectomy on a woman affected by breast cancer (Beatson, 1896). The tumour responded to the treatment even though it eventually progressed (Hayes and Robertson, 2002). This showed for the first time that breast cancer is deeply affected by hormonal variation and also that depletion of oestrogens could be a promising strategy to use for the treatment of this disease.

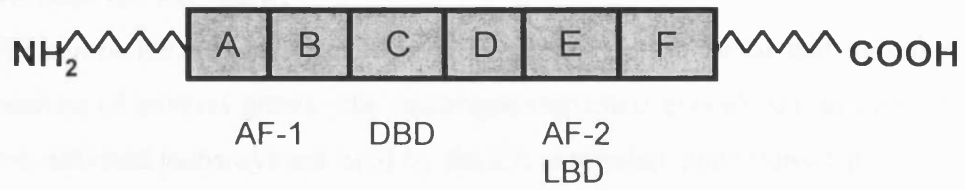
1.2.1. The oestrogen receptor (ER)

To achieve a better understanding of the connection between hormones and breast cancer, it is important to review the action of oestrogens and the molecular biology of the ER.

Oestrogens are vital for several physiological activities involved in the normal development of the female reproductive system. Furthermore, they are also key elements in the maintenance of the appropriate bone density and in the protection of the heart and of the blood vessels (Pettersen et al., 2000). Together with the receptors for gluco-corticoids, vitamin D₃, fatty acids, thyroid hormone, mineral-corticoids, androgens, progestins and other receptors for which the ligands have still to be identified (“orphan receptors”), the ER is a member of the nuclear receptor family. For several years only one type of ER was known, until in 1996, a second type of ER was discovered (Kuiper et al., 1996). Therefore, after this event, the nomenclature had to be modified and currently, we refer to the first identified ER as ER α and to the second identified as ER β . A huge amount of literature is available on ER α (the first discovered), but a large amount of information is now accumulating also on the ER β . A detailed description of the structure of the oestrogen receptor is beyond the scope of this thesis, therefore only a brief description will be provided.

ER α consists of 6 different domains, named from A to F (Vergote et al., 2000) (Fig. 1.3).

- The A/B domain is the N-terminus region. The activating function 1 (AF-1) involved in the transcriptional activity is located in this region.
- The C domain is the region where the DNA binding domain (DBD) is located. This domain contains two zinc fingers that are key for the recognition of the specific DNA-sequences.
- The D region is the part that separates the DBD from the ligand binding domain (LBD)
- The E region is the domain containing the hydrophobic part designed to bind the ligand (LBD). It also includes the AF-2 and the principal dimerization domain (the region responsible for the binding with another ER).
- The F region is the C-terminal domain; it seems to play a role in the



MW: \approx 67 kDa (varies depending on the degree of phosphorylation)
595 aminoacids

Fig. 1.3. Schematic representation of the structure and the functional domains of the ER α (adapted from Nicholson et al., 2002)

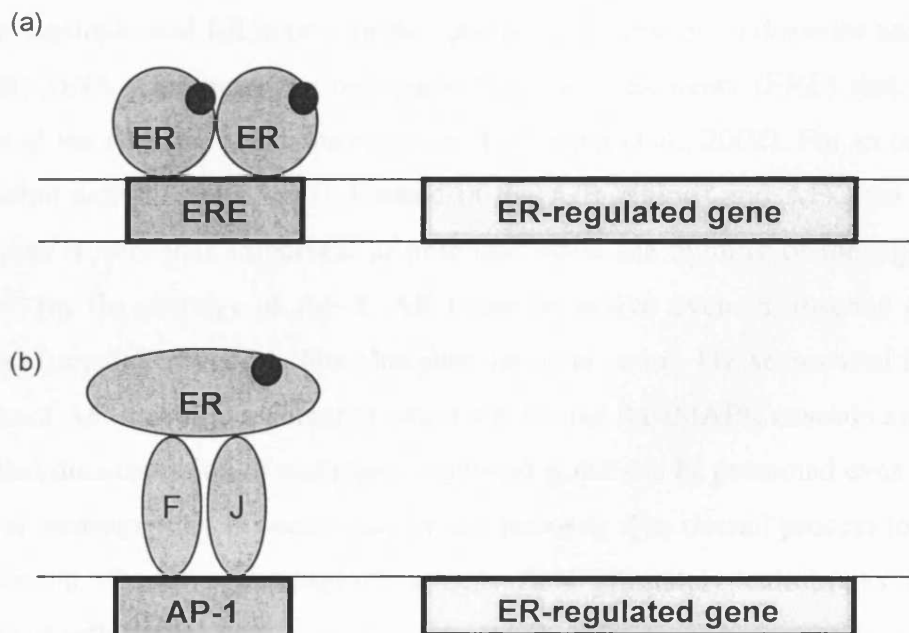


Fig. 1.4. Models of ER mechanism of action at classical ERE (a) and ER-dependent AP-1 response element (b). Blue circle represents the ligand, F = Fos, J = Jun (adapted from Paech et al., 1997)

transcriptional activation and repression of oestrogen-regulated genes by anti-oestrogens.

1.2.2. How does the ER work?

The ER can be defined as a ligand-regulated transcription factor that modulates the expressions of several genes (the oestrogen-regulated genes) (Gross and Yee, 2002). Two different pathways are used by the ER to regulate gene transcription:

- the classical signalling pathway where the ER binds directly to specific DNA sequences
- the non-classical pathway which seems to involve the binding to other proteins rather than directly to DNA (Fig. 1.4).

In the classical signalling pathways, oestrogens enter the cell by passive diffusion and bind to the ER. The binding of the ligand to the ER in the LBD triggers the displacement of heat-shock proteins and the phosphorylation of the ER at several sites. The ligand-bound ER is now in the optimal conformation to dimerise and bind to specific DNA sequences, the oestrogen responsive elements (ERE) that act as promoter of the oestrogen-responsive genes (Nicholson et al., 2002). For an optimal transcription activity both AF-1 (located in the A/B region) and AF-2 (in the E region) play a role. It is important to note that while the binding of the ligand is necessary for the activity of AF-2, AF-1 can be active even in absence of the oestrogens (or antioestrogens). The phosphorylation of serine-118 seems vital for the activation of AF-1, as it is a potential target site for the Ras/MAPK cascade and it is evident that the expression of oestrogen-regulated genes can be promoted even in the absence of oestrogens by the activation of this pathway. The overall process leads to the activation of oestrogen-responsive genes and ultimately culminates in the activation of cell proliferation.

As already mentioned, the activation of the non-classical pathway differs from the classical pathway as a direct binding between the ER and the DNA is not necessary, as demonstrated by Jakacka *et al.* (2001). In fact, the ER interacts with specific transcription factors, Fos (F) and Jun (J) which then bind with specific DNA sequences (Peach et al., 1997). In this second mechanism, AP-1 is the DNA fragment

involved, rather than the ERE. The ultimate effect is therefore the expression of genes having an AP-1 site within their promoters.

1.2.3. The ER β

Predictably, ER β shows a certain degree of homology with the ER α . The DBD of the two receptors has a 97 % similarity in their aminoacid sequence, while the LBD has 55 % homology. The different aminoacid sequence in the LBD offers a possible explanation for how the same ligand may induce different responses in the two receptor types. For example, tamoxifen exerts mixed agonist-antagonist (tissue-dependent) behaviour for the ER α while it shows a pure antagonist profile for the ER β (Pettersson and Gustafsson, 2001). Interestingly, Paech et al. (1997) showed that ER α and ER β give opposite responses at an AP1 site after activation by oestradiol. This indicates that the two ER subtypes may mediate different gene expression.

1.3. THERAPY OF BREAST CANCER

Therapy of breast cancer involves a variety of possibilities ranging from surgery to endocrine therapy (ET) and chemotherapy. In order to choose the most appropriate therapy, a number of considerations are made. Tumour stage is one of the most important factors to guide the therapeutic approach. Breast cancer ranges from stage 1 (small, extremely localised tumour mass with no involvement of lymph nodes) to stage 4 (metastatic breast cancer). Predictably, local therapies (eg. surgery) are usually first choice in primary (low stage) cancer often accompanied by adjuvant or neo-adjuvant (preoperative) systemic therapy (ET or chemotherapy). While surgery removes the primary tumour mass, adjuvant chemotherapy aims to treat non-detectable micrometastases that could potentially spread later on (Hortobagyi, 2002). For metastatic cancer the situation is more complex. Fig. 1.5 schematically shows the possible strategies to follow for the treatment of metastatic breast cancer.

The assessment of the ER and the progesterone receptor (PgR) status is important to guide the treatment as it is able to give indication on the possible response to ET. As the PgR is an oestrogen-induced protein, the simultaneous presence of the ER and PgR in a tumour tissue suggests that not only is the ER present but also functional.

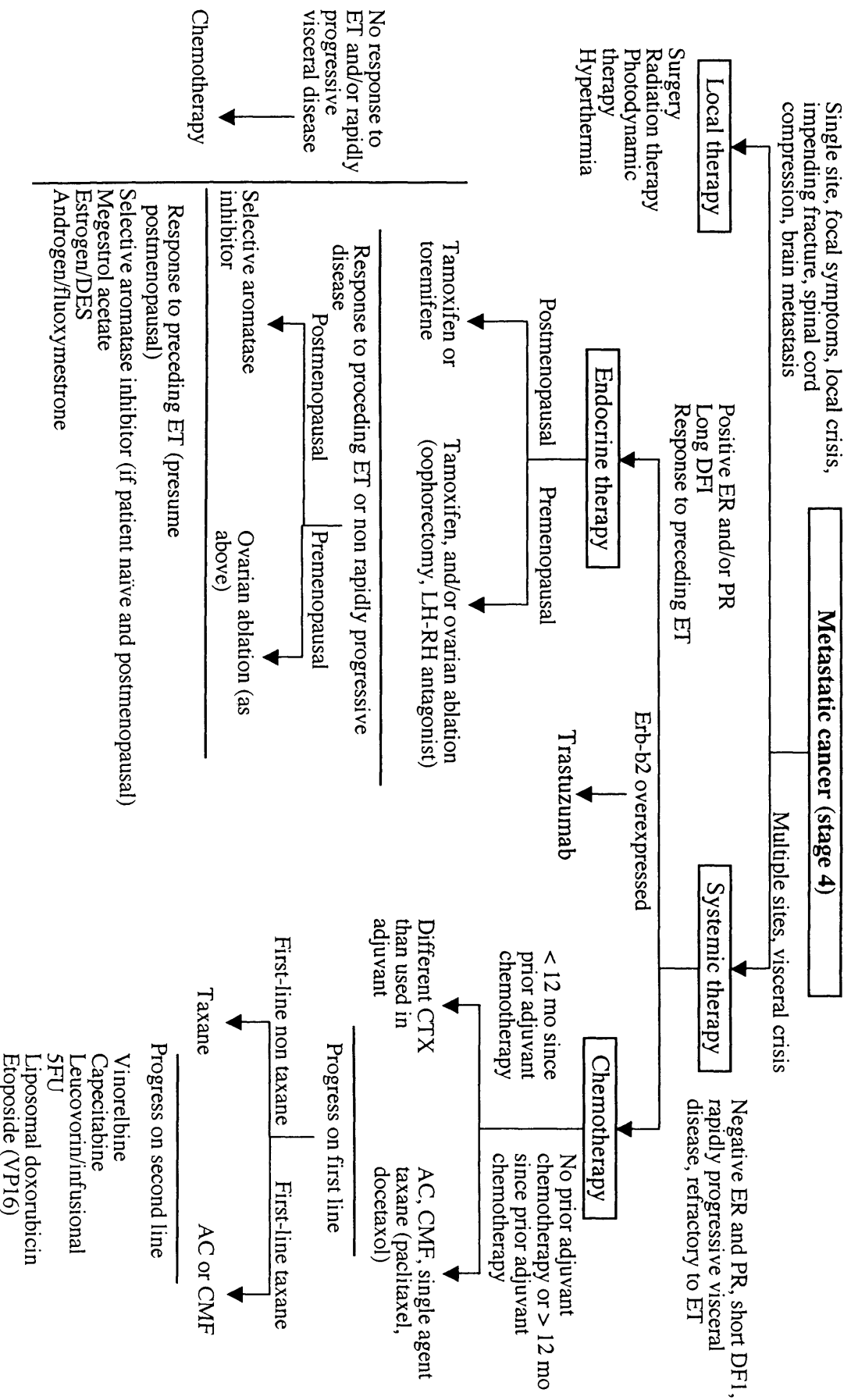


Fig. 1.5. Decision algorithm for patients with metastatic breast cancer (adapted from Ellis et al., 2000)

Table 1.1 Response to endocrine therapy by hormone receptor status

Oestrogen receptor	Progesterone receptor	Response to endocrine therapy
Negative	Negative	< 10 %
Positive	Negative	20 - 30 %
Negative	Positive	30 - 50 %
Positive	Positive	50 - 75 %

Taken from Ellis et al. (2000)

Therefore, tumours ER+ and PgR+ have a chance of responding to ET ranging from 50 % to 75 % (Ellis et al., 2000b) (Tab. 1.1). It is important to underline that an attempt with hormone therapy is usually made. In fact, hormone therapy has the advantage of providing a good quality of life compared to chemotherapy. On the contrary, if the tumour doesn't respond to hormone therapy and/or it is growing rapidly, chemotherapy would become the first choice (Ellis et al., 2000b).

1.3.1. Endocrine therapy

The experiment performed by Sir Beatson (1896) showed for the first time that depletion of oestrogens could be a promising strategy to use for the treatment of breast cancer. Nowadays, several elegant ways are used to reduce the circulating levels of oestrogens and/or their mitogenic activity on tumour cells. They are: anti-oestrogens, aromatase inhibitors, oestrogens, androgens, progestins, and LHRH agonists and antagonists. Finally, attention needs also to be given to new drugs acting on signalling transduction pathways.

Anti-oestrogenic drugs are extremely important drugs for the treatment of breast cancer. They are competitive antagonists of oestradiol. They bind to the oestrogen receptor, block it and thus reduce the oestrogen-induced cell growth (Fig. 1.6; Fig. 1.7; chemical structures Fig. 1.8) (Calabresi and Chabner, 1996). Tamoxifen, one of the most important examples of this class, is the treatment of choice today for the hormone treatment of all ER+ breast tumours (reviewed in Jordan, 2003). It is administered *per os* at a standard dose of 20 mg per day (Chang and Elledge, 2002). Its activity is due to its antagonist action on the breast cancer tissue. Nevertheless, it also has a partial agonist activity which may be responsible to some extent for drug resistance and tumour progression (Osborne and Fuqua, 1994; Sakamoto et al., 2002). Together with the emergence of resistance, other problems are associated with the use of tamoxifen, mainly, increased risk of developing endometrial cancer. For these reasons, alternative approaches have been considered like the development of aromatase inhibitors (discussed in the following section) or pure antagonists like Faslodex. Pure antagonists act on the ER at different levels from tamoxifen. In fact, not only do they more fully block the biological activity of the ER, but they cause receptor downregulation (Howell, 2000). Furthermore, it has been demonstrated that

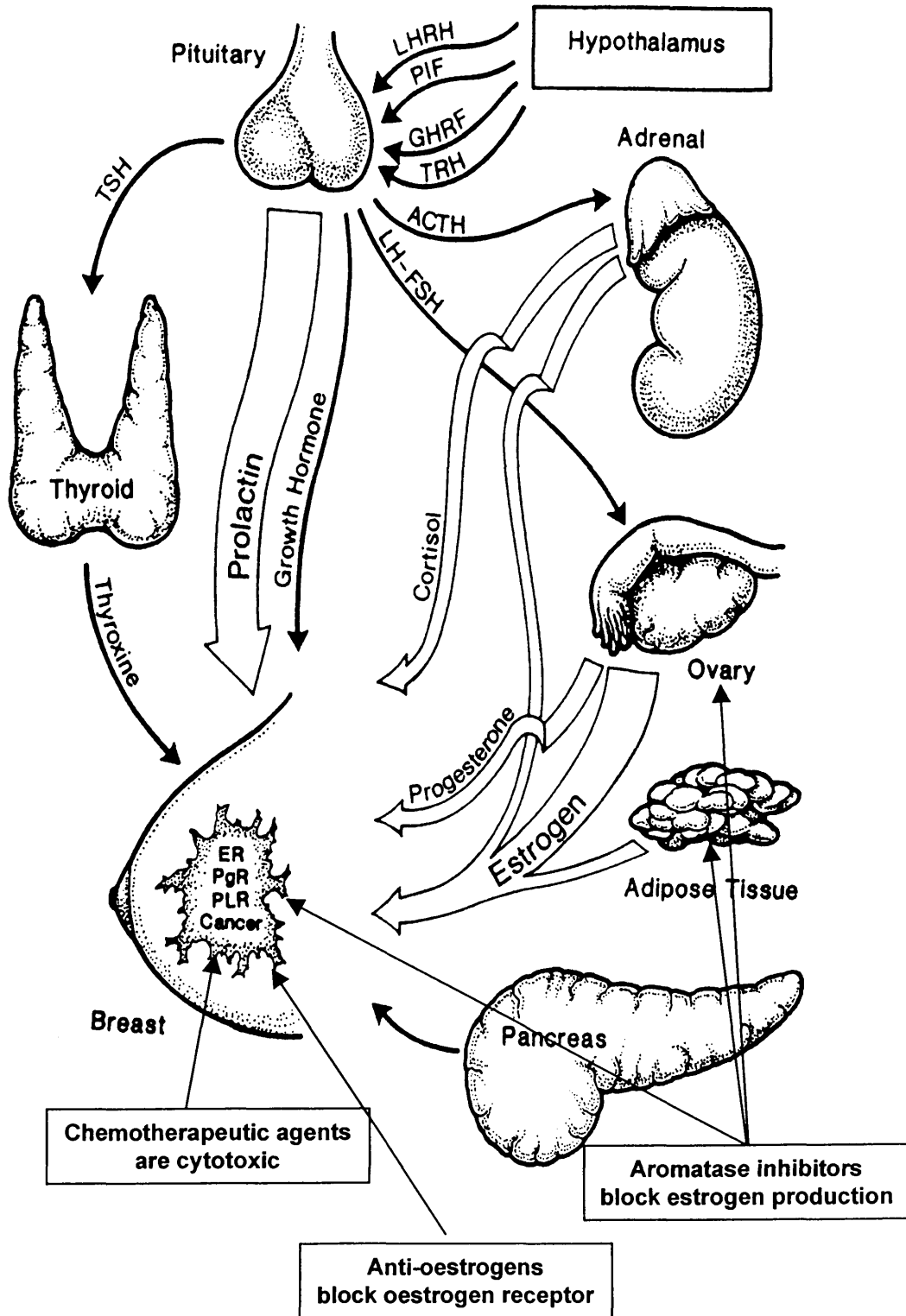
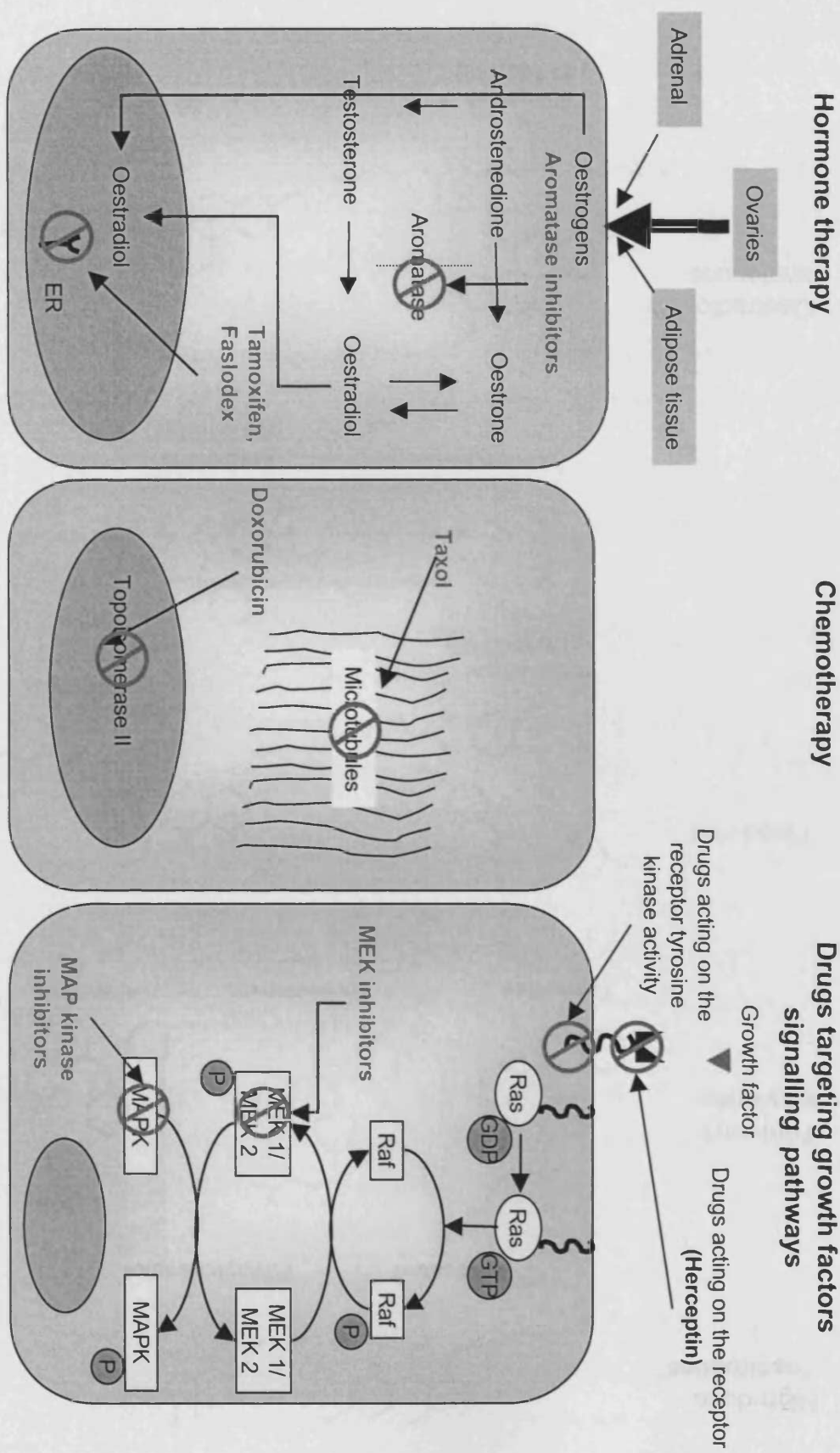
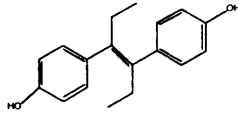


Fig. 1.6. Endocrine system interactions and main drugs sites of action (adapted from Kardinal, 1992)

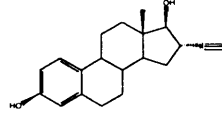
Fig. 1.7. Mechanism of action of the most commonly used drugs for the treatment of breast cancer



High-dose
"oestrogens"

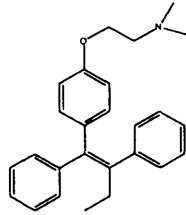


Stilbestrol

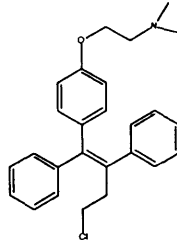


Ethinylestradiol

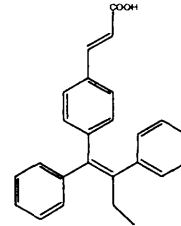
Triphenyl-
ethylenes



Tamoxifen

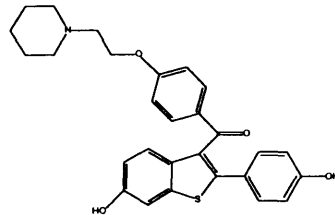


Toremifene

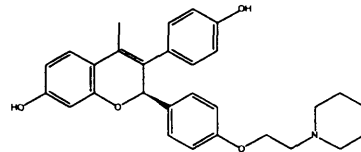


GW 5638

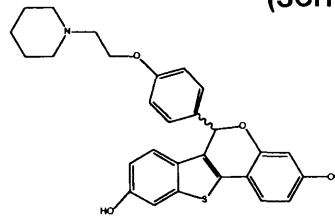
'Fixed-ring'



**Raloxifene
(LY 156,758)**

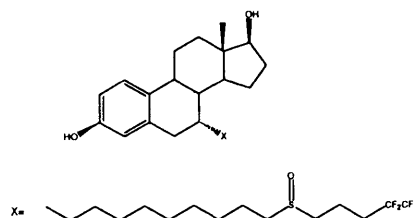


**EM-652
(SCH 57068)**

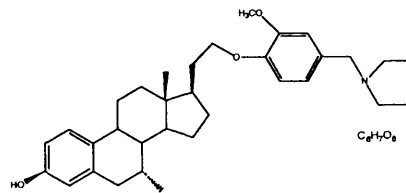


**Arzoxifene
(LY 353,381)**

Oestradiol
analogues



**Fulvestrant
(ICI 182,780)**



SR 16234

Fig. 1.8. Chemical structures of selective oestrogen receptor modulators (Howell and Johnston, 2002)

Faslodex has an inhibitory activity on aromatase enzyme *in vitro* (Long et al., 1998). As Faslodex is still active on tamoxifen resistant cells, the option of a sequential therapy seems very promising.

Aromatase inhibitors are an important class of compounds that is now getting substantial attention as recent clinical trials have shown the superiority of third-generation compounds versus tamoxifen. They act by interfering with the process of steroidogenesis. Oestrogens are synthesised by several tissues (Fig. 1.6), but in premenopausal women the ovaries are the main source of oestrogens. On the other hand, in post-menopausal women, other peripheral tissues, like the adipose tissue and the muscles, become the main site of oestrogen production (Fig. 1.6) (Goss and Strasser, 2002). Of particular relevance for this project is the observation that the tumour tissue itself can be a site of aromatisation and therefore, local oestrogens production can be essential for tumour development. Indeed, two thirds of breast carcinomas show aromatase activity and ability to produce oestrogens (Yue et al., 2002). Studies aiming to quantify the amount of “in situ” oestrogen production versus oestrogen uptake in nude mice bearing transfected MCF-7 showed the pivotal role of local biosynthesis (Yue et al., 1998). Aromatase inhibitors block P-450 aromatase complex, the enzyme that catalyses the last step of steroidogenesis (Fig. 1.9; Fig. 1.7). Selective inhibition of aromatase leads to reduced oestrogens production without interfering with the production of the other steroids hormones (Njar and Brodie, 1999).

The family of aromatase inhibitors can be classified according to their chemical structure as steroidal, (eg. formestane and exemestane) or non-steroidal (eg. letrozole and anastrozole) drugs (Fig. 1.10) (Njar and Brodie, 1999). The first compound that showed aromatase activity was aminoglutethimide (AGM). AGM belongs to the so-called first generation of aromatase inhibitors and has the disadvantage of being non-selective. In fact, not only does it act on aromatase, but it also blocks other P-450 enzymes like 11β -hydroxylase involved in the biosynthesis of corticosteroids (Fig. 1.9). Therefore, patients treated with AGM need to be supported by simultaneous administration of cortisol. It has nowadays mainly an historical value. Newer drugs in this class were synthesised to achieve higher selectivity and potency, for example the third generation compounds such as letrozole, anastrozole and exemestane (Goss

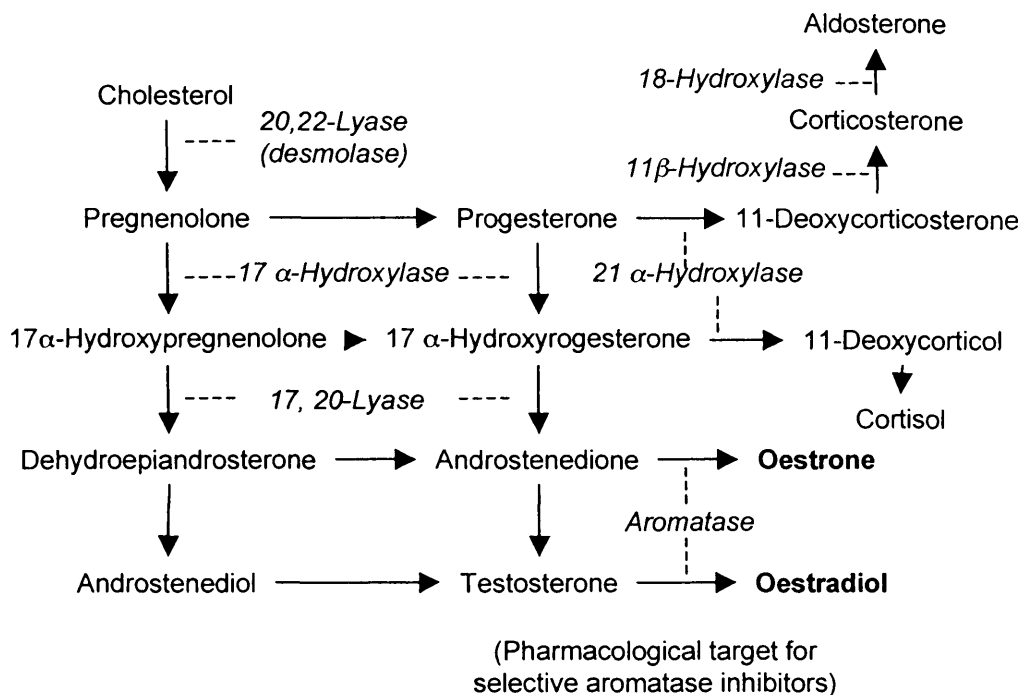


Fig. 1.9. Steroidogenesis pathway (taken from Njar 1999)

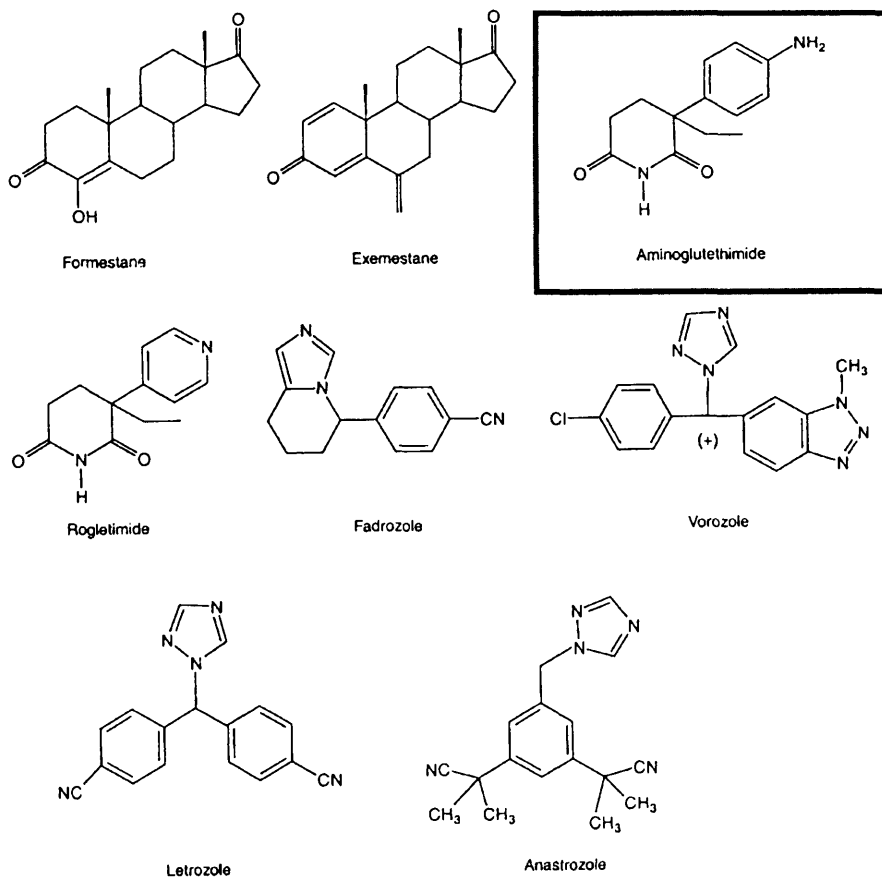


Fig. 1.10. Chemical structures of aromatase inhibitors (taken from Njar, 1999)

and Strasser, 2002; Long et al., 2002).

Aromatase inhibitors are poorly effective in pre-menopausal women because of their high levels of androstenedione, as the latter and the aromatase inhibitor compete for the active site of aromatase enzyme. However, these agents can be very useful in post-menopausal women or for women in whom the activity of the ovaries has been either pharmacologically or surgically reduced. As in the population of women affected by breast cancer, post-menopausal women account for 77% (American Cancer Society), the impact of aromatase inhibitors is potentially very high. Due to the problems associated with tamoxifen, several clinical trials have been carried out in recent years to assess the value of aromatase inhibitors as: early adjuvant therapy (where the aromatase inhibitor replaces the standard 5 years of tamoxifen); early sequential adjuvant therapy (aromatase inhibitor administered sequentially with tamoxifen during the 5-years post-surgery) and extended adjuvant therapy (the treatment with the aromatase inhibitor follows the standard 5 years tamoxifen therapy) (Mouridsen and Robert, 2005). The design of these clinical trials is summarised in Fig. 1.11, and several studies are still ongoing so only partial results are available. Nevertheless, it seems that aromatase inhibitors are at least as potent as tamoxifen. Interestingly, recent clinical trials showed that anastrozole (Arimidex®)(ATAC Trialists Group, 2005) and letrozole (The Breast International Group (BIG) 1-98 Collaborative Group, 2005) are superior to tamoxifen.

Oestrogens were the first choice therapy in advanced breast cancer before the introduction of anti-oestrogenic drugs (Perry, 1992). The mechanism of action of oestrogens on cancer is not completely clear. Nevertheless, high dosage oestrogens show antioestrogenic properties (Perry, 1992).

An important example of this class is DES (diethylstilbestrol) which used to be first line endocrine therapy before the introduction of tamoxifen. It is administered three times per day at a standard dose of 5 mg (Howell and Johnston, 2002). It is interesting to note that a polymer therapeutic containing DES has recently been described (Vicent et al., 2004). Another drug that has been used in breast cancer is ethynil estradiol.

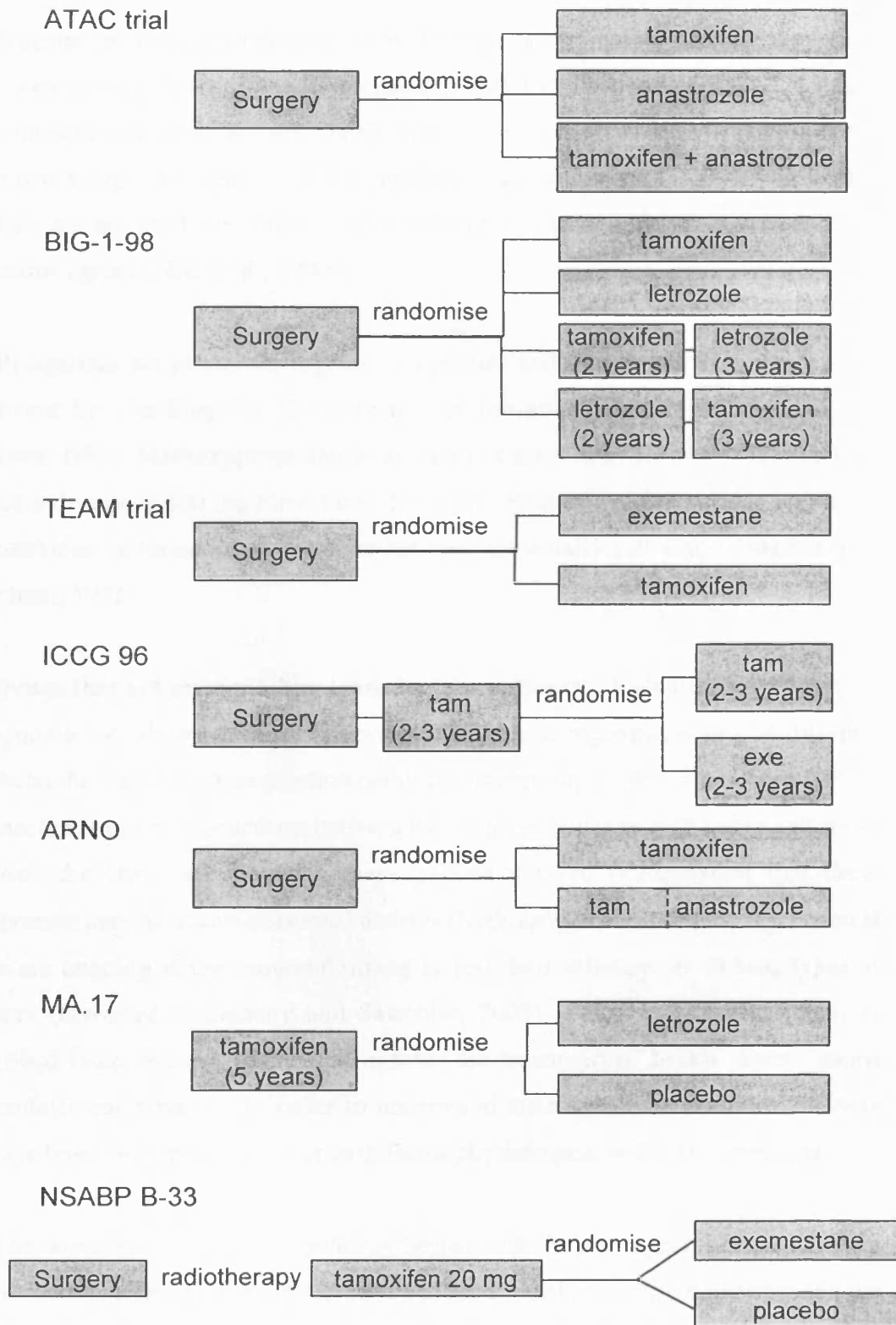


Fig. 1.11. Design of the clinical trials of aromatase inhibitors (Mouridsen and Robert, 2005)

Androgens can be used in the treatment of breast cancer mainly because they show anti-oestrogenic properties due to interactions with ER, PgR and androgen receptor. Nevertheless androgens are associated with side-effects of which virilisation is the most psychologically significant. An important drug of this class is fluoxymesterone but they are not used very often as they were proven to be less effective than other endocrine agents (Ellis et al., 2000b).

Progestins act as antioestrogenic compounds and the tumour response can be predicted by checking for the presence of hormone receptors (Calabresi and Chabner, 1996). Medroxyprogesterone acetate is a good example of this class and its standard dosage is 500 mg three times per week. Progestins have similar activity to tamoxifen on postmenopausal women but they are usually active for a shorter time (Kardinal, 1992).

Drugs that act on signalling transduction pathways. Recently, a new class of compounds has shown promising results. They are compounds acting at different levels on the signalling transduction pathways. Increasing evidence has been built in the last few years of interactions between the oestrogens and growth factor pathways. In fact, the cross-talk between these pathways is so fundamental that these compounds may have anti-hormonal activity (Nicholson et al. 2005). Several clinical trials are ongoing at the moment aiming to test their efficacy on various types of cancers (reviewed in Dancey and Sausville, 2003) (Table 1.2). Furthermore, as described later, the use of these drugs for the treatment of breast cancer seems particularly encouraging. In order to understand the mechanism of action of these drugs, a brief description of the growth factor physiological pathway is necessary.

The downstream signalling pathway begins with the interaction between growth factors and their receptors situated on the plasma membrane. The bond between the ligand and its receptor triggers the activation of a cascade of kinases, including the receptor's intrinsic tyrosine kinase activity, together with for example the mitogen-activated protein (MAP) cascade (reviewed in Dancey and Sausville, 2003). The activation of such pathways often promotes the transcription of specific genes responsible for cell proliferation (Darnell, 2002; reviewed in Downward, 2003). Overall, therefore, growth factor action is frequently mitogenic. While in normal

Table 1.2. Drugs acting on growth factor signalling pathway in clinical trials (taken from Dancey and Sausville, 2003)

Target	Name	Structure	Trial phase
Growth factor receptor inhibitors	EGFR	IMC-C225 cetuximab (Erbtux; Imclone)	Monoclonal antibody III
		ABX-EGF (Abgenix)	Monoclonal antibody II
		EMD 72000 (Merck KgaA Darmstadt)	Monoclonal antibody I
		RH3 (York Medical Bioscience Inc.)	Monoclonal antibody II
		MDX-447 (Medarex/Merck KgaA)	Monoclonal antibody bivalent I
		ZD1839 gefitinib (Iressa; AstraZeneca)	Small-molecule kinase inhibitor III
		OSI-774 erlotinib (Tarceva; OSI-Pharmaceuticals)	Small-molecule kinase inhibitor III
		CI-1033/PD183805 (Pfizer)	Small-molecule kinase inhibitor II
		EKB-569 (Wyeth Ayerst)	Small-molecule kinase inhibitor I
		GW2016/572016 (GlaxoSmithKline)	Small-molecule kinase inhibitor I
	HER-2/neu	Trastuzumab (Herceptin; Genentech)	Monoclonal antibody Registered
		MDX-210 (Medarex/Novartis)	Monoclonal antibody I
		2C4 (Genentech)	Monoclonal antibody I
	17-AAAG (Kosan)	Geldanamycin derivative inhibits HSP90 I	
PDGFR/c-KiVBCR-ABL	Imatinib (STI571/Gleevec; Novartis)	Small-molecule kinase inhibitor Registered	

Table 1.2. (continued)

Target	Name	Structure	Trial phase
Ras inhibitors	ISIS 2503 (Isis Pharmaceuticals)	Antisense oligonucleotide	II
	R115777 (Johnson and Johnson)	Farnesyl transferase inhibitor	II/III
	SCH66336 (Schering-Plough)	Farnesyl transferase inhibitor	II
	BMS214662 (Bristol Myers Squibb)	Farnesyl transferase inhibitor	I
Raf inhibitors	ISIS 5132/GPP69846A (ISIS Pharmaceuticals)	Antisense oligonucleotide	II
	L-779,450 (Merck)	Small-molecule kinase inhibitor	
	BAY 43-9006 (Onyx/Bayer)	Small-molecule kinase inhibitor	II
MEK inhibitors	PD 184352/CI-1040 (Pfizer)	Small-molecule kinase inhibitor	II
	U-0126 (Promega)	Small-molecule kinase inhibitor	I
mTOR inhibitors	CCI-779 (Wyeth)	Inhibits mTOR kinase by binding to FKBP12	II
	RAD001 (Novartis)	Inhibits mTOR kinase by binding to FKBP12	Phase I as a cancer therapeutic
			Phase II /III as an immunosuppressant
	Rapamycin/sirolimus (Wyeth)	Inhibits mTOR kinase by binding to FKBP12	Registered As an immunosuppressant

Table 1.2. (continued)

Target	Name	Structure	Trial phase
Cycline-dependent-kinase inhibitors	CDK	Flavopiridol/HMR-1275 (Aventis)	II
		E7070 (EISAI)	I
		CYC202 (Cyclacel)	I
		BMS-387032 (Bristol-Myers Squibb)	I
Other targets and agents	PKC	ISIS 3521/LY900003 Affinitak (ISIS Pharmaceuticals)	III
		CGP41251/PKC412 (Novartis)	II
		Bryostatins-1 (GPC Biotech)	II
		UCN-01 (Kyowa Hakko Kogyo)	I/II
		LY333531 (Ely Lilly)	Phase I oncology Phase II/III diabetic neuropathy
PDK1	UCN-01 (Kyowa Hakko Kogyo)	Staurosporine analogue	Phase I/II

cells a balance between activation of this pathway and its inhibition is highly regulated, during the pathogenesis of diseases like cancer, such signalling may be altered in several ways. For example, growth factors receptors such as epidermal growth factor (EGF) receptor (EGFR) and/or insulin-like growth factor receptor (IGFR) can be overexpressed. Consequently, the blockage of the growth factors downstream signalling pathway at any level should theoretically be beneficial in several cancer types.

In recent studies it has been interestingly pointed out that EGF and oestrogen signalling are strictly connected (Nicholson et al., 2001). In fact, not only are EGFRs over-expressed in cells previously treated with anti-hormonal drugs, but there is an active cross-talk between oestrogens and growth factors signalling pathways. The main connections between the pathways of oestrogens and growth factors have been summarised as follows (Nicholson and Gee, 2000):

- Growth factors like EGF, TGF- α and IGF are able to phosphorylate the serine 118 residue of ER. This process leads to the activation of the receptor even in absence of its ligand (oestrogen).
- Oestrogens are able to trigger positive elements involved in growth factors signalling cascade while they have an inhibitory effect on negative elements of this pathway.
- The ER enhances the activity of nuclear transcription factors induced by growth factors.

Finally, growth factors and steroids have as an eventual target the same pool of genes that promote cell mitogenic activity (Nicholson et al., 2002).

Importantly, oestrogen deprivation has been correlated with up-regulation of growth factor receptors such as EGFR. This seems to be an important mechanism of anti-hormonal resistance (Nicholson et al., 2001; Nicholson et al., 2005). Therefore, the treatment with drugs involving inhibitors of growth factors transduction pathways seems to be a promising solution even in the treatment of tumours resistant to hormone-therapy. It is also important to note that trastuzumab (Herceptin®), a monoclonal antibody targeting HER2 has been licensed and is used in metastatic disease after assessment of HER2 status (Ellis et al, 2000a).

Combination and sequential hormonal therapy. It is very important to underline that the above mentioned drugs can be used as sequential or combination therapy. According to Lonning (2000), the lack of cross-resistance between different hormonal treatments could be exploited using a sequential therapy. For instance, tamoxifen followed by aromatase inhibitors could be a good option to extend the efficacy of hormone treatment and life expectancy. Of particular promise seems to be the combination of anti-hormones with signal transduction inhibitors (discussed in Gee et al., 2005).

1.3.2. Chemotherapy

Chemotherapy agents are a very important category of compounds used in the treatment of breast cancer. Even though they show higher toxicity than endocrine therapy, they are widely used as pre/post surgery adjuvant therapy, in combination with hormone therapy and in endocrine resistant tumours. Several compounds are used as cytotoxic chemotherapy and in this section the principal classes are described.

Anthracyclines, such as Dox and epirubicin (Fig. 1.12), have had, and still have, a very important role in the treatment of breast cancer. They were considered the most effective drugs available until taxanes were introduced in clinical practice. Nowadays anthracyclines and taxanes are both first choice when a chemotherapy approach is chosen (Ellis et al., 2000b). Their exact mechanism of action is still controversial and several mechanisms have been proposed, including their capacity to damage the genetic material of the cancer cell; interfere with p53 expression (Liem et al., 2003); promote toxic actions at cell surface (Tritton, 1982; reviewed in Tritton 1991) and induce apoptosis by activation of caspases (reviewed in Gewirtz, 1999). The most widely accepted view, however, is that anthracyclines act at nuclear level and inhibit cell proliferation by interacting with topoisomerase II (Fig. 1.7) (Monneret, 2001; Calabresi and Chabner, 1996). For this reason it has been suggested that a quantification of the levels of this enzyme could be used as a predictor for anthracycline-sensitivity (reviewed in Barrett-Lee, 2005).

Although, anthracyclines are extremely potent drugs, their clinical use is limited by severe toxicity. Acute and chronic toxicity is seen. The former results from non-

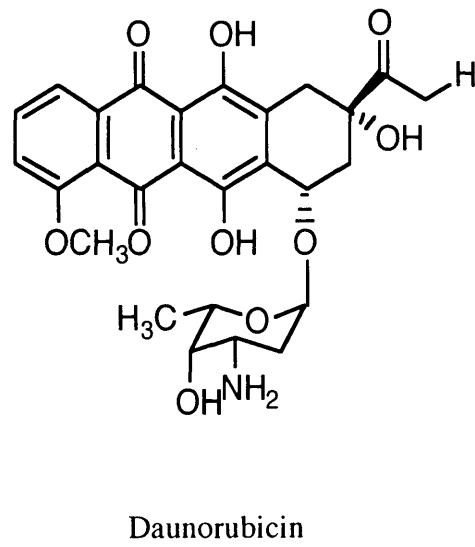
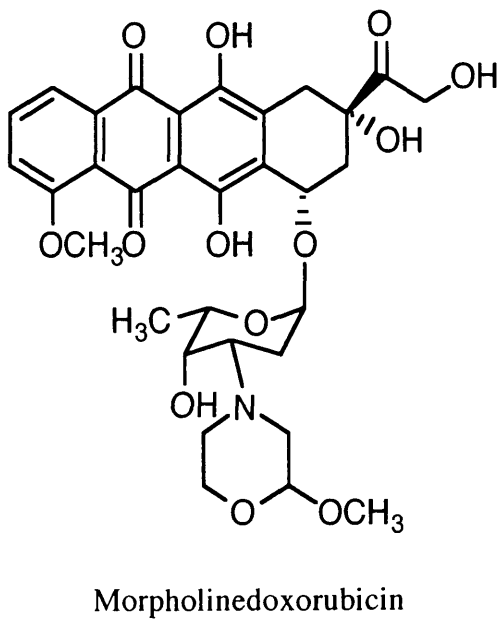
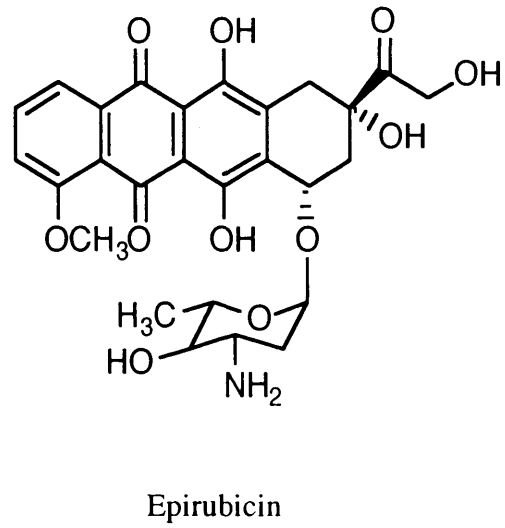
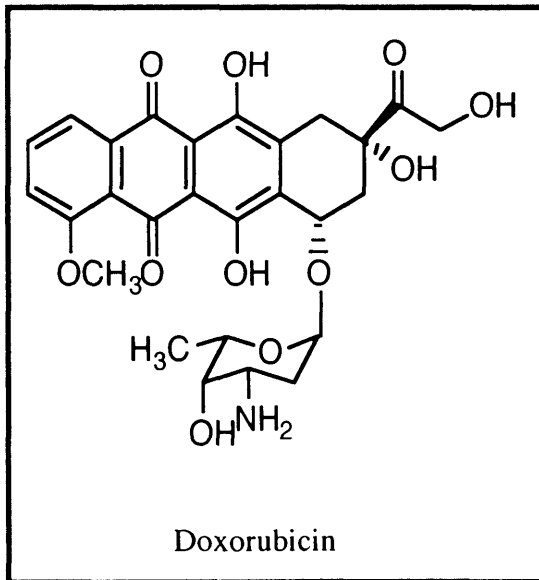


Fig. 1.12. Chemical structure of some anthracyclines

specific activity in other normal rapidly proliferating tissues of the body such as hemolymphopoietic system, the testes and gastrointestinal tract. Chronic toxicity is observed in the heart, liver, kidneys and peripheral nervous system (Mazue' et al., 1995). Dox cardiotoxicity is due to the aglycone metabolites produced in the liver by NADPH-dependent cytochrome P450 reductase (Danesi et al., 2002). It is interesting to note that even the administration route can influence the toxicity profile. Danesi et al. (2002) showed that anthracycline cardiotoxicity varies if the drug is administered as a bolus or as a continuous infusion, the latter being less toxic. Anthracyclines are often administered to patients in combination with other drugs, as described below. From a drug delivery point of view, it is interesting to note that a PEGylated liposomal formulation of Dox (Doxil[®]), is commonly used for the treatment of breast cancer.

Taxanes. Paclitaxel (Taxol[®]) and other taxanes are often employed in the treatment of breast cancer. They act at cellular level by inhibiting the function of microtubules, therefore preventing cell growth and multiplication (Fig. 1.7) (Calabresi and Chabner, 1996). Both paclitaxel and docetaxel (Taxotere[®]) are routinely used as chemotherapy agents for breast cancer. Docetaxel is rarely used as second choice after paclitaxel, even though there is an incomplete cross-resistance between the two. More often docetaxel is used as an alternative drug to paclitaxel (Hortobagyi, 2002) for example as second-line chemotherapy after anthracyclines (Crown et al., 2002) (Fig. 1.5).

Combination chemotherapy. Cytotoxic drugs are often administered in combination. Examples of this approach are CMF (Cyclophosphamide, Methotrexate, 5-FU) and CMFVP (Cyclophosphamide, Methotrexate, 5-FU, Vincristine, Prednisone) (Kardinal, 1992). Anthracycline based combinations are also widely used. Dox (trade name Adryamicin[®]), or its derivatives are usually combined with drugs such as cyclophosphamide (AC) and cyclophosphamide, 5-fluorouracyl (CAF) (Bonadonna et al., 1984; Hortobagyi, 2002). In recent trials combinations of taxanes and anthracyclines have been tested. Their combination is of particular interest for two main reasons. First, they are both effective as a first-line chemotherapy for breast cancer, but moreover, they have different mechanisms of

actions and thus do not show any cross-resistance (Friedrichs et al., 2002; Nabholz, 2003). It is also interesting to report that the monoclonal antibody HER-2, trastuzumab has shown increased activity when combined with chemotherapy such as paclitaxel (Marty et al., 2005).

1.4. POLYMER CONJUGATES

Despite the large number of drugs used for breast cancer, the survival rate of patients with high stage cancer is still very low (Fig. 1.2). In addition to the search for new molecular targets for a rational drug design, improved tumour drug targeting may also prove beneficial and the design of polymer conjugates may potentially enhance the performances of chemotherapy and hormonal therapy.

Polymer conjugates were proposed as a new concept approximately 30 years ago, (Ringsdorf, 1975) since then, research of Duncan and Kopecek (Duncan et al. 1992; Duncan and Kopecek 1984; reviewed in Duncan 2003b) transferred the first polymer anticancer conjugate into clinical trials in 1994 (Table 1.3) (reviewed in Duncan, 2003a) and now 11 polymer-anticancer drug conjugate are in Phase I, II or III clinical trials.

The structure of polymer anticancer drug conjugates is made by three different components: a polymeric backbone, a linker, a drug and, optionally, a targeting group (Fig. 1.13).

- **Polymeric backbone.** The polymer is used as a platform to carry drug molecules. As the conjugates are designed for intravenous administration, it is important that the polymer is water soluble, non-toxic and non-immunogenic. Several polymeric carriers have been suggested, including, HPMA copolymers (Duncan et al., 1987), polyethylene glycol (PEG) (Veronese et al., 2005), polyglutamic acid (PGA), dextran (Guu et al., 2002), hyaluronic acid (Cera et al., 1992) alginates (Al-Shamkhani and Duncan, 1995) and poly-amino acid (Zunino et al., 1984). However, so far, only HPMA copolymers, PEG, PGA and oxidised dextran have made it to clinical trials (Table 1.3). When HPMA copolymer-Dox entered clinical trials in 1994, HPMA was tested on humans for the first time. The study didn't show any evidence of polymer-related toxicity (Vasey et al., 1999; reviewed in Duncan

Table 1.3. Polymer conjugates in clinical trials (adapted from Duncan 2003)

Polymer-drug	Status
HPMA copolymer-doxorubicin (PK1, FCE 28068)	Phase II
HPMA copolymer-doxorubicin-galactosamine (FCE 28069)	Phase I/II
HPMA copolymer-paclitaxel (PNU166945)	Phase I
HPMA copolymer-camptothecin (MAG-CPT, PNU 166148)	Phase I
HPMA copolymer-platinite (AP 5280)	Phase I
PG-paclitaxel (CT-2103)	Phase II/III
PG-camptothecin (CT-2106)	Phase I
PEG-camptothecin (PROTHECAN®)	Phase I

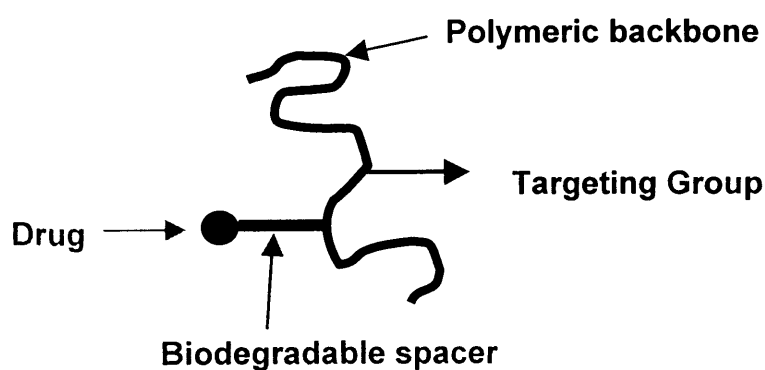


Fig. 1.13. Ringsdorf model of polymer conjugate (adapted from Ringsdorf 1975)

2003b). Subsequent studies on other conjugates based on HPMA confirmed the safety of this polymer (Schoemaker et al 2002; Meerum Terwogt et al. 2001; Nowotnik 2004).

- **Linker/spacer.** The drug is attached to the polymeric backbone through a linker/spacer designed to be degraded at cellular level to obtain the eventual release of the drug. It is a key feature as its careful and rational design may allow a finely modulated release in specific intracellular compartments at specific rates (Duncan, 2002).

Therefore, the choice of the linker depends on where the drug is designed to be released. Most conjugates prepared so far are designed for lysosomotropic delivery, i.e. they are designed to be internalised by the cell and to eventually release the drug in the lysosomal compartment (Fig. 1.14) (De Duve et al., 1974). There are two different approaches that can lead to lysosomal release: enzymatic release (exploiting the large number of lysosomal enzymes) and pH-dependent release (exploiting the low lysosomal pH).

Enzymatic release consists of designing a linker that can be selectively cleaved by lysosomal enzymes (enzymatic release). For this purpose several peptidic linkers have been tested both *in vitro* using tritosomes (lysosomal hepatic enzymes) and *in vivo* (Brocchini and Duncan, 1999; Duncan et al., 1980; Kopecek et al 1981). Kopecek et al. (1981) linked *p*-nitroaniline to an HPMA polymeric backbone through different peptidic linkers and measured the release of *p*-nitroaniline in rats. The experiment showed that both the rate and the amount of the release depend on the linker used. In a broad sense, tetrapeptides give a faster release than tripeptide which release faster than dipeptide linkers.

pH-dependent release consists of exploiting the decrease in pH in different cellular compartments in order to obtain the release of the drug. pH-sensitive linkers can be designed to be degraded at lysosomal pH. For example, Dox has been conjugated with HPMA through Gly-Gly or Gly-Phe-Leu-Gly spacer and a hydrazone linker to obtain a hydrolytically labile bond at acidic pH (Etrych et al., 2001; Ulbrich et al., 2004). *In vitro* tests in different buffers showed different release

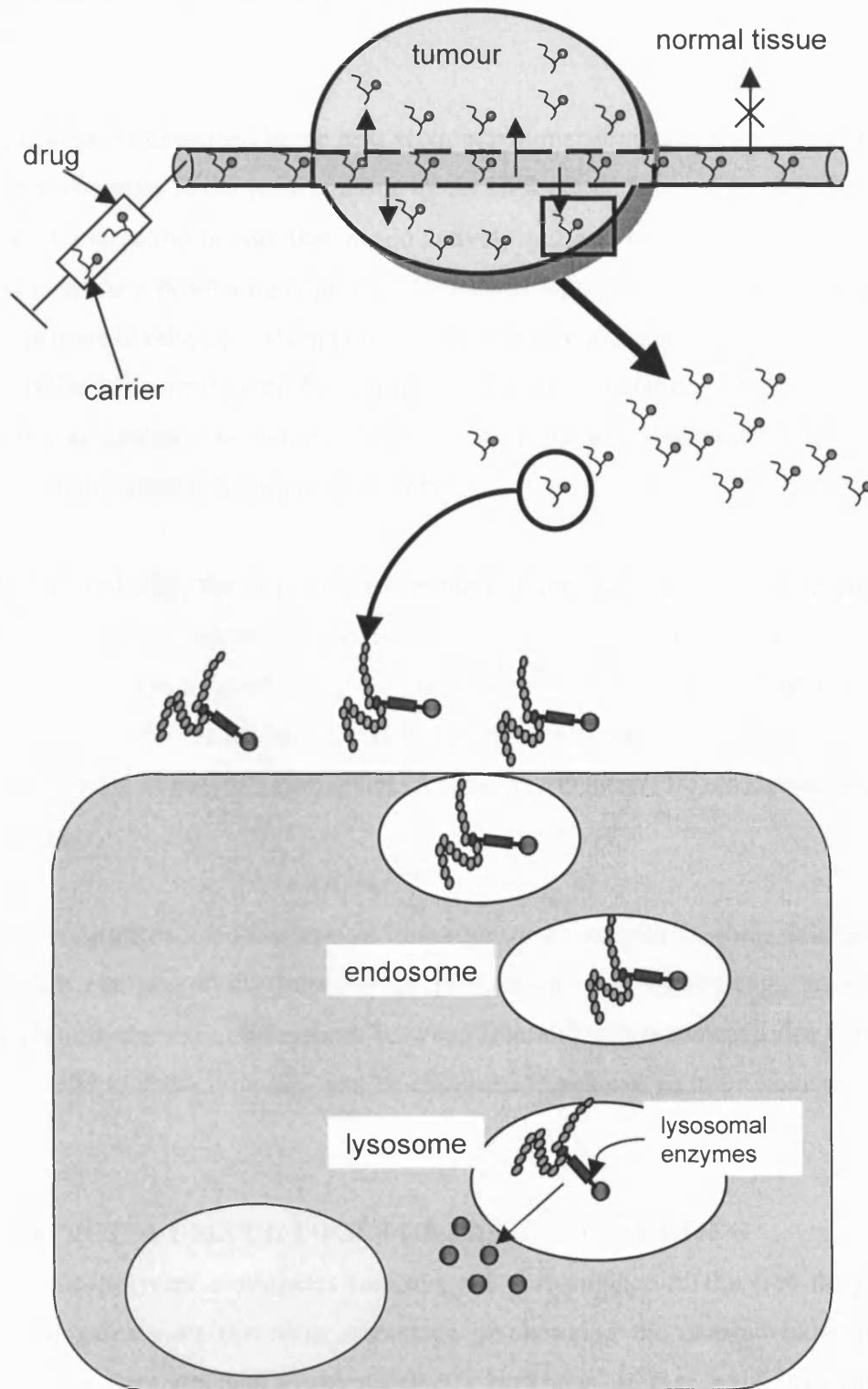


Fig. 1.14. Tumour passive targeting through the EPR effect and lysosomotropic delivery. (adapted from Duncan, 1999)

rate depending on the pH. Maximum release was achieved at pH 5 suggesting that a selective intracellular release could be achieved using the appropriate linker (Etrych et al., 2001).

Targeting group. As described in the next section, polymer-drug conjugates are able to passively accumulate in the tumour tissue by the EPR effect. It has been suggested that the use of a targeting moiety that would actively address the conjugate towards the tumour tissue is a promising approach. Nevertheless, of the 11 anticancer drug conjugates that are in clinical trials only one bears a targeting group (Table 1.3). This is the HEMA copolymer-Dox-galactosamine (called PK2, FCE 28069) and was designed to achieve liver targeting by selective binding to the asialoglycoprotein receptor (Seymour et al., 2002).

Drug. Theoretically, the drug carried by the polymer conjugate could be any anticancer drug that is resistant to lysosomal pH and to lysosomal enzymes. In addition, it should have a functional group that can be used to bind the drug to the linker. Dox, camptothecin, paclitaxel and cisplatin are examples of drugs that are now in clinical trials as polymer conjugates (reviewed in Duncan 2003a; Thanou and Duncan, 2003).

Polymer conjugates are therefore an important new category of drug delivery systems which can potentially improve the performances of many drugs. In the following section, the main differences between free and polymer-bound drug are analysed in order to show how they can be exploited to achieve an improvement of the therapy.

1.5. EPR EFFECT: A USEFUL TOOL FOR PASSIVE TARGETING

Why should polymer conjugates improve the performance of the free drug? Polymer conjugates have the main advantage of changing the pharmacokinetic properties of the drug attached to the polymeric backbone. In fact, exploiting the EPR effect described in this paragraph, they are able to change the drug body-distribution and accumulate in the tumour thus achieving a passive targeting. Tumours originate from one single cell bearing genetic modifications. Initially, it grows and multiplies taking nutritive substances from the surrounding vasculature,

but as soon as the cancerous mass becomes bigger, its need for nutrients increases. Thus, tumours start producing their own vessels to support their growth. This process is known as angiogenesis (reviewed in Folkman, 1992).

Cancerous vessels have proven to be anatomically different from normal vessels. In fact, cell junctions are looser than in normal vessels and the basement membrane is either lacking or incomplete. Furthermore, tumour vasculature often lacks of muscle layer and is not homogeneous. All these feature make the cancerous capillaries more permeable (enhanced permeability) allowing increased polymer access (Duncan, 1999; Maeda, 1994; Maeda et al., 2001). Not only the permeability of the vessel is increased but also the lymphatic system is less effective in tumour vasculature. Consequently, the clearance of the drug from the cancerous tissue is decreased (enhanced retention). The EPR effect has proven to be ideal to achieve passive targeting. In fact, while low molecular weight drugs can easily pass both through normal and cancerous vessels, macromolecular carriers can accumulate selectively in tumour tissues (Fig. 1.13). It is important to notice that the conjugation of a drug to a polymeric backbone increases its distribution half-life. For example, Dox distribution half-life changes from 4.8 min (if administered as free drug) (Danesi et al., 2002) to 1.8 h (in HPMA-copolymer-Dox) (Vasey et al., 1999). The prolonged circulation time therefore achieved potentially magnifies the EPR effect. *In vivo* studies performed on solid B16F10 tumour model showed that HPMA copolymer-Dox is able to accumulate in the tumour at higher extent than the free drug (10-15 fold more) (Seymour et al., 1994). Similar results were found testing HPMA copolymer-Gly-Phe-Leu-Gly-en-Pt *in vivo* (Gianasi et al., 1999).

1.6. AIM OF THE PROJECT

The use of polymer conjugates to deliver selectively standard chemotherapeutic agents to the tumour tissue is well established (reviewed in Duncan, 2003a). The use of combinations of drugs to maximise the therapeutic effect is also well established (discussed in section 1.3.2). Therefore, the design of a conjugate that carries and delivers simultaneously both chemotherapy and endocrine therapy to the tumour tissue has a high therapeutic potential.

At the outset, the aim of this project was to develop a new family of polymer-conjugates for the treatment of breast cancer carrying only chemotherapy, only endocrine therapy or their combination and to assess the advantages of polymer-based combination therapy *in vitro*.

Firstly, it was necessary to synthesise and characterise this novel family of conjugates (Chapter 3). Then, the conjugates were tested to assess cytotoxicity and ability to inhibit aromatase *in vitro* (Chapter 4). As the internalisation of a polymer conjugate is a key step for its biological activity, the uptake rate and mechanism of HPMA copolymer-Dox and HPMA copolymer-AGM-Dox were compared *in vitro* (Chapter 5). Finally, in an attempt to gain an insight into the cellular mechanism of action, immunocytochemistry was used to investigate the impact of the two conjugates on cell growth and survival (Chapter 6).

Chapter 2:

Materials and General Methods

2.1. EQUIPMENT

2.1.1. Analytical

HPLC analysis was performed using one or two JASCO HPLC pumps with a gradient mixer with a μ Bondapak C18 (150 x 3.9 mm) column. The 717 plus autosampler was from Waters Ltd, UK. The machine was equipped with 2 detectors: a spectroflow 783 UV detector, Kratos Analytical, UK and a fluoromonitorTM III fluorescence detector, LDC/Milton Roy, UK. HPLC chromatograms were collected and analysed with PowerChrom hardware and software (version 2.0.7).

Fluorescence was measured with a Fluostar Optima fluorescence plate reader from BMG Labtechnologies, Germany and with an Amnico-Bowman Series 2 luminescence spectrophotometer from Spectronic Instruments, USA.

Ultraviolet (UV) absorbance was read with a Sunrise UV absorbance plate reader from Tecan, Austria and with a Cary 1G UV-visible spectrophotometer from Varian, Australia.

Gel permeation chromatography (GPC) analysis was performed using aqueous GPC equipped with a JASCO HPLC pump, with two TSK-gel columns in series (G3000 PW followed by G2000 PW) and a guard column (Progel PWXL). The eluent was monitored using a differential refractometer (Gilson 153) and an UV-visible spectrophotometer at 254 nm (UV Savern Analytical SA6504) in series. PL Caliber Instrument software was used for data analysis.

Thin-layer chromatography (TLC) was performed on Merck silica gel plates (DC-60 F254 and Kieselgel ALU 60 F254). Size exclusion chromatography was performed with Sephadex LH20 (Amersham Biosciences, Sweden) in column 5 x 50 cm. Spectra/Pore 7 dialysis membrane (2,000 g/mol cut-off) was from Spectrum Laboratories Inc, USA.

Freeze drier. Freeze dried products were obtained with a Flexi Dry FD-1.540 freeze dryer from FTS systems, USA equipped with a vacuum pump from Javac, Australia.

Flow cytometry. Uptake studies were performed with a FACSCalibur flow cytometer (Becton Dickinson, UK) equipped with a single argon laser (excitation wavelength 486 nm). Data were acquired in 1024 channels with band pass filters (FL-1 530 ± 30 nm; FL-2 585 ± 42 nm; FL-3 670 long pass filter). Data were acquired and analysed with Cell Quest software (version 3.3).

Fluorescence microscopy. Visualisation of the cellular uptake was performed with an inverted Leica DM IRB fluorescence microscope, Germany with an incident 450 – 490 nm and long pass filter 515 nm (for Dox fluorescence). Images were taken with a 12 – bit cooled monochrome Retiga 1300 camera from Qimaging, Canada and handled with Openlab software (version 3.0.9) from Improvision, UK. The same microscope was also used to collect bright-field images.

Microscopy for immunocytochemistry. Cells stained by immunocytochemistry were visualised using an Olympus BH-2 microscope, Japan and images were acquired with an Olympus DP12 camera, Japan.

2.1.2. Cell culture

With the exception of the centrifugation steps, work with cells was performed in Bioair and Microflow class II laminar flow hoods (Bioair, Italy and Servicecare, UK, respectively). For general tissue culture work an inverted bright-field microscope was used (Leica, Germany). For routine cell counting, a silver stained Neubauer haemocytometer (Marienfeld, Germany) was used. Tissue culture flasks (25, 75 and 150 cm²) and tissue culture sterile plates (96-well; 24-well; 12-well; 6-well) were from Corning Inc, USA. Sterile pipettes were from Elkay, UK as well as 7 mL bijous, universal containers and 60 mL pots. Cells were scraped with a tailor made rubber policeman, from the European Molecular Biology Laboratory, Germany.

2.2. MATERIALS

2.2.1. Chemical reagents

Anhydrous dimethylsulfoxide (DMSO), anhydrous dimethylformamide (DMF), 1,3-dicyclohexylcarbodiimide (DCC), 1-amino-2-propanol, sodium hydroxide pellets, chlorpromazine, cytochalasin B, methyl-β-cyclodextrin, lovostatin and 1-hydroxy benzotriazol (HOBt) were supplied by Sigma-Aldrich, UK. Methanol, ethanol, propan-2-ol (HPLC grade), diethylether, triethylamine, dichloromethane,

acetone, acetic acid, hydrochloric acid, were provided by Fisher Scientific, UK. AGM was provided by Sigma-Aldrich, UK while orthophosphoric acid was from Fluka Biochemica, UK. Dox.HCl was kindly donated by Pharmacia, Italy.

2.2.2. HPMA copolymers

HPMA copolymer-GFLG-ONp (5 mol %), HPMA copolymer-GFLG-ONp (10 mol %) and HPMA copolymer-GG-ONp (5 mol %) were supplied by Polymer Laboratories, UK. HPMA copolymer-GFLG-Dox was kindly donated by Pharmacia, Italy.

2.2.3. Cell culture

MCF-7 is a human oestrogen-dependent breast cancer cell line and MCF-7ca is the same cell line transfected in order to over-express the aromatase enzyme (Brodie 2002; Brodie and Njar, 2000). Both cell lines were provided by Tenovus Centre for Cancer Research (Cardiff, UK). B16F10 are murine melanoma cells and they were from ATCC, USA. RPMI 1640 with L-glutamine (with and without the pH indicator phenol red), 0.05 %w/v trypsin - 0.53 mM EDTA and foetal bovine serum (FBS) were provided by Invitrogen Life Technologies, UK. 3-(4,5-dimethylthiazol-2-yl)-2,5-diphenyl-2H-tetrazoliumbromide (MTT), trypan blue, androstenedione, oestradiol, testosterone, and sterile DMSO were from Sigma-Aldrich, UK. Geneticin (G418) solution (50 mg/mL) was from Invitrogen, UK. [1,2,6,7-³H]androst-4-ene-3,17dione ([³H]androstenedione) was supplied by Amersham Biosciences (UK). Formic acid was from Aldrich (UK) while the liquid scintillation cocktail, OptiPhase 'HiSafe' 3 was from Perkin Elmer (UK) and mercuric chloride was purchased from BDH Chemicals (UK).

2.2.4. Western blots

Trizma base, Triton X-100, ethylene glycol-bis(beta-aminoethyl ether)-N,N,N',N'-tetraacetic acid (EGTA), all the protease inhibitors (sodium vanadate (NaVO₄), phenylmethanesulfonyl fluoride (PMSF), sodium molybdate, phenylarsine, sodium fluoride (NaF), aprotinin, leupeptin), sodium dodecyl sulfate (SDS), glycerol, lower buffer, upper buffer, dithiothreitol (DTT), 30 % acrylamide solution, ammonium persulfate (APS), tetramethylethylenediamine (TEMED) were from Sigma-Aldrich, UK. Bromo-phenol blue was from BDH Chemicals, UK. Mouse

anti-human cytochrome P450 aromatase was from Serotec, UK (Turner et al., 2002). The kit used for developing the blot, SuperSignal® WestDura Extended Duration Substrate was from Pierce, USA. The composition of the solutions, and the various buffers used for lysing cells, SDS-PAGE and Western blotting is summarised in Tables 2.1-2.2.

2.2.5. Immunocytochemistry

The solvents used for fixation (methanol, acetone) were from Fisher Scientific, UK as was the formaldehyde solution (40 %). ER primary antibody (clone 6F11) was from Vector, California. The monoclonal mouse primary antibodies against the PgR (clone 636), against the Ki67 antigen (clone MIB-1) and against the Bcl-2 oncoprotein (clone 124) were all supplied by DakoCytomation, California. The rabbit polyclonal primary antibody against pS2 was from Novacastra, UK. The polyclonal goat anti-mouse (GAM) immunoglobulins, the peroxidase anti peroxidase (PAP), the diaminobenzidine (DAB) were from DakoCytomation, California. EnVision mouse (labelled polymer-HRP anti-mouse) and EnVision rabbit (labelled polymer-HRP anti-rabbit) were also from DakoCytomation, California. Supersensitive concentrated detection kit (i.e. link (biotinylated anti-mouse immunoglobulins) and concentrated label (streptavidin peroxidase)) were from Biogenex, California. The DPX mountant for histology was from Sigma-Aldrich, UK, as were the tween and the methyl green while glycerol and sucrose were from Fisher scientific, UK.

2.3. GENERAL METHODS

This section gives a detailed description of the methods used in this thesis. When the development of a method was considered to be an important part of the results, its description was provided in the related experimental chapter.

The first aim of this project was to prepare a library of HPMA copolymer-AGM \pm Dox conjugates. The synthesis and characterisation of HPMA copolymer-Dox is widely described in the literature (Rejmanova et al. 1977; Duncan et al. 1988). On the contrary, the synthesis of conjugates containing AGM and their characterisation was more challenging. Only the methods used to prepare and characterise HPMA copolymer-Dox will be described in this chapter while the synthesis and

Table 2.1. Summary of the composition of the lysis buffer and protease inhibitors.

Lysis buffer	Protease inhibitors solutions to be added to 10 mL of lysis buffer		
	Protease inhibitor	concentration of stock solution	final concentration
0.6 g TRIZMA base	200 μ L NaVO ₄	100 mM	2 mM
0.875 g NaCl	100 μ L PMSF	100 mM in propanol	1 mM
0.19 g EGTA	100 μ L sodium molibdate	1 M	100 mM
1 % TRITON X-100	10 μ L phenylarsine	20 mM in chloroform	20 μ L
pH = 7.6	100 μ L NaF	2.5 M	250 mM
	50 μ L aprotinin	2 mg/mL	10 μ g/mL
	20 μ L leupeptin	5 mg/mL	4 μ g/mL

39

Table 2.2. Summary of the composition of buffers and solutions used for SDS page and Western blot

2 X loading buffer	lower gel:	upper (stacking) gel:	running buffer:	transfer buffer:	TBS tween:
4 mL 10% SDS	4.8 mL H ₂ O	6.1 mL H ₂ O	3.3 g TRIZMA base	10.8 g glycine	1.21 g TRIZMA base
2 mL glycerol	2.5 mL lower buffer	2.5 mL upper buffer	14.4 g glycine	2.28 g Tris base	5.8 g NaCl
2.4 mL upper buffer	2.5 mL 30% acrylamide	(0.5 M TRIS, pH 6.8)	1 g SDS	600 mL H ₂ O	0.5 mL Tween 20
1.6 mL H ₂ O	100 μ L 10% SDS	1.3 mL 30% acrylamide	pH 8.3	150 mL methanol	1.5 mL 5M HCl
0.01 % Bromophenol blue	100 μ L 10% APS	100 μ L 10% SDS			
0.1 M DTT	6 μ L TEMED	50 μ L 10% APS			
		10 μ L TEMED			

characterisation of HPMA copolymers containing AGM is considered to be part of the results and is therefore described in Chapter 3.

2.3.1. Synthesis of HPMA copolymer-Dox conjugate by aminolysis

The aminolysis reaction was performed according to the procedure described in the literature (Rejmanova et al 1977; Duncan et al. 1988) (Fig. 2.1). One equivalent of the precursor (HPMA copolymer-ONp) and Dox.HCl were dissolved in the minimum amount of anhydrous DMSO in a N₂ atmosphere. Triethylamine (1 equiv.) was added dropwise to the copolymer solution to neutralise the hydrochloric acid and obtain Dox as free amine. The reaction was allowed to proceed at room temperature for approximately 5 h and quenched by addition of 1-amino-2-aminopropanol. The reaction was monitored by UV (release of ONp at 400 nm (Fig. 2.2)) and by TLC (mobile phase: acetic acid 0.5 butanol 6.5 H₂O 3; R_f_{Dox} = 0.55, R_f_{polymer} ~ 0). The non-specific hydrolysis of the ester is a competitive reaction and this was prevented by carrying the reaction out in dry solvents and under a N₂ atmosphere.

2.3.2. Purification of HPMA copolymer-Dox

DMSO was evaporated under reduced pressure. The polymer conjugate was dissolved in a minimal amount of methanol, precipitated into a vigorously stirred mixture of acetone : diethylether (4 : 1) and then filtered. The polymer conjugate was purified by gel filtration chromatography using Sephadex LH20 (column 5 x 50 cm, eluent MeOH) and the purified compound was then dissolved in a minimal amount of water and freeze-dried. The overall yields based on polymer weight were 70 - 80 %.

2.3.3. Synthesis of HPMA copolymers-aminopropanol

As a control polymer for chemical characterisation and also biological studies, HPMA copolymers-aminopropanol derivatives were prepared as follows. HPMA copolymers-ONp were dissolved in dry DMF in a N₂ atmosphere and an excess of aminopropanol (10 equiv.) was added to the solution. The reaction was allowed to proceed for approximately 4 h and it was monitored spectrophotometrically (release of ONp at 400 nm). DMF was evaporated at reduced pressure. The reaction mixture was then dissolved in ddH₂O and dialysed (2 days, 2,000 Mw membrane cut-off) to remove unreacted aminopropanol and released ONp.

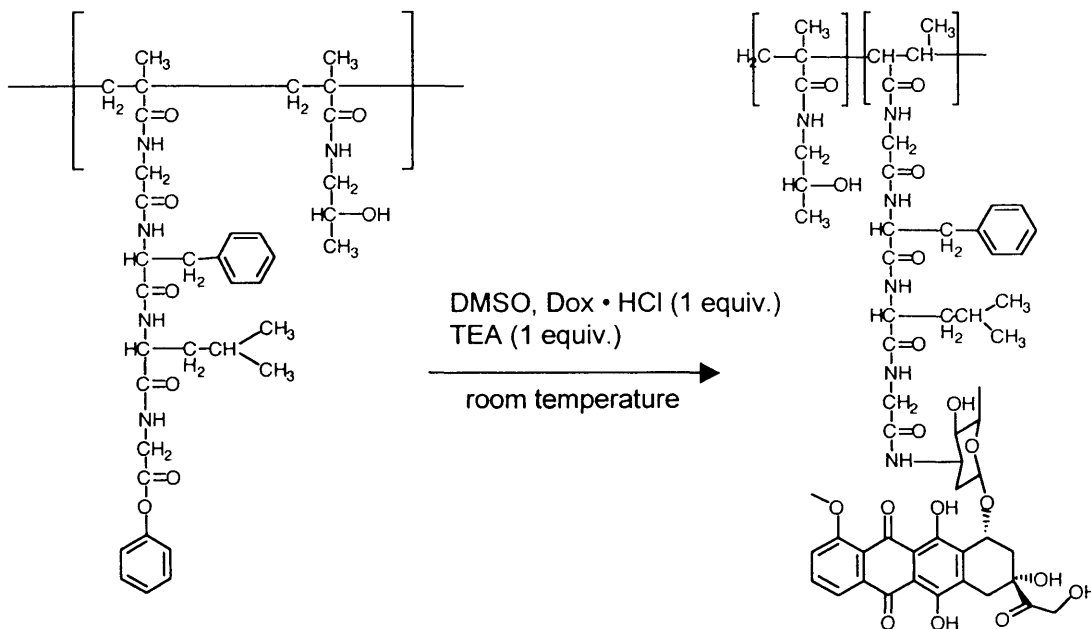


Fig. 2.1. Aminolysis reaction

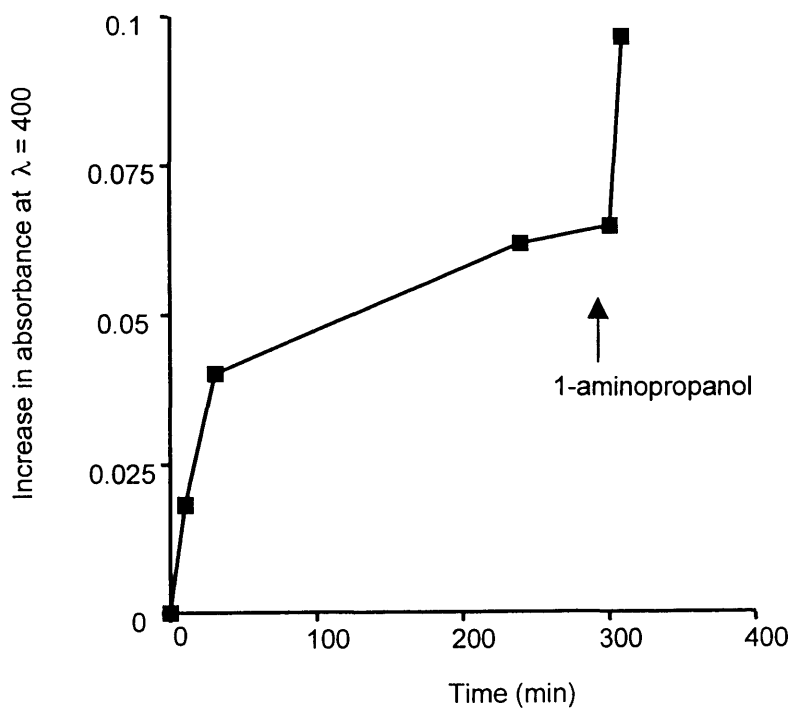


Fig. 2.2. Monitoring the aminolysis reaction by UV (release of ONp)

2.3.4. Determination of total and free Dox by HPLC

Total Dox. This procedure is schematically summarised in Fig. 2.3. Aqueous solutions of HPMA copolymer conjugates (1 mg/mL) were prepared. An aliquot (100 μ L) was transferred into a polypropylene tube, 100 μ L of an aqueous solution of daunomycin (1 μ g/mL; used as internal standard) were added and the volume was then made up to 1 mL with water. Then 1 mL of 2 M HCl was added and the tubes were heated at 80 °C for 30 min in order to obtain Dox aglycone. After cooling down to room temperature, 1 mL of 2 M NaOH was added and the pH of the samples was adjusted to 8.5 with ammonium formate buffer (150 μ L, 1 M, pH 8.5). Then, a mixture of HPLC grade chloroform : propan-2-ol at a ratio of 4 : 1 (5 mL) was added. Samples were then thoroughly extracted by vortexing (3 x 30 s). The upper aqueous layer was carefully removed and the solvent was evaporated under N₂. The dry residue was re-dissolved in 100 μ L of HPLC grade methanol. In parallel the same procedure was carried out for the standard (i.e. the free drug (Dox)) using 100 μ L of a 1 mg/mL stock aqueous solution. Addition of 1 mL of methanol to re-dissolve the product gave a 100 μ g/mL stock from which a range of concentrations were prepared (2 to 60 μ g/mL) in order to obtain a calibration curve (Fig. 2.4). The mobile phase was 29 % propan-2-ol in ddH₂O, to which orthophosphoric acid was added to reach a pH of 3.2 (flow rate 1 mL/min) total run 12 min. The columns used were Guard-PAK™ μ Bondpak™C18 Modul; analytical μ Bondpak™C18 (150 x 3.9 mm) Stainless Steel. To monitor Dox and daunomycin aglycones, a Fluoromonitor III fitted with interference filters at 485 nm for excitation and 560 nm for emission was used. The retention times were 4.3 min for Dox aglycone and 6.7 min for daunomycin aglycone.

Free Dox. This procedure is schematically summarised in Fig. 2.3. Aqueous solutions of HPMA copolymer-AGM \pm Dox conjugates (1 mg/mL) were prepared, and an aliquot (200 μ L) was added to a polypropylene tube. 100 μ L of a solution of a 1 μ g/mL aqueous solution of daunomycin (used as internal standard) were added and the volume was then made up to 1 mL with water. The extraction procedure was as described above. A stock solution of 10 μ g/mL Dox was used as standard (Fig. 2.4). HPLC conditions as described above. The retention times were 2.8 min for free Dox and 3.9 min for free daunomycin.

EXTRACTION OF FREE AND TOTAL DOX

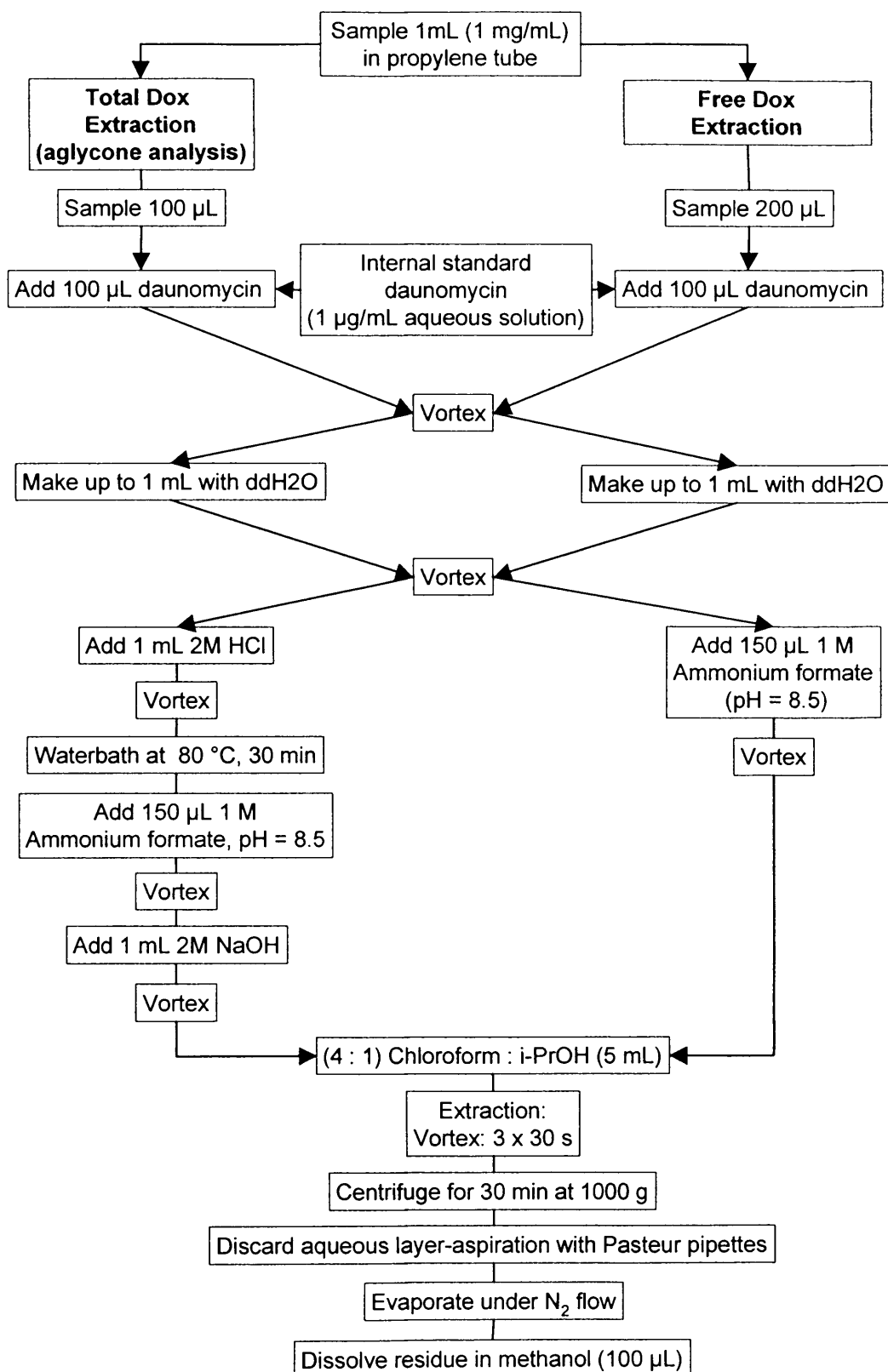


Fig. 2.3. Scheme of the extraction procedure used to determine free and total Dox with HPLC

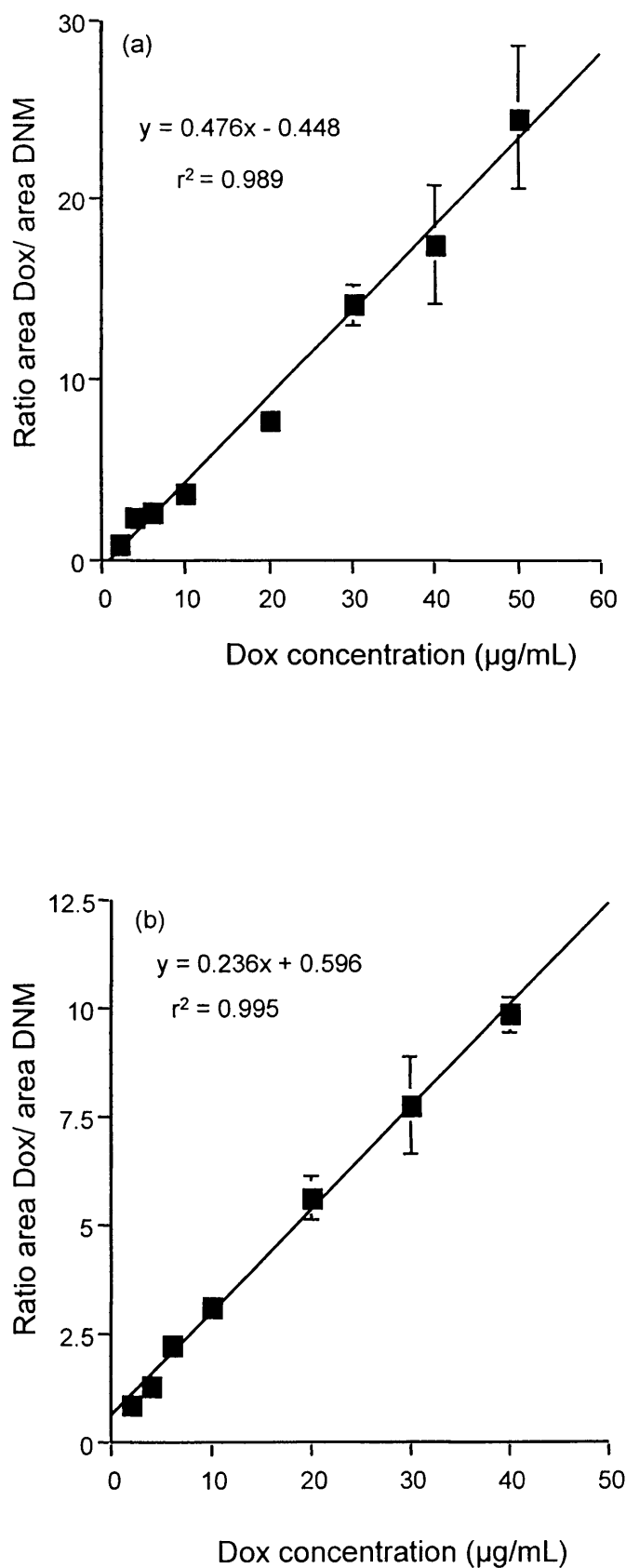


Fig. 2.4. Quantification of free and total Dox by HPLC. Calibration curve of Dox aglycone (panel a) and of free Dox (panel b). Data represent mean \pm S.E.M., $n = 3$

2.3.5. Characterisation of HPMA copolymers by GPC

HPMA copolymers were analysed using aqueous phase GPC. Polysaccharide standards (pullulan) (M_w from 11800 to 210000 g/mol) were used to produce a calibration curve (Fig. 2.5). All samples were prepared in PBS (3 mg/mL), filtered (0.2 μ m) and approximately 80 μ L were injected (injection loop 20 μ L). PBS was used as mobile phase (flow rate 1.0 mL/min). RI detection was used.

2.3.6. General cell culture

Cell culture was performed according to the guidelines given by The United Kingdom Co-ordinating Committee on Cancer Research (UKCCCR) (UKCCR, 2000). To preserve the sterile environment of the incubator and of the safety cabinets all the equipment was sprayed with 70 % ethanol (v/v in water).

2.3.6.1. Defrosting cells

Cells were grown from frozen stock vials (containing 1 mL of cells suspension) by warming the vial to 37 °C in a water bath. The thawed suspension was collected in a universal container and 9 mL of RPMI 1640 with 20 % FBS were added. Cells were centrifuged at room temperature for 5 min at 243 g, the supernatant was aspirated and cells were resuspended in 5 mL of RPMI 1640 with 5 % FBS (10 % for B16F10). The whole suspension was then put in the incubator in a 25 cm² flask. After 24 h medium was replaced with fresh medium and cells were then allowed to grow and passaged when confluency was reached.

2.3.6.2. Cell maintenance and passaging

MCF-7, MCF-7ca and B16F10 were grown in vented 75 cm² tissue culture flasks in RPMI 1640 (with L-glutamine) supplemented with 5 % FBS (10 % for B16F10) at 37 °C in humidified atmosphere with 5 % CO₂ (MCF-7ca were further supplemented with geneticin in order to maintain the transfected strain (15 μ L of a 50 mg/mL solution). Cells were passaged as described below when 70 - 90 % confluency was reached. Old medium was removed by aspiration and cells were washed with 10 mL of sterile PBS in order to remove dead cells and any residual medium. Trypsin EDTA solution was added (1 mL) and cells were incubated with it for approximately 3-5 min (until detached). Fresh medium (10 mL) was added and the cell suspension was collected in a universal container and centrifuged for 5 min at 243 g at room

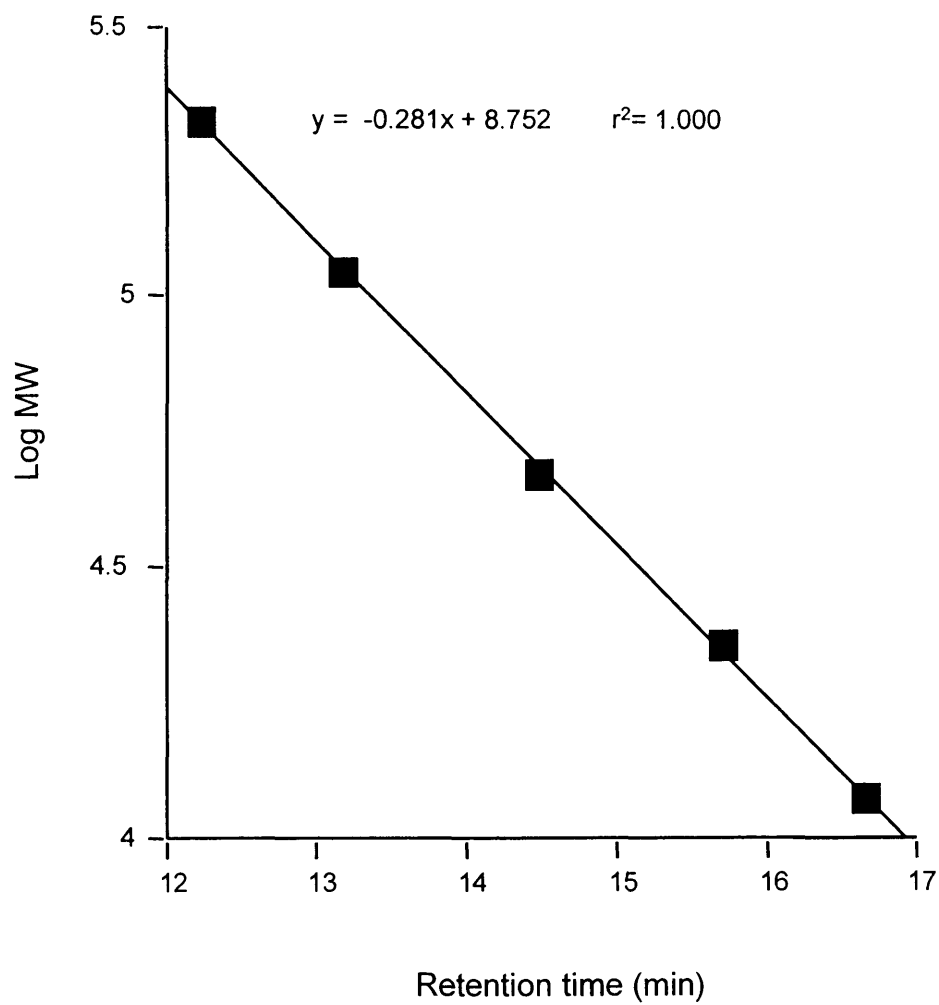


Fig. 2.5. Typical GPC calibration curve for polysaccharide standards

temperature. The supernatant was removed and the cells were resuspended in fresh medium. New flasks were prepared from this suspension after a 1 : 10 dilution. It is important to underline that experiments on B16F10 were carried out in medium having the same composition as the culturing medium (i.e. RPMI 1640 + 10 % FBS). In the case of MCF-7 and MCF-7ca cells, RPMI 1640 without the pH indicator was used in all the experiment as phenol red has mitogenic activity (Devleeschouwer et al., 1992) and might therefore interfere with oestrogen signalling pathways. The growth of MCF-7 is highly influenced by the presence or absence of oestradiol. Consequently, the presence of steroids in the serum was controlled by using charcoal-stripped FBS (SFBS). If the presence of steroids was required WRPMI + 5% SFBS + the desired steroid concentration was used. Cell culturing conditions are summarised in Table 2.3.

2.3.6.3. Counting and seeding cells

Cells were washed with PBS, trypsinised, and resuspended in medium as described above. In order to obtain a homogenous suspension of single cells, cells were passed through a needle (23 G). An aliquot of the suspension (100 μ L) was removed and diluted with an equal volume of trypan blue (0.2 % trypan blue in PBS). After 1 min, the cells suspension was placed into a haemocytometer. Cells from ten 0.1 mm³ squares (five from the top and five from the bottom chamber of the haemocytometer) were counted. Non-viable cells (stained with trypan blue) were excluded. Cell concentration was then determined using the following formula:

$$\text{cells/mL} = \text{mean} \times 2 \times 10^4$$

Where: mean is the arithmetic mean of the 10 values
 2 takes into account of the trypan blue dilution
 10⁴ accounts for the conversion from 0.1 mm³ to mL

The cells suspension was then diluted with medium in order to obtain the appropriate seeding density needed for the experiment.

2.3.6.4. Freezing cells

Cells were periodically frozen to maintain a stock. Cells were trypsinised and an aliquot of the cell suspension was analysed to quantify the amount of cells as

Table 2.3. Cell culture conditions for the different cell lines used

Cell line	Origin	Medium		Frequency of splitting			Freezing medium
		(a) for maintenance	(b) for experiments	(a)	(b)	(c)	
MCF-7	human breast carcinoma	(a) RPMI 1640 + 5% FBS		(a) once a week		90% FBS	
		(b) RPMI 1640 without phenol red + 5% SFCS *		(b) 3/4 days		10% DMSO	
				(c) 1:10			
MCF-7ca	human breast carcinoma	(a) RPMI 1640 + 5% FBS #		(a) once a week		90% FBS	
		(b) RPMI 1640 without phenol red + 5% SFCS * #		(b) 3/4 days		10% DMSO	
				(c) 1:10			
B16F10	murine melanoma	(a) RPMI 1640 + 10% FBS		(a) twice a week		90% FBS	
				(b) 3/4 days		10% DMSO	
				(c) 1:10			

*± steroids at the concentrations stated in each experiment
supplemented with 15 µL of geneticin

described in section 2.3.1.2. The cells were centrifuged, the supernatant was removed and the pellet resuspended in the appropriate volume of freezing medium (90 % serum + 10 % sterile DMSO) to obtain the concentration of 10^6 cells/mL. Aliquots (1 mL) of this suspension were then transferred into sterile cryogenic vials. To obtain a slow freezing (approximately 1 °C/min) vials were wrapped in tissue paper and placed at – 20 °C for 1 h and then at – 80 °C overnight. Finally, vials were transferred to liquid nitrogen and stored there until use.

2.3.6.5. Preparation of SFBS

FBS (500 mL) was adjusted to pH 4.2 with hydrochloric acid 5 M and equilibrated to 4 °C. A charcoal suspension was prepared adding 18 mL of ddH₂O, 0.2 g of Norit A charcoal and 0.01 g of dextran T-70. An aliquot (25 mL) of this suspension was then added to the cold PBS. The suspension was stirred for 16 h at 4 °C. Then, it was centrifuged (40 min at 12000 g) and the charcoal was removed by coarse filtration. The pH was re-adjusted to 7.2 with sodium hydroxide 5 M, and the SFBS obtained was sterile-filtered with millipore filters 0.2 µm and stored in universal containers at –20 °C.

2.3.7. Counting cells with the Coulter counter: growth curve for MCF-7

Coulter counter is an instrument routinely used to count the number and the size of particles in suspension. A known volume of suspension is sucked by a pump and forced to pass through a small hole in a tube. Two electrodes are placed inside and outside the tube in order to measure variations of the electrical impedance caused by the passage of the particles in suspension through the hole (Fig. 2.6). The number of cells can thus be determined. After trypsination (section 2.3.1.2.), cell suspension (100 µL) was transferred to a Coulter counter vial containing 10 mL of isotonic solution. The number of cells contained in the sample was then determined. Cells were diluted to obtain 4×10^4 cells/mL, seeded in a 24 well plate and allowed to adhere for 24 h. The medium was removed and replaced with fresh medium. To test the influence of oestradiol on cell growth, two different types of medium were prepared. One, referred to as oestradiol medium, was prepared by adding 5 µL of oestradiol solution (stock solution in ethanol at 10^{-5} M) to 50 mL of medium (final concentration of oestradiol, 10^{-9} M). The other (control medium) was prepared

(a)



(b)

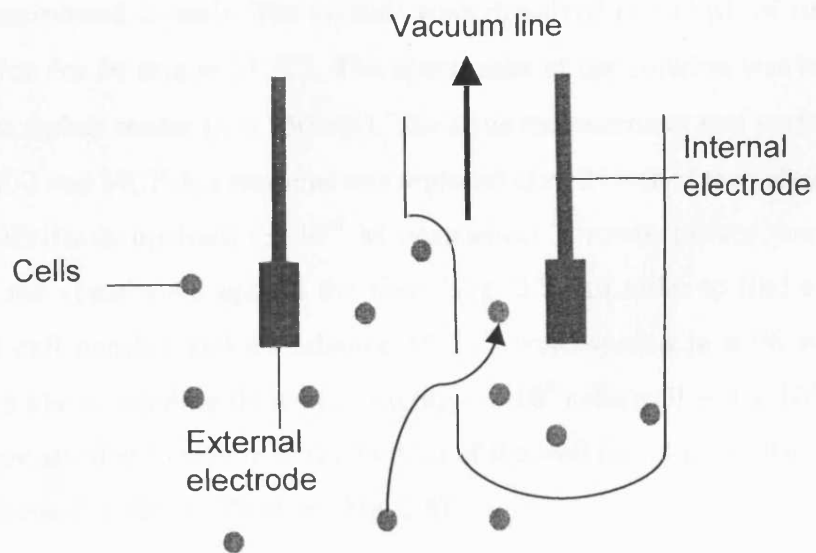


Fig. 2.6. The Coulter counter. Picture of the instrument (panel a) and the schematic representation of the counting system (panel b)

dissolving 5 μL of ethanol in 50 mL of medium. The medium was replaced every 3 - 4 days and cells were counted with the Coulter counter on day 1, 4, 6, 8, 11, 13. To count cells, the medium was removed from the well and 1 mL of trypsin was added. Trypsinised cells were collected in a Coulter counter vial containing 6 mL of isotonic solution. The well was then washed (3 x 1 mL) with isotonic solution and the washings were added to the Coulter counter vial to achieve a final volume of 10 mL. The cell suspension obtained was then counted. Growth curves were produced plotting cell number against the time (Fig. 2.7).

2.3.8. MTT assay as means to assess cell viability: growth curve

The MTT assay, introduced by Mosmann (1983) is a method used to assess cell viability. In viable cells, a yellow solution of the substrate (MTT 5 mg/mL in PBS) is reduced into blue insoluble crystals after a REDOX reaction with mitochondrial respiration products NADH and NADPH (Fig. 2.8) (Denizot and Lang, 1986; Sgouras and Duncan, 1990; Twentyman and Luscombe, 1987; Vistica et al., 1991). MCF-7, MCF-7ca and B16F10 were seeded in 96 well plates (4×10^4 , 4×10^4 , 10^4 cells/mL, respectively) and allowed to adhere for 24 h. MTT sterile filtered solution (20 μL) was added to each well and the reaction was allowed to proceed for 5 h at 37 °C. The solution of MTT and medium was then removed carefully avoiding removal of the precipitated crystals. The crystals were dissolved in 100 μL of sterile DMSO (incubation for 30 min at 37 °C). The absorbance of the solution was read in a UV absorbance plate reader ($\lambda = 550 \text{ nm}$). The same measurement was performed daily. For MCF-7 and MCF-7ca medium was replaced after 24 h (and then after every 3 - 4 days) with fresh medium ($\pm 10^{-9} \text{ M}$ oestradiol). Growth curves were produced plotting the absorbance against the time (Fig. 2.7). In order to find a correlation between cell number and absorbance MCF-7 were seeded in a 96 well plate as described above (seeding densities ranging 4×10^3 cells/well \div 4×10^4 cells/well). Cells were allowed to adhere to the bottom of the well for 24 h and then MTT assay was performed on the whole plate (Fig. 2.8).

2.3.9. Evaluation of cytotoxicity using the MTT assay

The MTT assay (as described in the previous section) was also used to establish the cytotoxicity of antitumour drugs and of HPMA copolymer-conjugates. To be able

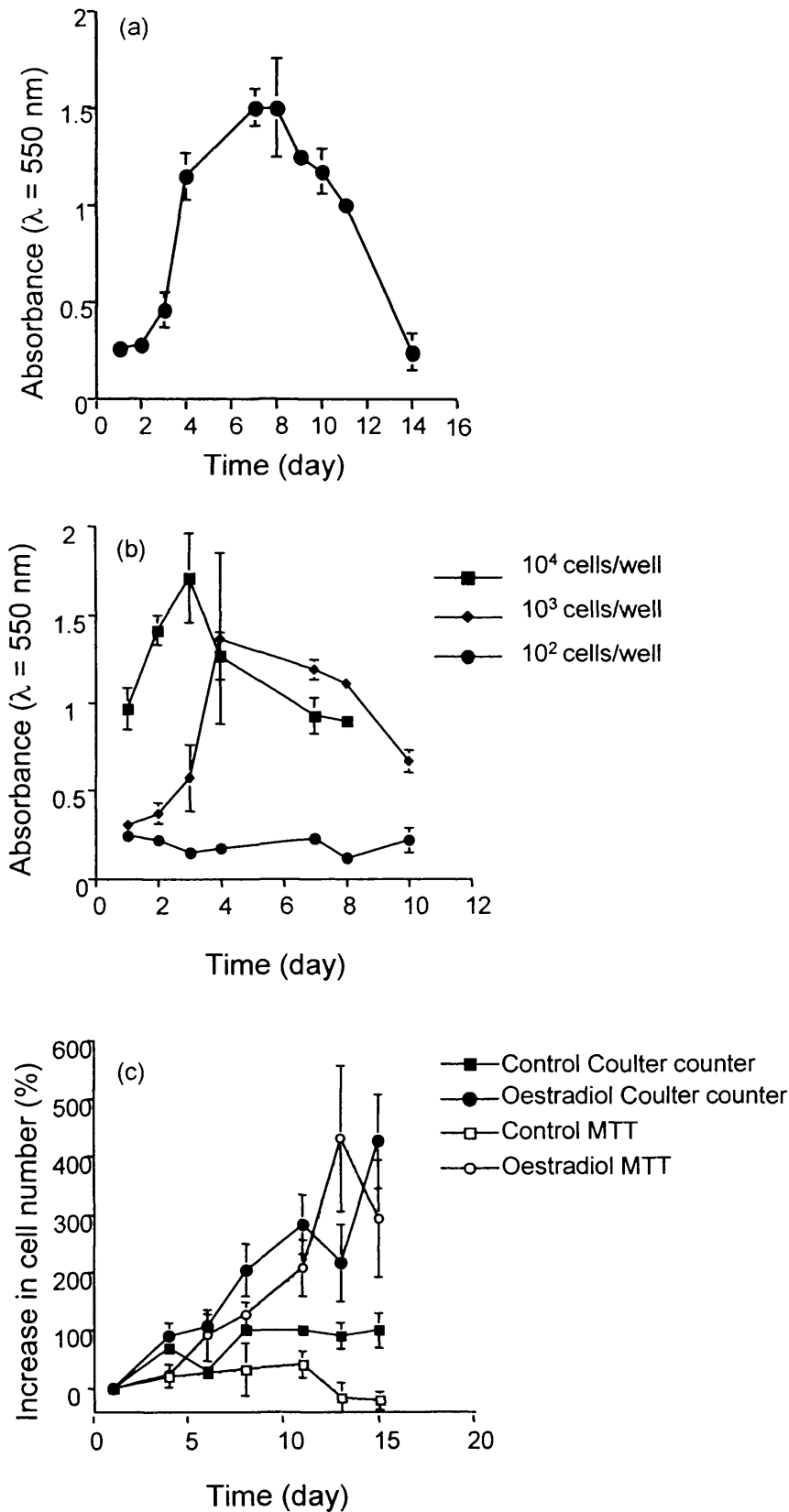


Fig. 2.7. Growth curves of B16F10 and MCF-7 cells. Panel (a) shows the growth of B16F10 at a seeding density of 10^3 cells / well; data represent mean \pm S.D., $n = 6$. Panel (b) shows the growth of B16F10 seeded at 10^2 , 10^3 or 10^4 cells / well; data show mean \pm S.D., $n = 6$. Panel (c) shows the growth curve of MCF-7 in presence and absence of oestradiol measured with the Coulter counter or with the MTT assay; data show mean \pm S.D., $n = 3$ for Coulter counter and $n = 6$ for MTT assay

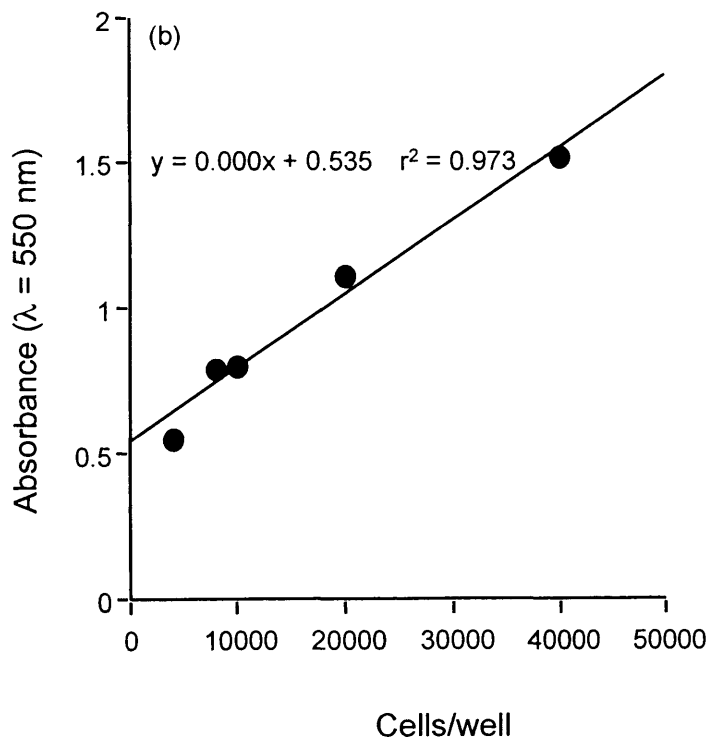
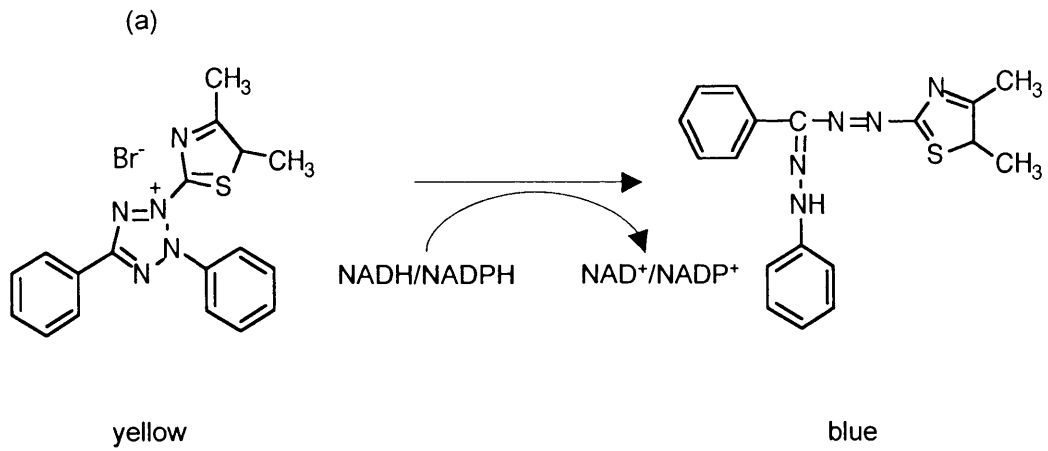


Fig. 2.8. Mechanism of action of MTT assay (panel a) and correlation between cell number and absorbance in MTT assay (panel b). In panel b data show mean \pm S.E.M., $n = 12$. When error bars are not visible they are hidden by the symbol

to see cytotoxic effects, it is important that cells are incubated with the drug while they are in exponential growing phase. MCF-7 and MCF-7ca cells were seeded in a 96-well plate (4×10^4 cells/mL; $100 \mu\text{L}$ cell suspension/well) in WRPMI supplemented with 5 % SFBS and allowed to adhere for 24 h. The medium was then replaced with fresh medium (either control medium or oestradiol-supplemented (10^{-9} M) medium). On day 5, the medium was replaced with a solution of the drug in medium (fresh medium only was used for control wells) and cells were incubated for 67 h. In this way, cells were incubated for 72 h with the compounds whilst in their exponential growing phase (day 5 to day 8). Then, MTT solution ($20 \mu\text{L}$; 5 mg/mL in PBS) was added. After 72 h the solution was removed, the crystals were dissolved in optical grade DMSO (30 min at 37°C) and the UV absorbance was measured ($\lambda = 550 \text{ nm}$).

Results were expressed as percentage viability of the control cells, according to the following formula:

$$\text{Cell viability (\%)} = \text{Abs}_{550\text{a}} \times 100 / \text{Abs}_{550\text{c}}$$

Where: $\text{Abs}_{550\text{a}}$ = absorbance measured for the compound at a certain concentration.

$\text{Abs}_{550\text{c}}$ = absorbance measured for the control cells.

2.3.10. Determination of the effect of androstenedione/testosterone on the growth of MCF-7 and MCF-7ca

In this experiment the effect of the substrates of aromatase (androstenedione and testosterone) on the growth of MCF-7 and MCF-7ca was investigated. Both cell lines were seeded as described previously (section 2.3.6.3) at a seeding density of 4×10^4 cells/mL in medium deprived of steroids (WRPMI + 5 % SFBS) and allowed to adhere for 24 h. The medium was then replaced with fresh medium containing different concentrations of androstenedione ($10^{-6} \div 10^{-11}$ M) and of testosterone ($10^{-6} \div 10^{-11}$ M). The medium was changed every 3 - 4 days and cell growth was measured on day 8 and on day 11 with MTT assay. Medium containing androstenedione and testosterone was prepared diluting stock medium of androstenedione and testosterone (10^{-2} M in ethanol) to achieve the final concentration desired. Therefore, control

medium contained an equivalent amount of ethanol. Data were presented according to the following formula:

$$\text{Cell growth (\% of control)} = A_{550\text{and or test}} \times 100 / A_{550\text{cont}}$$

Where: $A_{550\text{and or test}}$ = average absorbance obtained in presence of a given concentration of androstenedione or testosterone.

A_{550c} = average absorbance obtained for the control.

2.3.11. Effect of AGM (free and polymer-bound) on the mitogenic properties of androstenedione

MCF-7ca cells were seeded in 96 well plates as described in section 2.3.6.3. at a seeding density of 4×10^4 cells/mL in medium deprived of steroids (WRPMI + 5 % SFBS) and allowed to adhere for 24 h. Medium was then replaced with fresh medium containing:

- a) WRPMI + 5 % SFBS + ethanol
- b) WRPMI + 5 % SFBS + 5×10^{-8} M androstenedione
- c) WRPMI + 5 % SFBS + 5×10^{-8} M androstenedione + free or polymer bound AGM (0.1 – 0.8 mg/mL AGM eq.).

The cells were then allowed to grow under standard tissue culture conditions for 11 days when MTT assay was performed to assess cell growth. Old medium was replaced with fresh medium every 3 - 4 days.

2.3.12. Radiometric evaluation of isolated aromatase activity using placental microsomes

The isolated placental enzymes used in this assay were kindly provided by Dr. Claire Simons at the Welsh School of Pharmacy, Cardiff, UK.

Preparation of [^3H]androstenedione solution. 50 μL of 0.5 mM androstenedione in EtOH was diluted to 1 mL with iPrOH : EtOH 1 : 1 v/v to give a 0.025 mM stock solution. To this 35 μL of [^3H]androstenedione (37 Mbq/mL) was added.

Procedure. The substrate androstenedione was prepared from a mixture of labelled [^3H]androstenedione and non-labelled substrate as described above. Frozen placental microsomes were thawed under cold running water prior to the incubation and used

immediately. AGM solutions were prepared in ethanol and were added to the incubation mixture in a volume of 10 μL . It was more convenient (save in material and more practical) to prepare the polymer conjugate solutions directly in the 420 μL of PBS. The final mixture contained the inhibitors (10 μL of ethanol), substrate (10 μL = 0.0125 MBq), NADPH (50 μL , 0.16 mmol/L), 50 mM PBS, pH = 7.4 (420 μL) and placental microsomes (10 μL , final protein concentration 0.26 mg/mL). In control tubes, 10 μL ethanol was substituted for the inhibitors. Determinations were conducted in duplicate. Following the addition of the microsomal suspension the tubes were shaken with a vortex to ensure the thorough mixing. Incubations (15 min) were carried out in a shaking water bath at 37 °C. The reaction was then terminated by mixing the incubation mixture with a solution of mercuric chloride (0.1 mM, 300 μL), that combines with sulphhydryl groups on the enzyme leading to deactivation. Activated charcoal (1 %, 900 μL) was then added to remove residual substrate. The charcoal was separated by centrifugation (at 1638 g for 15 min) leaving the tritiated water in the supernatant. An aliquot (1 mL) of the supernatant was removed and transferred to counting vials containing scintillation fluid (2 mL, OptiPhase “HiSafe 3”), mixed thoroughly with vortex. The [^3H]H $_2\text{O}$ formed was counted on a liquid scintillation counter to determine the extent of aromatisation. The activity recorded was assumed to be a direct measurement of the production of oestrogens.

2.3.13. Radiometric assay of aromatase activity in cells

Three days before the experiment, cells were deprived of oestrogens by replacing the old medium with fresh steroid-free medium (WRPMI + 5 % SFBS). MCF-7ca were seeded into a 6 well plate (3 x 10⁵ cells/mL) and allowed to adhere for 24 h. Old medium was removed and replaced with fresh medium (0.5 mL) containing 15 μL of the [^3H]androstenedione solution (described in section 2.3.12) and different concentrations of free and polymer bound AGM (0.1 - 0.8 mg/mL AGM eq; control wells AGM = 0 mg/mL). Cells were then incubated at 37 °C for 2 h. Then, the medium was transferred to a glass tube, 0.5 mL of water were added, 1 % aqueous formic acid (0.3 mL) was also added and the mixture was vortexed briefly to quench the reaction (protein inactivation). Chloroform (2 mL) was then added to remove un-reacted steroids. The two phases were allowed to separate and an aliquot (1 mL) from the top (aqueous) phase was transferred into a clean glass tube. Aqueous charcoal suspension (1 mL, 1 % charcoal in ddH $_2\text{O}$) was then added and the mixture,

after being vortexed, was centrifuged (15 min, 1638 g). The supernatant liquid (1 mL) was placed in a scintillation vial to which 2 mL of scintillation fluid (OptiPhase “HiSafe 3”) was added. The [³H]H₂O contained in each vial was then determined using a scintillation counter.

2.3.14. Cell lysis for protein extraction

The MCF-7 and MCF-7ca cells were seeded as described in section 2.3.6.3 in 60 mm Petri dishes in WRPMI + 5 % SFBS (5 X 10⁵ cells per dish). Cells were grown under standard culturing condition until approximately 80 % of confluency was reached. Proteases inhibitors were added to the lysis buffer, to prevent protein degradation (see Table 2.1). The buffer prepared was then kept on ice until use. Medium was aspirated from the dishes and cells were washed with warm PBS three times. Then approximately 175 μL of lysis buffer were added to each dish (checking that the whole surface was covered) and cells were placed on ice. Cells were scraped with a cell scraper, coarsely mixed with a pipette and the suspension was collected in a 1.5 mL eppendorf. No more than 4 dishes were processed per time. Cells were then spun down in a pre-cooled centrifuge (15 min 15800 g 4 °C). Supernatant was aliquoted (50 μL aliquots) and stored at – 20 °C until use. Protein content was determined using the Lowry assay as described in the following section.

2.3.15. Quantification of the protein content: Lowry assay

To quantify the amount of proteins, the DC protein assay (from BIO RAD) was used. This assay is a colorimetric method based on a modification of the Lowry assay. It is based on the reaction that occurs between protein, an alkaline copper tartrate solution and Folin reagent. The latter is reduced by several amino acids (primarily tyrosine and tryptophan) to metabolites that have a blue colour (maximum absorbance at 750 nm). Bovine serum albumin (BSA) standards (1.45 mg/mL kept as stock at –20 °C) were used to build a calibration curve (diluted to a final volume of 50 μL with lysis buffer to obtain concentrations ranging 1.45 ÷ 0.25 μg/mL). A sample containing 50 μL of lysis buffer was used as a blank. For the samples, an aliquot (10 μL) of the cell lysate was diluted to 50 μL with lysis buffer and was processed in parallel with the standards. The kit provided by BIO RAD was used. A solution was made mixing Reagent A (250 μL per sample to be analysed) with substrate S (20 μL per sample). An aliquot (250 μL) of the solution obtained was

added to each sample. Then, 2 mL of reagent B were added to all samples. The solution was allowed to react for approximately 15 min to obtain the development of the colour. Standards and samples absorbance was read at a spectrophotometer ($\lambda = 750$ nm). The protein concentration in the sample was then extrapolated from the calibration curve.

2.3.16. Detection of aromatase enzyme in MCF-7 and MCF-7ca by Western blot

SDS-PAGE. SDS-PAGE apparatus was assembled. The lower gel was prepared (Table 2.2) and gently pipetted into the chamber formed by the two glasses. A small amount (200 μ L) of H₂O was applied on top of the gel to obtain a smoother border. The gel was then left to set for approximately 15 min. Stacking gel was then prepared (Table 2.2), the water was removed from the lower gel and the upper gel was then pipetted above it. Combs were then gently pushed in the upper gel to create the wells that would host the sample. The gel was allowed to set for approximately 20 minutes. The appropriate volume of protein (80, 60, 40 or 20 μ g) was placed in an eppendorf and an equivalent volume of 2 x loading buffer (Table 2.2) was added. Samples were then heated for 10 min at 100 °C. The combs were removed, the running apparatus was assembled and its middle section was filled with running buffer (Table 2.2). Samples were loaded using the appropriate tip in each well (rainbow proteins were loaded in the first lane). The apparatus was then connected to power and run at 150 V for ~ 1 h.

Western blotting. The transfer buffer was prepared (Table 2.2). Four pieces of filter paper, two of nitrocellulose and four sponges were soaked in this buffer. The blot was assembled in this order: black side of plastic housing, sponge, filter paper, gel, nitrocellulose, filter paper, sponge, clear side of plastic housing. The tank was filled with transfer buffer, an ice block and a stirring magnet. Cartridges were inserted and the system was run at 100 V for 1 h. The blot was then blocked for 1 h under gentle agitation in milk (5 % in tris-buffered saline (TBS) tween). The milk was removed and a solution of the primary antibody was added (1 mL western block reagent, 19 mL TBS tween, 200 μ L NaN₃ and 20 μ L antibody) for 2-3 h. For the detection of aromatase a mouse anti human cytochrome P450 aromatase was used (Turner et al., 2002). The blot was then washed with TBS tween (Table 2.2) (3 x 20 mL x 5 min) and incubated with the secondary antibody (antimouse, 2 μ L in 20 mL

of TBS tween) for 1 h. Then, washings with TBS tween were performed (5 x 20 mL x 5 min). The blot was developed with chemiluminescent substrate.

2.3.17. Determination of the cellular uptake of polymer conjugates by flow cytometry

Flow cytometry was used to assess the uptake of polymer conjugates by MCF-7 and MCF-7ca cells using the inherent fluorescence of Dox as marker. Cells were seeded in 6 well plates (1×10^6 cells/mL) in WRPMI + 5 % SFBS and allowed to adhere for 24 h. The experiment was performed at 37 °C and at 4 °C (to account for the external binding). Polymer solutions were prepared in medium and equilibrated to 37 °C or 4 °C. For the 37 °C condition, cells were kept under cell culture condition for the incubation period. For the 4 °C experiment, cells were placed on ice 30 min prior the addition of the polymer. HPMA copolymer-Dox conjugate was added at a concentration of 0.1 mg/mL in medium (≈ 0.01 mM Dox-equiv.). For HPMA copolymer-AGM-Dox conjugate the concentration of the polymer was adjusted to achieve an equivalent concentration of fluorophore (Dox). Cells were then incubated for times up to 60 min at 37 °C or 4 °C. At the end of the incubation period, the plates were placed on ice to prevent further uptake and kept at 4 °C. The cells were washed three times with ice-chilled PBS (3 x 5 mL). Then PBS (1 mL) was added and cells were scraped from the plate, collected in falcon tubes and centrifuged at 4 °C, 600 x g for 5 min. Finally, cells were re-suspended in ice-chilled PBS (200 μ L) and analysed using Becton Dickinson FACSCalibur cytometer (California, USA) equipped with an argon laser (488 nm) and emission filter for 550 nm. Data were collected with 25,000 events per sample and processed using CELLQuest™ version 3.3 software. Control cells (incubated with medium only) were used in all cases to account for background fluorescence output. Data was acquired in 1024 channels with band pass filter FL2 (585 nm \pm 42 nm).

2.3.18. Analysis of flow cytometry data

To best interpret the flow cytometry data, several options were taken into account. Increase in the fluorescence of the cell population can be estimated considering two different parameters. First of all, one can consider the increase in the average fluorescence of the population. The mean, the geometric mean and the median are the 3 different variables that can be used for this. Otherwise, the

increased number of cells taking up the fluorescently labelled compound can be used. In this second case, it is first necessary to define a population of non-fluorescent cells (negative) to account for background fluorescence. Two regions were therefore arbitrarily set (Fig. 2.9). Region M1 was arbitrarily defined as the region covering 98 % of the events in the control population. M2 covered any area at higher fluorescence than M1. Obviously, an increased number of fluorescence-associated cells would lead to an increased number of events in the M2 region. As the geometric mean of log data corresponds to the median of the linear data, it was decided that presenting the data as the geometric mean of the entire population was the best way to mirror the variation in fluorescence of the whole population.

2.4. STATISTICAL ANALYSIS

Data are expressed as mean \pm Standard Error of the Mean (S.E.M.), unless otherwise stated. Statistical significance was set at $p < 0.05$ (indicated with *). When only two groups were compared, Student's t test for small sample size was used. If more than two groups were compared evaluation of significance was performed using one way - Analysis Of Variance (ANOVA) followed by Bonferroni *post hoc* test.

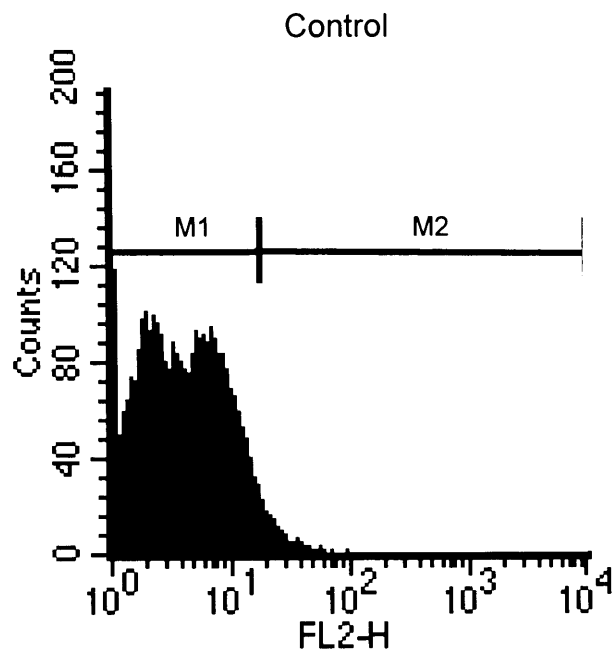


Fig. 2.9. Setting the M1 and M2 region for the interpretation of the data of flow cytometry

Chapter 3:

Synthesis and Characterisation of HPMA copolymer-AGM \pm Dox
Conjugates

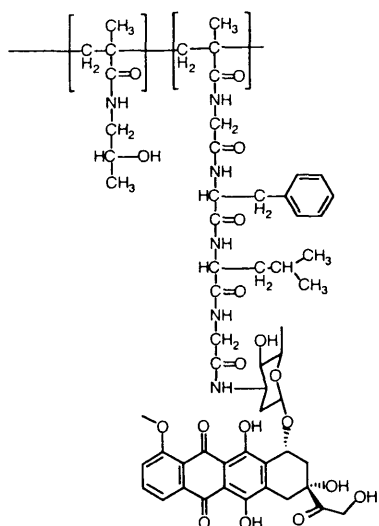
3.1. INTRODUCTION

At the beginning of this project it was important to synthesise and characterise the conjugates carrying both endocrine therapy (AGM) and chemotherapy (Dox). Several issues were considered before starting, particularly the choice of the polymeric carrier and the choice of the drugs to be used as the first model compounds. The chemical approach to be used for synthesis was also considered, and thought was given to the linkers that might be used for creation of optimal drug conjugates.

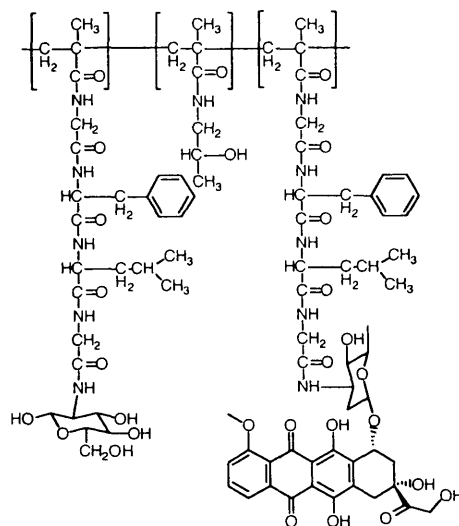
The general aim of this project was to investigate the potential advantage of combining endocrine and chemotherapy on the same polymeric carrier. Thus, it was decided to avoid using experimental polymers and architectures whose biological behaviour is not yet understood as this would be an extra-variable in the system. Only four polymeric carriers have been used to prepare the polymer-anticancer drug conjugates being tested clinically. These are HPMA copolymers, PGA, PEG and oxidised dextran (Fig. 3.1). The wealth of literature available on HPMA copolymers and the history of their use in our group made them ideal candidates for this project (reviewed in Duncan 2005). HPMA copolymers have proven safe both in animal models (Duncan et al., 1992; Duncan et al., 1998), and in humans (Meerum Terwogt et al., 2001; Schoemaker et al., 2002; Vasey et al., 1999; Seymour et al., 2002; also reviewed in Duncan, 2005). Of the six HPMA copolymer drug conjugates transferred into clinical trials (HPMA copolymer-Dox, HPMA copolymer-Dox-galactosamine, HPMA copolymer-paclitaxel, HPMA copolymer-camptothecin and HPMA copolymer platinates) (Fig. 3.1) none showed evidence of polymer-related toxicity (reviewed in Duncan 2003b). Even more interestingly for this project, HPMA copolymer-Dox has already shown activity in breast cancer (Vasey et al., 1999; Cassidy, 2000).

The choice of an appropriate linker is another vital parameter for a rational design of polymer-drug conjugates. Whilst stable in the bloodstream, the linker must be degradable when the site of action is reached. Several linkers have been explored, most importantly, peptidyl (Duncan et al., 1980) and ester linkers have been used to synthesise those polymer-drug conjugates transferred into clinical trials (reviewed in Brocchini and Duncan, 1999). Despite the successful use of an ester linkage to

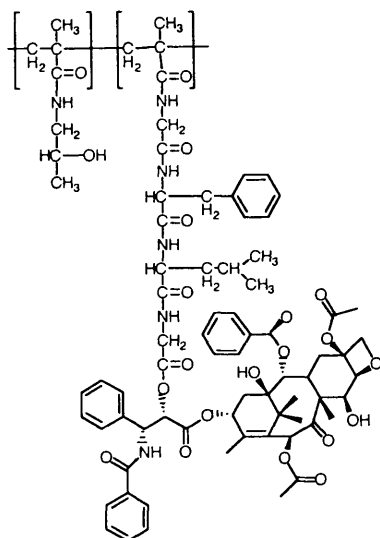
(a) HPMA copolymer-Dox,
PK1, FCE28068



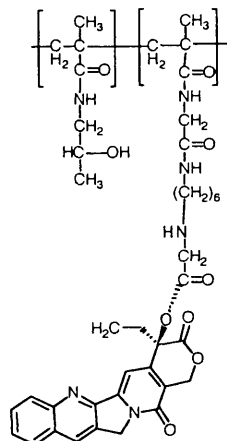
(b) HPMA copolymer-Dox-galactosamine,
PK2, FCE28069



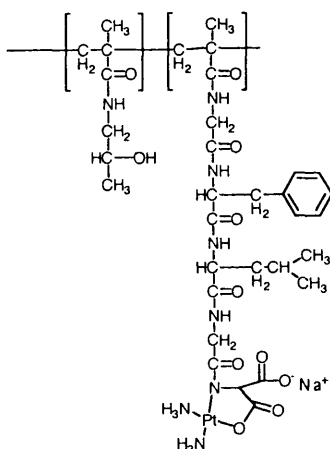
(c) HPMA copolymer-paclitaxel
PNU166954



(d) HPMA copolymer-camptothecin
MAG-CPT, PNU166148



(e) HPMA copolymer-platinite
AP5280



(f) HPMA copolymer-platinite
AP5346

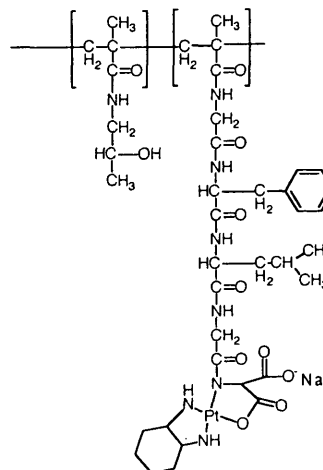
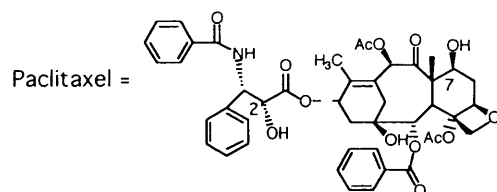
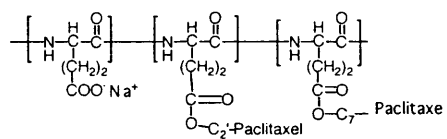


Fig. 3.1. Examples of chemical structure of the polymer conjugates that have undergone clinical evaluation

(g) Polyglutamate-paclitaxel
CT-2103, XYOTAX



(h) Polyglutamate-camptothecin
CT-2106

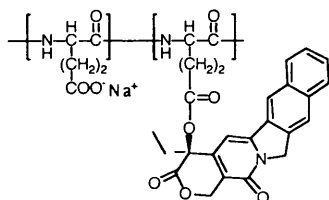


Fig. 3.1. Continued

conjugate paclitaxel to PGA, both HPMA copolymer-paclitaxel and HPMA copolymer-camptothecin showed toxicity that can, at least partially, be attributed to a premature release of the drug from the conjugate due to the susceptibility of the ester linkage to blood esterases (Schoemaker et al., 2002; reviewed in Duncan 2003b). The stability of the linker is influenced by the drug, the loading (Searle et al., 2001) and also the conformation that the conjugate has in solution, which affects the accessibility of the linker. Consequently, theoretically each case is different. However, the data presented above on the use of an ester linkage in HPMA copolymer conjugates and data reporting the stability of peptidyl linkers and their degradation by lysosomal enzymes, made the choice of a peptidyl linker a better option for this project. Therefore, the peptidyl linker GFLG degradable by the thiol-dependent protease cathepsin B (already used in the HPMA copolymer-Dox) was used. The non-biodegradable linker, GG, was also used as a control.

Once the polymeric carrier and the linker were chosen, it was necessary to identify the drugs to be used as model compounds for chemotherapy and endocrine therapy. Dox was an obvious choice as it is a first line chemotherapy treatment for breast cancer (Ellis et al., 2000b), and also as HPMA copolymer-Dox had shown activity in a Phase I study in anthracycline-resistant breast cancer (Vasey et al., 1999). Phase II clinical trials of HPMA copolymer-Dox (for colon, breast and non small cell lung cancer (NSCLC)) confirmed the activity in breast cancer as partial responses were found for this type of tumour (Cassidy, 2000; reviewed in Duncan, 2005).

The selection of the model drug for endocrine therapy was more difficult, and the rationale for choosing the aromatase inhibitor AGM has already been outlined in detail in the introduction (paragraph 1.3.1). The fact that AGM carries an amino group (Fig. 1.10) makes it an ideal candidate for conjugation to HPMA copolymers via a peptidyl linker. Moreover, as this first generation aromatase inhibitor is a relatively old drug, it was not protected by patent.

Many routes to synthesise HPMA copolymer-drug conjugates have been described (reviewed in Duncan and Kopecek, 1984; Duncan, 2005). Two main

approaches can be used to prepare conjugates where the drug is covalently bound to the polymer via a side chain:

- The drug can be incorporated into the polymer backbone during the polymerisation reaction. In this case, the drug itself or a monomeric derivative containing the drug is polymerised into the polymer backbone.
- Polymer analogous reaction. In this procedure the drug is bound to a pre-synthesised polymeric intermediate (Fig. 3.2) (reviewed in Duncan and Kopecek, 1984).

The first option has the potential disadvantage of leading to the formation of conjugates with different molecular weight as different monomers have different reactivity. This is important as a Mw lower than 40 KDa is essential for the eventual renal elimination of the polymer. Using the polymer analogous reaction it is possible to synthesise a common activated intermediate. From this, a library of HPMA copolymers can be synthesised where the Mw and Mw/Mn is the same. Consequently, the second option was selected and HPMA copolymer-ONp were used as a polymer intermediate throughout this PhD thesis. As Dox and AGM both carry an amino group, direct aminolysis exploiting the activated HPMA copolymer-ONp seemed to be an obvious option for drug conjugation as it had been previously used successfully for the synthesis of HPMA copolymer-Dox and HPMA copolymer-Dox-galactosamine. Nevertheless, the amino group of AGM is aromatic and therefore less nucleophilic. As described by Vicent et al. (2005), the use of DCC coupling produced higher loading than the aminolysis reaction, therefore this method was chosen to prepare HPMA copolymer-AGM conjugates.

Thus the general aims of this study were to reproduce the synthesis described by Vicent et al. (2005) and prepare the library of HPMA copolymers summarised in Fig. 3.3. It was important to characterise the conjugates in respect of total drug content and residual free drug by HPLC, UV and their Mw by GPC. Having standardised these methods it was also important to prepare reproducible batches of each compound for use in the subsequent biological tests.

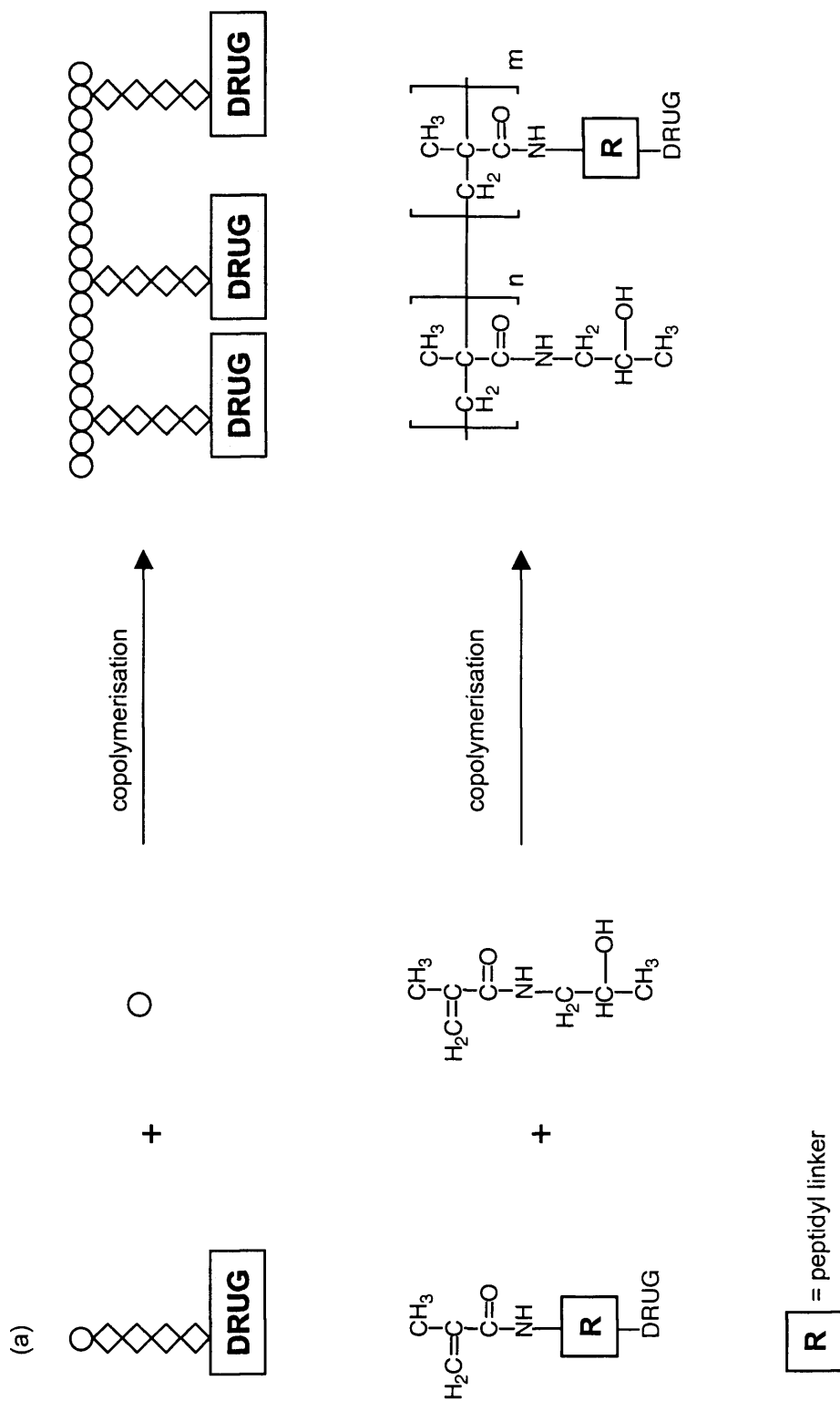
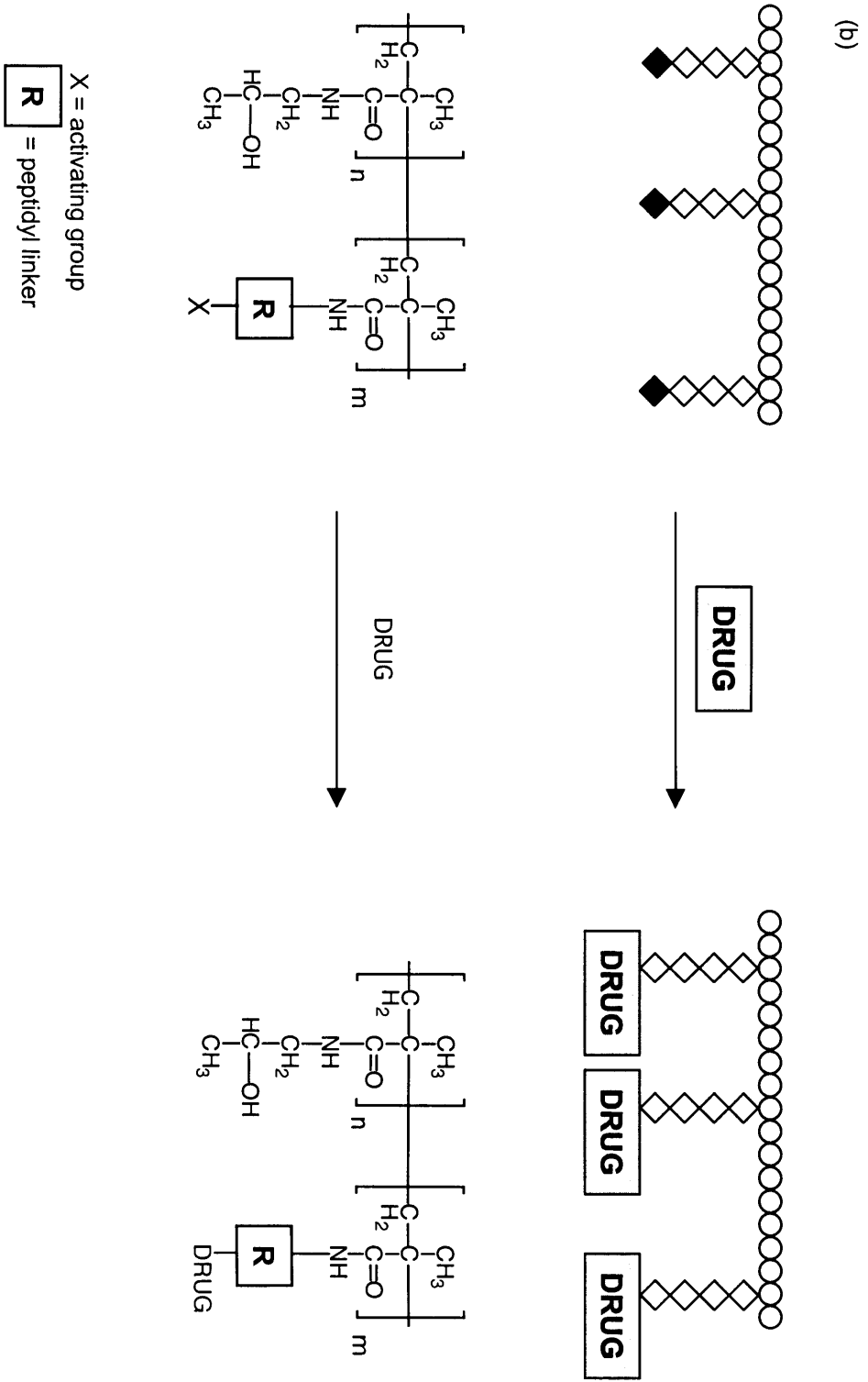


Fig. 3.2. Schematic representation of the two main approaches used to prepare HPMA copolymer-drug conjugates

Fig. 3.2. Continued



3.2. METHODS

The general methods used in this study have already been described in detail in Chapter 2. These were: the aminolysis reaction (section 2.3.1 - 2.3.3), the HPLC method for the determination of the total and free Dox content in the HPMA copolymer-Dox (section 2.3.4) and the characterisation of the Mw by GPC (section 2.3.5).

3.2.1. Synthesis and purification of HPMA copolymer-AGM \pm Dox conjugates.

The library of HPMA copolymer conjugates shown in Fig. 3.3, and the HPMA copolymer-aminopropanol derivatives were synthesised following these synthetic routes:

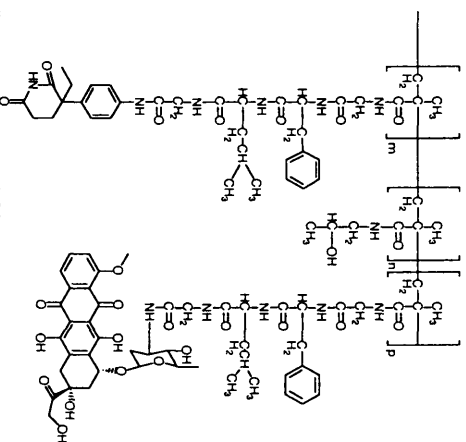
- HPMA copolymer-Dox conjugate and HPMA copolymer-aminopropanol conjugates were synthesised by aminolysis as described previously (paragraph 2.3.1 and 2.3.3, respectively; also described in Rejmanova, 1977).
- HPMA copolymer-AGM conjugates were synthesised by DCC coupling as described below.
- HPMA copolymer-AGM-Dox conjugate was synthesised also by DCC coupling as described below.

Synthesis of HPMA copolymer-GFLG (5 and 10 mol%)-AGM and HPMA copolymer-GG (5 mol%)-AGM conjugates.

The reaction procedure used is summarised in Fig. 3.4. It consists of 3 steps: hydrolysis of the HPMA copolymer-ONp derivative, conjugation of AGM and finally purification (Vicent et al., 2005).

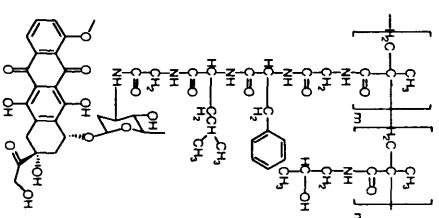
Step 1: A typical method to hydrolyse HPMA copolymer-GFLG (5 mol %)-ONp (or HPMA copolymer-GFLG (10 mol %)-ONp or HPMA copolymer-GG (5 mol %)-ONp) is described. The quantities referred to relate to HPMA copolymer-GFLG (5 mol %)-ONp as an example. HPMA copolymer-GFLG (5 mol %)-ONp (150 mg, 0.044 mmol ONp groups) was dissolved in ddH₂O (~ 5 mL) and a 0.1 M NaOH solution (1.32 mL) was added. The reaction was allowed to proceed for 4 h at room temperature. To monitor the reaction, an aliquot from the reaction mixture (5 μ L) was added in a quartz cuvette containing ddH₂O (995 μ L) and the resulting solution was analysed by UV spectroscopy to measure the displacement of ONp

HPMA copolymer-GFLG-AGM-Dox



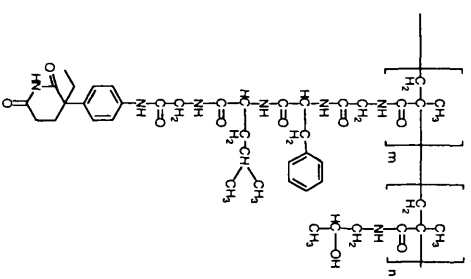
Where m = 5 mol %, p = 5 mol %, n = 90 mol %

HPMA copolymer-GFLG-Dox



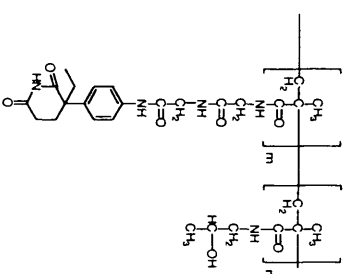
Where m = 5 mol %, n = 95 mol %

HPMA copolymer-GFLG-AGM



Where m = 5 mol %, n = 95 mol %
or 10 mol % n = 90 mol %

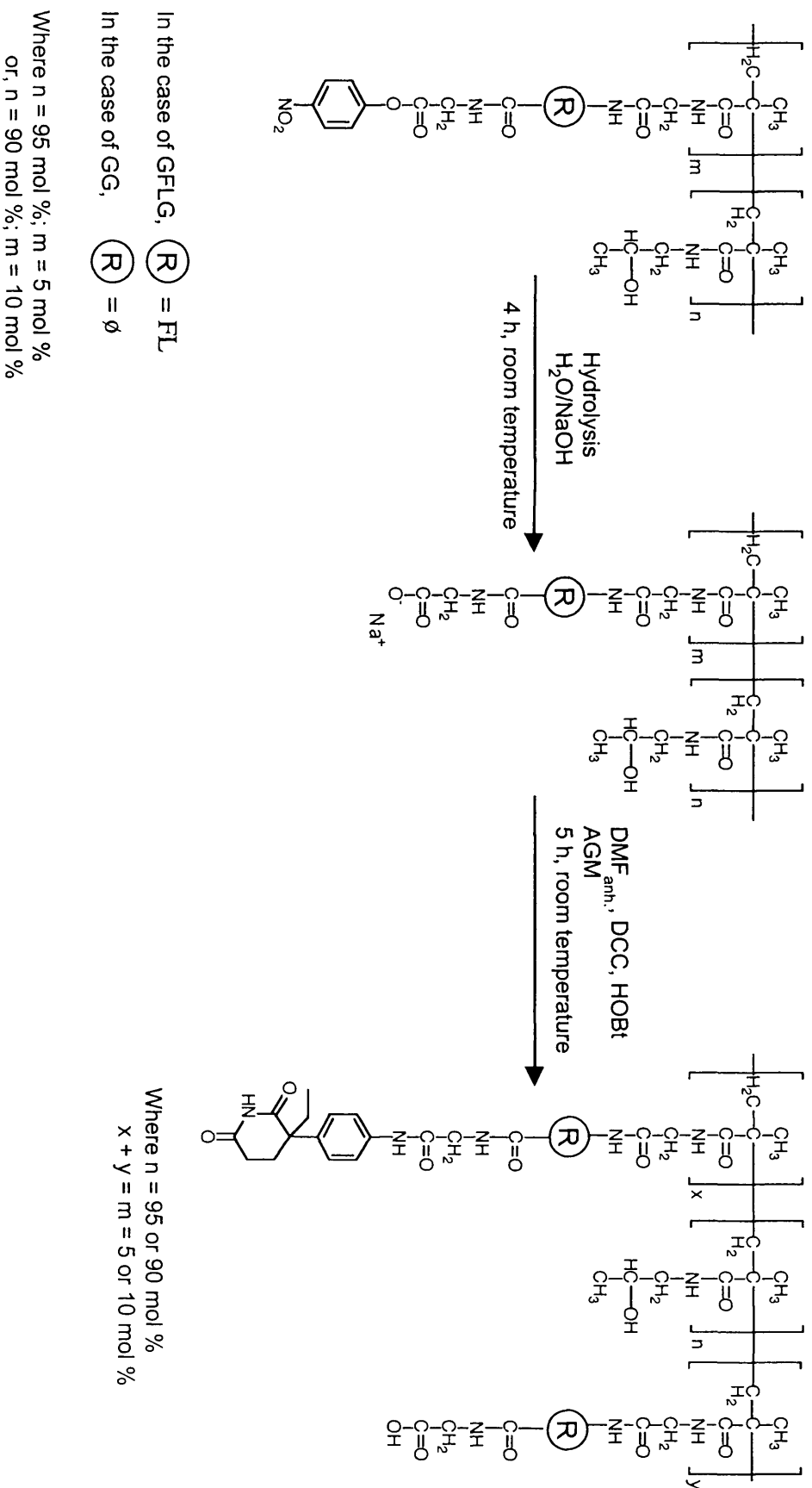
HPMA copolymer-GG-AGM



Where m = 5 mol %, n = 95 mol %

Fig. 3.3. Chemical structures of the library of target compounds. HPMA copolymer conjugates containing Dox, AGM or their combination

Fig. 3.4. Synthesis of HPMA copolymer-GFLG (5% or 10%)-AGM and HPMACopolymer-GG (5%)-AGM by DCC coupling



(Schwarzenbach et al., 1988; Ketelaar and Hellingman, 1951). Another quartz cuvette containing 1 mL ddH₂O was used as blank. The reaction mixture was then purified by dialysis (membrane: Mw cut-off ~ 2,000 g/mol) against ddH₂O in a conical flask (approximately 5 L of ddH₂O) for 2 days under constant stirring (the ddH₂O was changed approximately 5 times a day) and then freeze-dried to obtain a white solid.

Step 2: Conjugation of AGM. HPMA copolymer-GFLG (5 mol %)-COOH (150 mg; 0.046 mmol in respect of the –COOH) was dissolved in anhydrous DMF (1 mL), under nitrogen atmosphere. Then DCC (19 mg, 0.092 mmol) was added as a solid. After 10 min, HOBt (12.5 mg, 0.092 mmol) was added, also as a solid, and the reaction was allowed to proceed for 30 min. AGM (10.7 mg, 0.046 mmol) was dissolved in a minimal amount of anhydrous DMF (~ 0.2 mL), and then added to the reaction mixture. The reaction was allowed to proceed under a nitrogen atmosphere for approximately 5 h and was monitored by TLC (mobile phase CHCl₃ : MeOH 95 : 5 (v/v); R_f free AGM = 0.53, R_f conjugate = 0).

Step 3: The protocol followed for the purification is schematically described in Fig. 3.5. At the end of the reaction the precipitated urea was filtered-off, and DMF was partially evaporated under reduced pressure. The product was first purified by precipitation in a mixture of acetone : ether (4 : 1 (v/v); ~ 250 mL). The precipitated compound was filtered with a Buchner funnel (size 3). After the filtration, the acetone and ether were evaporated and this residue (R1) was kept for HPLC analysis. The filtered compound was collected and dissolved in MeOH (~ 0.5 mL) for further purification by column chromatography. This methanolic solution was applied to a sephadex LH20 column (5 x 50 cm, eluent MeOH). Fractions were collected (~ 5 mL each) and analysed by TLC (mobile phase CHCl₃ : MeOH 95 : 5 (v/v); R_f free AGM = 0.53, R_f conjugate = 0). The first fractions, containing the purified polymer conjugate, were collected, the MeOH was removed and the compound was dissolved in a minimal amount of water and freeze-dried. The impure fractions containing the free drug (AGM) were collected and the MeOH was evaporated. The resulting residue (R2) was added to R1 and together analysed at HPLC to quantitate directly the residual AGM and therefore estimate indirectly the content of AGM in the

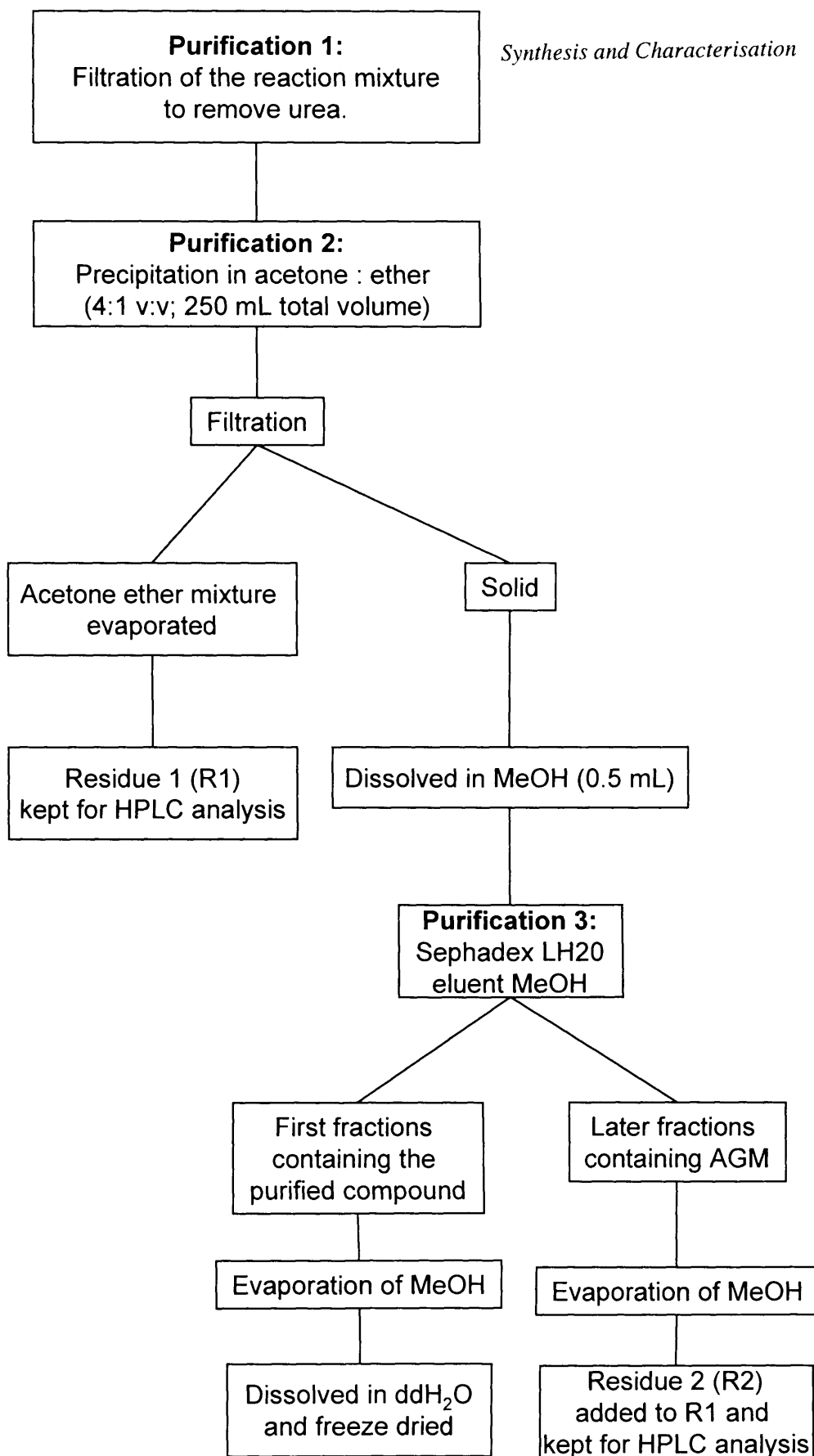


Fig. 3.5. Schematic representation of the purification steps following the synthesis of HPMa copolymer-AGM conjugates

conjugates, as described below. The overall yields based on polymer weight were 70-80 %.

Synthesis of HPMA copolymer GFLG (10 mol %)-AGM-Dox conjugate

The procedure for this reaction is summarised in Fig. 3.6 and consists of 3 steps: hydrolysis of the HPMA copolymer-ONp derivative, conjugation of AGM and Dox, and finally purification.

Step 1: HPMA copolymer-GFLG (10 mol %)-ONp was hydrolysed using the procedure described above.

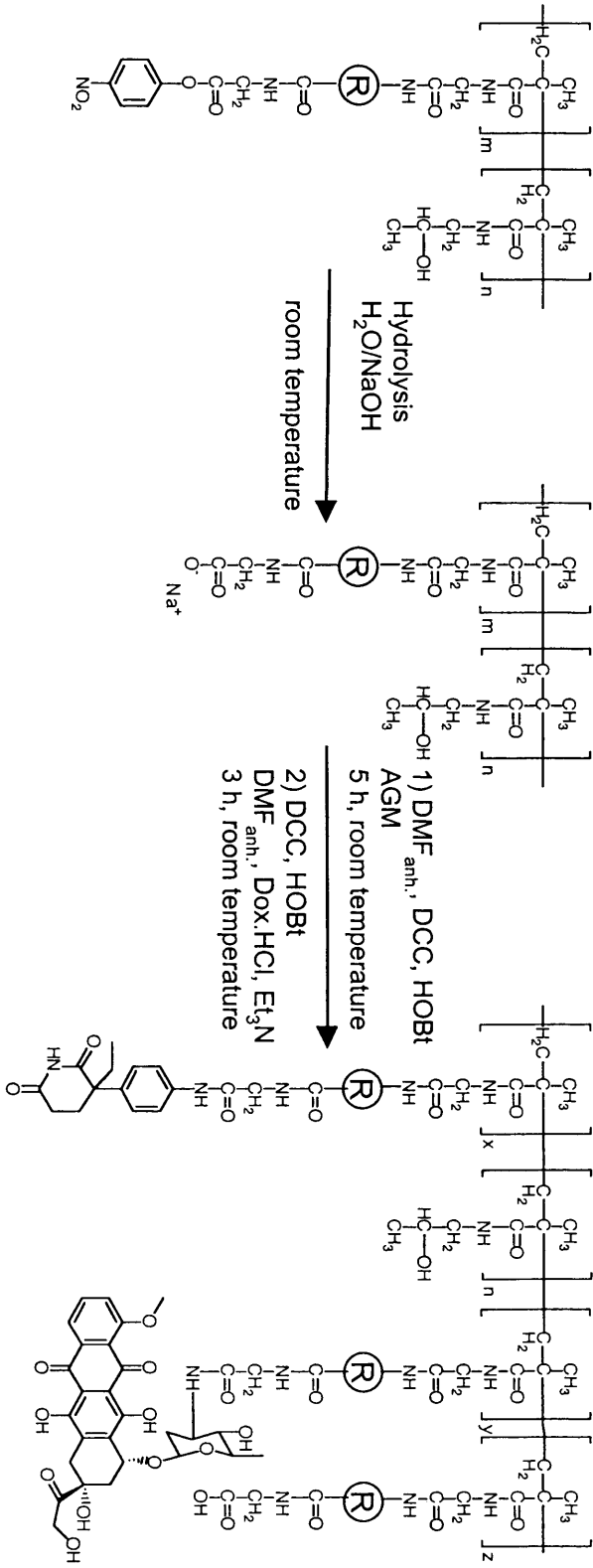
Step 2: HPMA copolymer-GFLG (10 mol %)-COOH (150 mg; 0.079 mmol in respect of the -COOH) was dissolved in anhydrous DMF (1 mL), under nitrogen atmosphere, then DCC (16.43 mg, 0.079 mmol) was added as a solid and the reaction stirred for 10 min. Then, HOBt (10.69 mg, 0.079 mmol) was added, also as a solid and the reaction allowed to proceed for 30 min. AGM (9.06 mg, 0.039 mmol) was dissolved in a minimal amount of anhydrous DMF (~ 0.2 mL) and added to the reaction mixture. The reaction was allowed to proceed under a nitrogen atmosphere for approximately 5 h and was monitored by TLC as described above. DCC (16.43 mg, 0.079 mmol) was again added as a solid. After 10 min HOBt (10.69 mg, 0.079 mmol) was added as well as a solid. After 30 min, a solution of Dox.HCl (22.6 mg, 0.039 mmol) in DMF anhydrous and triethylamine (3.95 mg, 5.4 μ L, 0.039 mmol) were added. The reaction was allowed to proceed for approximately 3 h and monitored by TLC (MeOH : AcOH 99.5: 0.5; R_f free AGM = 0.89, R_f free Dox = 0.44, R_f conjugate = 0).

Step 3: The reaction mixture was then purified to obtain the final product as described above.

3.2.2. Characterisation of HPMA copolymer-AGM \pm Dox conjugates

HPMA copolymer-AGM \pm Dox conjugates were characterised in respect of the total and free drug content (HPLC or UV). The methods used to determine free and total Dox are described in section 2.3.4 (Wedge, 1991; Vicent et al., 2005). The methods used to determine AGM content (total and free) are described below.

Fig. 3.6. Synthesis of HEMA copolymer-GFLG-Dox-AGM conjugate by DCC



\textcircled{R} = FL

Where n = 90 mol %; m = 10 mol %

Where n = 90 mol %
m = x + y + z = 10 mol %

Determination of total AGM content by UV spectroscopy

A glycine-AGM derivative (Gly-AGM) was first synthesised (in our laboratories by Dr. Vicent) and used as a standard to produce a calibration curve. Free AGM and Gly-AGM were dissolved in HPLC grade MeOH to produce a stock solution (1 mg/mL). This was then diluted to produce a range of concentrations (0 - 50 $\mu\text{g/mL}$ for AGM and 0 - 130 $\mu\text{g/mL}$ for Gly-AGM). UV absorbance of each sample over the range 200 - 300 nm was then determined. A calibration curve was then constituted and used to determine the total AGM content of HPMA copolymers-AGM \pm Dox conjugates. Each conjugate was dissolved in HPLC grade MeOH (1 mg/mL) and absorbance at 200 to 300 nm was measured. Relevant HPMA copolymer-aminopropanol derivatives in HPLC grade MeOH (1 mg/mL) were used as blank to remove any background effect due to the polymer chain.

Determination of total AGM using HPLC

The method used was a modification of the extraction procedure used to quantify total and free Dox content (section 2.3.4 and Fig. 2.3) (Vicent al., 2005; Wedge, 1991). The dried residue obtained following conjugation and purification (R1 + R2; see paragraph 3.2.1) was dissolved in HPLC grade CH_2Cl_2 and any precipitate was filtered off. As AGM is completely soluble in this solvent, none was lost during this procedure. The solvent was then evaporated and a stock solution in MeOH was prepared (5 mL), and samples (3 x 100 μL) were taken and placed into polypropylene tubes. Each sample was made up to 1 mL with H_2O , the pH was adjusted to 8.5 by addition of ammonium formate buffer (100 μL , 1M, pH 8.5) and the sample thoroughly mixed by vortexing.

A mixture of chloroform : propan-2-ol (4 : 1) was then added (5 mL), and the samples were extracted alternating vortexing and shaking (3 x 30 s vortexing and 1 shaking) and the two phases were allowed to separate. The upper aqueous layer was removed and discarded while the lower organic phase was evaporated using a N_2 flow. The dry residue was re-dissolved in 100 μL of HPLC grade MeOH. In parallel, AGM reference samples (3 x 100 μL of a 1 mg/mL stock aqueous solution) were also processed as a standard. Addition of 1 mL of HPLC grade MeOH led to a stock solution (100 $\mu\text{g/mL}$), which was then diluted to produce a calibration curve (2 to 80 $\mu\text{g/mL}$). All standards and the samples were then analysed by HPLC using a

μ Bondapak C18 (150 x 3.9 mm) column. A gradient elution profile and the conditions listed below were used:

- **solvent A**- propan-2-ol : H₂O 12 : 88 v/v.
- **solvent B**-propan-2-ol : H₂O 29 : 71 v/v adjusted to pH 3.2 by addition of orthophosphoric acid).
- **Flow rate** was 1 mL/min, the total run time was 20 min
- **gradient profile:**
 - t = 5 min A 100 %
 - t = 9 min A 0 %,
 - t = 14 min A 0 %,
 - t = 16 min A 50 %,
 - t = 18 min A 100 %.

AGM was detected by a UV detector ($\lambda = 254$ nm), retention time (t_r) was 5.3 min. Data were acquired and processed using PowerChrom hardware and software. From the standards, a calibration curve was produced and used to estimate AGM content.

Determination of the free AGM and the free Dox content by HPLC

An aqueous solution of each HPMA copolymer-AGM-Dox conjugate (1 mg/mL) was prepared. An aliquot of the solution (400 μ L) was then placed into a polypropylene tube and a DNM internal standard was added to each sample (100 μ L of a 1 μ g/mL stock aqueous solution). and the volume was made up to 1 mL with H₂O. The extraction procedure described above was used.

For quantitation of free Dox the standards were produced processing a solution (10 μ g/mL) and then diluting it to give a calibration curve. HPLC conditions were the same as described above for quantitation of total AGM (t_r for free Dox was 13.7 min and free DNM was 15.1 min). Also in this case a calibration curve was produced and used to determine the free residual Dox.

3.3. RESULTS

A library of HPMA copolymer conjugates was synthesised containing Dox, AGM or a combination of both drugs linked to the same polymer chain. To prepare conjugates using DCC coupling, it was first necessary to hydrolyse the polymeric precursor. This reaction was monitored by UV to follow the release of ONp (Fig. 3.7

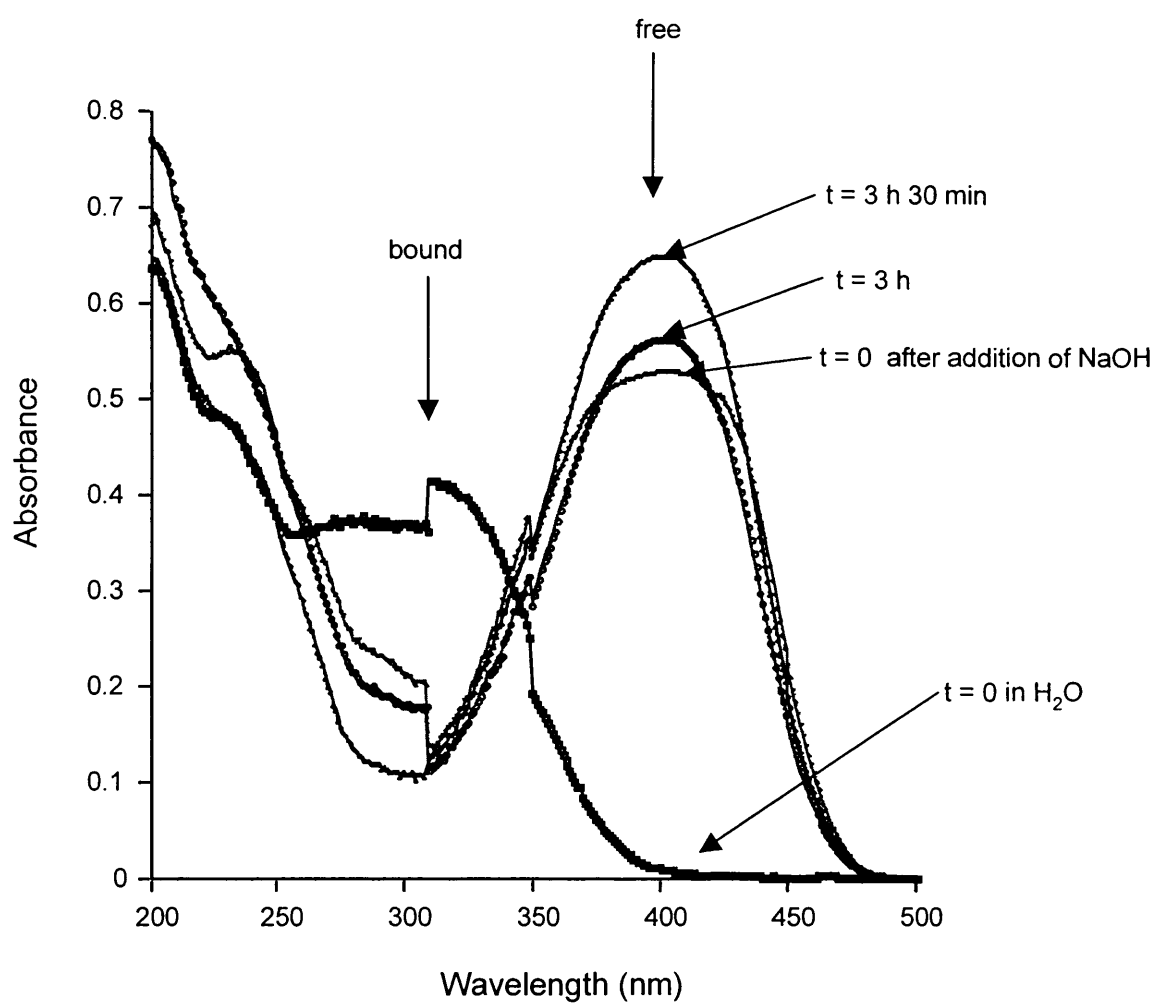


Fig. 3.7. UV scan of the hydrolysis reaction of HPMA-copolymer-ONp. Scans are taken at t = 0 (before and after addition of NaOH), after 3 h and after 3 h and 30 min

indicating ONp liberation). When HPMA copolymer-ONp was dissolved in H₂O, no absorbance was registered at 400 nm, but addition of NaOH quickly led to the appearance of a peak at 400 nm. Further release continued over 3.5 h. The yield of this reaction was approximately 80 - 90%.

3.3.1. Content of total and free drug in HPMA copolymer conjugates

Two methods were used, a direct analysis of the conjugate by UV (for total AGM) and HPLC analysis (for total and free AGM and Dox).

The total Dox content of the conjugate was quantified by HPLC. Fig. 3.8a shows the chromatogram of the aglycone produced by acid degradation of Dox. The fluorescence was increasing with increasing concentration in a linear manner ($r^2 = 0.998$), in the range of concentrations considered (Fig. 3.8b). The aglycone produced by hydrolysis and extraction from the sample had the same retention time (t_r) as the standards (Fig. 3.8a). Figure 3.9a shows a typical chromatogram of a standard for free Dox. The calibration curve showed a linear dependency (Fig. 3.9b). The free Dox extracted from the sample had the same t_r as the standard (Fig. 3.9a).

The total AGM content was estimated indirectly by HPLC (quantification of the remaining, non-reacted AGM). The content of free AGM was determined by HPLC after extraction from the polymer. In both cases AGM was used as standard. A linear dependency was found for AGM standard ($r^2 = 0.999$). The free AGM extracted from the sample had the same t_r as the standards (Fig. 3.10).

Total AGM by UV. In the attempt of quantifying the total content of AGM directly, UV analysis was performed. Free AGM was, in the first instance, used as standard. The UV spectrum of free AGM in MeOH showed a maximum peak of absorbance at 238 nm (Fig. 3.11a). The respective calibration curve (Fig. 3.11b) showed a linear dependence ($r^2 = 0.999$) in the range of concentrations tested (0 - 0.025 mg/mL). With the aim of mimicking the electronic distribution of polymer bound AGM, the use of Gly-AGM as standard seemed more appropriate. UV scans of Gly-AGM in MeOH, showed a shift of the maximum absorbance (from 238 to 257 nm) and also a change in the extinction coefficient ($\epsilon_{AGM} > \epsilon_{GlyAGM}$) (Fig. 3.12).

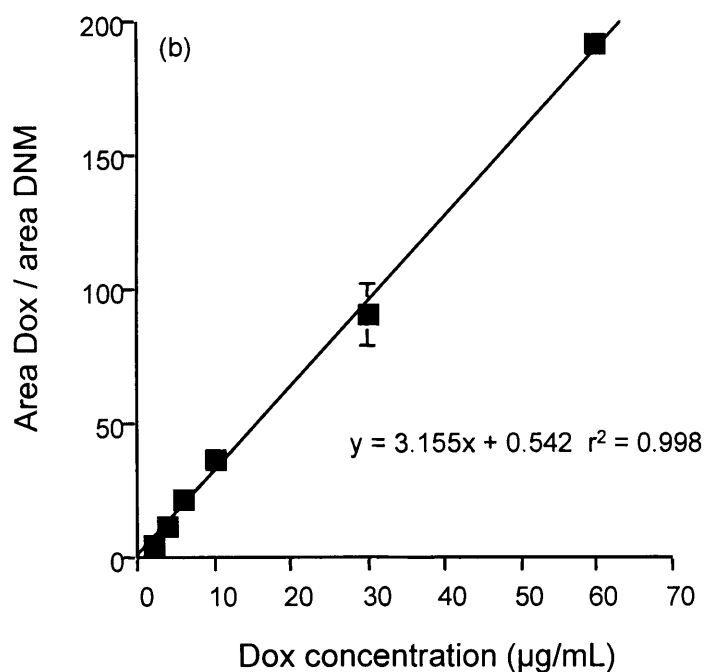
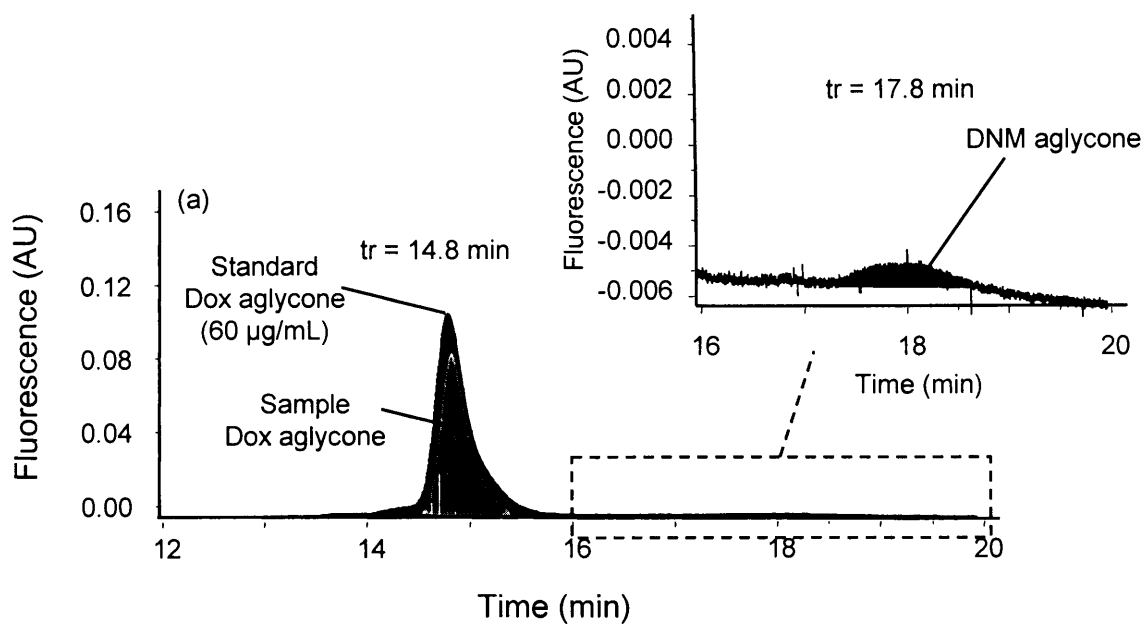


Fig. 3.8. HPLC analysis of Dox aglycone. Panel (a) shows the chromatogram of the standards and sample, panel (b) shows the calibration curve. Data indicate mean \pm S.E.M., $n = 3$

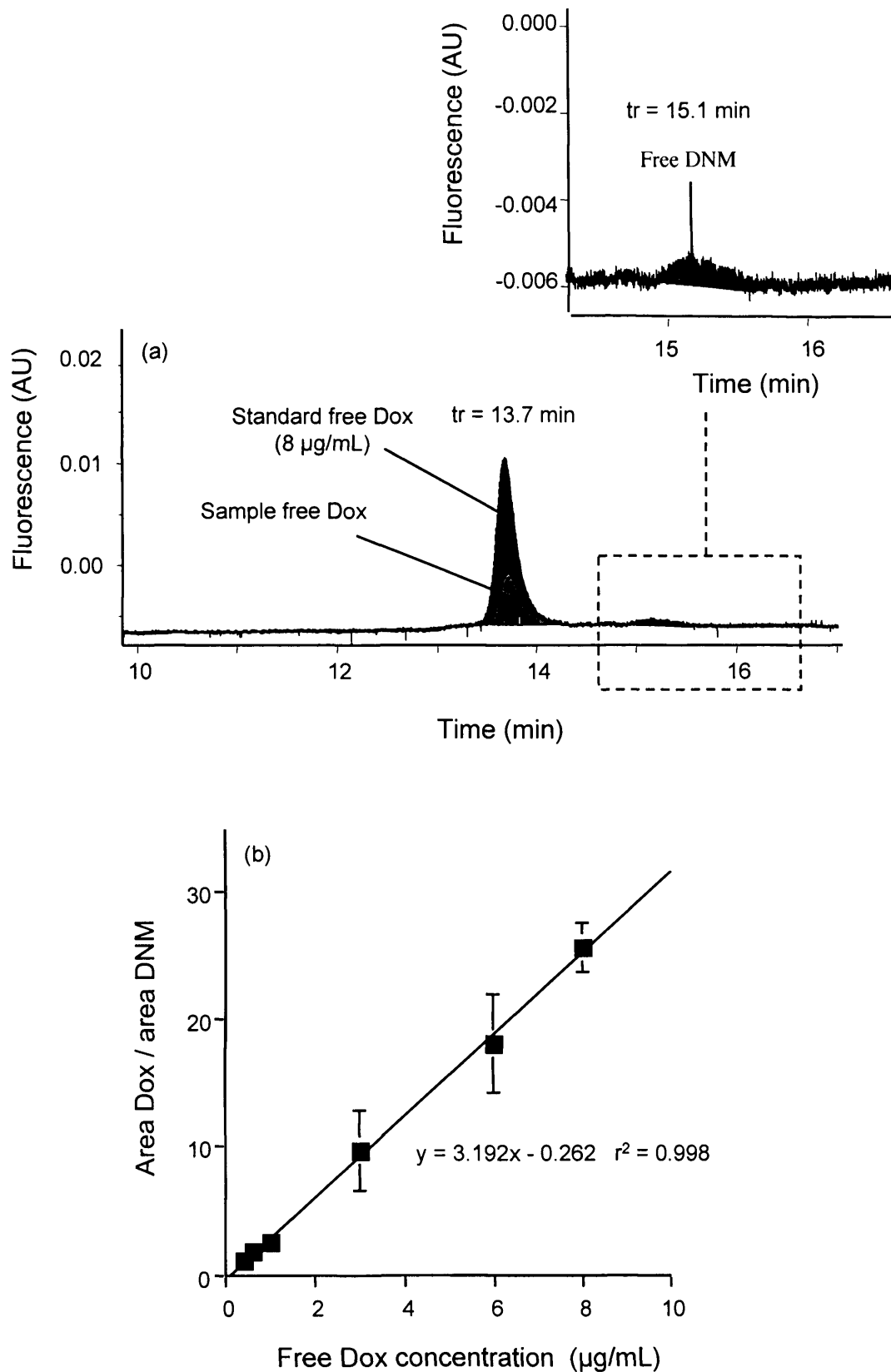


Fig. 3.9. HPLC analysis of free Dox. Panel (a) shows the chromatogram of the standards and sample panel (b) shows the calibration curve. Data indicate mean \pm S.E.M., $n = 3$

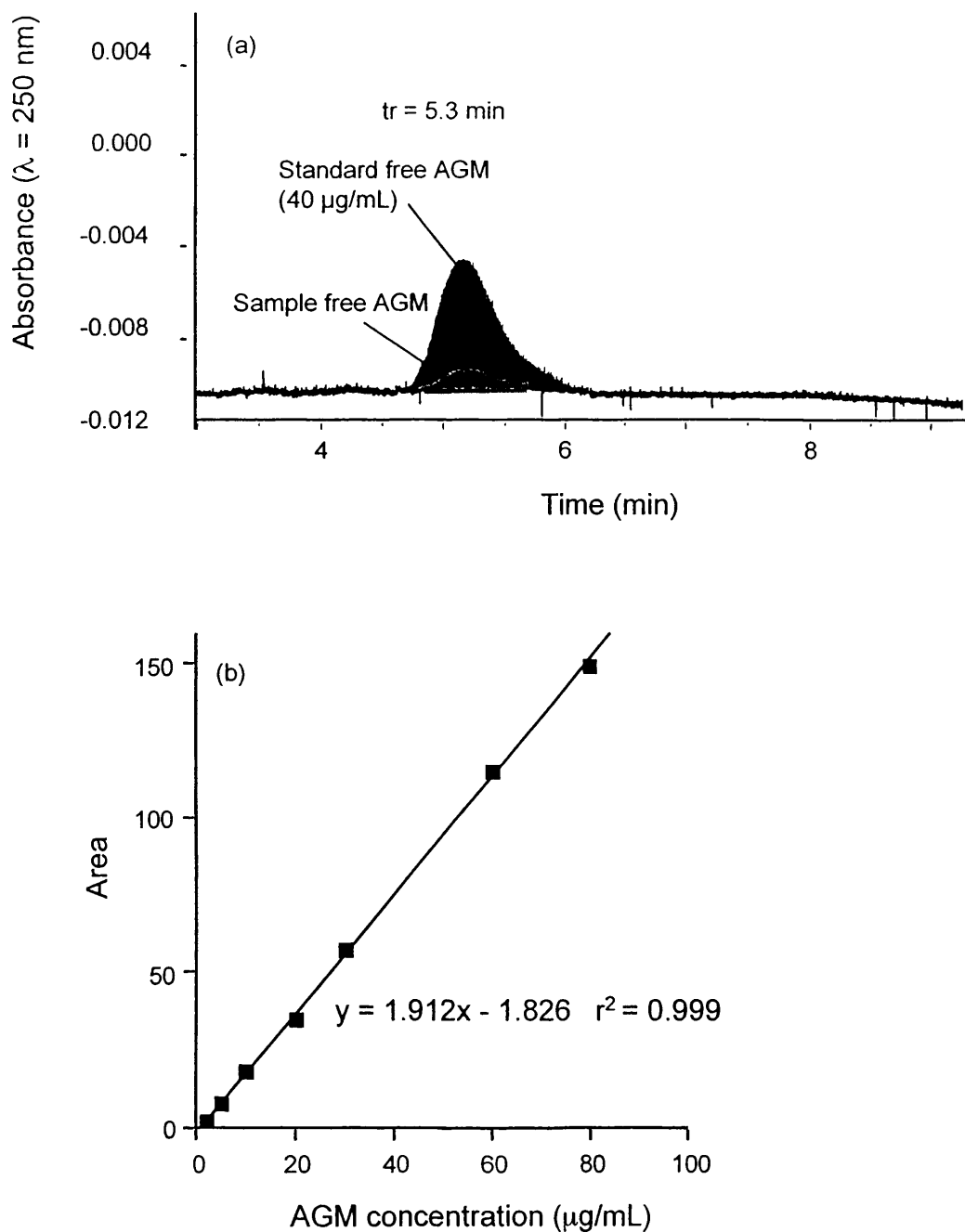


Fig.3.10. HPLC analysis of free and total AGM. Panel (a) shows the chromatogram of the standard and an example of free, panel (b) shows the calibration curve. Data indicate mean \pm S.E.M., $n = 3$

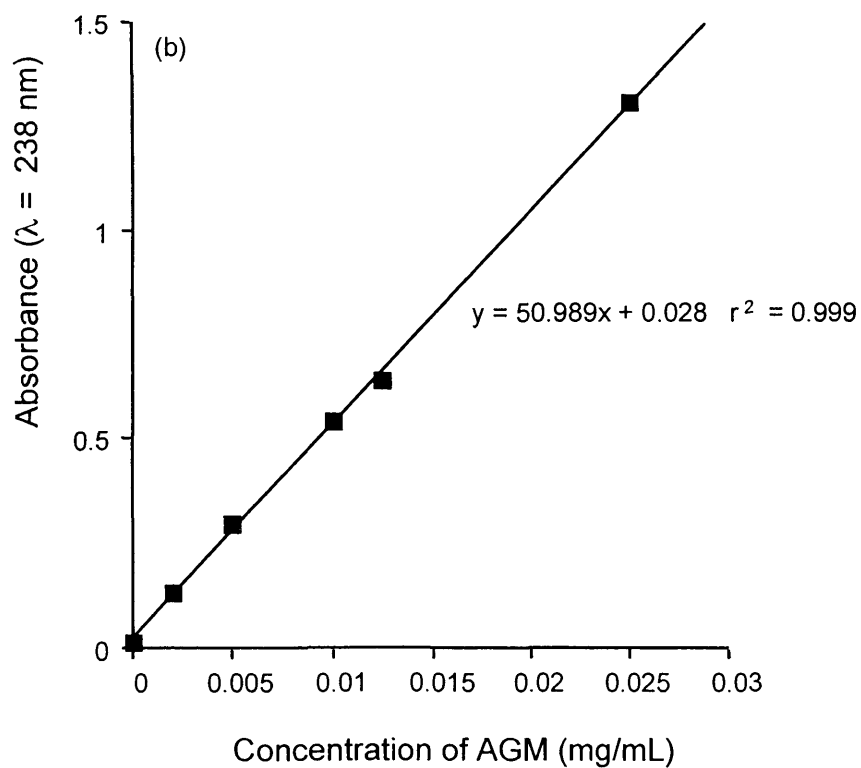
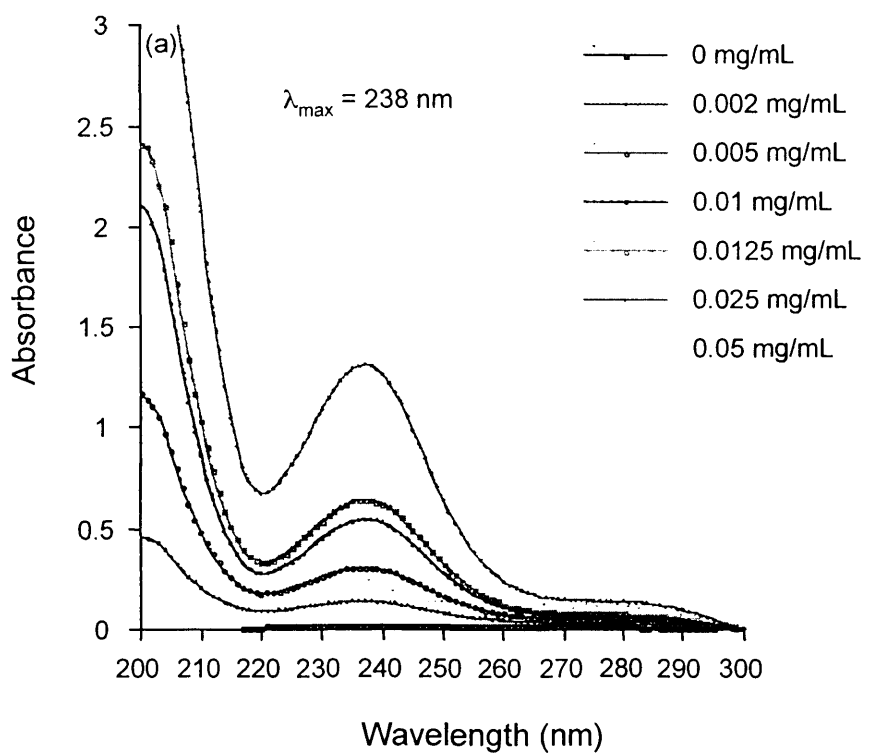


Fig. 3.11. UV scan of free AGM in MeOH, panel (a) and the corresponding calibration curve, panel (b)

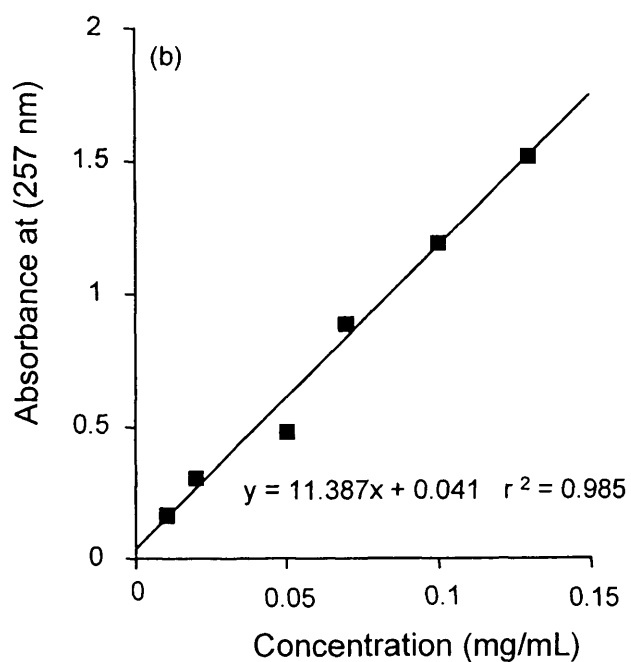
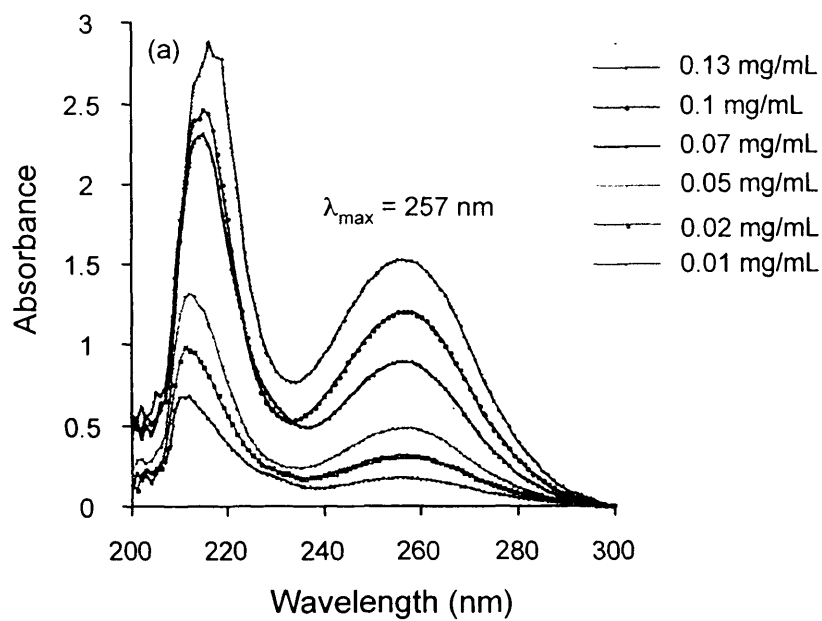


Fig. 3.12. UV spectrum of Gly-AGM in MeOH panel (a) and the corresponding calibration curve panel (b)

When the HPMA copolymers carrying AGM were analysed by UV, they showed a maximum absorbance at 251 nm, which closely resembles that seen for Gly-AGM. The HPMA copolymer backbone interfered with the absorbance of polymer bound AGM. This could be seen if MeOH alone was used as blank (Fig. 3.13). On the other hand, if the aminopropanolated derivative in MeOH was used as blank, the interference was abolished (Fig. 3.13).

3.3.3. Characterisation of the conjugates by GPC

After determination of the content of total and free drug, GPC was used to determine M_w , M_n and the polydispersity. First the bed volume and the void volume of the column were determined using sucrose and pullulan ($M_w = 788,000$ g/mol), respectively (Fig. 3.14a). Then, HPMA copolymer conjugates containing AGM and/or Dox were analysed. Also the hydrolysed precursor and the HPMA copolymer-Ap derivatives were analysed (Fig. 3.14b). The determination of the exact molecular weight was not possible as the polysaccharides standards are not suitable for HPMA copolymers. However, it was noticed that if each conjugate was compared with the parent compounds (HPMA copolymer-Ap and HPMA copolymer-COOH), the retention time was the longest for the conjugate, then for the HPMA copolymer-Ap derivatives and finally the HPMA copolymer-COOH had the shortest retention time.

3.3.4. Summary of the conjugates synthesised and their characteristics

The library of HPMA copolymer conjugates synthesised and their characteristics are summarised in Table 3.1. Two batches of HPMA copolymer-Dox were synthesised by aminolysis. Whilst the first one had a low Dox content (2.1 % wt), the second had higher loading (6.8 % wt). DCC coupling was used to synthesise HPMA copolymers containing AGM alone or AGM combined with Dox. A good batch to batch reproducibility was found. In the polymers containing only AGM, the total drug content was approximately 6 % wt, ranging between 5.5 - 8.6 % wt. Predictably, the highest content of total AGM was found in the conjugate containing 10 mol % of side chain (a total AGM loading 8.6 % wt). In the conjugate carrying both AGM and Dox, the content of each individual drug was approximately 5 % wt with a range of 5.1 - 5.4 for AGM and 2.8 - 7.2 for Dox. In all cases, the content of free drug was always low (< 1.4 % of the total drug bound).

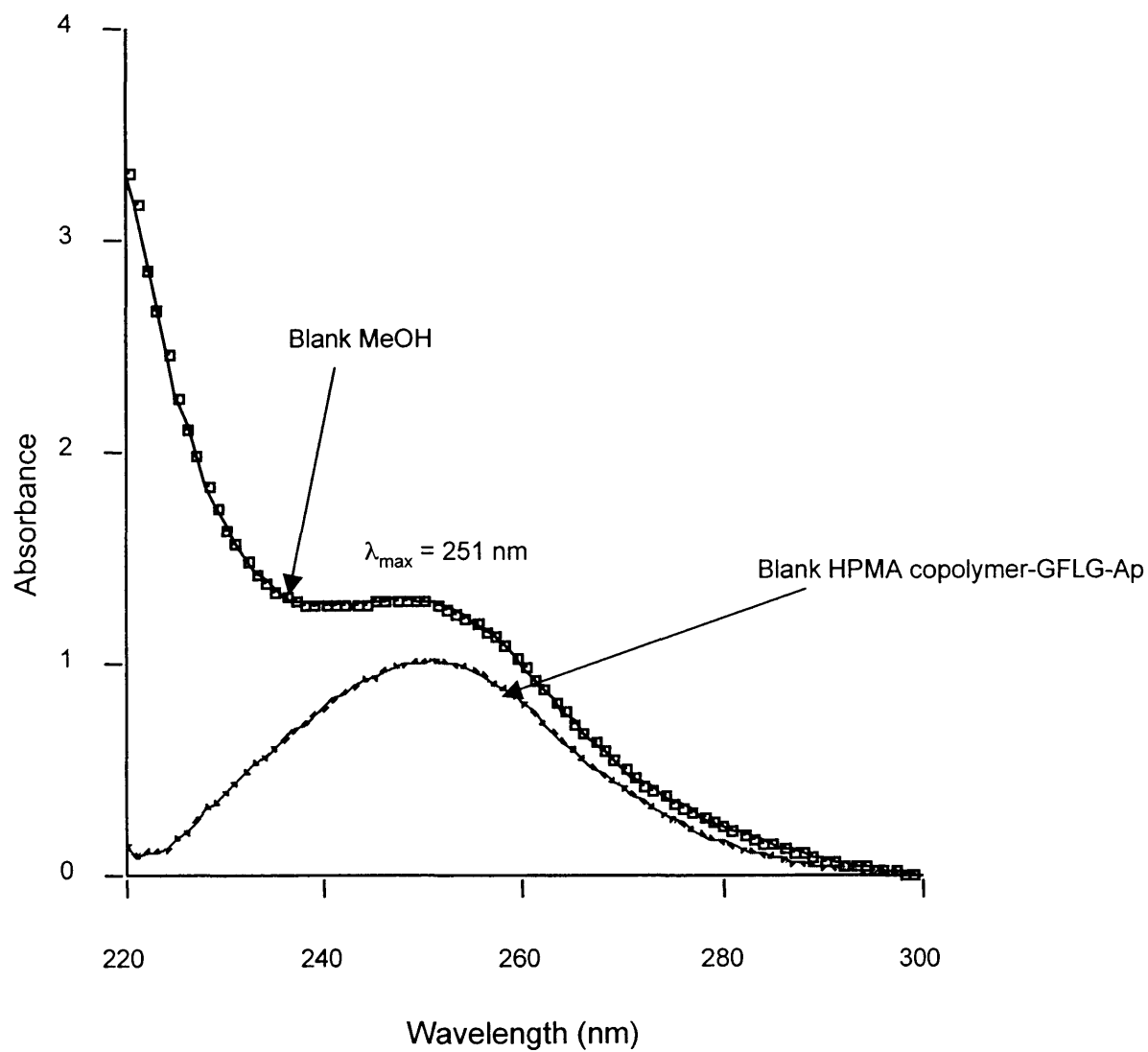


Fig. 3.13. UV spectrum of HPMA copolymer GFLG (5 mol%)-AGM using as blank either MeOH or a solution of HPMA copolymer GFLG (5 mol%)-Ap in MeOH at the same concentration

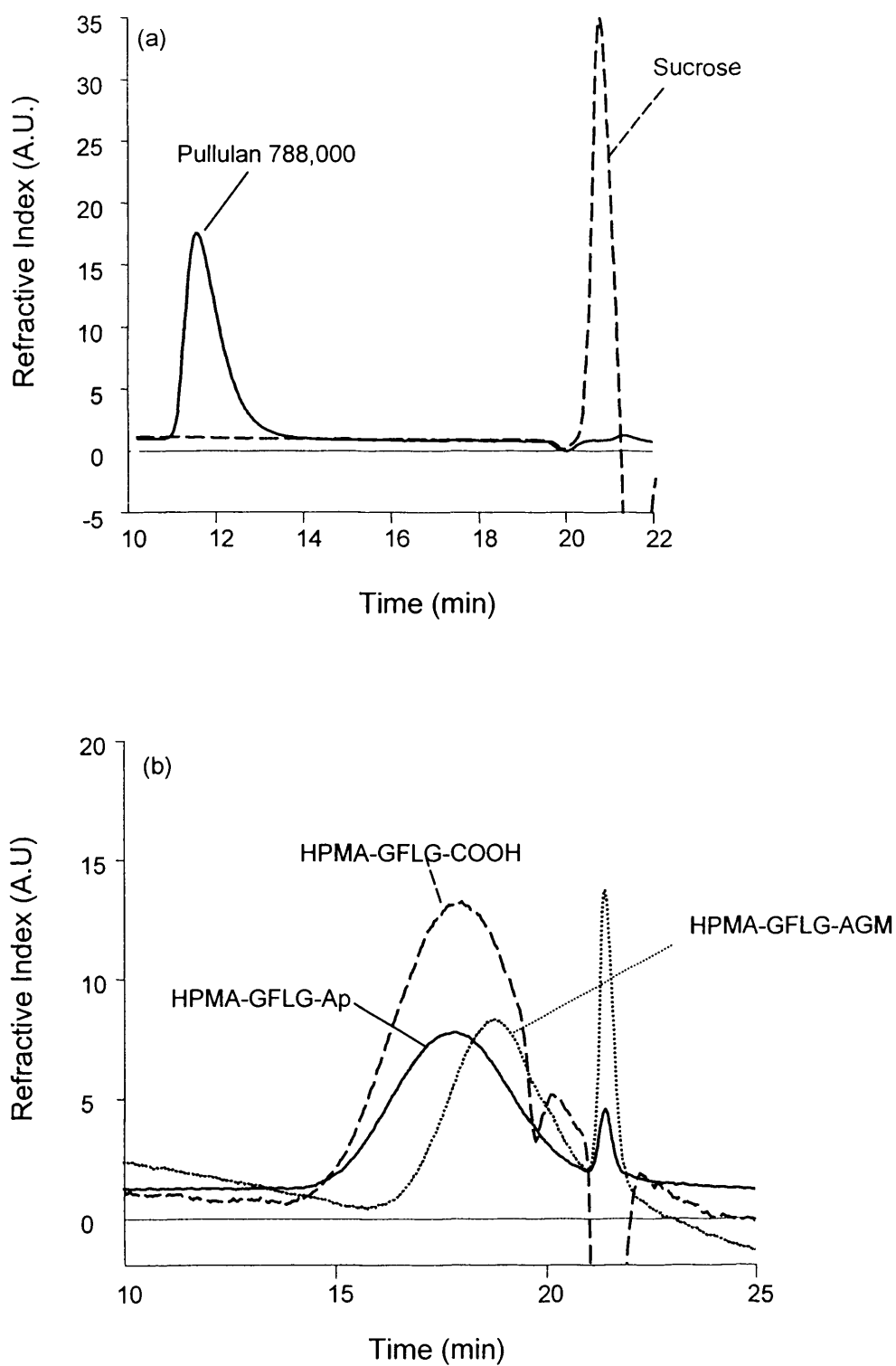


Fig. 3.14. GPC profiles of HPMA copolymer conjugates. Panel (a) GPC profile of pullulan ($M_w = 788,000$ g/mol) and sucrose to determine the void volume and the bed volume, respectively. Panel (b) GPC profile of HPMA copolymer GFLG (5 mol %)-COOH, HPMA copolymer GFLG (5 mol %)-Ap and HPMA copolymer GFLG (5 mol %)-AGM

3.4. DISCUSSION

At the beginning of this project it was essential to first prepare the library of HPMA copolymer conjugates desired and carefully characterise them (Table 3.1). The synthesis of HPMA copolymer-Dox was achieved by aminolysis as widely described in literature (Rejmanova, 1977). However, as the aromatic amino group of AGM is poorly nucleophile (the electron doublet of the amino group is partially delocalised on the aromatic system), activation of the carboxylic group using DCC (Fig. 3.15) and HOBT to promote AGM conjugation to HPMA copolymer intermediates bearing $-\text{COOH}$ was preferred (Camplo et al., 1996; Vicent et al., 2005).

One of the characteristics, possibly the most significant, that differentiates polymer drug conjugates from other drug delivery systems like liposomes or micelles is the covalent attachment of the drug to the polymeric carrier. The presence of covalent linkage is often demonstrated by NMR. However, the interference of the signals from the protons of the polymeric backbone can make the interpretation of the results more difficult. The formation of an amide bond between Dox and HPMA copolymer was elegantly proven previously by NOESY and TOCSY (Pinciroli et al., 1997). Evidence for covalent conjugation of AGM was also obtained by ^1H NMR analysis (Vicent et al., 2005), as the appearance of a band at 9.8 ppm, clearly indicated the formation of an aromatic amide. Furthermore, a positive NOE correlation between the imide group of AGM ($\delta = 11.0$ ppm) and the methylene group of the first Gly in the spacer ($\delta = 4.0$ ppm) was also observed (Fig. 3.16).

Once the chemical identity of the conjugates was proven, it was important to determine the total and free Dox and AGM content for each drug. One of the main challenges was the optimisation of a method that would allow the quantitation of total AGM. Although there is a well established HPLC method for Dox quantitation (Wedge, 1991; Configliacchi et al., 1996), this method was not suitable for AGM. The method used to quantify total Dox uses acid hydrolysis to liberate Dox aglycone which can then be extracted and quantified (Wedge, 1991; Configliacchi et al., 1996). However, hydrolysis of HPMA copolymer-AGM conjugates would need conditions able to hydrolyse the terminal amide linkage. This would also degrade the peptidyl

Table 3.1 HPMA copolymer conjugates synthesised

Sample	Side chain (mol %)	Batch/code	Total AGM (% w/w)	Free AGM (% total)	Total Dox (% w/w)	Free Dox (% total)
HPMA-GFLG-Dox	~ 5	FG/1a	N/A*	N/A	2.1	0.9
		FG/1b	N/A	N/A	6.8	0.5
HPMA-GFLG-AGM	~ 5	FG/2a	6.4	nd [†]	N/A	N/A
		FG/2b	6.0	0.6	N/A	N/A
		FG/2c	6.4	1.2	N/A	N/A
		FG/2d	5.9	0.2	N/A	N/A
HPMA-GFLG-AGM	~ 10	FG/3a	8.6	nd	N/A	N/A
HPMA-GG-AGM	~ 5	FG/4a	6.3	nd	N/A	N/A
		FG/4b	5.6	1.1	N/A	N/A
		FG/4c	5.2	1.4	N/A	N/A
HPMA-GFLG-Dox-AGM	~ 10	FG/4d	5.5	0.2	N/A	N/A
		FG/5a	5.1	1.0	2.8	1.1
		FG/5b	5.1	0.7	5	0.8
		FG/5c	5.4	0.7	7.2	0.2

* N/A = not applicable

[†] nd = non detectable

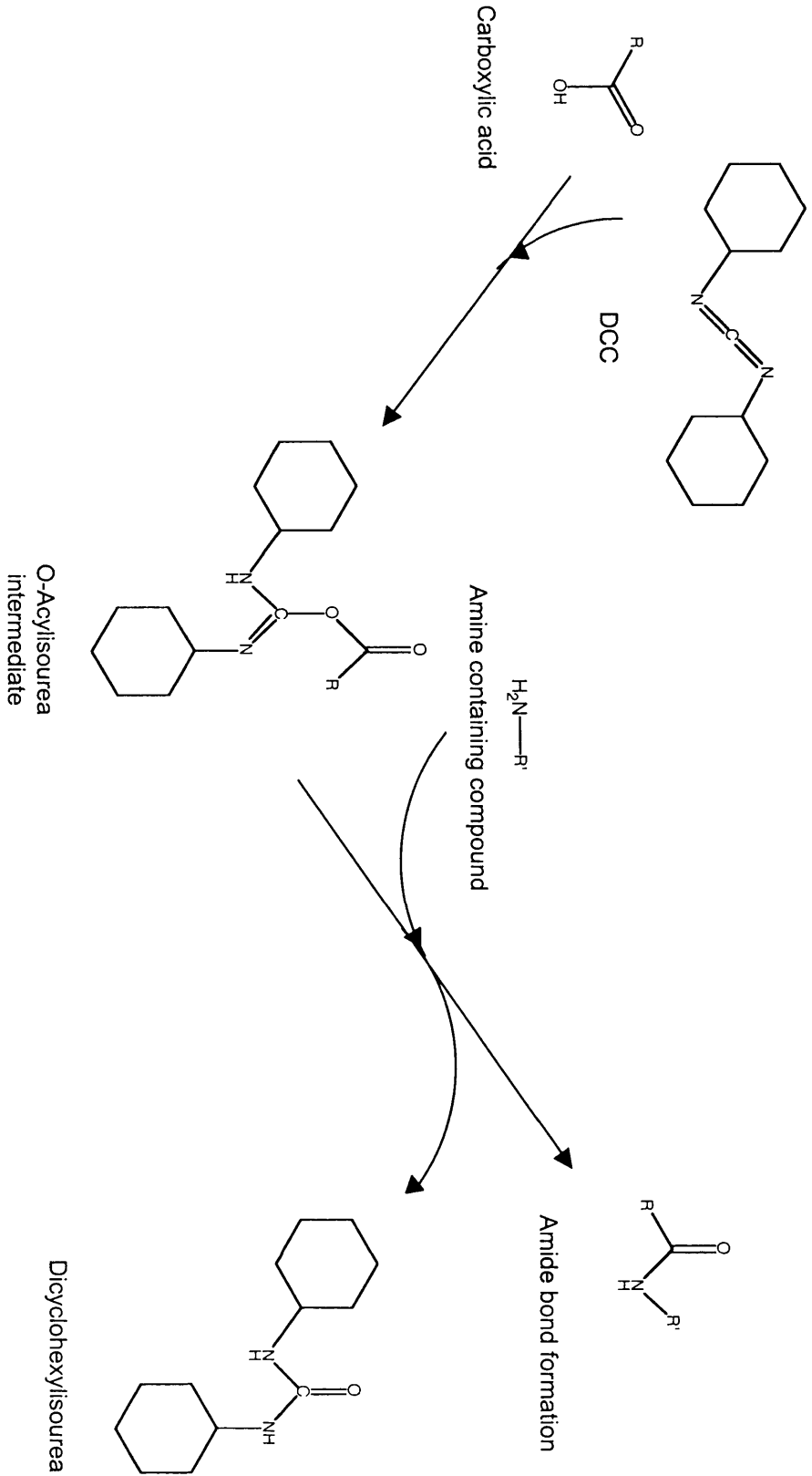


Fig. 3.15. Mechanism of the DCC coupling reaction (adapted from Hermanson, 1996)

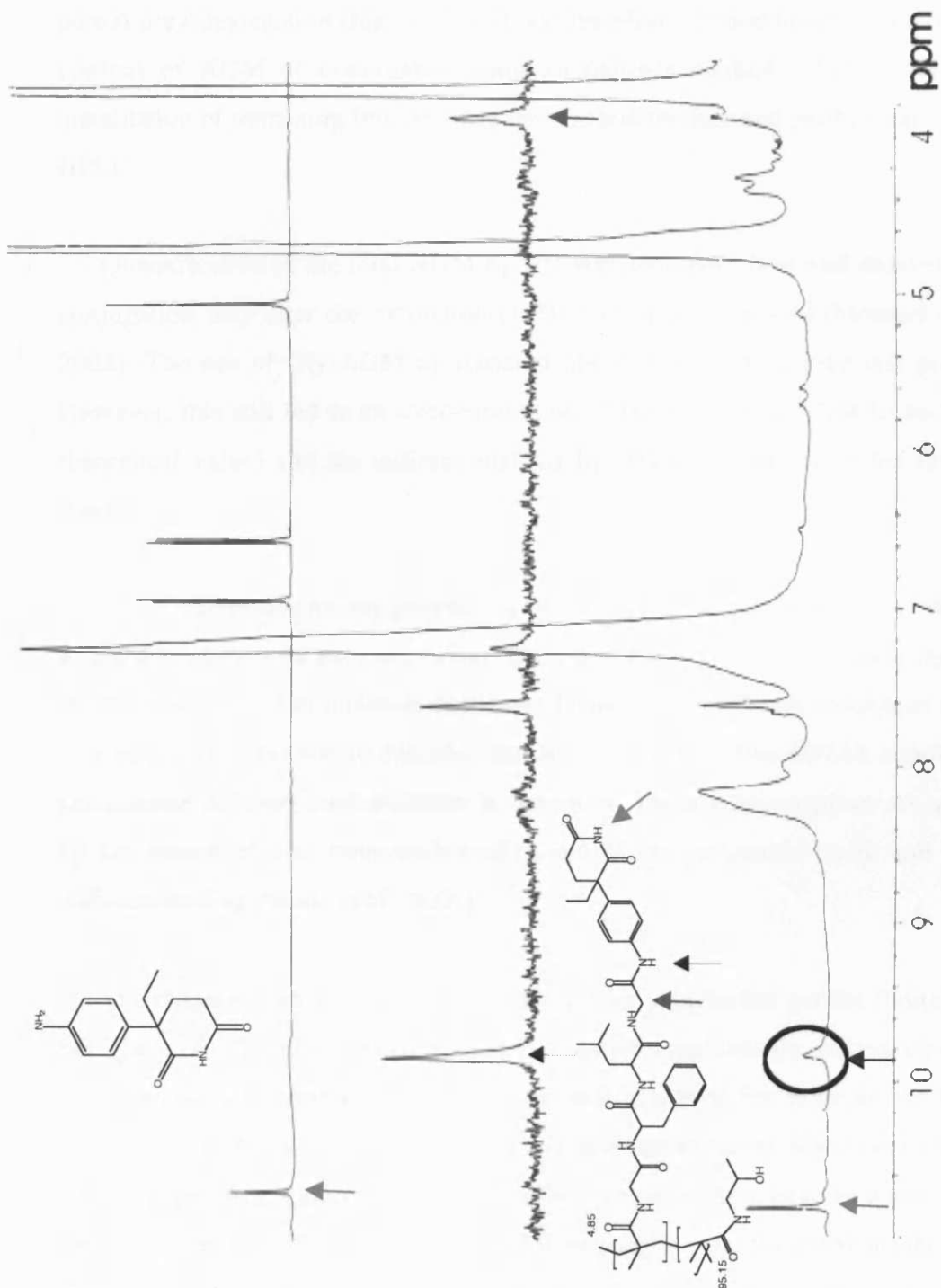


Fig. 3.16. NOE ^1H -NMR spectra of HPMA copolymer GFLG (10 mol%)-AGM conjugate (adapted from Vicent et al., 2005). Black arrows indicate the aromatic amide, red arrows the imide and blue arrows the methylene of the Gly.

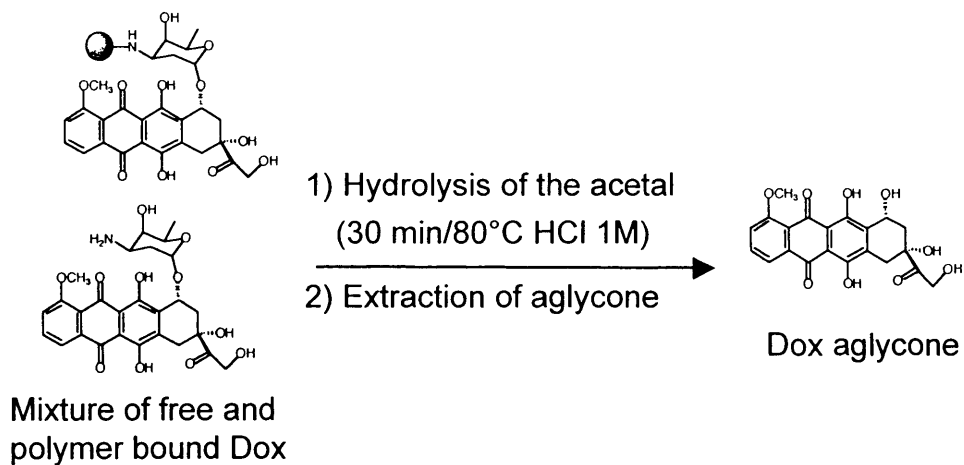
side chain probably leading to a complex mixture of free AGM, peptidyl derivatives (i.e. G-AGM, LG-AGM, FLG-AGM, GFLG-AGM), free aminoacids and products deriving from the degradation of HPMA (i.e. aminopropanol) (Fig. 3.17c). Furthermore, the AGM imide would probably also be hydrolysed leading to at least partial drug degradation (Fig. 3.17c). It was therefore decided to determine the total content of AGM of conjugates using an indirect method. This involved the quantitation of remaining free AGM in the reaction mixture and purification steps by HPLC.

Quantification of the total AGM by UV was also used. It is well described that conjugation may alter the extinction coefficient of a compound (Mendichi et al., 2002). The use of Gly-AGM as standard allowed us to overcome this problem. However, this still led to an over-estimation of the content of AGM (> maximum theoretical value) and the indirect analysis by HPLC was therefore the favourite route.

When characterising any polymer-drug conjugate, the determination of the Mw, and polydispersity is very important. Only a conjugate Mw lower than the renal threshold allows the elimination of the non biodegradable HPMA copolymer carrier. It is also very important to consider that linear polymers, like HPMA copolymers, can assume different conformations in solutions. These conformations are affected by the nature of the compounds conjugated to the polymeric chain and by the different loading (Searle et al., 2001).

The characterisation by GPC presented in this chapter has got the limitation of not giving an accurate Mw (due to inappropriate standards i.e. polysaccharides). However, some interesting observations can still be drawn. For example, the HPMA copolymer-AGM (and/or Dox) conjugates have an apparent Mw lower than the HPMA copolymer-aminopropanol derivatives. These, in turn, have an apparent Mw lower than the HPMA copolymer-COOH. This suggests that the covalent attachment of a less hydrophylic group (hydrophylicity: AGM/Dox < Ap < COOH) leads to a more compact structure (Fig. 3.18).

(a) Determination of **total** Dox



(b) Determination of **free** Dox

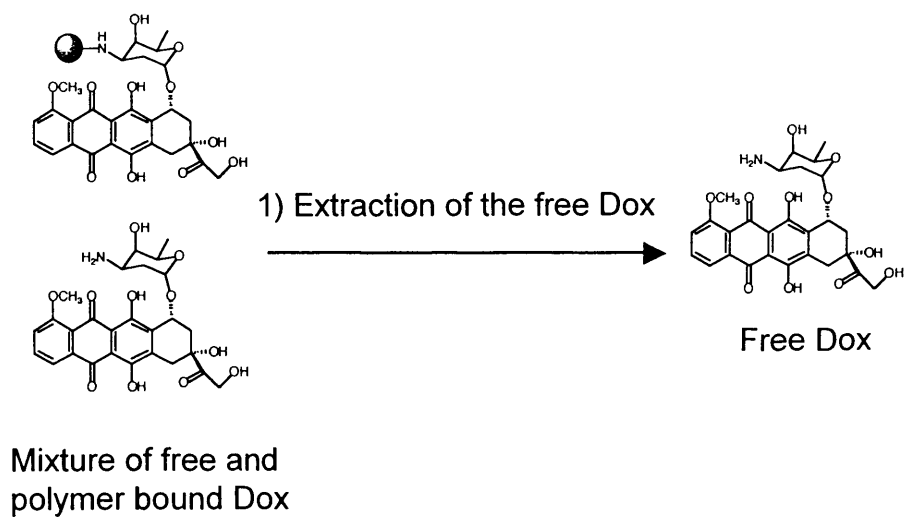
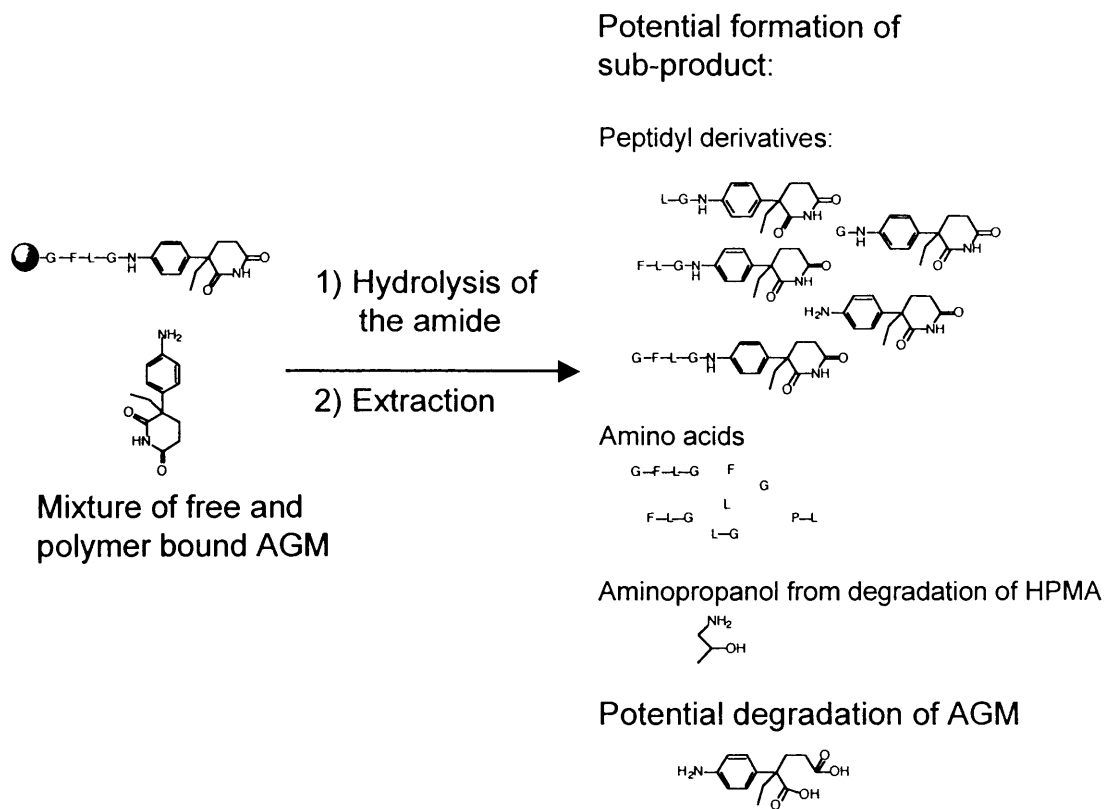


Fig. 3.17. Rationale for the HPLC method used for Dox illustrating the potential disadvantages for the quantitation of total AGM

(c) Hypothetical direct determination of **total** AGM



(d) Determination of **free** AGM

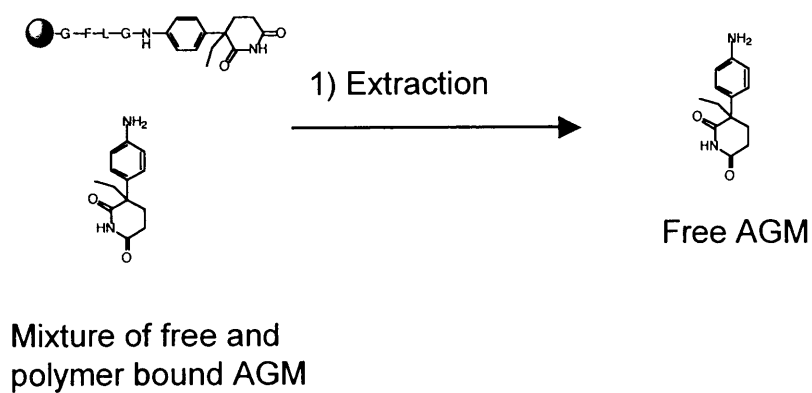


Fig. 3.17. Continued



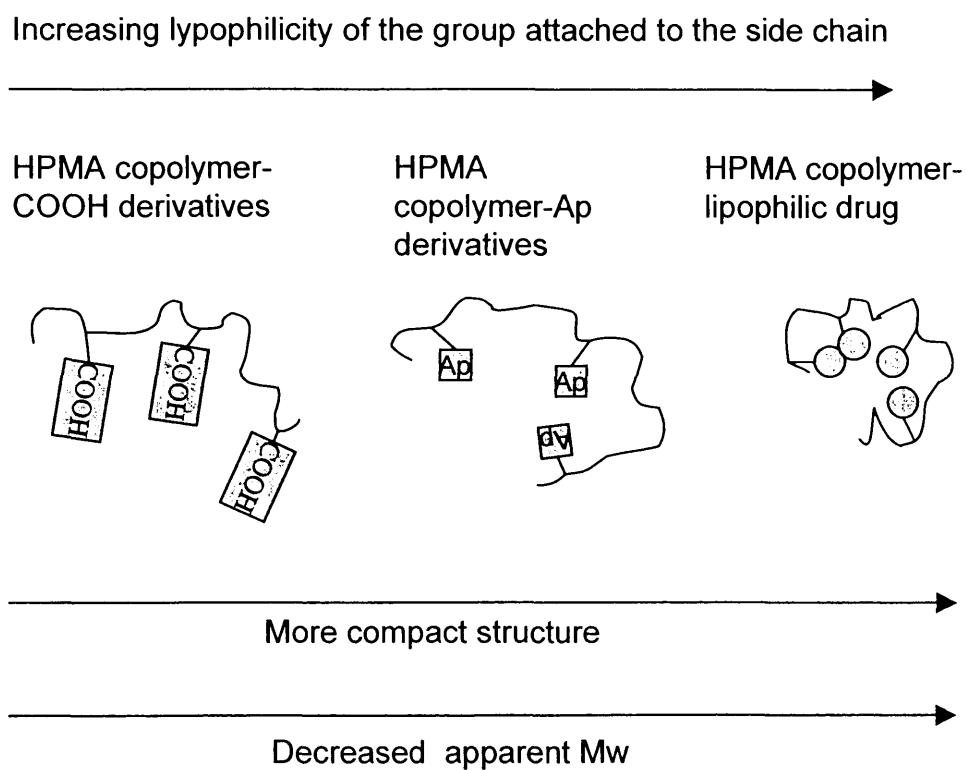


Figure. 3.18. Schematic representation of the potential explanation of the results obtained by GPC

HPMA copolymers have a high number of degrees of freedom and would more frequently have the most thermodynamically stable conformation. It has been suggested that HPMA copolymer-Dox exists in solution as unimolecular micelle (Uchegbu et al.,1996). This is a structure in which a single polymeric chain is arranged to expose the hydrophobic drug in the centre (hydrophobic core) leaving the hydrophilic chain on the outside. At present, however, physical evidence to support this hypothesis is still missing. Small angle neutron scattering SANS has successfully been applied to investigate the conformation in solution of polymer therapeutics (Wan et al., 2004). Recently, the HPMA copolymer presented in this work were analysed by SANS. The Gaussian coil model for polymer conformation showed the best fit to the raw scattering data (Vicent et al., 2005). HPMA copolymer-GFLG-Dox and HPMA copolymer-GFLG-AGM (both 5 mol%) had a similar Rg (7.7 and 7.9 nm, respectively). The increase in the side-chain content (from 5 to 10 mol%) led to an increase of the Rg to 16.5 nm for the AGM conjugate but only to 12.5 nm for the Dox conjugate. Indeed, the HPMA copolymer-GFLG-AGM-Dox also had a Rg of 12.8 nm. This suggests that the presence of Dox leads to a more compact structure, which could be explained by its tendency to display π - π stacking. These results clearly indicate that the drug loading and the chemical structure of the drug influence the polymer-conjugate conformation.

In conclusion, a library of HPMA copolymers containing Dox and/or AGM was synthesised and characterised. An acceptable loading of Dox and AGM was achieved so it was considered possible to move onto their biological evaluation (cytotoxicity and inhibition of the aromatase enzyme) (Chapter 4).

Chapter 4:

Evaluation of the cytotoxicity of HPMA copolymers-Dox \pm AGM and assessment of aromatase inhibition.

4.1. INTRODUCTION

In the previous chapter the synthesis and the characterisation of a family of conjugates carrying endocrine therapy and/or chemotherapy was described. Here the cytotoxicity of all conjugates is assessed and the ability of the HPMA copolymer-AGM conjugate to inhibit the aromatase enzyme is determined.

Cytotoxicity.

It was first necessary to choose an assay to assess cytotoxicity. Although MTT assay has been widely used to compare cytotoxicities of low molecular weight antitumour agents (Mosmann, 1983), HPMA copolymer conjugates (Wedge, 1991) and to determine the biocompatibility of novel polymers (Sgouras and Duncan, 1990), it is difficult to obtain an objective comparison between free and polymer-bound drug *in vitro* (discussed in Wedge, 1991; Duncan et al., 1992; Duncan 2003b). The chemical conjugation of a low molecular weight drug to a polymer leads to a marked change in its pharmacokinetic profile at cellular level. While low molecular weight drugs, including Dox or AGM, can rapidly pass across the cellular membrane, and immediately exert their biological effect, a polymer-drug conjugate has completely different cellular pharmacokinetics.

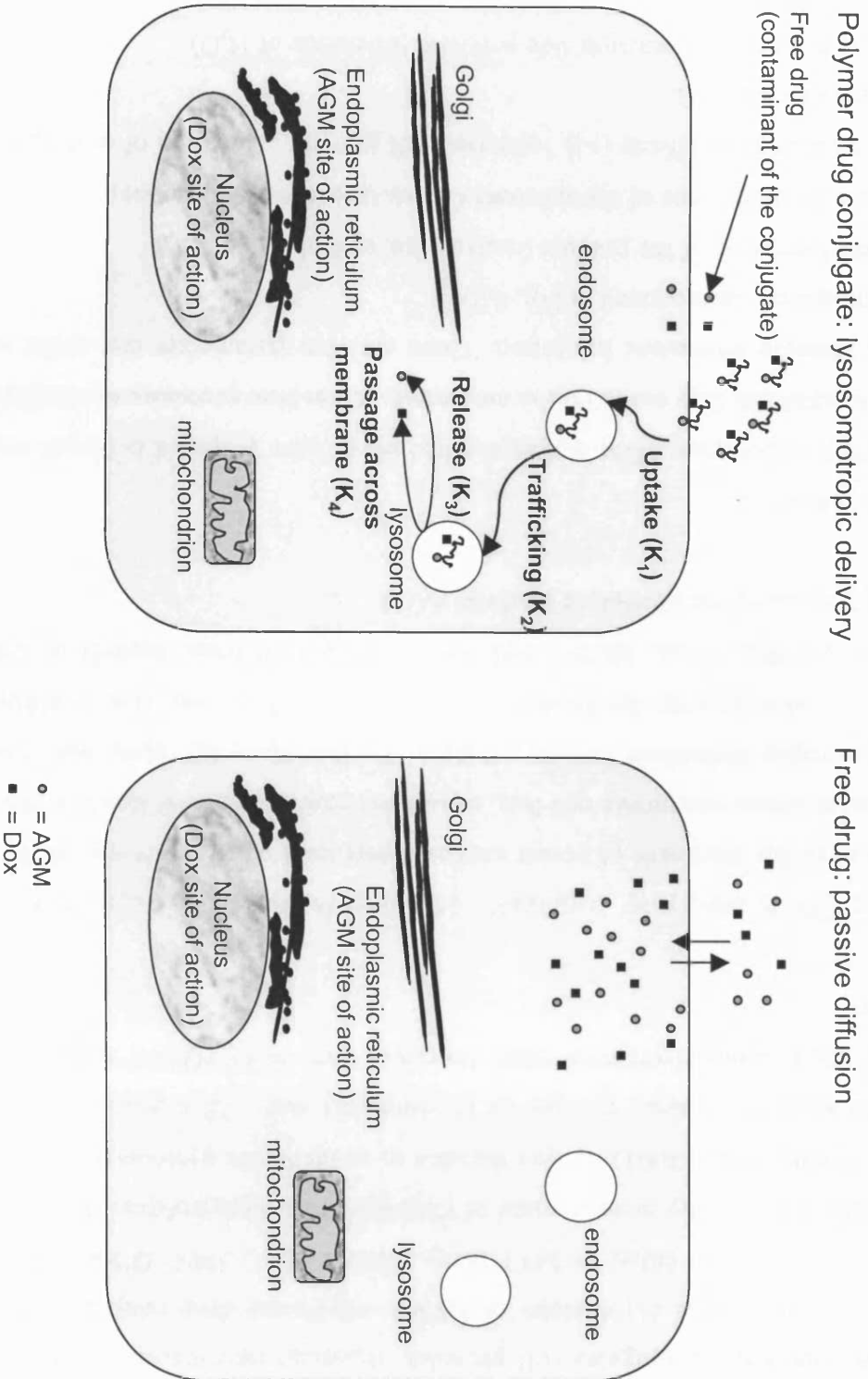
There are four steps that govern the ‘availability’ of a polymer-conjugated drug:

- (i) cellular uptake (K_1),
- (ii) trafficking to the lysosomal compartment (K_2)
- (iii) release of the drug from the polymer (K_3) mediated by cathepsin B
- (iv) passage of drug across the lysosomal membrane into the cytosol (K_4)

(reviewed in Lloyd, 2000) (Fig. 4.1).

As a result, the free drug typically shows higher toxicity *in vitro* than the conjugated drug (Duncan et al., 1992; O’Hare et al., 1993). Indeed, the *in vitro* activity of a conjugate has often been correlated with the activity of the residual contaminant free drug (Duncan et al., 1992) (Fig.4.1). For example, the HPMA copolymer-Dox conjugate which displayed activity clinically (Vasey et al., 1999) and enhanced antitumour activity compared to free Dox in many tumour models *in vivo* (Duncan et al. 1992; reviewed in Duncan, 2005) is almost completely inactive *in vitro* (~ 100 fold less active than free Dox) (Wedge, 1991; Duncan et al., 1992;

Fig. 4.1. Differences in the cellular pharmacokinetic of free drug and polymer-drug conjugates. Adapted from Tomlinson, 2003



Seymour et al., 1990). Nevertheless, it was felt that evaluation of the cytotoxicity of the HPMA copolymer conjugates still provides important information as to their relative cytotoxicity. The cytotoxicity of HPMA copolymer-drug conjugates has generally been evaluated either by MTT assay (Gianasi et al., 1999; O'Hare et al., 1993; Wedge, 1991) or by measurement of [³H] thymidine incorporation (Kovar et al., 2004; Rihova et al., 2001). It was decided to evaluate the cytotoxicity of the compounds using MTT assay because of its simplicity and a 72 h incubation was chosen to allow comparison with other literature data using HPMA copolymer conjugates.

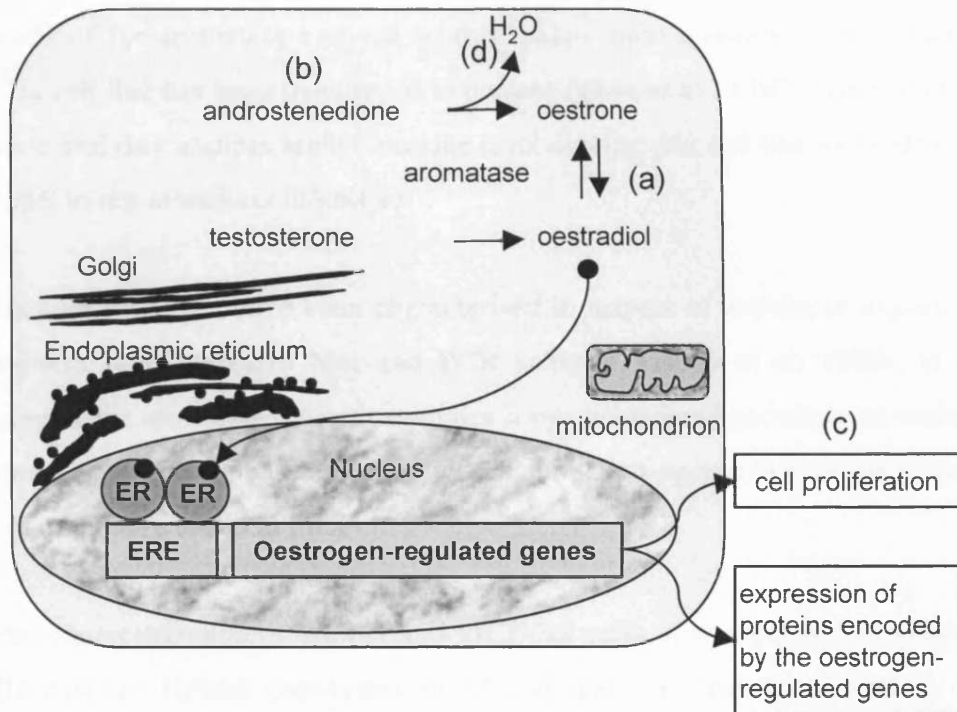
As the HPMA copolymer conjugates described in this study were designed specifically for the treatment of breast cancer it seemed logical to choose MCF-7 cells, a human breast carcinoma cell line, as *in vitro* model. This cell line is widely used as oestrogen-dependent *in vitro* system. Furthermore, the same cell line transfected to over-express the aromatase enzyme (MCF-7ca) was also available (Zhou et al., 1990). Thus, MCF-7 and MCF-7ca seemed ideal models to test conjugates containing the aromatase inhibitor AGM.

Aromatase inhibition

As HPMA copolymer-AGM conjugates had never been prepared before it was important to establish they could inhibit aromatase. It was first necessary to establish models to measure aromatase inhibition. There are four parameters that could in theory be measured (summarised in Fig. 4.2):

- a) the formation of the product (oestrone/oestradiol)
- b) the disappearance of the substrate (androstenedione/testosterone).
- c) the biological effects (e.g. increased cell growth; expression of oestrogen-regulated genes).
- d) the formation of reaction side-products (liberation of H₂O)

For these studies, cell-based assays and an isolated enzyme assay were used to study polymer conjugate aromatase inhibition.



Possible ways to monitor aromatase activity:

- (a) measure formation of the product (oestrone / oestradiol).
- (b) measure disappearance of the substrate (androstenedione / testosterone).
- (c) measure the biological effects (cell-proliferation/ expression of proteins encoded by the oestrogen-regulated genes).
- (d) measure formation of reaction side-products (H_2O).

Fig. 4.2. Parameters that can be measured to evaluate the enzymatic activity: formation of oestrogens (panel a); disappearance of androstenedione (panel b); cell proliferation (panel c); formation of side products – H_2O – (panel d)

Cell-based aromatase assay

Several *in vitro* and *in vivo* models have been described in the literature that allow measurement of aromatase activity (summarised in Table 4.1 and reviewed in Njar and Brodie, 1999). Wild type MCF-7 cells have been used as an *in vitro* model to test aromatase inhibitors (Kitawaki et al., 1993). However, they contain relatively low levels of the aromatase enzyme so this makes them a relatively poor model. MCF-7ca cell line has been transfected to contain (Zhou et al., 1990) higher level of aromatase and they express higher enzyme level making this cell line more efficient as a model to test aromatase inhibitors.

Although MCF-7ca have been characterised in respect of aromatase expression by Southern blot, Northern blot and PCR analysis, (Zhou et al. 1990), at the beginning of the aromatase inhibition studies it was considered necessary to evaluate the expression of the aromatase protein by Western Blotting and to compare it to the levels of aromatase found in MCF-7.

After characterisation of MCF-7 and MCF-7ca cells, it was decided to measure the effect of the HPMA copolymer-AGM conjugate on growth induced by the substrate. The aromatase enzyme has two substrates that are converted to oestrogens: testosterone and androstenedione. Androstenedione has been described to promote cell growth in MCF-7ca cells across a range of concentrations (1 to 100 nM) and this mitogenic effect was completely reverted in the presence of the aromatase inhibitor fadrozole hydrochloride (Santner et al. 1993). This is a relatively simple assay and although it requires a long incubation time, it is also inexpensive. It was decided to first, test the effect of both androstenedione and testosterone on the growth of MCF-7ca in order to select the substrate and the concentration that gave the maximum stimulatory effect. Then, free AGM and HPMA copolymer-AGM were tested with this system.

As the growth stimulation assay is an indirect measurement it was considered important to try and measure directly the effect on intracellular aromatase. A radiometric assay was used where cells were incubated with the aromatase substrate [³H]androstenedione. The [³H]H₂O released from its metabolism in the presence and

Table 4.1. Experimental models used to assess aromatase activity

System	Type of system	References
<i>In vitro</i>		
• microsomal preparation from human placenta	enzymatic mixture	Ryan, 1959
• JEG-3 or JEG	Human choriocarcinoma cells	Johnston <i>et al.</i> , 1984
• MCF-7	oestrogen-dependent breast cancer cells	Kitawaki <i>et al.</i> , 1993 Macaulay <i>et al.</i> , 1994
• MCF-7ca	MCF-7 transfected with aromatase	Zhou <i>et al.</i> , 1990
<i>In vivo</i>		
• female rat	determination of inhibition of ovarian ovulation	Brodie <i>et al.</i> , 1976
• MCF-7ca inoculated into ovariectomised nude mice	anti-tumour effect	Yue <i>et al.</i> , 1995
• male rhesus monkey	it is a model where most of the circulating oestrogen is of extragonadal origin.	Brodie <i>et al.</i> 1980 Longcope <i>et al.</i> 1988

absence of AGM and HPMA copolymer-AGM could then be measured (Long et al., 2002).

Enzymatic aromatase assay

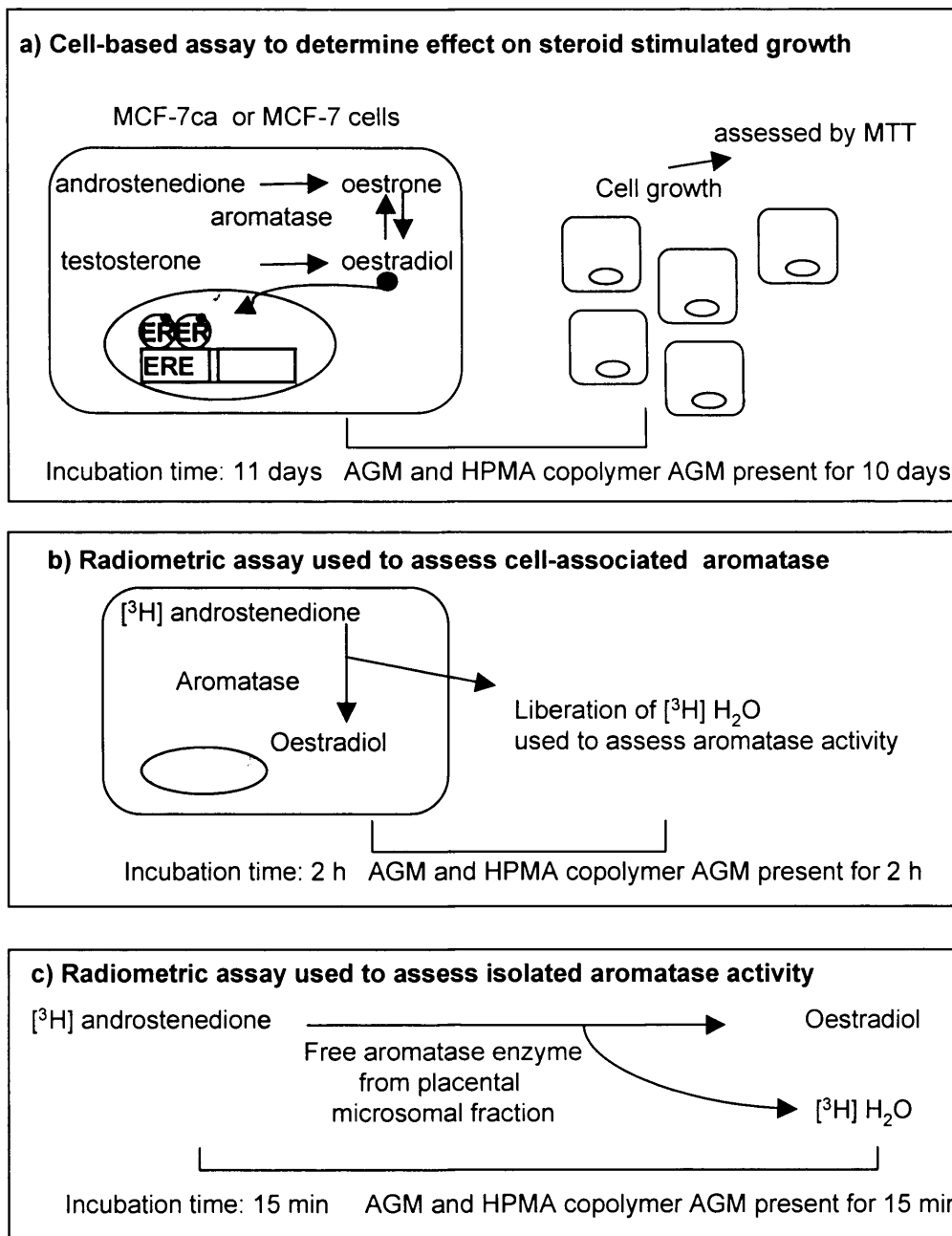
To see more directly the effect of free AGM and HPMA copolymer-AGM on the free enzyme, a microsomal extract from placenta was selected as model using the same radiometric assay described above. For clarity, the *in vitro* systems used in this chapter to assess aromatase activity (with their advantages and disadvantages) are summarised in Fig. 4.3.

To summarise, the aims of this study were: (i) to evaluate the levels of aromatase in MCF-7 and MCF7ca cells by Western blotting, (ii) to test the cytotoxicity of free Dox and AGM, the HPMA copolymer-Dox, the HPMA copolymer-AGM and the combination conjugate HPMA copolymer-Dox-AGM, and (iii), to establish whether HPMA copolymer-AGM could inhibit the aromatase enzyme, and to compare its activity with free AGM. Three different assays were used for this purpose.

4.2. METHODS

Most of the methods used here were described previously in Chapter 2. The method used for Western blot analysis was described in section 2.3.16. For determination of cytotoxicity against MCF-7 and MCF-7ca, free and polymer-bound drugs were tested by MTT assay (described in section 2.3.9) at the following concentration ranges:

Dox:	0.05 – 100 $\mu\text{g}/\text{mL}$
AGM:	0.01 – 2 mg/mL
AGM + Dox:	0.002 – 2 mg/mL AGM 0.1 – 100 $\mu\text{g}/\text{mL}$ Dox
HPMA copolymer-Dox:	0.629 – 126 $\mu\text{g}/\text{mL}$
HPMA copolymer-AGM:	4.6 – 186 $\mu\text{g}/\text{mL}$
HPMA copolymer-Dox + HPMA copolymer-AGM:	1.57 – 157 $\mu\text{g}/\text{mL}$ Dox-equiv. 1.5 – 150.7 $\mu\text{g}/\text{mL}$ AGM-equiv.
HPMA copolymer-AGM-Dox:	0.47 – 235 $\mu\text{g}/\text{mL}$ Dox-equiv. 0.51 – 254 $\mu\text{g}/\text{mL}$ AGM-equiv.



Method	Advantages	Disadvantages
a)	Easy Non expensive	Non specific Long
b)	More specific	
c)	More specific	Artificial system

Fig. 4.3. The three model systems used to evaluate inhibition of aromatase, their advantages and disadvantages

HPMA copolymer-Dox + free AGM: 12.6 - 126 $\mu\text{g/mL}$ Dox-equiv.
0.2 – 2 mg/mL AGM

The method used to determine whether the polymer conjugates interfere with the MTT assay is described below. The protocols used for assessment of aromatase activity in cells (sections 2.3.10, 2.3.11, 2.3.13), and against the free enzyme (2.3.12) were described in Chapter 2. As the cytotoxicity of Dox precludes evaluation of aromatase inhibition by the combination conjugate, these studies were designed to examine the mechanism of action only of the HPMA copolymer-GFLG (5%)-AGM and to compare it to free AGM.

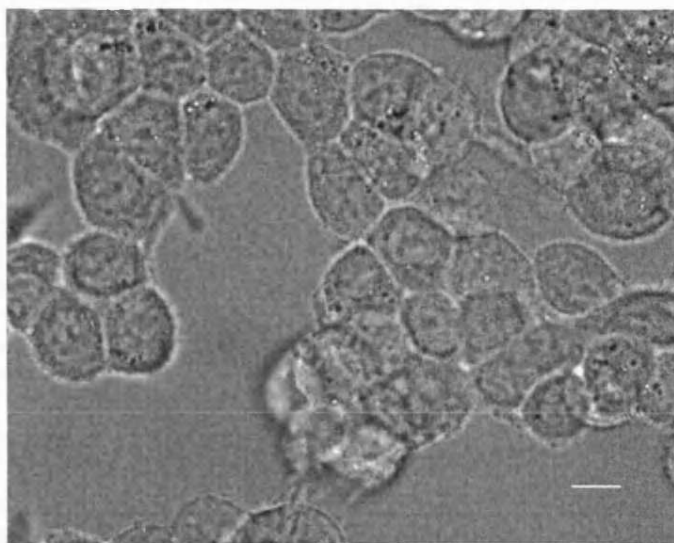
4.2.1. Evaluation of potential interferences of the HPMA copolymer conjugates with the MTT assay

MCF-7 cells were harvested and seeded as described before (section 2.3.6.3) in WRPMI + 5 % SFBS at a seeding density of 4×10^4 cells/mL in a 96-well plate. Cells were allowed to grow for 8 days during which time the medium was periodically replaced with fresh medium (on day 1 and day 5). On day 8, the medium was removed and fresh medium containing the polymer solution was added (concentrations used 0 – 5 mg/mL). The MTT solution (20 μL of 5 mg/mL in PBS) was also added to each well and the plates were placed into the incubator for 5 h. At the end of the incubation period the supernatant was removed and the crystals produced by reaction of the MTT with the cellular NADH and NADPH were dissolved by addition of DMSO (100 μL). The plates were placed again in the incubator for 30 min, to allow complete dissolution of the crystals and the absorbance was then measured at 550 nm. Data are expressed as absorbance measured at 550 nm for each polymer concentration.

4.3. RESULTS

The morphology of MCF-7 and MCF-7ca cells is similar and it is shown in Fig. 4.4. When the cell lines were assessed for the presence of aromatase by Western blotting, a band was observed at ~ 55 KDa for both cell lines (consistent with aromatase molecular weight) (Turner et al., 2002). The enzyme levels were higher in MCF-7ca than in MCF-7 cells (Fig. 4.5).

(a) MCF-7ca



(b) MCF-7

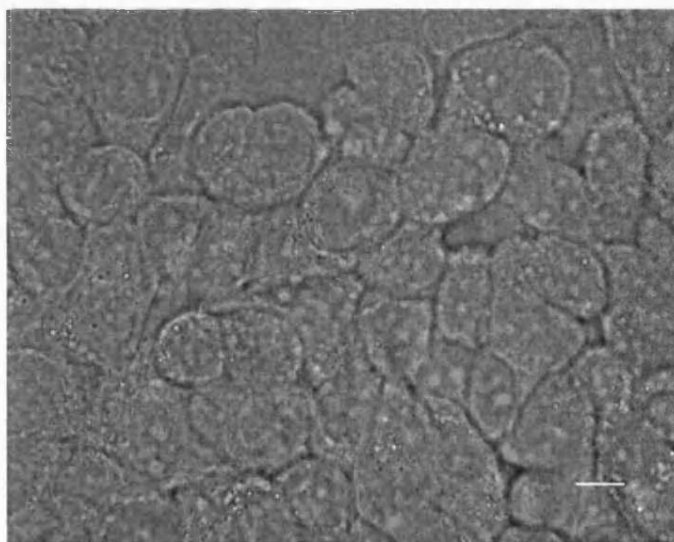


Fig. 4.4. Morphology of MCF-7ca (panel a) and MCF-7 (panel b). Pictures taken by bright field microscopy. Size bar = 10 μm

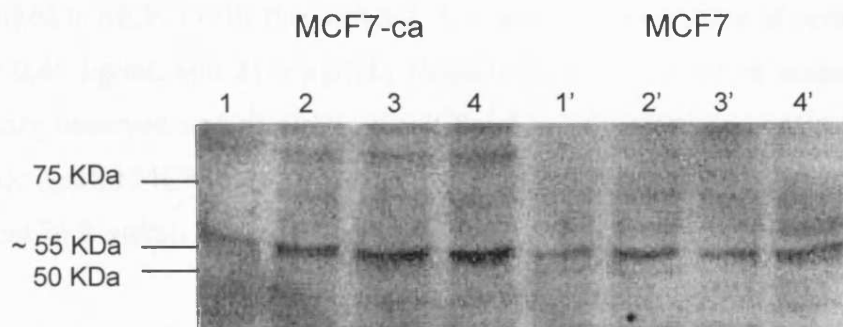


Fig. 4.5. Aromatase expression in MCF-7 and MCF-7ca. Example of western blot showing the aromatase enzyme in MCF-7 and MCF-7ca. Loading was adjusted to protein content, as determined using a modification of the Lowry assay (lane 1 and 1' = 20 μ g of protein; lane 2 and 2' = 40 μ g of protein; lane 3 and 3' = 60 μ g of protein; lane 4 and 4' = 80 μ g of protein)

Cytotoxicity

The cytotoxicity of the free drugs AGM and Dox alone or in combination and their conjugates was investigated in presence of oestradiol (10^{-9} M) or in its absence (Fig. 4.6a - h). Tables 4.2 and 4.3 summarise the IC_{50} values found. The results obtained can be summarised as follows:

Free Dox was cytotoxic in both cell lines (Fig. 4.6a). However, toxicity was more marked in MCF-7 cells than in MCF-7ca cells (in the presence of oestradiol the IC_{50} was 0.41 $\mu\text{g/mL}$ and 21.6 $\mu\text{g/mL}$, respectively). In absence of oestradiol, the cytotoxicity observed was similar to that obtained in its presence. Again, Dox was more toxic against MCF-7 cells than against MCF-7ca cells (the IC_{50} values were 1.9 $\mu\text{g/mL}$ and 26.8 $\mu\text{g/mL}$ for MCF-7 and MCF-7ca, respectively).

Free AGM was relatively non-toxic up to 0.5 mg/mL. Above this concentration, cell viability started to decrease more (Fig. 4.6b). AGM had a similar cytotoxicity in the two cell lines. In presence of oestradiol, the IC_{50} was 1.2 mg/mL and 1.04 mg/mL for the MCF-7 and MCF-7ca cells, respectively). In absence of oestradiol, no cytotoxicity was observed over the range of concentrations tested ($IC_{50} > 2$ mg/mL for both MCF-7 and MCF-7ca cells).

Free AGM + free Dox. When these drugs were added together as a simple mixture, the pattern of cytotoxicity observed clearly resembled that of free Dox (Fig. 4.6c).

HPMA copolymer-Dox. The conjugate carrying only Dox was non-toxic at all concentration tested and in both cell lines ($IC_{50} > 125.8$ $\mu\text{g/mL}$ Dox-equiv.) (Fig. 4.6d). At the highest concentrations (approximately above 90 $\mu\text{g/mL}$ Dox-equiv.) an increase in the MTT-related absorbance was seen.

HPMA copolymer-AGM. Also in the case of the HPMA copolymer-AGM, no toxicity was observed over the range of concentrations tested ($IC_{50} > 180$ $\mu\text{g/mL}$) (Fig. 4.6e). Again, increased MTT-related absorbance was seen at higher concentrations of polymer.

Table 4.2. IC₅₀ values of free and polymer-bound AGM and Dox and their combinations (with 10⁹ M oestradiol)

Compounds	IC ₅₀ (µg/mL Dox-equiv.)*		IC ₅₀ (µg/mL AGM-equiv.)*	
	MCF-7	MCF-7 ca	MCF-7	MCF-7 ca
AGM	NA	NA	1223.3 ± 274	1043 ± 441
Dox	0.41 ± 0.16	21.6 ± 8.5	NA	NA
Dox + AGM	0.38 ± 0.09	15.6 ± 7.6	7.4 ± 1.7	307.7 ± 150.7
HPMA-AGM	NA	NA	> 180	> 180
HPMA-Dox	> 125.8	> 125.8	NA	NA
HPMA-Dox + AGM	62.3 ± 11.7	60.0 ± 8.9	986.7 ± 177.0	966.7 ± 145.2
HPMA-Dox + HPMA-AGM	> 157.2	> 157.2	> 150.7	> 150.7
HPMA-AGM-Dox	75.4 ± 45.2	8.2 ± 3.1	76.85 ± 45.3	8.8 ± 3.5

* IC₅₀ values are expressed as mean ± S.E.M, n = 3.

NA = not applicable

Table 4.3. IC₅₀ values of free and polymer-bound AGM and Dox and their combinations (without oestradiol)

Compounds	IC ₅₀ (µg/mL Dox-equiv.)*		IC ₅₀ (µg/mL AGM-equiv.)*	
	MCF-7	MCF-7 ca	MCF-7	MCF-7 ca
AGM	N/A	NA	> 2000	> 2000
Dox	1.9 ± 1.2	26.75 ± 3.9	NA	NA
Dox +AGM	11.16 ± 10.4	31.2 ± 8.3	210 ± 195	608.3 ± 169.2
HPMA-AGM	NA	NA	> 180	> 180
HPMA-Dox	> 125.8	> 125.8	NA	NA
HPMA-Dox + AGM	68.5 ± 13.0	69.8 ± 9.3	1100.0 ± 200.0	948.3 ± 61.2
HPMA-Dox + HPMA-AGM	> 157.2	> 157.2	> 150.7	> 150.7
HPMA-AGM-Dox	21.8 ± 8.5	12 ± 7.6	22.5 ± 8.9	9.9 ± 5.1

* IC₅₀ values are expressed as mean ± S.E.M, n = 3.

NA = not applicable

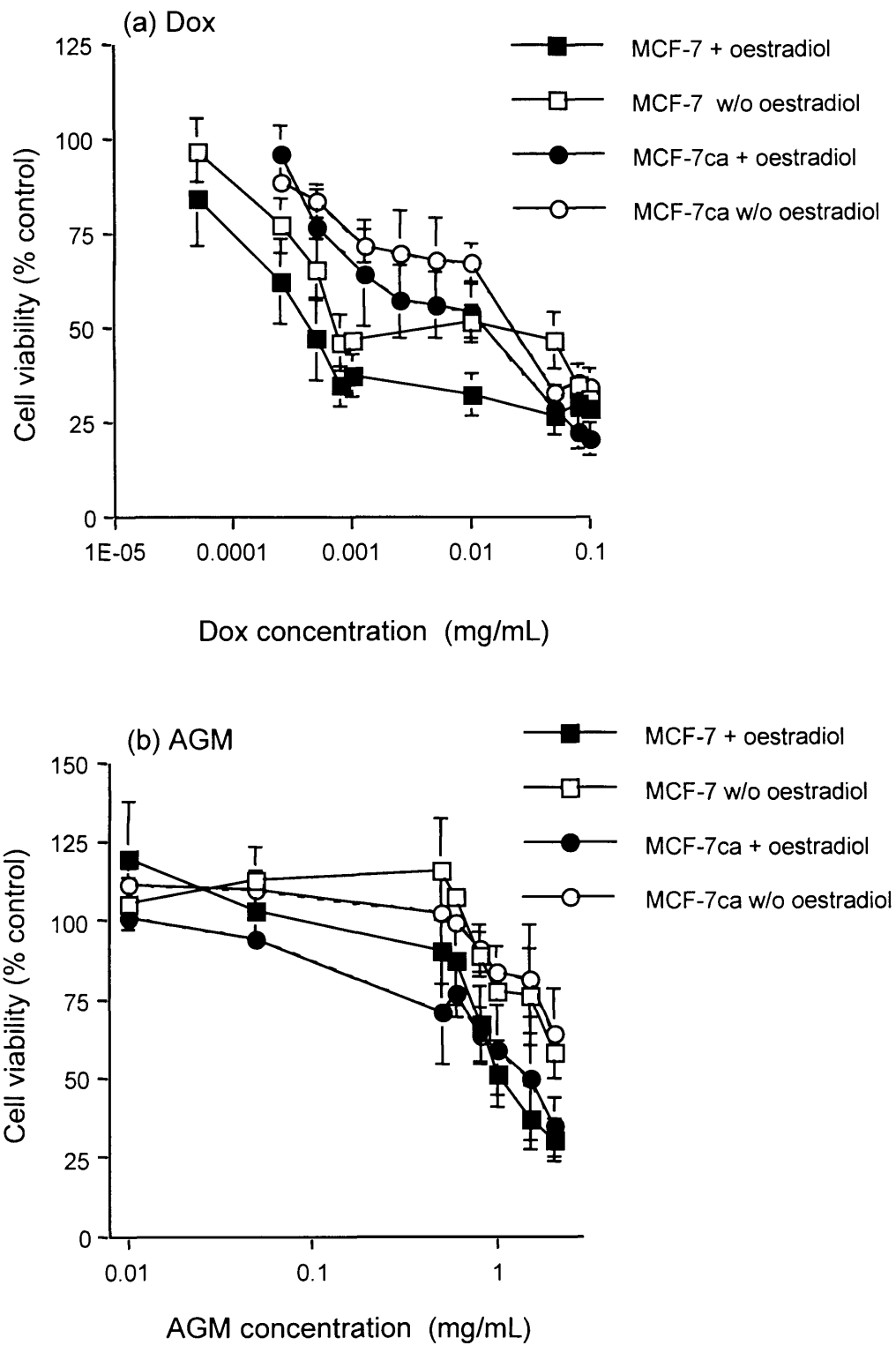


Fig. 4.6. *In vitro* cytotoxicity of Dox, AGM, and the HPMA copolymer conjugates. The data shown are against MCF-7 (□) and MCF-7ca (○) cells grown in the presence (full symbol) and absence (empty symbol) of oestradiol. Dox (panel a), AGM (panel b), Dox + AGM (panel c), HPMA copolymer-Dox (panel d) HPMA copolymer-AGM (panel e) HPMA copolymer-AGM + HPMA copolymer-Dox (panel f) HPMA copolymer-Dox-AGM (panel g) and HPMA copolymer-Dox + AGM (panel h). Data shown represent mean \pm SEM; n = 3

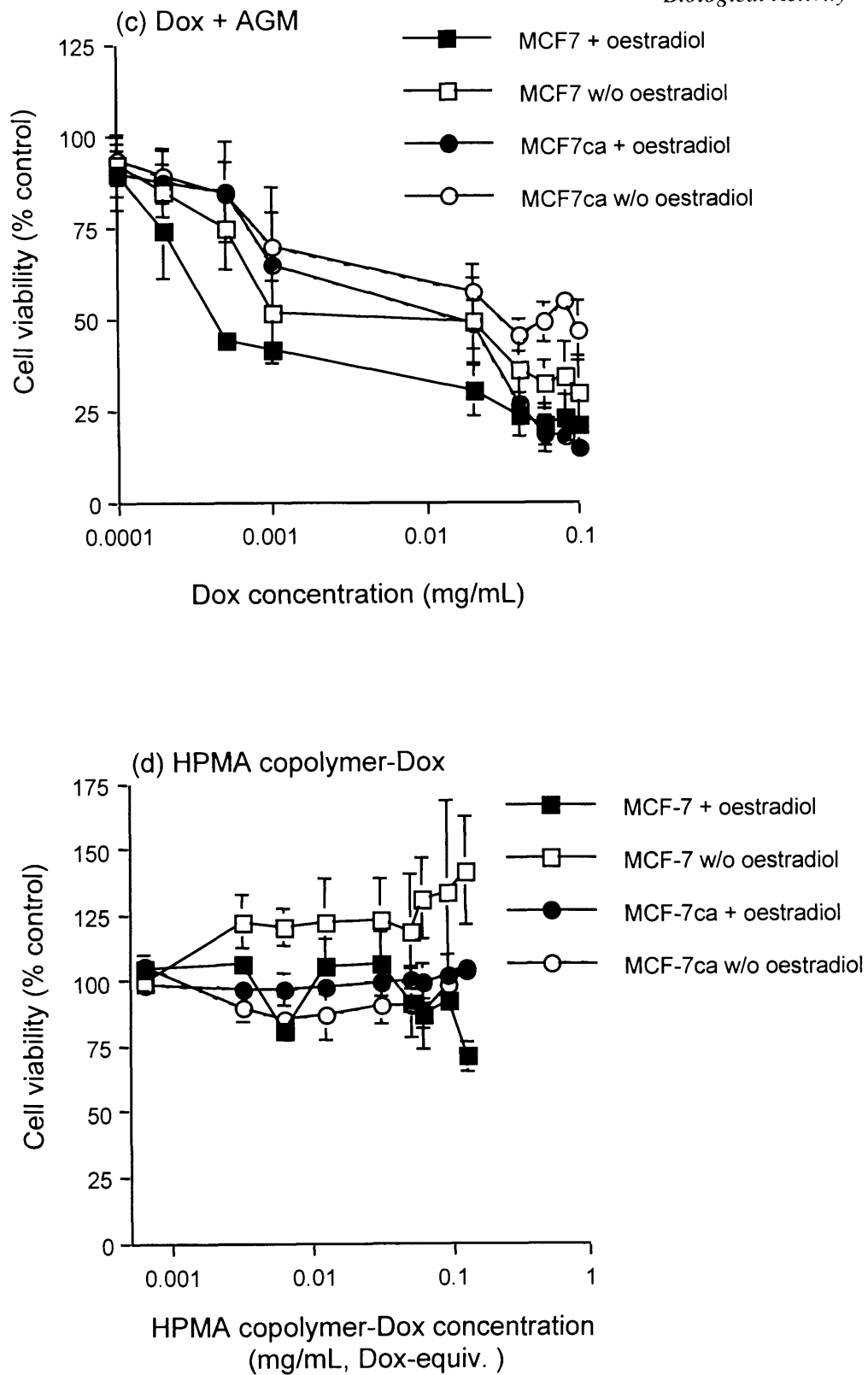


Fig. 4.6. Continued

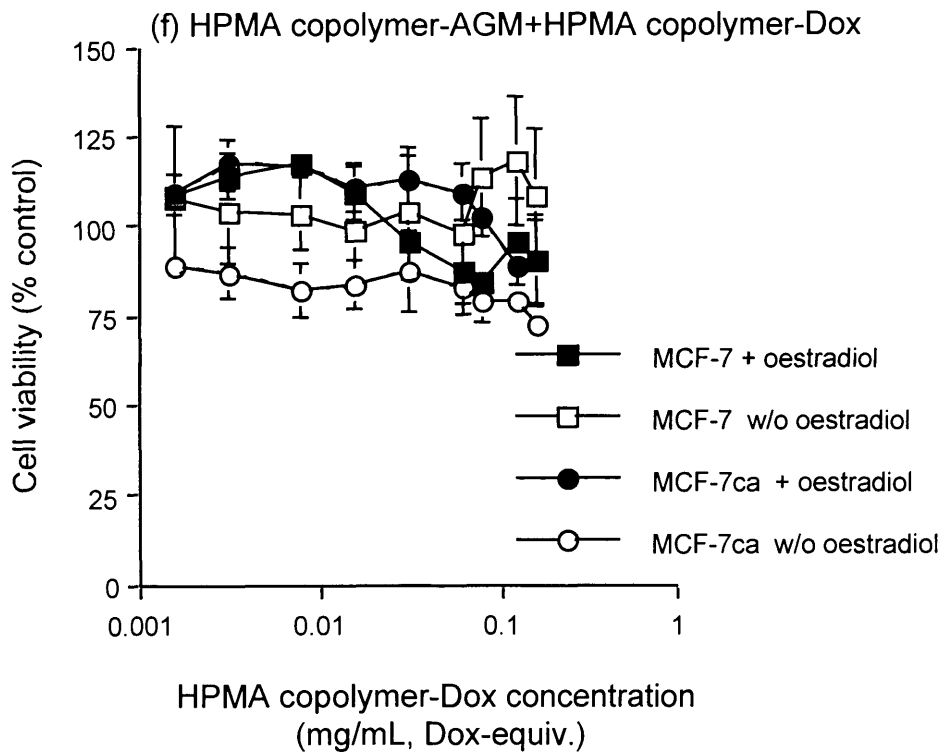
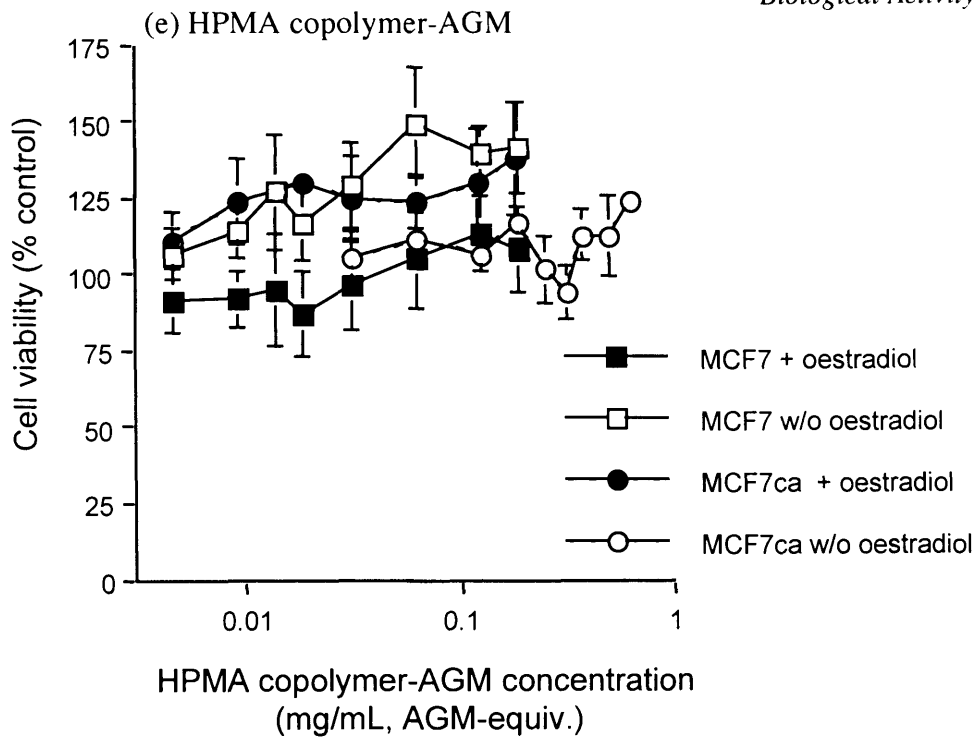


Fig. 4.6. Continued

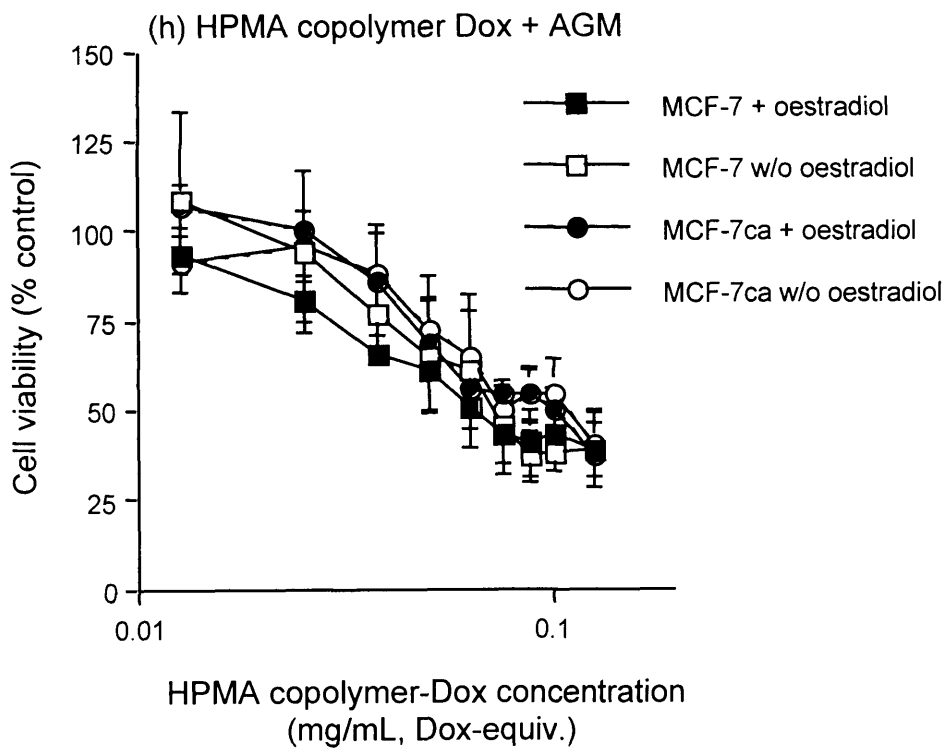
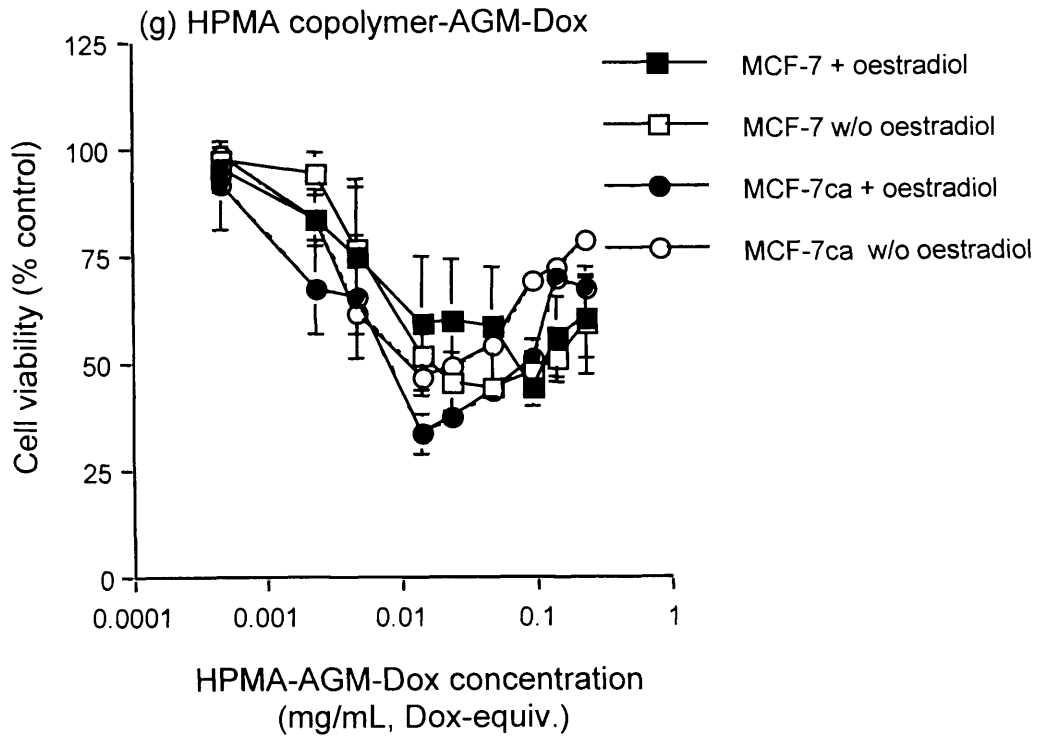


Fig. 4.6. Continued

HPMA copolymer-Dox + HPMA copolymer-AGM. When the HPMA copolymer-Dox and the HPMA copolymer-AGM were simultaneously added as a mixture no increase in cytotoxicity was seen (Fig. 4.6f). Indeed, this mixture was non-toxic over the concentration range tested ($IC_{50} > 157.2 \mu\text{g/mL Dox-equiv.}$ and $IC_{50} > 150.7 \mu\text{g/mL AGM-equiv.}$).

HPMA copolymer-AGM-Dox. Interestingly, when the two drugs were simultaneously attached to the same HPMA copolymer backbone greater cytotoxicity was seen for the HPMA copolymers carrying individual drugs as well as for the mixture of individual conjugates (Fig. 4.6g). This increased cytotoxicity was most dramatic in MCF-7ca cells where the HPMA copolymer-AGM-Dox conjugate had equivalent toxicity to that of the free Dox (Fig. 4.6g). In all cases, the cell viability decreased rapidly at lower concentrations ($< 10 \mu\text{g/mL Dox-equiv.}$), then the curve started plateauing and, eventually rising at higher concentrations ($> 100 \mu\text{g/mL Dox-equiv.}$).

HPMA copolymer-Dox + free AGM. The mixture of HPMA copolymer-Dox with free AGM led to an *apparent* increased cytotoxicity if Dox concentrations are considered ($IC_{50} \sim 60 \mu\text{g/mL Dox-equiv.}$ in all cases). However, this effect was only due to the free AGM as clear when a comparison is made with the cytotoxicity profile obtained for free AGM (Fig.4.6b) and with the IC_{50} values obtained for free AGM (Table 4.2 – 4.3).

To investigate why an increased absorbance was seen at higher concentrations of polymer, the effect of the presence of the conjugates on the MTT assay was examined. The addition of HPMA copolymer-AGM-Dox, immediately prior to the start of the assay led to increased absorbance which was dependent on the conjugate concentration added (Fig. 4.7a). At the highest concentration tested (5 mg/mL of polymer conjugate), the absorbance was double the absorbance seen in the absence of the conjugate. To exclude the possibility that this effect was just due to the colour of Dox, the same experiment was repeated for the HPMA copolymer carrying only AGM. In this case an increased absorbance was also observed in presence of the conjugate (at 5 mg/mL 1.5 fold than the control). However, in this case the increase seen was lower than for the HPMA copolymer-AGM-Dox conjugate (Fig. 4.7b).

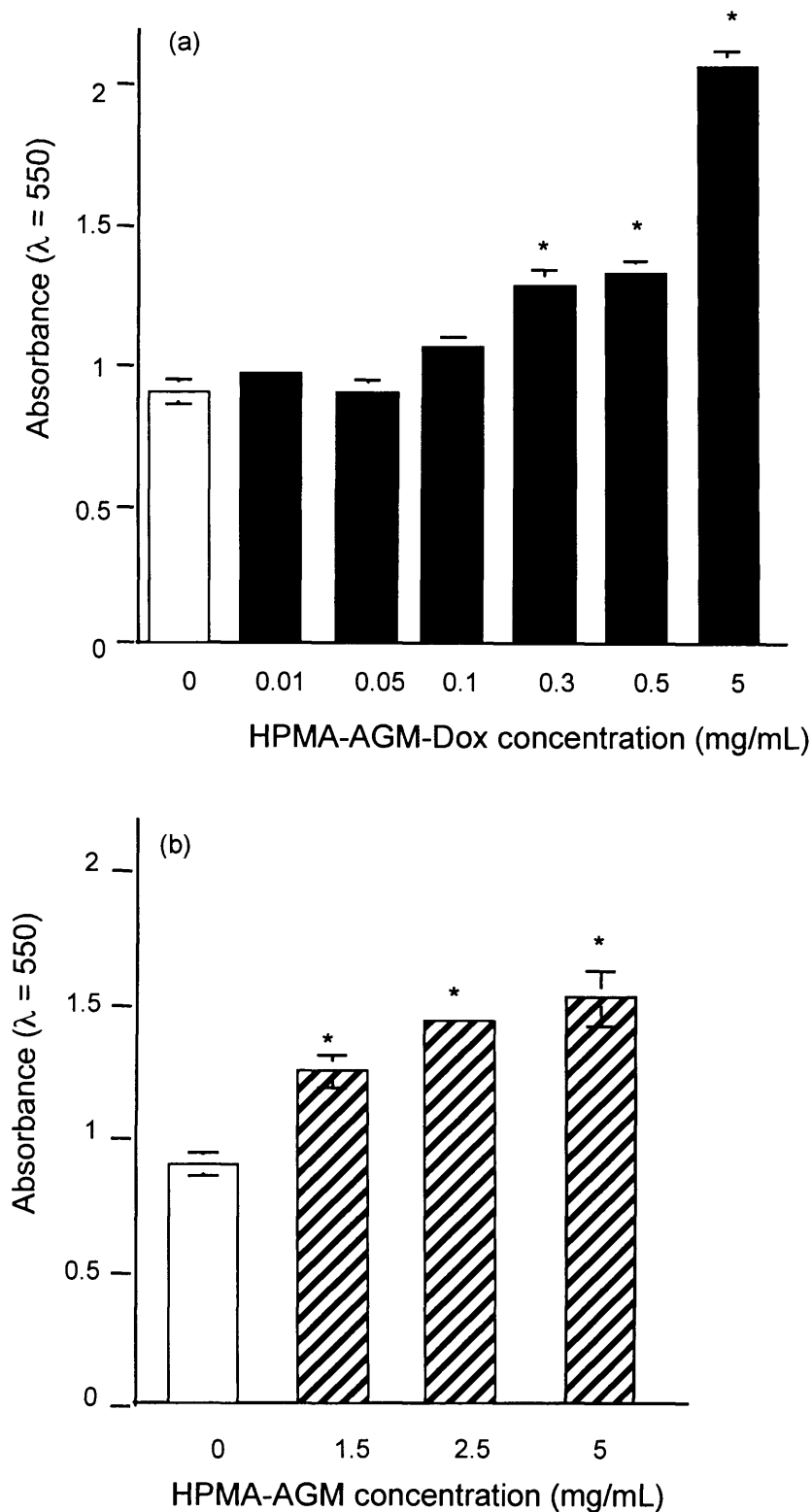


Fig. 4.7. Investigation of possible interference of HPMA copolymer conjugates with the MTT assay. Panel (a) shows the absorbance observed in presence of HPMA copolymer-AGM-Dox and panel (b) in presence of HPMA copolymer-AGM at the concentrations indicated. Statistical significance against control (0 mg/mL) was determined at $p \leq 0.05$ (*) using one-way ANOVA and Bonferroni post hoc test. Values represent mean \pm S.E.M. $n = 3$

Aromatase inhibition

To establish a cell-based model to study aromatase inhibition, cell growth was stimulated by addition of the aromatase substrates testosterone and androstenedione. The experiments with testosterone were performed in the Centre for Polymer Therapeutics by Neal Penning under my supervision.

Testosterone showed mitogenic activity in MCF-7ca cells at concentrations of 10^{-6} - 10^{-7} M (Fig. 4.8b). Lower concentrations had no effect. Neither testosterone nor androstenedione had an effect on the growth of MCF-7 (Fig. 4.8a and 4.9a). Androstenedione also had a mitogenic effect on MCF-7ca cells, and this was more marked than seen for testosterone. In addition, androstenedione-stimulated growth occurred across a broader range of concentrations (10^{-8} – 10^{-6} M) (Fig. 4.9b).

Therefore an androstenedione concentration of 5×10^{-8} M was chosen for further experiments. A time-dependent study showed that although growth stimulation was already seen after 8 days, it was more marked on day 11 (Fig. 4.9c). Consequently, MCF-7ca cells and an incubation time of 11 days were selected for further studies.

Addition of free AGM to the MCF-7ca cells incubated in the presence of androstenedione caused a concentration-dependent reduction in growth (Fig. 4.10a). At 0.2 mg/mL AGM completely inhibited the androstenedione-mediated growth stimulation. Similarly, the HPMA copolymer-GLFG-AGM conjugate caused a concentration-dependent growth inhibition (Fig. 4.10b). At higher concentrations, both free and polymer-bound AGM decreased cell viability to a level that was lower than seen for the controls with or without androstenedione (Fig. 4.10).

When the MCF-7ca aromatase activity was further investigated using a radiometric assay, free AGM (Fig. 4.11a) decreased enzyme activity in a concentration dependent manner to give a maximum inhibition of ~ 25 %. HPMA copolymer-AGM produced a similar pattern of inhibition results at 0.2-0.4 mg/mL AGM-equiv. (Fig. 4.11b). However, surprisingly at the highest HPMA copolymer-AGM concentrations (0.8 mg/mL AGM-equiv.) aromatase inhibition was lost. Interestingly, the maximum inhibition caused by AGM and HPMA copolymer-AGM was equivalent to the baseline activity seen in MCF-7 cells.

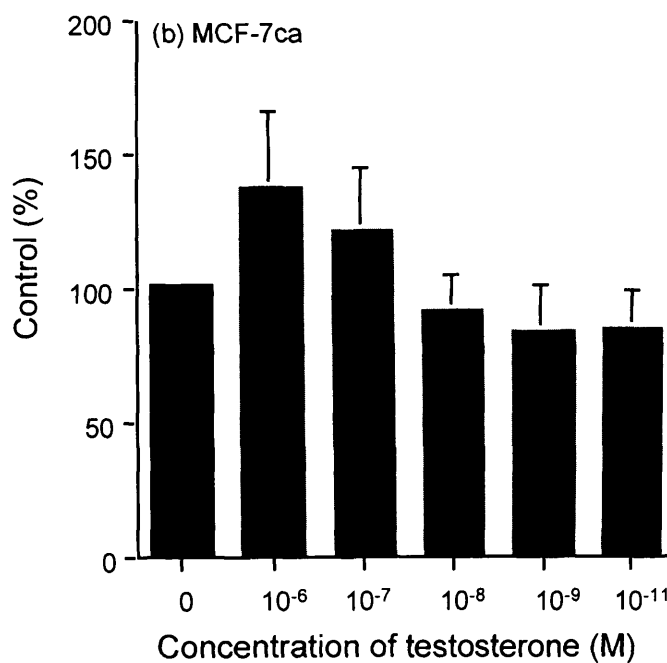
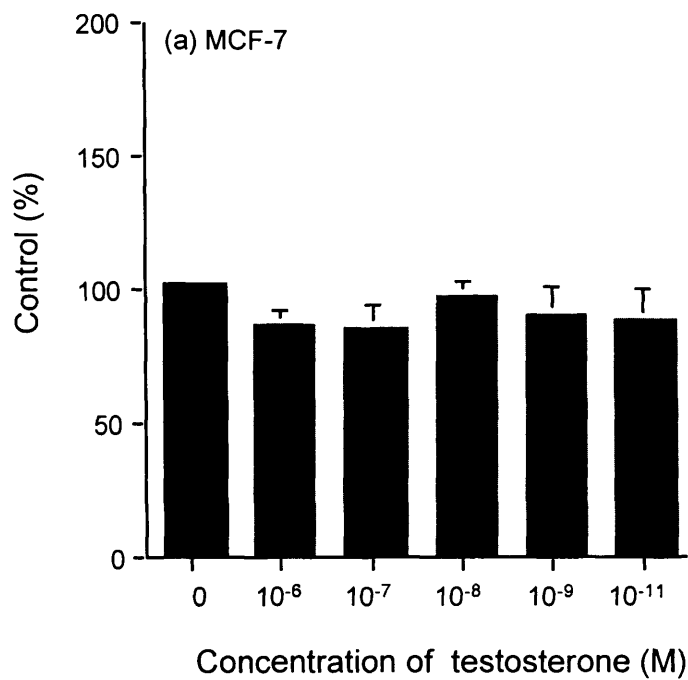


Fig. 4.8. Effect of testosterone on MCF-7 (panel a) and MCF-7ca (panel b) cell growth. The growth of cells in the presence of these steroids (at the concentrations shown) was measured on day 11 using the MTT assay. The results are expressed as percentage of the control with no addition. The values represent mean \pm SEM; n = at least 3

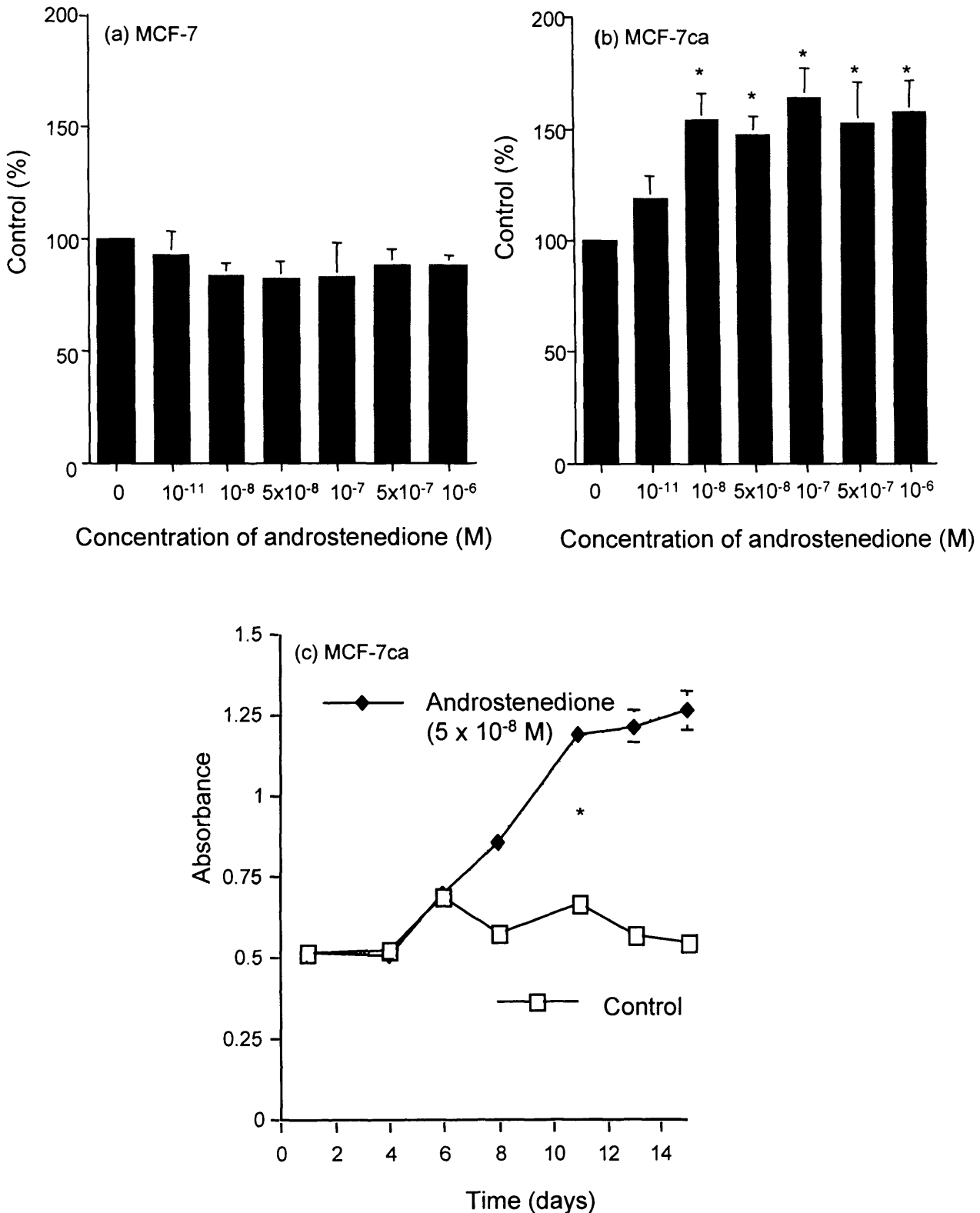


Fig. 4.9. Effect of androstenedione on MCF-7 and MCF-7ca cell growth. In panels a and b the growth of cells in the presence of this steroid (at the concentrations shown) was measured on day 11 using the MTT assay. The results are expressed as percentage of the control with no addition. For panel (c) cell growth was measured every 2 - 3 days until day 15 using MTT assay. Statistical significance against control (0 M) was determined at $p \leq 0.05$ (*) using one-way ANOVA and Bonferroni post hoc test for panel (a) and (b); and at day 11 by Student's t test for panel (c). The values represent mean \pm SEM; n = at least 3

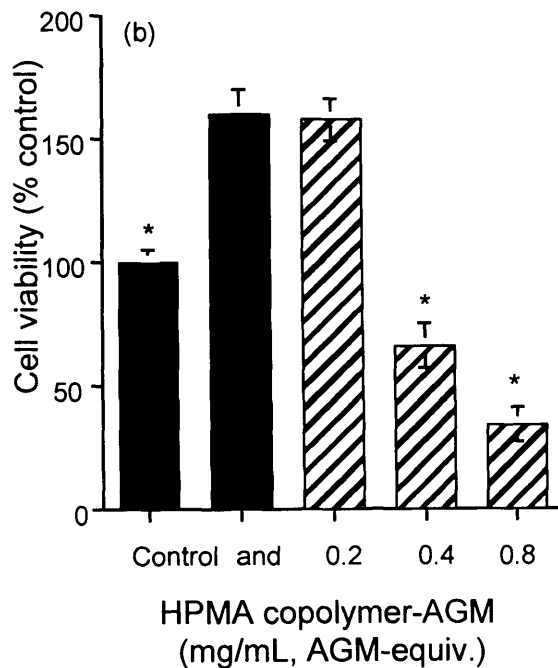
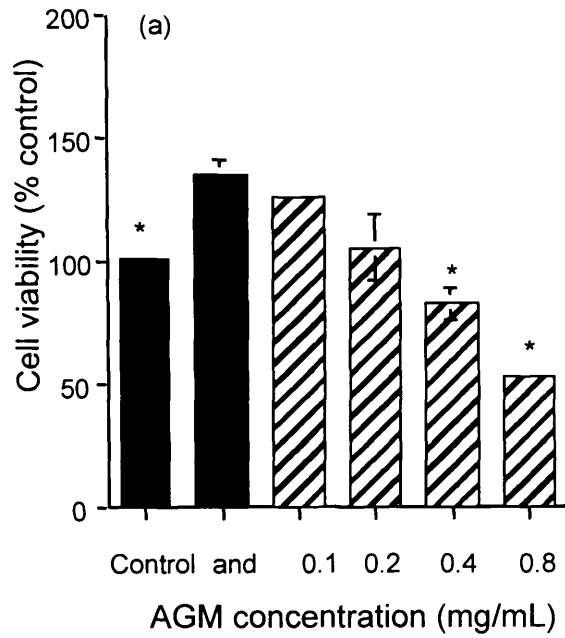


Fig. 4.10. Inhibition of the mitogenic effect of androstenedione by free AGM (panel a), and HPMa copolymer-GFLG-AGM (panel b). Cell growth was measured after 11 days using MTT assay and the results are expressed as percentage of the control without addition. The values represent mean \pm SEM; $n = 3$ for AGM and $n = 6$ HPMa copolymers-AGM, respectively. Statistical significance against androstenedione sample was determined at $p \leq 0.05$ (*) using one-way ANOVA and Bonferroni post hoc test

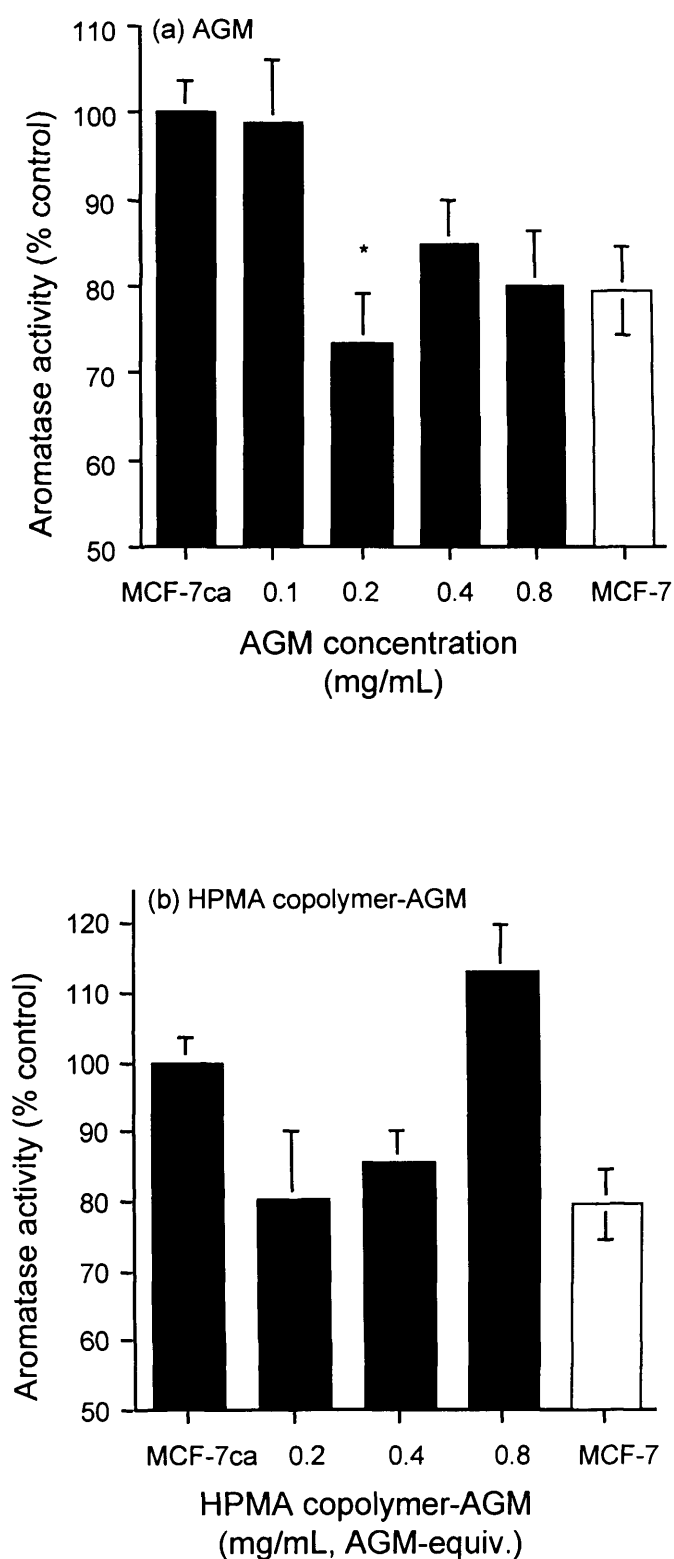


Fig. 4.11. Effect of free and polymer-bound AGM on aromatase activity in MCF-7ca cells. Panel (a) free AGM and panel (b) HPMA copolymer-AGM at the concentrations shown. Results obtained with MCF-7 cells with no addition are shown for comparison. Data are expressed as a percentage of the activity seen in MCF-7ca without addition, mean \pm SEM and $n \geq 12$. Statistical significance was determined at $p \leq 0.05$ (*) using one-way ANOVA and Bonferroni post hoc test

Finally, aromatase inhibition was also studied using isolated microsomal enzymes. Whilst, free AGM showed marked dose-dependent aromatase inhibition (Fig. 4.12a), the HPMA copolymer-AGM did not cause any aromatase inhibition (Fig. 4.12a and b). Indeed, no inhibition occurred even at concentrations 10-fold higher than those used for free AGM (Fig. 4.12).

4.4. DISCUSSION

Although the use of polymer anticancer-drug conjugates to deliver well-known cytotoxic drugs including Dox (Vasey et al., 1999), platinates (Rademaker-Lakhai et al. 2004; Rice & Howell, 2004) and paclitaxel (Singer et al., 2005) more selectively to tumour tissue is becoming well established (reviewed in Duncan, 2003a; Duncan 003b), the use of drug delivery systems to deliver endocrine therapy is largely unexplored. A limited amount of studies are described where a drug delivery system is used to improve endocrine therapy efficacy. Tamoxifen has been encapsulated in nanospheres (Brigger et al., 2001), in micelles (Cavallaro et al., 2004) and in nanoparticles (Fontana et al., 2005; Shenoy and Amiji, 2005). *In vitro* evaluation of these systems is often limited to the assessment of their cytotoxicity, generally by MTT assay against MCF-7 (Fontana et al., 2005; Cavallaro et al. 2004). A polymeric drug was also described that contained diethyl-stilbestrol (Vicent et al., 2004). Also in this case, only *in vitro* evaluation of cytotoxicity was described (by MTT assay - 72 h incubation-). However, the activity of this polymer therapeutic on the effects and the signalling of steroids was not evaluated. Due to the limited amount of studies describing drug delivery systems for endocrine therapy and to the lack of *in vitro* models designed for the assessment of drug delivery systems such as polymer-drug conjugates, it was considered important to determine the activity of the HPMA conjugates containing Dox and AGM (in particular the activity against the aromatase enzyme) in models routinely used to evaluate low molecular weight cytotoxic and endocrine therapies.

The *in vitro* cytotoxicity studies highlighted a dramatic increase in the activity of the HPMA copolymer conjugate when AGM and Dox were both bound on the same polymeric chain. This observation might be explained by an additive or synergistic effect of the two drugs given together. However, as no enhanced activity was observed when the HPMA copolymer-AGM and HPMA copolymer-Dox were added

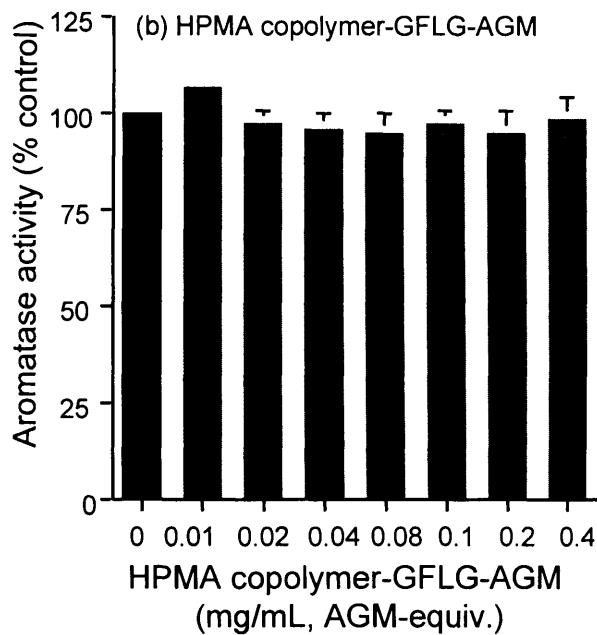
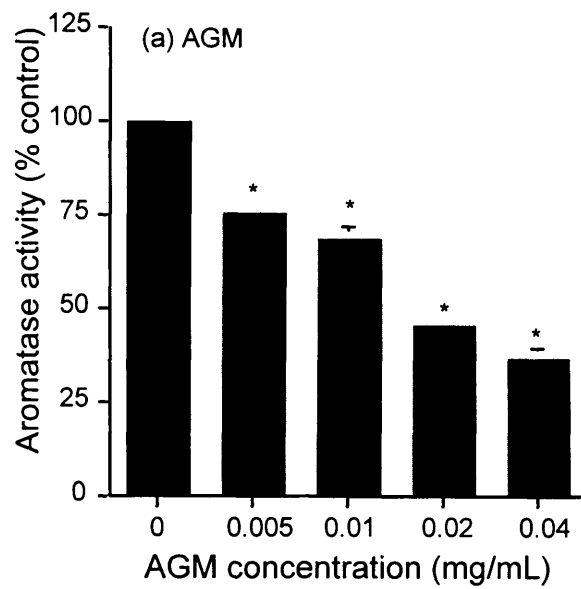


Fig. 4.12. Effect of free and polymer-bound AGM on aromatase activity in isolated human placental microsomal extract. Panel (a) free AGM and panel (b) HPMA copolymer-GFLG-AGM at the concentrations shown. Data are expressed as a percentage of the activity without addition; mean \pm SEM and $n \geq 4$. Statistical significance was determined at $p \leq 0.05$ (*) using one-way ANOVA and Bonferroni post hoc test

together as a mixture, a more complex explanation must account for the fact that HPMA copolymer-Dox-AGM is much more potent than HPMA copolymer-Dox.

Vicent et al. (2005) reported two important differences between the two conjugates. Firstly, the release rate and pattern of release after incubation of the conjugates with a mixture of lysosomal enzymes (tritosomes) were very different in the conjugate carrying only Dox than from that observed in the conjugate carrying both AGM and Dox (Vicent et al., 2005). Whilst HPMA copolymer-Dox showed a linear Dox-release profile with time, and drug liberation started immediately after addition of the enzyme, the combination conjugate displayed a non-linear progression with a marked lag phase with little release over the first 30 min for both drug. Also it was observed that the conjugate size (and thus conformation) in solution, and therefore the accessibility of the linker, was quite different in the two conjugates (the R_g was 7.7 and 12.8 nm for HPMA copolymer-Dox and HPMA copolymer-AGM-Dox, respectively) (Vicent et al., 2005).

The simultaneous delivery of the two agents through a single polymeric carrier coupled with different release kinetics could at least partially explain the increased activity observed. However, other factors might also be playing an important role. For instance, differences in the uptake of the conjugates by MCF-7 and MCF-7ca cells need to be considered. It has been suggested that HPMA copolymer-Dox is as cytotoxic as free Dox if intracellular concentration of the drugs are considered (Minko et al., 1999). If this is the case, a more marked uptake of the combination polymer by MCF-7 and MCF-7ca cells could well explain its increased activity. This issue is investigated in Chapter 5.

It is also possible that the HPMA copolymer-Dox and the HPMA copolymer-AGM-Dox have a different mechanism of toxicity. Several authors have highlighted differences in the mechanism of toxicity of free Dox compared to HPMA copolymer-Dox. *In vitro* studies suggested that the HPMA copolymer-Dox toxicity can be attributed to induction of the apoptotic cascade (Minko et al., 2001). Furthermore, the presence of AGM on the same polymeric chain might ultimately be responsible for the activation of other pathways. These topics concerning the cellular mechanism of action are addressed in Chapter 6.

To better understand the mechanism of action of these conjugates it was considered important to assess the ability of the HPMA copolymer-AGM to inhibit aromatase.

Oestrogens play an important role in the growth of breast cancers. Indeed, the majority of breast tumours are oestrogen-dependent (Ali and Coombes, 2002). As mentioned previously, oestradiol promotes the growth of both MCF-7 and MCF-7ca cells (Fig. 2.6). Consistent with the observations of Santner et al. (1993), we showed that addition of the aromatase substrates androstenedione and testosterone stimulated growth of MCF-7ca cells, but not MCF-7. The latter suggests that although testosterone and androstenedione have a similar structure to oestradiol, they do not act as direct ER agonists. This is coherent with data reported previously showing that the addition of the antiandrogen 2-hydroxyflutamide does not affect the mitogenic activity of androstenedione (Santner et al. 1993).

It is also important to note that androstenedione is first transformed to oestrone (less potent than oestradiol) and only in a second step to oestradiol. In contrast, testosterone is transformed directly to oestradiol. Consequently, it might seem a paradox that the highest mitogenic activity was seen in presence of androstenedione. This is probably due to the higher affinity of androstenedione for the aromatase enzyme (reviewed in Lonning 2004) and explains why androstenedione is preferentially used as substrate for aromatase in the vast majority of the *in vitro* system reported in literature, rather than testosterone (reviewed in Njar and Brodie, 1999).

Both free AGM and HPMA copolymers-AGM were able to reverse the mitogenic activity of androstenedione, and indeed at higher AGM concentration, cell growth was even lower than that seen in the control. This could be attributable to the fact that charcoal-stripped serum might still contain some residual steroids, allowing AGM to block their transformation into oestrogens. Alternatively, and most likely, high levels of AGM show some non-specific cytotoxic activity.

The radiometric assay provided more direct evidence that HPMA copolymer-AGM, like AGM (Burak Jr et al., 1997), were able to inhibit cell-associated aromatase. It is however fair to say that the activity seen in MCF-7ca was only 20 % higher than that seen in MCF-7. This suggests that, consistently with the indications resulting from the previous experiments (mitogenic effect of androstenedione and Western Blot) MCF-7ca do not have a *dramatically* higher level of aromatase than MCF-7. Consequently, although all these results suggest some evidence of aromatase inhibition, conclusions on dose-dependence can be difficult.

The results described above suggest that HPMA copolymer-AGM can act like free AGM in cell-based systems. The experiments conducted with isolated human placental microsomal aromatase showed that polymer-bound-AGM is completely inactive, whereas as expected free AGM is able to prevent aromatase action in this system at concentrations comparable to those reported in the literature (Miller and Dixon, 2000; reviewed in Miller and Dixon 2002). This lack of activity of the conjugate can probably be attributed to steric hindrance caused by the polymer backbone. Furthermore, this decrease in activity was predictable as even acetyl-AGM (one of AGM metabolites), shows reduced activity compared to the parent compound (< 50 %) (Aboul-Enein, 1986). These observations confirm that intracellular release of AGM is a critical step for the aromatase inhibitory activity of HPMA copolymer conjugates.

4.5. CONCLUSIONS

In this chapter a first evaluation of the activity of the drug conjugates previously synthesised was described. Two main findings need to be highlighted. First, the polymer carrying the combination of endocrine and chemotherapy was more active than all of the other polymeric system and their combinations. Secondly, evidence of the ability to retain aromatase activity was found for HPMA copolymers containing AGM.

The increased activity seen in the HPMA copolymer-AGM-Dox is exciting as not only does it suggest that the simultaneous administration of chemotherapy and endocrine therapy can be beneficial but it can also represent an improvement against a conventional regime that is already in clinical trial (polymer-drug conjugates

containing only chemotherapy like HPMA copolymer-Dox). However, the reasons for this behaviour are yet to be understood. Indeed, the next two chapters aim to investigate the mechanism of action of the combination polymer. More specifically, in the next chapter the uptake of HPMA copolymer-Dox and HPMA copolymer-Dox-AGM are evaluated to determine if the different cytotoxicity can be attributed to a different uptake rate or mechanism.

Chapter 5:

Comparison of the cellular uptake of HPMA-copolymer Dox
and HPMA copolymer-Dox-AGM

5.1. INTRODUCTION

The evaluation of the polymer-drug conjugates carried out in the previous chapter showed that the HPMA copolymer carrying the combination of Dox and AGM was markedly more active than any of the individual polymer-drug conjugates or their mixtures. In particular, HPMA copolymer-AGM-Dox was markedly more cytotoxic than HPMA copolymer-Dox that has shown activity in breast cancer patients clinically (Vasey et al., 1999; Cassidy, 2000). This effect might be potentially attributed to:

- 1) differences in the rate of endocytic uptake of the conjugates
- 2) differences in the intracellular trafficking of the conjugates (thus exposure to cathepsin B)
- 3) differences in the rate of liberation of drugs from the conjugates
- 4) and/or the synergistic activity of Dox and AGM.

The aim of this study was to investigate whether the *rate* of endocytic uptake and/or the *mechanism* of uptake of HPMA copolymer-AGM-Dox were different from HPMA copolymer-Dox. Before starting the experiments, the marker and the technique to be used to measure the uptake were both considered. In addition, the inhibitors of endocytic pathways that might allow dissection of the mechanisms of endocytic internalisation of the two conjugates were also considered.

The marker and the technique. All the early studies on endocytosis of HPMA copolymers used [¹²⁵I]-labelled polymers (e.g. Duncan et al., 1986; Flanagan et al., 1989). Also, radioiodination of HPMA copolymers has been successfully used for monitoring the distribution of HPMA copolymers in animals (Seymour and Duncan, 1987) and man (Julyan et al., 1999). The development of an HPLC technique to monitor the *in vivo* (Wedge et al., 1991) and clinical biodistribution of HPMA copolymer-Dox conjugate has been an important alternative as it allows detection of free and bound drug (Wedge, 1991).

Fluorescence labelling has been widely used to monitor cellular uptake of compounds by flow cytometry (Dordal et al., 1995), and also using fluorescence microscopy to visualise the intracellular localisation of the probe (Crivellato et al.,

1999). However, it is well-known that labelling with a fluorescent probe can affect the physico-chemical and consequently the biological behaviour of the polymer (Waggoner, 1990). Importantly, the two conjugates used in this study contain Dox which is inherently fluorescent. This allows detection of the polymer-drug conjugate without need of further modification. So combination of the intrinsic fluorescence of Dox and FACS and fluorescence microscopy were chosen as techniques to examine the cellular fate of the HPMA copolymer conjugates.

It is well described that fluorescence output can be affected by several parameters, most importantly pH and drug concentration (Waggoner, 1990). Consequently, preliminary studies were carried out to assess the influence of these parameters on the fluorescence of free and polymer-bound Dox. Two different techniques were used. FACS was used to quantitate cellular uptake at 37 °C, while cell binding was estimated performing the experiment at 4 °C. In parallel, fluorescence microscopy was used to visualise the intracellular fate of the probes.

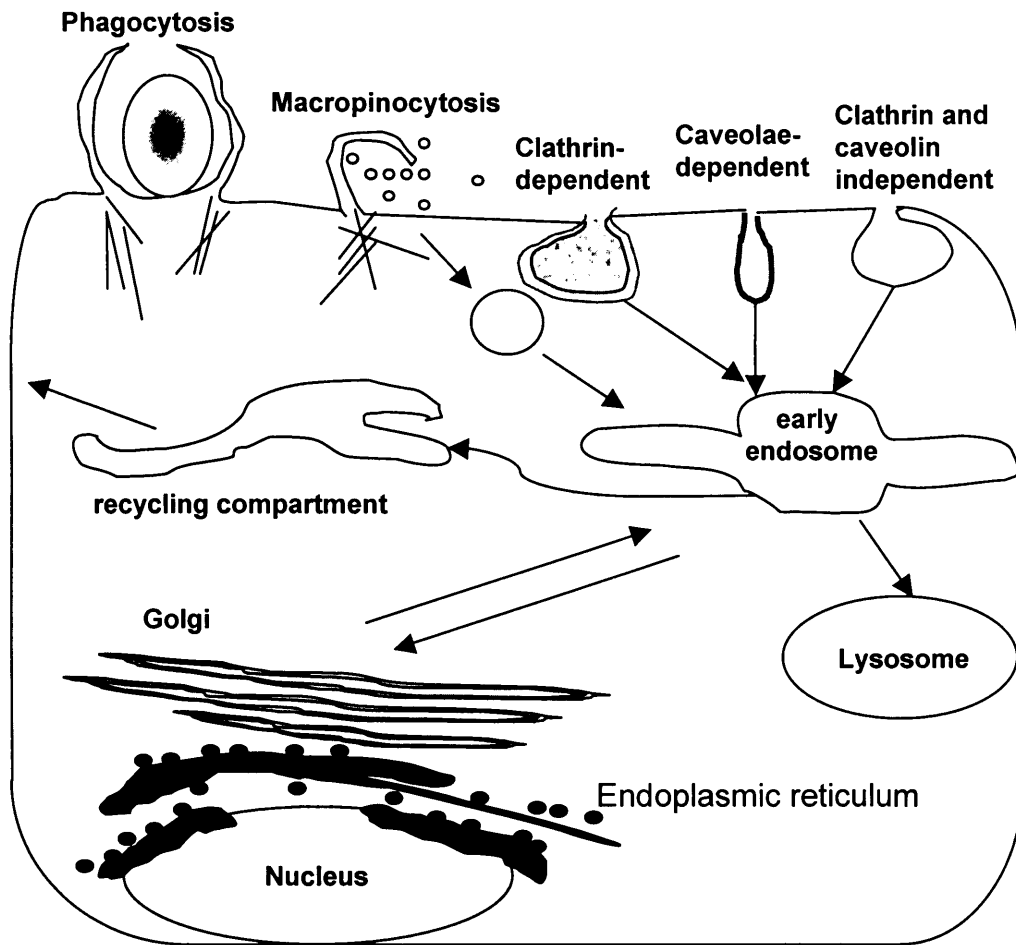
Mechanism of uptake. In the context of this project establishing differences in the uptake route of the HPMA copolymer-Dox and the HPMA copolymer-AGM-Dox is extremely important as recent studies suggest that uptake through different portals might be responsible for the different intracellular fate (reviewed in Johannes and Lamaze, 2002). For HPMA copolymer-Dox conjugates to exhibit biological action, the cellular uptake and subsequent transfer to lysosomes are essential steps, as drug liberation requires exposure of the GFLG linker to lysosomal thiol-dependent proteases (reviewed in Duncan, 2005). It is possible that HPMA copolymer-Dox and HPMA copolymer-AGM-Dox have different routes of internalisation. Therefore, here preliminary experiments were carried out to investigate the route of uptake of the two conjugates.

A brief description of the endocytic internalisation of polymer conjugates was given previously (section 1.4). As the HPMA copolymer-Dox and HPMA copolymer-AGM-Dox have a size of ~ 8 nm and 13 nm, respectively (Vicent et al., 2005), here, the possible endocytic uptake routes they could theoretically be internalised by are

briefly analysed. Several pinocytotic routes have been described, at present they can be summarised as follows:

- 1) Clathrin-mediated endocytosis. It is the best described endocytic route. The assembly of clathrin forms the so-called clathrin-coat. This leads to membrane invagination and the eventual formation of clathrin-coated vesicles (~ 120 nm). This pathway is used by several endogenous molecules such as transferrin and the low density lipoprotein receptor (reviewed in Johannes and Lamaze, 2002). Conjugates carrying Dox and transferrin as targeting moiety have been described. However, as the transferrin receptor undergoes rapid recycle and never reaches the lysosomal compartment, an enzymatic-degradable linker is not suitable for this type of conjugates. For instance, the HPMA copolymer-DNM-transferrin showed reduced antitumour activity *in vivo* (Flanagan et al., 1992 and reviewed in Duncan 2005). From a drug delivery point of view, it is also interesting to note that clathrin-mediated endocytosis has recently been described as the uptake route followed by lipoplex in COS-7 cells (Zuhorn et al., 2002).
- 2) Caveolae-mediated endocytosis. Caveolae are omega-shaped vesicles with a diameter of approximately 50 nm, characterised by the presence of the protein caveolin-1. This protein is usually located in glycolipid rich domains of the plasma membrane (lipid rafts) and has affinity for cholesterol (Nichols, 2003). It is interesting to note that the internalisation of the cholera toxin via caveolae leads to trafficking of the toxin to the Golgi (Orlandi and Fishman, 1998).
- 3) Macropinocytosis. Is the process associated with the formation of membrane ruffles and subsequent formation of big (~ 1 μm) vesicles called macropinosomes. It is dependent on the actin cytoskeleton (Swanson and Watts, 1995).
- 4) Non-clathrin, non-caveolin-dependent endocytosis (Fig. 5.1). It is an umbrella term that encompasses the other endocytic routes that cannot be identified in the categories described above (reviewed in Conner and Schmid, 2003).

After internalisation, all compounds are directed to early endosomes. From there, they can be directed to: (i) the degradative pathway (endosomes – lysosomes); (ii) the recycling pathway and (iii) the trafficking through trans-Golgi network to the Golgi apparatus to the endoplasmic reticulum. Of these options, for the HPMA copolymer-Dox only the first pathway will lead to exposure to lysosomal cathepsin B and to the



- 1) Phagocytosis (particle-dependent)
- 2) Macropinocytosis ($> 1 \mu\text{m}$)
- 3) Clathrin-mediated endocytosis ($\sim 120 \text{ nm}$)
- 4) Caveolin-mediated endocytosis ($\sim 60 \text{ nm}$)
- 5) Clathrin and caveolin-independent endocytosis ($\sim 90 \text{ nm}$)

Fig.5.1. Simplified scheme of the possible routes of uptake of the conjugates. Adapted from Conner & Schmid (2003) and Sorokin (2000)

enzymatic release of the drug(s) from the polymeric backbone. So far there has been no correlation between entry route for polymer anticancer drug conjugates and the subsequent trafficking. However, differences in the mechanism of internalisation of the HPMA copolymer-Dox conjugates could potentially determine the efficiency of trafficking to the lysosomal compartment and hence provide a potential explanation for the increased biological activity observed previously (Chapter 4).

To investigate whether HPMA copolymer-Dox or HPMA copolymer-AGM-Dox follow different endocytic routes, their uptake was measured in presence of inhibitors of the different endocytic pathways. Several such inhibitors have been used by others and they are summarised in table 5.1. As both HPMA copolymers Dox conjugates have a Rg smaller than 20 nm (by SANS), they could be theoretically internalised by any of the pathways described above. Methyl- β -cyclodextrin (M β CD) was used in order to first investigate whether a cholesterol-dependent pathway was involved. This compound depletes cholesterol in the plasma membrane (Ilangumaran and Hoessli, 1998; Ivanov et al., 2004; Rodal et al., 1999) and, to prevent endogenous synthesis of cholesterol, M β CD is usually supplemented with lovastatin. Then, to discriminate between clathrin-dependent or caveolin-dependent endocytosis, chlorpromazine was chosen as an inhibitor. It is reported to inhibit clathrin-dependent endocytosis (Zuhorn et al., 2002). Finally, to investigate if macropinocytosis was involved in the uptake of the conjugates, cytochalasin B was selected as the third and final inhibitor (Kee et al., 2004).

In summary, first, the effect of pH and concentration on the fluorescence of the two conjugates was determined to ensure appropriate interpretation of the results obtained in the subsequent studies. Then, the cellular uptake (37 °C) and binding (4 °C) of HPMA copolymer-Dox and HPMA copolymer-AGM-Dox in MCF-7 and MCF-7ca cells was compared using flow cytometry. Also fluorescence microscopy (epifluorescence microscopy) studies were carried out to visualise the intracellular fate of the conjugates. Finally, preliminary experiments were undertaken to investigate which endocytic route of entry was used by the two conjugates.

Table 5.1. Inhibitors of specific routes of endocytic uptake

Inhibitor	Mechanism of action	Type of uptake blocked	Concentration used	Reference
M β CD	Cholesterol depletion from plasma membrane	Clathrin- and caveolin-dependent	10 mM	Manunta et al. (2004)
			10 mM	Ivanov et al. (2004)
			10 mM	Rejman et al. (2004)
			10 mM	Zuhorn et al. (2002)
Chlorpromazine		Clathrin-mediated endocytosis	15 μ M	Kee et al. (2004)
Monodansylcadaverine	Stabilisation of clathrin cage assembly	Clathrin-mediated endocytosis	10 μ g/ml 400 μ M	Rejman et al. (2004) Claing et al. (1999)
Phenylarsine oxide	Prevents assembly of clathrin coated pits or their pinching off from the plasma membrane	Clathrin-mediated endocytosis	20 μ M	Ivanov et al (2004)
Nyastatin	Incorporates into lipid membranes and chelates cholesterol	Clathrin-independent internalisation / caveolae dependent	25 μ g/ml	Manunta et al. (2004)
Filipin III	Incorporates into lipid membranes and chelates cholesterol	Caveolae	15 μ M 5 μ g/ml	Kee et al (2004) Manunta et al (2004)
Cholesterol oxidase	Enzymatic modification of cholesterol	Caveolar-mediated pathway	1 μ g/ml 5 μ g/ml 2 μ M 2 units/ml	Zuhorn et al. (2002) Rejman et al. (2004) Kee et al. (2004) Ivanov et al (2004)

Table 5.1. Continued

Amiloride	Na ⁺ /H ⁺ transporter inhibition	Macropinocytosis	1 mM	Ivanov et al. (2004)
5-(<i>N</i> -ethyl- <i>N</i> -isopropyl) amiloride	Na ⁺ /H ⁺ transporter inhibition	Macropinocytosis	100 μM	Ivanov et al. (2004)
Cytochalasin B	Actin depolarising agent	Macropinocytosis	10 μM	Rejman et al. (2004)
Nocodazole	Disruption of microtubule structure	Macropinocytosis	100 μM	Kee et al (2004)
Rapamycin	Suppression of actin synthesis	Macropinocytosis	25 μM	Kee et al (2004)
			33 μM	Kee et al (2004)
			1 – 100 ng/mL	Hackstein H. (2002)

5.2. METHODS

The methods used for the flow cytometry studies and the data analysis have been already described in sections 2.3.15 and 2.3.16. The concentration of conjugates used in these studies was always adjusted to obtain 6.3 $\mu\text{g}/\text{mL}$ Dox-equiv. This concentration is lower than IC_{50} values determined for the two conjugates in the two cell lines. It is also important to note that while the cytotoxicity studies were performed after an incubation of 72 h, the longest exposure time in the uptake studies was 1 h. This ensured that the concentration chosen for all uptake studies were non-toxic.

5.2.1. Characterisation of Dox, HPMA copolymer-Dox and HPMA copolymer-Dox-AGM fluorescence

First, the fluorescence spectra of Dox, HPMA copolymer-Dox and HPMA copolymer-Dox-AGM were defined. Each compound was dissolved in HPLC grade methanol at a concentration of 0.03 $\mu\text{g}/\text{mL}$ for the free Dox, 5 $\mu\text{g}/\text{mL}$ (i.e. 0.31 $\mu\text{g}/\text{mL}$ Dox-equiv.) for the HPMA copolymer-Dox and 5 $\mu\text{g}/\text{mL}$ (i.e. 0.39 $\mu\text{g}/\text{mL}$ Dox-equiv.), placed into a polystyrene cuvette (3 mL of solution per sample) and analysed at a fluorescence spectrophotometer. Each emission spectrum was recorded; excitation 488 nm and emission in the range 400 – 800 nm.

The effect of *concentration* and *pH* on the fluorescence output was also determined. In this case, HPMA copolymer-Dox and HPMA copolymer-Dox-AGM were dissolved into two different buffers. Phosphate buffer (pH 7.4 and 6.4) and citrate buffer (pH 5.5) were used. For each polymer conjugate, a stock solution in each buffer was prepared (62.9 ng/mL Dox equiv.). From the stock solution, serial dilutions with the buffer were performed to achieve a range of concentrations (0.629 - 62.9 ng/mL) for each buffer. Fluorescence was then recorded in a plate reader. The fluorescence recorded was then plotted against the concentration to obtain the concentration-dependence.

5.2.2. Fluorescence microscopy. Live-cell imaging

Cells were seeded in glass bottom culture dishes (10^6 cells per plate) in WRPMI supplemented with 5% of SFCS and allowed to adhere for 24 h. The medium was

then replaced with fresh medium containing HPMA copolymer-Dox or HPMA copolymer-Dox-AGM, at the same concentration used for the uptake studies, (6.3 $\mu\text{g}/\text{mL}$ Dox equiv.) and incubated for either 5, 30 or 60 min. Then the medium was removed and the cells were washed 3 times with warm (37 °C) PBS (3 x 3 mL). After the third wash, fresh clear medium was added (WRPMI + 5% SFCS; 1 mL per dish) and the cells were analysed at the microscope for a maximum of 30 min. Cells were visualised using an inverted epifluorescence microscope with the appropriate filter settings for Dox and by manually adjusting the gain. Control cells with no treatment were also analysed to account for the cell autofluorescence.

5.2.3. Cytotoxicity of the inhibitors

The experiments described in this and the following section (5.2.4) were done in the Centre for Polymer Therapeutics in part by Siobhan Gee, under my supervision.

MCF-7 and MCF-7ca were seeded in 24 well plates (3.2×10^5 cells/ml; 500 μL per well) in WRPMI + 5% SFCS. Cells seeding density was adjusted to obtain the same concentration (cells/area) used in the uptake experiment with flow cytometry. After 24 h, cells were washed with warm (37°C) PBS (500 μL) in order to remove dead cells and residual serum. A solution containing the inhibitor in medium was added (500 μL). The three inhibitors used for this study were:

- M β CD (0-15 mM) and lovastatin (1 μM)
- chlorpromazine (0-50 μM)
- cytochalasin B (0-25 μM).

The solutions were prepared by diluting a stock solution of the inhibitor in medium. After a 2 h incubation with the inhibitors, the medium was removed, cells were washed with warm (37 °C) PBS (3 x 500 μL). Then, 150 μL of a trypan blue solution (0.2% trypan blue in PBS) were added to each well. The total number of stained cells in the visual field was counted (SC_{vis}). The total number of cells in the visual field (TC_{vis} , i.e. stained and unstained) was determined applying a grid that allowed the counting of 25 % of the cells in the visual field. The data were expressed as % of dead cells:

$$\% \text{ dead} = (SC_{\text{vis}} / TC) \times 100$$

5.2.4. Effect of inhibitors on the endocytic uptake of HPMA copolymer conjugates.

Cells were seeded in a 6-well plate (10^6 cells/well) using WRPMI supplemented with 5% of SFCS and they were allowed to adhere for 24 h. Then, cells were washed with warm (37°C) PBS (1mL) and fresh medium ($900\ \mu\text{L}$) containing the endocytosis inhibitor (either M β CD + lovastatin ($10\ \text{mM} + 1\ \mu\text{M}$), chlorpromazine ($15\ \mu\text{M}$) or cytochalasin B ($25\ \mu\text{M}$)) was added. As described above, the solutions were prepared in medium starting from stock solutions of the inhibitor. The final concentrations were $10\ \text{mM} + 1\ \mu\text{M}$, $25\ \mu\text{M}$ and $15\ \mu\text{M}$ for M β CD + lovastatin, cytochalasin B and chlorpromazine, respectively. In each case it was ensured that the remaining solvents from the stock solutions were present at non-toxic concentrations (always lower than 0.6 %).

After 1 h pre-incubation with the inhibitors at $37^\circ\ \text{C}$, a solution of HPMA copolymer-Dox or HPMA copolymer-AGM-Dox ($100\ \mu\text{L}$ in medium) was added to give a final Dox-equiv. concentration of $6.3\ \mu\text{g}/\text{mL}$ (same concentration used for the uptake studies). Cells were then incubated with the conjugate for 1 h. After the incubation period, the uptake was stopped by placing the plates on ice and by replacing the polymer and inhibitor solution with ice cold PBS ($5\ \text{mL}/\text{well}$). The cells were then washed with cold ($4^\circ\ \text{C}$) PBS three times ($3 \times 5\ \text{mL}$) and then $1\ \text{mL}$ of PBS was added. The cells were scraped with a rubber policeman and the cell suspension was then collected into a falcon tube and centrifuged for 5 min (at $4^\circ\ \text{C}$, $600 \times g$). Finally, the cells were re-suspended in ice-chilled PBS and promptly analysed using Becton Dickinson FACSCalibur cytometer. The settings used were the same as in the uptake studies (section 2.3.15). Data were presented as a percentage of the geometric mean obtained in absence of the inhibitor. Further details on the flow cytometry data analysis have been previously described (section 2.3.16).

5.3. RESULTS

5.3.1. Characterisation of the fluorescent probes

The fluorescence spectra of Dox, HPMA copolymer-Dox and HPMA copolymer-AGM-Dox (excitation at $488\ \text{nm}$) were very similar (Fig. 5.2). All the compounds

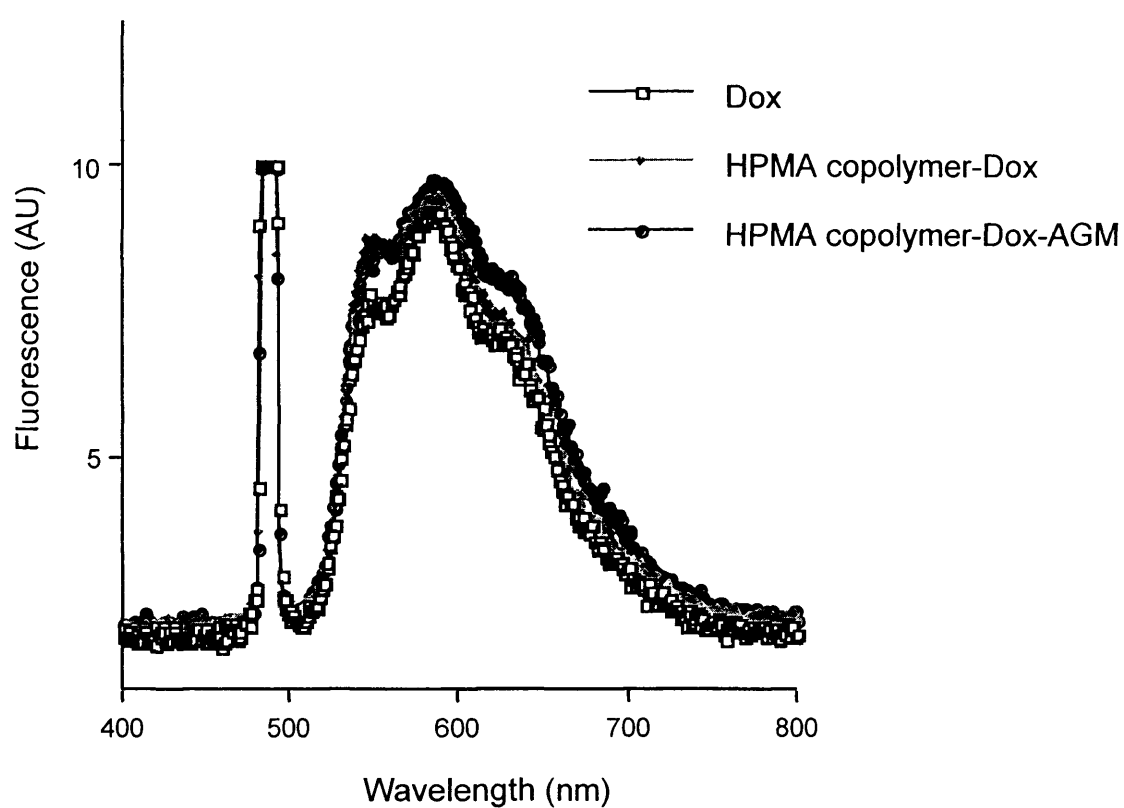


Fig.5.2. Fluorescence emission scan of Dox ($0.03 \mu\text{g/mL}$), HPMA copolymer-Dox ($5 \mu\text{g/mL}$ of conjugate i.e. $0.315 \mu\text{g/mL}$ Dox equiv.) and HPMA copolymer-Dox-AGM ($5 \mu\text{g/mL}$ of conjugate i.e. $0.39 \mu\text{g/mL}$ Dox equiv.). All the samples were dissolved in HPLC grade MeOH and excited at 488 nm. The emission scan was recorded at 400 – 800 nm

showed three peaks at ~ 560, 590 and 630 nm. However, it should be noted that free Dox had a higher fluorescence output than the conjugates. This is clear when the concentrations used to create the spectra seen in Fig. 5.2 are compared. It also appeared that the HPMA copolymer-AGM-Dox had lower fluorescence than the HPMA copolymer-Dox as a lower concentration of free Dox (0.31 $\mu\text{g/mL}$) gave a similar fluorescence output to HPMA copolymer-AGM-Dox (0.39 $\mu\text{g/mL}$ Dox-equiv.). When the fluorescence of HPMA copolymer-Dox and HPMA copolymer-AGM-Dox was measured across a range of concentrations and at different pH (Fig. 5.3) it could be seen that the conjugates fluorescence was concentration-dependent. At higher concentrations (0.02 – 0.06 mg/mL Dox-equiv.) the fluorescence of HPMA copolymer-Dox started plateauing. In addition, it was evident that HPMA copolymer-Dox had greater fluorescence output than HPMA copolymer-AGM-Dox at concentrations greater than 0.02 mg/mL (Fig. 5.4). Fluorescence of the conjugates did not show pH-dependence (Fig. 5.3 and 5.4).

5.3.2. Uptake of HPMA copolymer-Dox and HPMA copolymer-AGM-Dox by MCF-7 and MCF-7ca using flow cytometry or fluorescence microscopy.

Incubation of cells with the HPMA copolymer conjugates led to an immediate shift in their fluorescence, i.e. at time 0 (Fig. 5.5). A further shift was seen when the cells were incubated with the conjugates for 1h (Fig. 5.5). As the incubation time increased, the fluorescence became more marked (Fig. 5.6) and this was more evident after incubation of cells with HPMA copolymer-Dox than with HPMA copolymer-AGM-Dox. For both HPMA copolymer-Dox and HPMA copolymer-AGM-Dox (in both cell lines) the cell-associated fluorescence was higher at 37 °C than at 4 °C. The uptake was rapid in the first minutes but no time-dependent increase was seen at later time points (10 – 60 min). HPMA copolymer-Dox showed a more marked membrane binding than HPMA copolymer-AGM-Dox (cell-associated fluorescence of HPMA copolymer-Dox at 37 °C > than cell-associated fluorescence of HPMA copolymer-AGM-Dox at 37 °C or 4 °C). Also a higher uptake was seen for HPMA copolymer-Dox than for HPMA copolymer-AGM-Dox as the difference in fluorescence between 37 °C and 4°C is higher for the first than for the latter

(i.e. $F_{\text{HPMA copolymer-Dox } 37^\circ\text{C}} - F_{\text{HPMA copolymer-Dox } 4^\circ\text{C}} > F_{\text{HPMA copolymer-AGM-Dox } 37^\circ\text{C}} - F_{\text{HPMA copolymer-AGM-Dox } 4^\circ\text{C}}$).

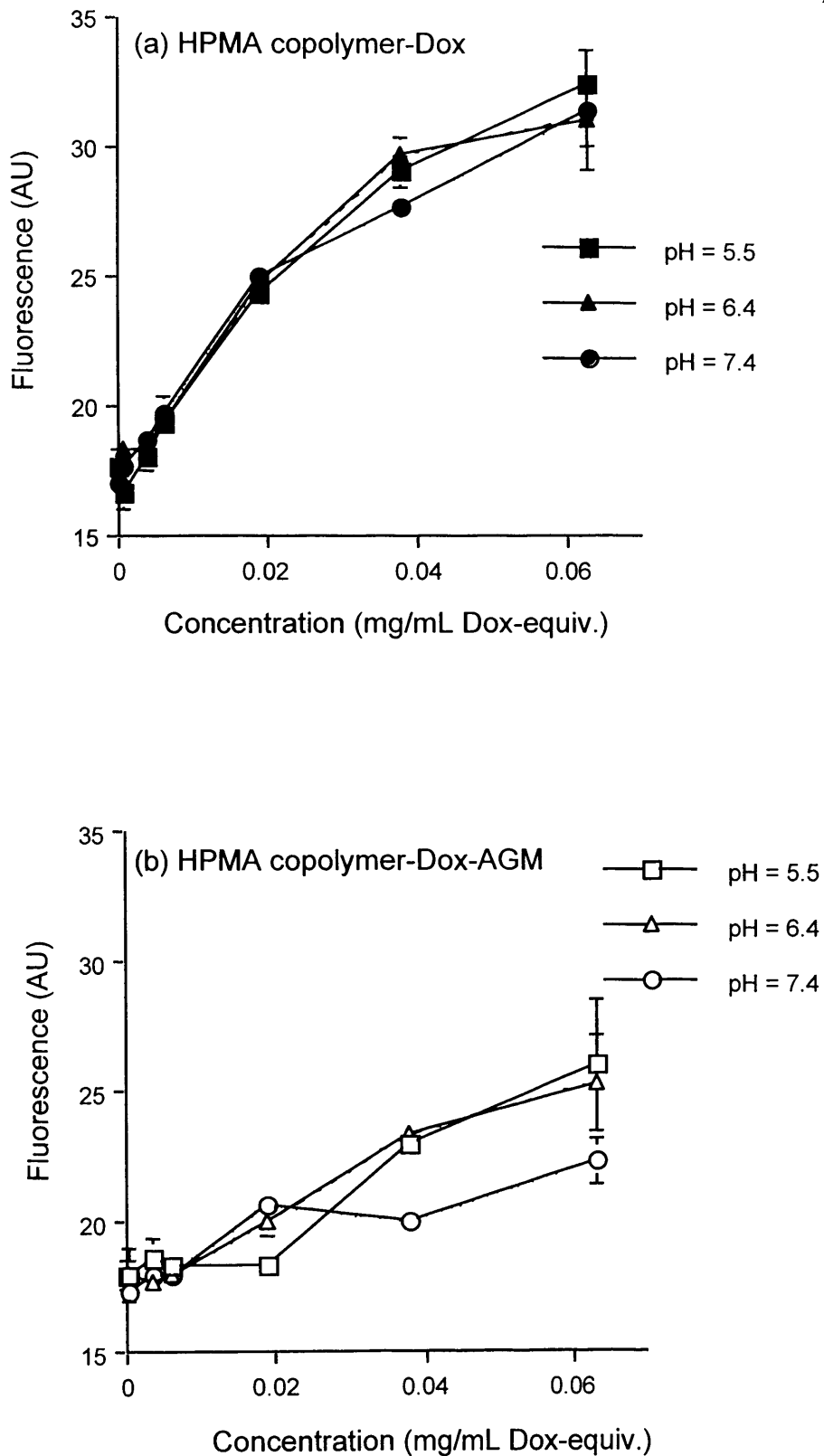


Fig.5.3. Effect of concentration and pH (7.4, 6.4, 5.5) on the fluorescence output of HPMA copolymer-Dox (panel a) and HPMA copolymer-Dox-AGM (panel b)

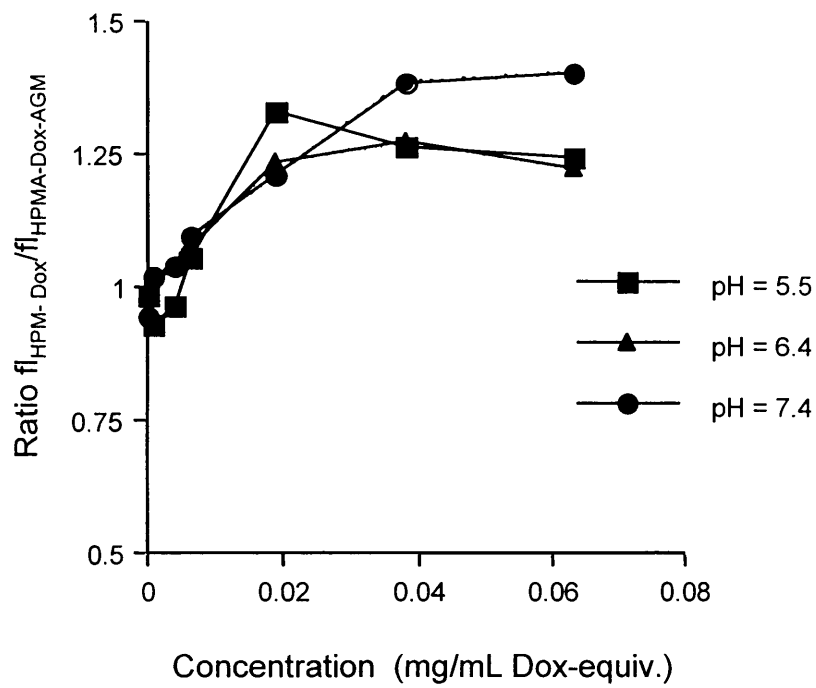


Fig.5.4. Ratio between the fluorescence output of HPMA copolymer-Dox and HPMA copolymer-AGM-Dox at 3 different pH (7.4, 6.2, 5.5)

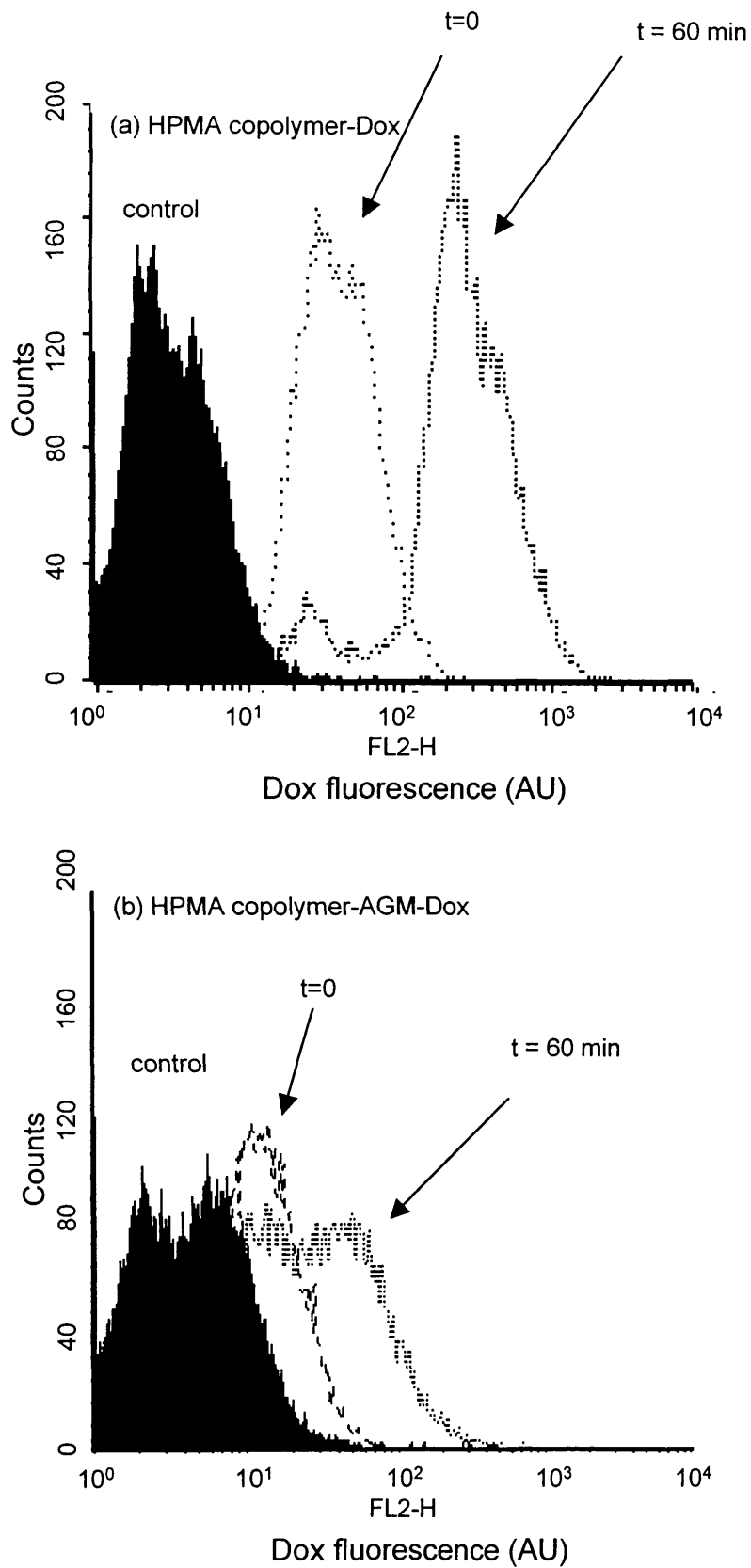


Fig.5.5. Uptake of HPMA copolymer Dox conjugates by MCF-7ca cells. HPMA copolymer-Dox in panel (a) and HPMA copolymer-Dox-AGM in panel (b) ($t = 0$ or $t = 1$ h). Control cells (incubated only with medium) are shown in black

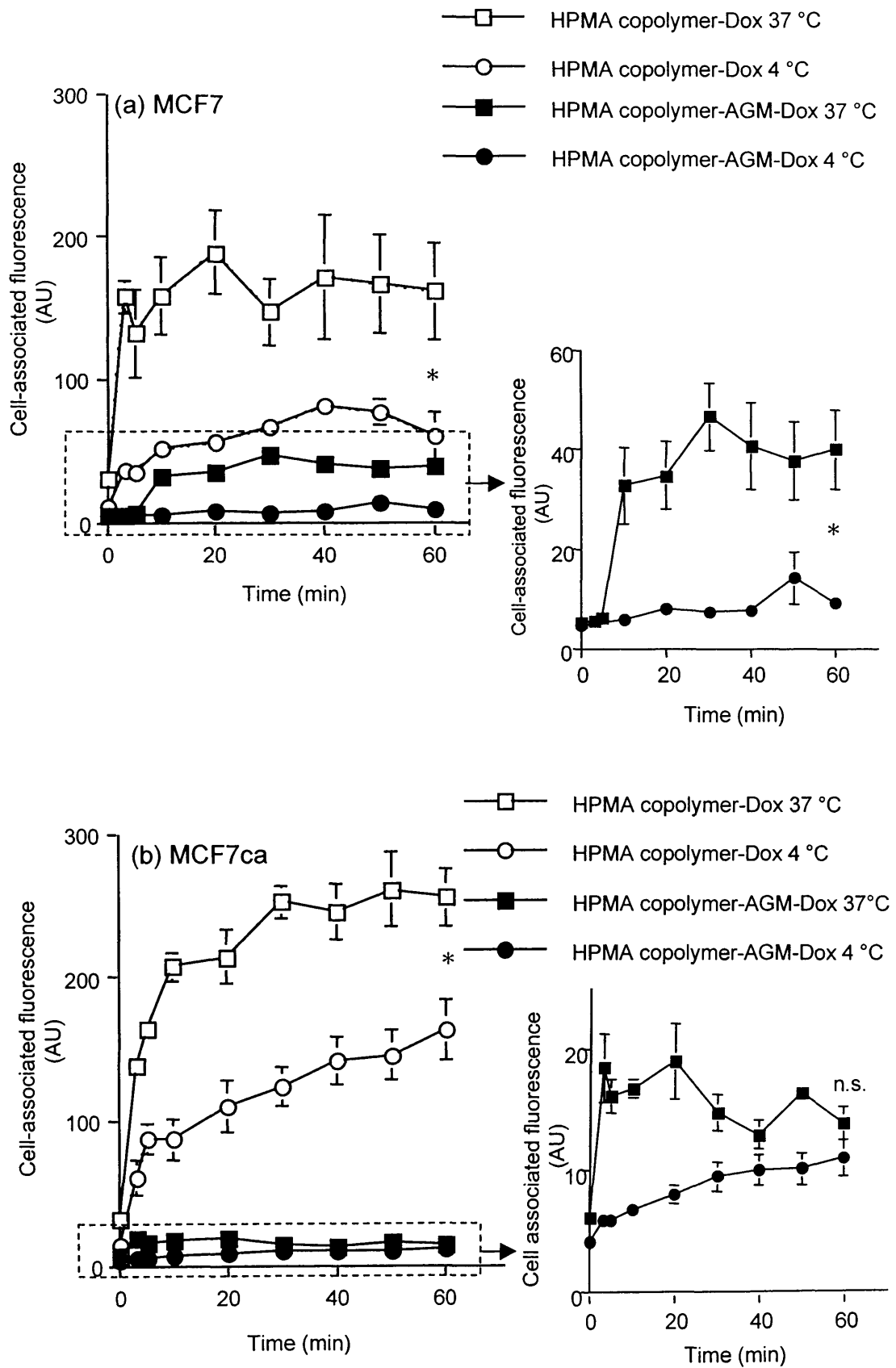


Fig.5.6. Uptake of HPMA copolymer-Dox (\pm AGM) by MCF-7 (panel a) and MCF-7ca cells (panel b). Data represent mean \pm SEM, $n =$ at least 4. Statistical significance between 37 °C and 4 °C at 60 min was determined at $p < 0.05$ (*) by Student's t test

A similar profile was seen in MCF-7ca (Fig. 5.7b). In this case, a time-dependent increase of the fluorescence was seen for HPMA copolymer-Dox at 37 °C and 4 °C. As a result the internalisation of HPMA copolymer-Dox (FI 37 °C - FI 4 °C) did not increase with time.

Also, the fluorescence microscopy studies showed no time-dependent increase of the cell-associated fluorescence (Fig. 5.7) (although it should be noted that these are qualitative studies). In both cell lines, evidence of marked membrane binding was seen both for HPMA copolymer-Dox and HPMA copolymer-AGM-Dox (Fig. 5.8). Although, visualisation of fluorescence was complicated by the photobleaching (Fig. 5.9), it was also seen to a lesser extent in vesicular compartments (Fig. 5.8).

5.3.3. Evaluation of the toxicity of the endocytosis inhibitors and the effect of inhibitors on the uptake of HPMA copolymer-Dox and HPMA copolymer-AGM-Dox

Prior to the start of the uptake studies with the endocytosis inhibitors (M β CD, chlorpromazine and cytochalasin B cytotoxicity), their cytotoxicity was investigated using MCF-7 and MCF-7ca cells. Each compound was tested at 3 different concentrations (as described in paragraph 5.2.3), which were chosen in the range of those routinely used in the literature. In MCF-7 cells, all the compounds showed a dose-dependent toxicity M β CD had a maximum toxicity of approximately 20% (at 15 mM) (Fig. 5.10a). Cytochalasin B had a toxicity that was always below 10 % even at the maximum concentration tested (25 μ M) (Fig. 5.10b). Chlorpromazine at 50 μ M was the most toxic (100 %) while at lower concentrations its toxicity was less than 10 %. The results obtained in MCF-7ca cells showed similar profiles (Fig. 5.11). Again chlorpromazine was the most toxic (~ 30 % at 50 μ M). As the concentrations commonly used in literature (10 mM for M β CD, 15 μ M for chlorpromazine and 25 μ M for cytochalasin B) were all below the maximum accepted cell death (arbitrarily set \leq 10 %) these were therefore used for the following studies.

When the uptake of HPMA copolymer-Dox and of HPMA copolymer-AGM-Dox by MCF-7 and MCF-7ca were measured in presence of the inhibitors, it was seen that M β CD decreased the uptake of both conjugates in both cell-lines (in MCF-7ca uptake

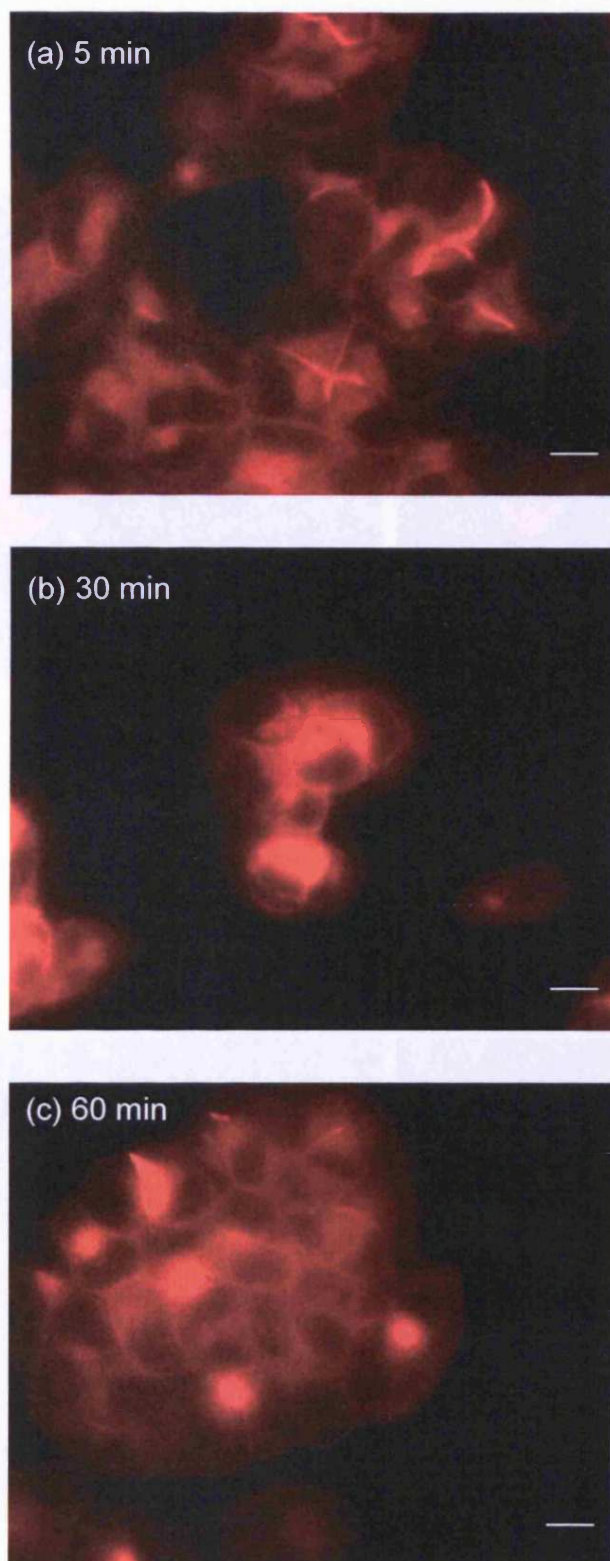


Fig.5.7. Fluorescence microscopy pictures of MCF-7ca cells after incubation with HPMA copolymer-Dox. Pictures were taken following a 5 min incubation (panel a), a 30 min incubation (panel b) or a 1 h incubation (panel c) (Size bar = 10 μm)

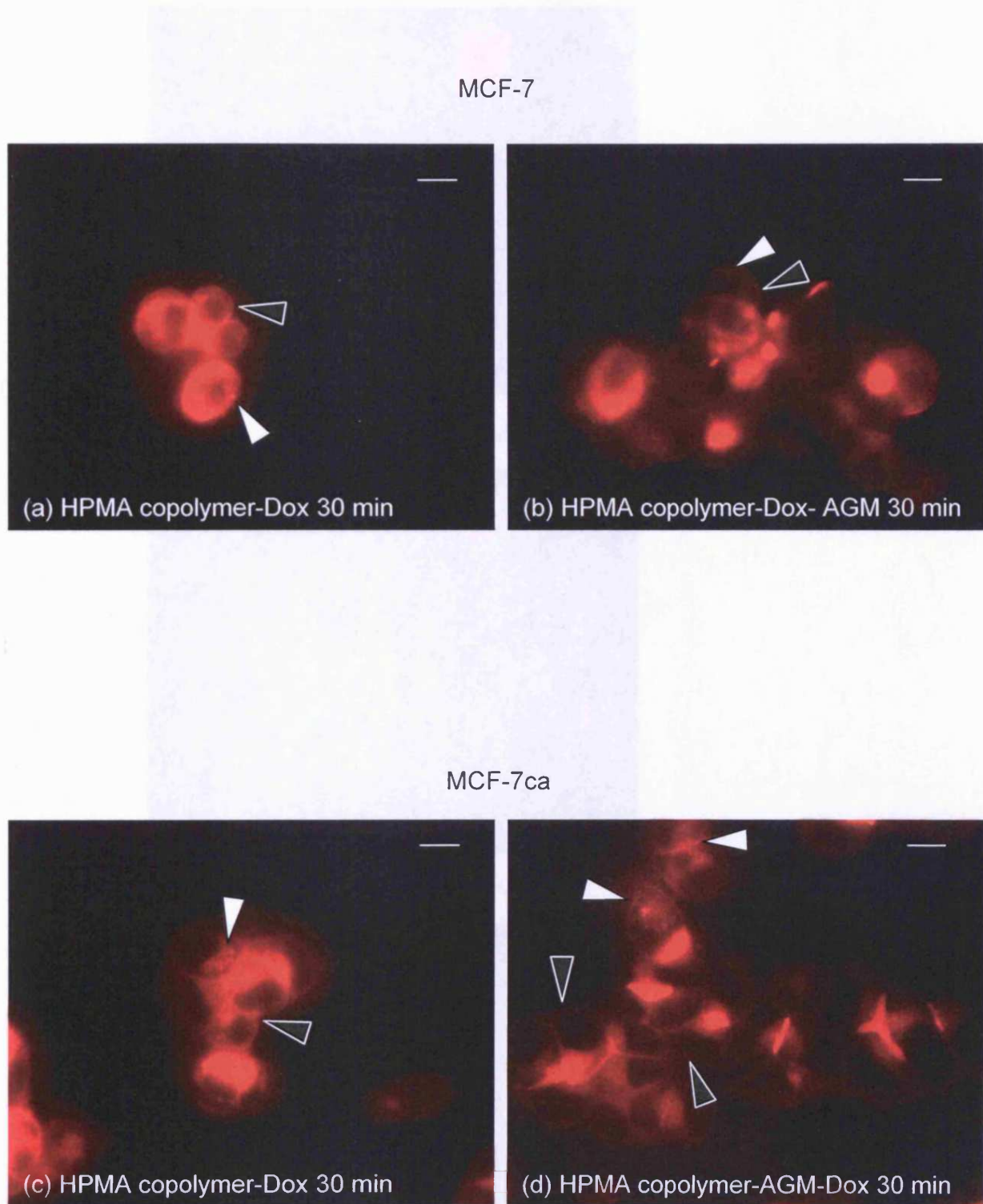


Fig.5.8. Fluorescence microscopy pictures of MCF-7 after 30 min incubation with HPMA copolymer-Dox (panel a) or HPMA copolymer-Dox-AGM (panel b) and of MCF-7ca after 30 min incubation with HPMA copolymer-Dox (panel c) or HPMA copolymer-Dox-AGM (panel d) (Size bar = 10 μ m). White arrows indicate fluorescence localised in vesicular compartments; black arrows indicate membrane labelling

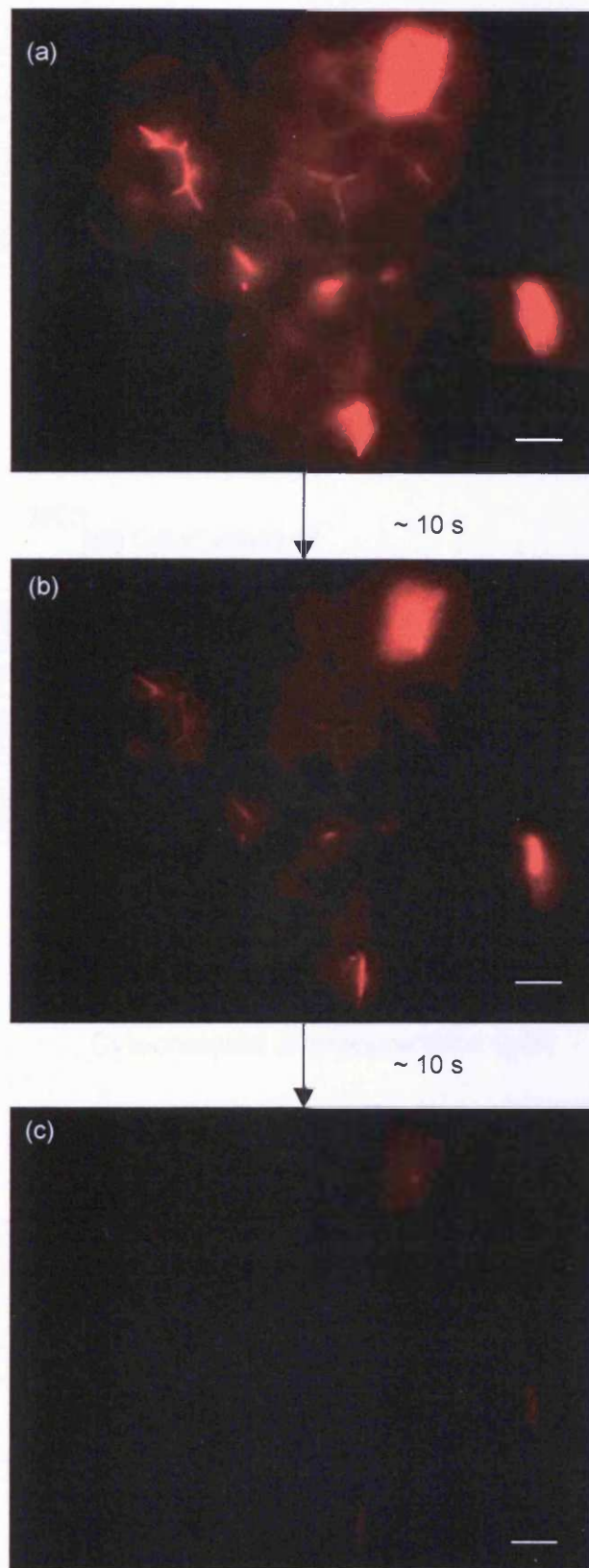


Fig. 5.9. Example of photo-bleaching in MCF-7ca incubated with HPMA copolymer-Dox. Panel (a) shows a picture taken immediately after excitation, panel (b) approximately 10 s later and panel c approximately a further 10 s later (Size bar = 10 μm)

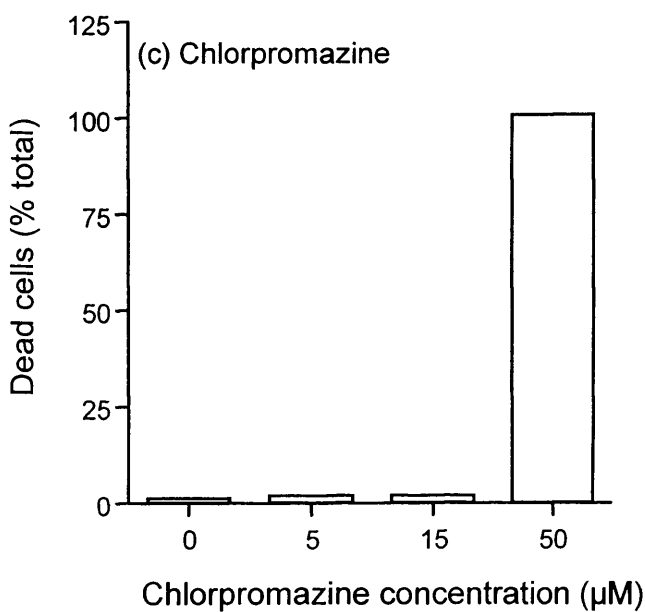
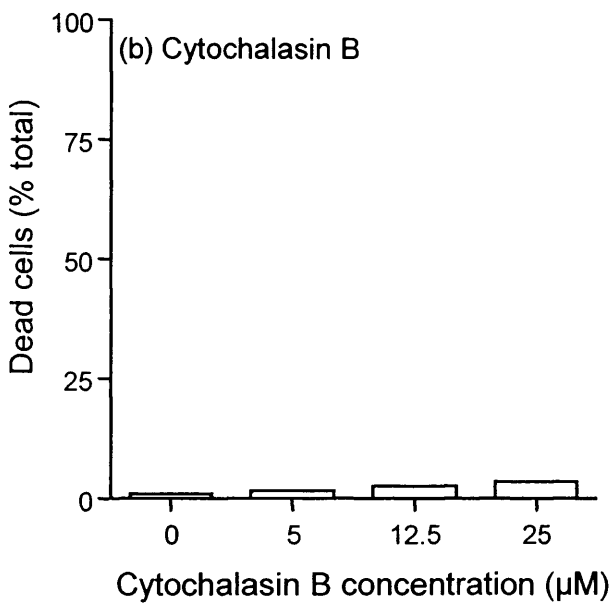
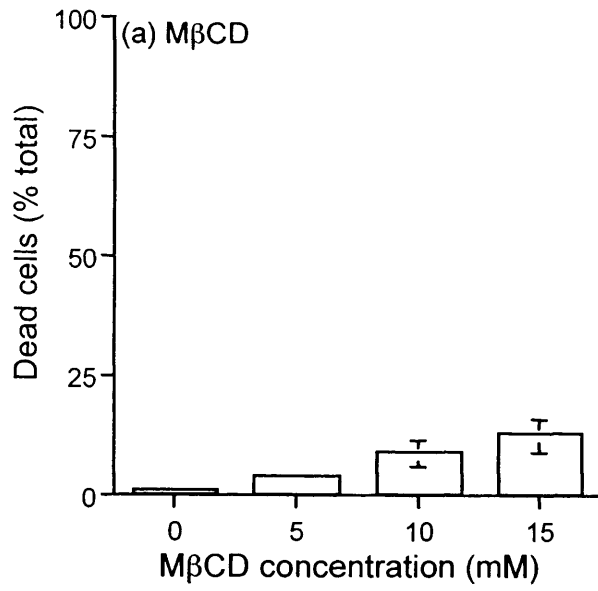


Fig. 5.10. Cytotoxicity of the inhibitors of endocytic pathways (M β CD, cytochalasin B and chlorpromazine) against MCF-7. Data represent mean \pm S.E.M., n at least 6

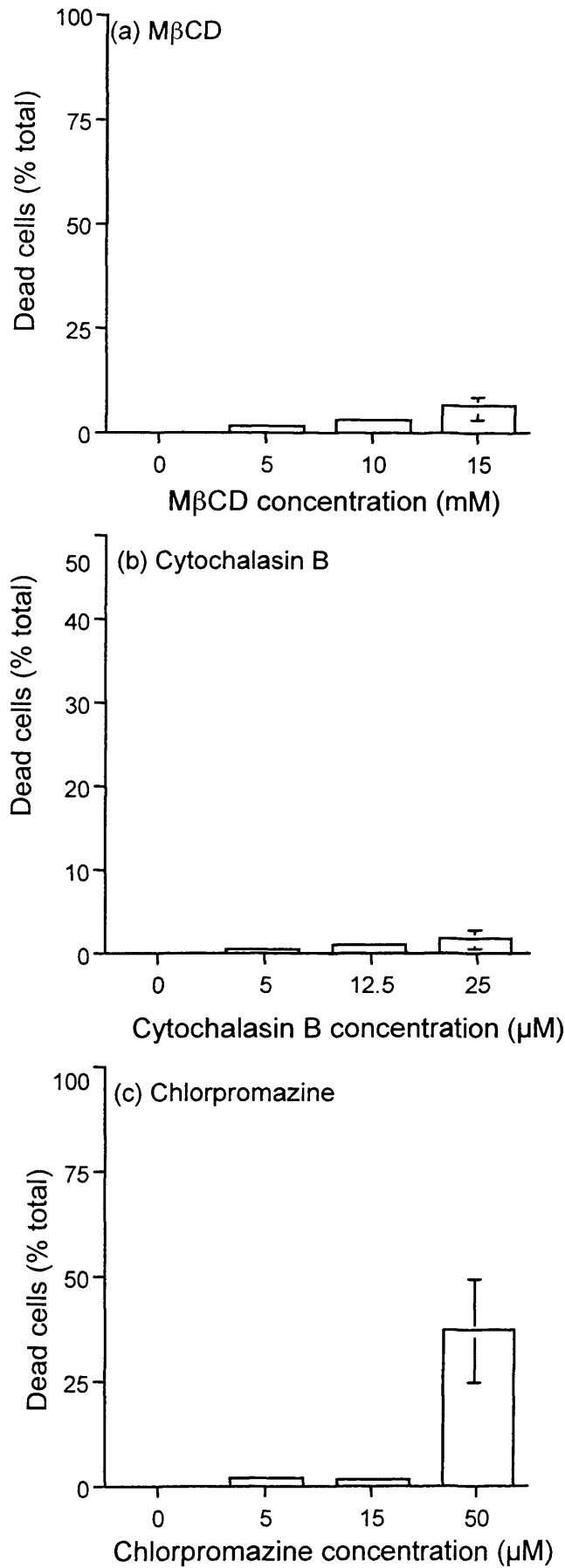


Fig. 5.11. Cytotoxicity of the inhibitors of endocytic pathways (M β CD, cytochalasin B and chlorpromazine) against MCF-7ca cells. Data represent mean \pm S.E.M., n at least 6

< 75 % after 1h incubation; in MCF-7 uptake < 60 % after 1 h incubation). A certain degree of inhibition was also seen in presence of chlorpromazine (Fig. 5.12; 5.13) although in all cases this was lower than the effect seen with M β CD. In all the cases cytochalasin B did not show any effect on the uptake of the conjugates.

5.4. DISCUSSION

In order to compare the uptake of HPMA copolymer-Dox and HPMA copolymer-AGM-Dox by MCF-7 and MCF-7ca cells, it was first necessary to characterise their fluorescence output in the different environments that would be encountered following endocytic internalisation. Intracellular trafficking is an extremely dynamic process. Also, the intracellular compartmentalization is responsible for the presence of markedly different environments within the same cell. Cellular pH varies from as high as 7.4 (the external environment) to as low as 5 (in the lysosomes). As the fluorescence output can be deeply influenced by the pH, preliminary assessments were performed prior to the uptake studies.

To investigate pH dependency, three pHs (7.4, 6.4 and 5.5) were chosen as representative of the extracellular environment, the endosomes and the lysosomes, respectively. pH-dependent probes can cause difficulties in the quantification of the uptake as the same amount of probe would lead to different fluorescence output depending on the pH of the compartment where it is located. To our advantage, the fluorescence of HPMA copolymer-Dox and of HPMA copolymer-AGM-Dox did not show pH-dependence. This means that the fluorescence output of a given concentration of conjugate will be independent from the cellular compartment in which the conjugate is localised.

It is also well-known that the fusion of the intracellular vesicles can lead to accumulation and therefore concentration of drugs (Tulkens and Trouet, 1978). Studies investigating the uptake and the accumulation of the HPMA-copolymer-Dox in B16F10 cells showed that the lysosomal concentration of the conjugate was up to 5 fold higher than that present in the extracellular environment (Seib, 2005). For this reason, the concentration dependence was also investigated. The fluorescence quenching found for concentrations greater than 0.02 mg/mL Dox equiv. is consistent

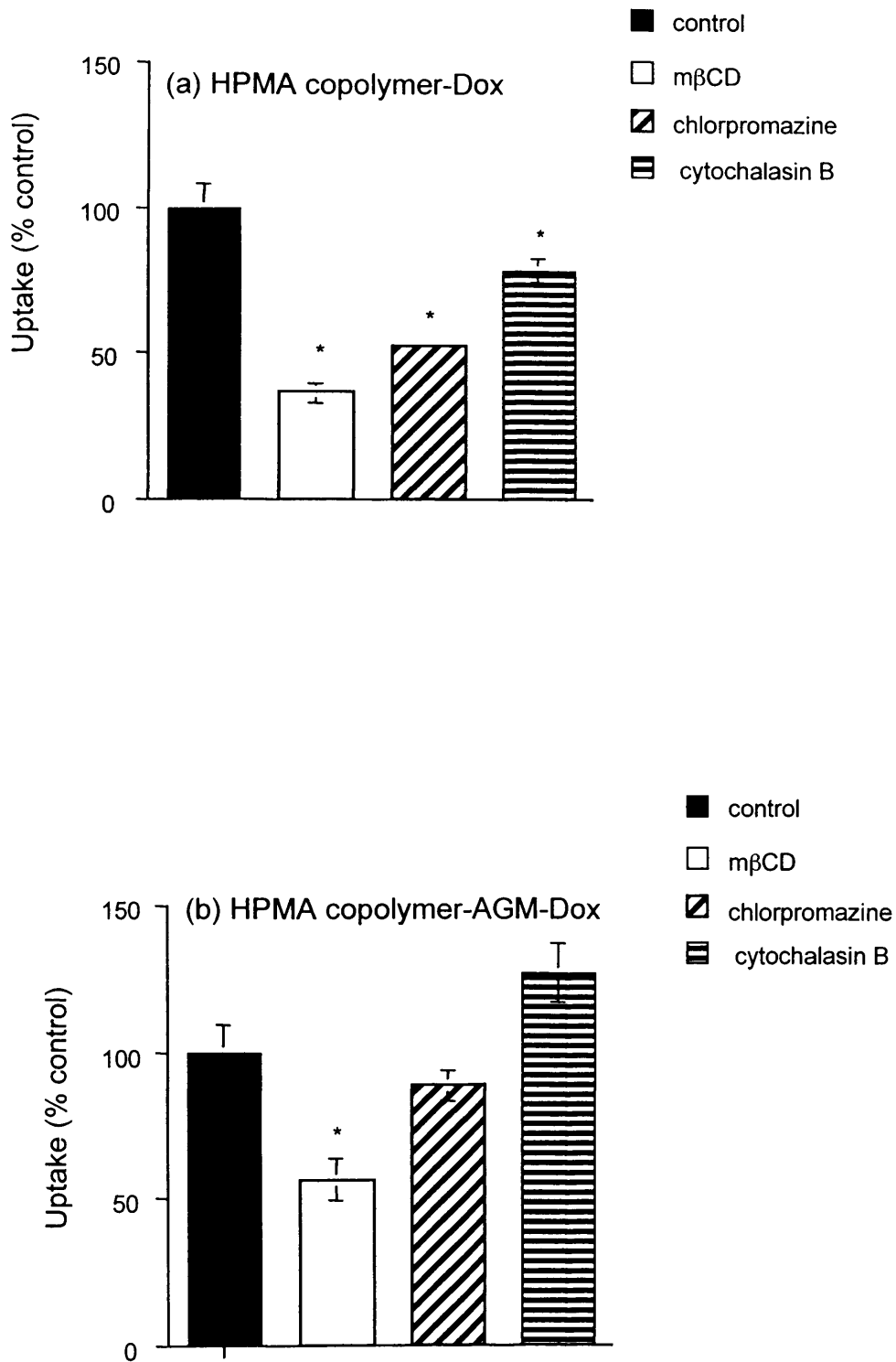


Fig. 5.12. Effect of M β CD, chlorpromazine and cytochalasin B on the uptake of HPMA copolymer-Dox (panel a) and HPMA copolymer-Dox-AGM (panel b) by MCF-7 cells (incubation time $t = 60$ min). Statistical significance against control (in absence of inhibitor) was determined at $p < 0.05$ (*) by ANOVA followed by Bonferroni post hoc test. Data represent mean \pm S.E.M., $n = 5$

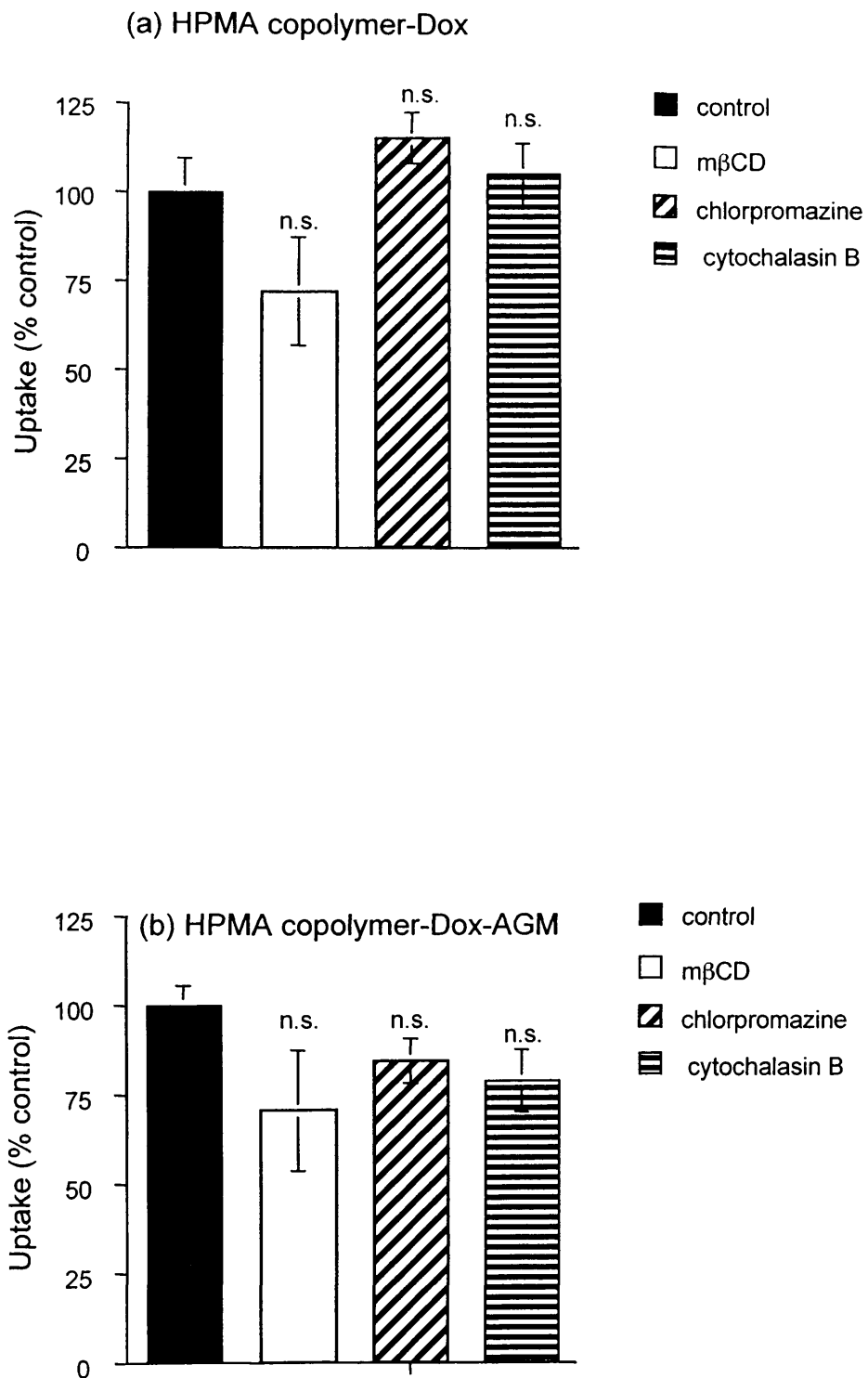


Fig. 5.13. Effect of MβCD, chlorpromazine and cytochalasin B on the uptake of HPMA copolymer-Dox (panel a) and HPMA copolymer-Dox-AGM (panel b) by MCF-7ca cells (incubation time = 60 min). Statistical significance against control (in absence of inhibitor) was determined at $p < 0.05$ (*) by ANOVA followed by Bonferroni post hoc test. Data represent mean \pm S.E.M., $n = 6$

with other studies that also reported fluorescence quenching for HPMA copolymer-Dox in the same range of concentrations (0.04 to 1 mg/mL Dox equiv) (Seib, 2005). This observation has important implications. The conjugates described in this study are designed to achieve lysosomotropic delivery. However, accumulation of the conjugate in the lysosomal compartment might not lead to a proportional increase in fluorescence leading to underestimation of the amount of conjugate internalised.

While low molecular weight drugs can enter cells by passive diffusion, the uptake of macromolecules is restricted to the endocytic route. Internalisation of HPMA copolymers via pinocytosis has been described using a variety of techniques, for instance, HPLC analysis (Wedge, 1991; Wedge et al., 1991), confocal fluorescence microscopy (Omelyanenko et al., 1998), flow cytometry (Kovar et al., 2004) and monitoring [¹²⁵I]-labelled conjugates (Duncan et al., 1981; Flanagan et al., 1989). The studies presented here confirmed internalisation of both conjugates in both cell lines. The visualisation of their uptake by fluorescence microscopy showed fluorescence in vesicular compartments which was consistent with an endocytic uptake and with previous studies also showing localisation of the HPMA copolymer-Dox in cytoplasmic vesicles (Hovorka et al., 2002; Omelyanenko et al., 1998). However, the absence of time-dependent uptake after 10 min is interesting. It is well known that cells have a complex trafficking network that can lead to rapid recycling within a relatively short (5 - 10 min) time frame (reviewed in Jones et al., 2003; Maxfield and McGraw, 2004). Therefore, one possibility is that after 10 min an equilibrium between the endocytosis and exocytosis rate of the copolymer is established. Another possibility is occurrence of fluorescence quenching due to progressive accumulation of the conjugates in the vesicles and consequent under-estimation of the amount of conjugate internalised.

Other authors have investigated the uptake of HPMA copolymer-Dox by flow cytometry and compared it to the uptake of free Dox and of Dox conjugated to HPMA via a pH-sensitive linker (Kovar et al., 2004). They showed a markedly higher cell-associated fluorescence for HPMA copolymer-Dox than for free Dox (Kovar et al., 2004). However, a quantitative comparison is difficult as different quantities of fluorophore (Dox) were used in that study (3 x IC₅₀ value was used for each

compound). On the contrary, to allow an easier comparison, in the study presented here, the amount of fluorophore was kept constant. Although both conjugates showed evidence of internalisation, a higher uptake was seen for HPMA copolymer-Dox. The higher fluorescence output of this conjugate can only partially account for this. It should be noted that the trafficking of the HPMA copolymers to the lysosomal compartment can lead to the release of the free drug (markedly more fluorescence than the polymer bound). The release studies performed incubating the HPMA copolymer-Dox and the HPMA copolymer-AGM-Dox with a mixture of lysosomal enzymes (Vicent et al., 2005) showed that their release rates were different. While HPMA-copolymer-AGM-Dox showed 5 % release of Dox after 1 h, the amount of Dox liberated from the HPMA copolymer-Dox was double in the same time frame (Vicent et al., 2005). These observations suggest that the liberated free Dox could be partially responsible for higher cell-associated fluorescence seen in HPMA copolymer-Dox.

Some authors have reported evidence of drug liberation and presence of free DNM in the nucleus following endocytic uptake of HPMA copolymer-DNM (Wedge et al., 1991). Another research group, in confocal microscopy studies performed on HepG2 cells, observed nuclear fluorescence after incubation with HPMA copolymer-Dox (Omelyanenko et al., 1998). However, other studies performed on a number of cell lines (EL-4 mouse T-cell lymphoma, SW620 human colorectal carcinoma and OVCAR-3 human ovarian adenocarcinoma cells) did not detect any free drug in the nucleus after incubation with HPMA copolymer-Dox, even after 72 h (Hovorka et al., 2002). The authors suggest that the cytotoxicity of HPMA copolymer Dox might be the result of a different mechanism of action than free Dox. Indeed, they suggest that the HPMA copolymer-Dox initiates cell death at membrane level (Hovorka et al., 2002). Interestingly, in the study presented here, evidence of marked membrane binding was found for both conjugates. This was clear from the FACS results and confirmed by the microscopy data. Although these conjugates were designed for lysosomotropic delivery and intracellular liberation of the drugs the possibility of membrane-action needs at least to be taken into consideration. More observations regarding the mechanism of action of HPMA copolymer-Dox conjugates are discussed in Chapter 6.

In order to understand what was the preferential route of uptake of HPMA copolymer-Dox and HPMA copolymer-AGM-Dox by the model cell lines (MCF-7 and MCF-7ca) and, most importantly to compare the uptake of the two conjugates, 3 different inhibitors were used. To ensure that any decrease of the uptake was due to the blockage of endocytic route rather than to non-specific toxicity of the inhibitor the three inhibitors were firstly screened for toxicity. The concentrations of inhibitors described in the literatures for this type of studies showed a toxicity lower than 10 % and were consequently used.

The decreased uptake of HPMA copolymer-Dox and HPMA copolymer-AGM-Dox by MCF-7 and MCF-7ca seen in presence of M β CD suggests that both these conjugates rely on a cholesterol-dependent pathway to enter the cells (Rejman et al., 2004). Both clathrin- and caveolin-dependent pathways are cholesterol-dependent (Conner and Schmid, 2003; Hailstones et al., 1998; Rodal et al., 1999). However, as wild type MCF-7 cells do not express a detectable amount of caveolin (Fiucci et al., 2002), the caveolin-dependent route seems extremely unlikely. To investigate if a clathrin-dependent pathway was involved in the uptake of the conjugates, uptake studies were also performed in presence of chlorpromazine, which inhibits only clathrin-dependent uptake (Kee et al., 2004; Rejman et al., 2004; Sun et al., 2005). The certain degree of inhibition seen in the presence of this compound, suggests that clathrin-dependent pathway might play a certain role in the uptake of these conjugates. However, it does not seem to account for the whole inhibition seen after cholesterol depletion. Therefore, a cholesterol-dependent but clathrin-independent pathway is the most likely uptake route used by these conjugates.

Although, more investigations could be performed to compare the uptake of these conjugates and although compensatory pathways might be used by the conjugates in presence of inhibitors, the data here analysed indicate that at this stage, the uptake of HPMA copolymer-Dox does not significantly differ from that of HPMA copolymer-AGM-Dox. This suggests that the uptake seems to be driven more by the characteristics of the polymeric carrier rather than by the presence of one or two

drugs. It also indicates that differences in the uptake are unlikely to account for the different activity of the conjugates.

5.5. CONCLUSIONS

In this study it was hypothesised that differences in the uptake of HPMA copolymer-Dox and HPMA copolymer-AGM-Dox were responsible for their different biological activity. Flow cytometry and fluorescence microscopy showed that both conjugates are internalised by the two breast cancer cell lines previously selected as models. Preliminary studies investigating the route of uptake suggested that both conjugates are internalised via a cholesterol-dependent pathway. Although, further investigations could potentially highlight differences in the uptake of the conjugates, no apparent differences were found in the study presented here. The next chapter will attempt to investigate the cellular mechanism of action of the HPMA copolymer-Dox and the HPMA copolymer-AGM-Dox.

Chapter 6:

Using immunocytochemistry to investigate the effect of the HPMA copolymer-Dox and the HPMA copolymer-AGM-Dox on the cellular markers ER, PgR, pS2, Ki67 and Bcl-2

6.1. INTRODUCTION

The observation that the HPMA copolymer conjugate carrying the combination of AGM and Dox on the same backbone was much more cytotoxic than the HPMA copolymer-Dox was an important finding (Chapter 4). In an attempt to explain this behaviour, it was shown that the HPMA copolymer-AGM inhibits intracellular aromatase activity, and that AGM release from the conjugate is required for this effect (section 4.3). Studies in Chapter 5 suggest that differences in the rate and mechanism of endocytic uptake of the HPMA copolymer-Dox and the combination conjugate by MCF-7 and MCF-7ca cells are *not* responsible for their marked difference in cytotoxicity. It seems most likely that the rate, and pattern of, AGM and Dox liberation from the conjugate (Vicent et al., 2005) and synergistic pharmacological activity are responsible for the marked enhanced cytotoxicity of the combination. To try to identify more precisely the cellular mechanism of action, immunocytochemistry was used here to study the effect of HPMA copolymer-Dox and HPMA copolymer-AGM-Dox on some of the cellular markers classically used to monitor activity of breast cancer therapies.

Immunohistochemical analysis of clinical tissue is routinely used to predict a breast cancer patient's likely response to anti-hormone treatments and their prognosis (discussed in Gee et al., 2002). Established cellular markers include the ER and the oestrogen-regulated proteins PgR (Collett et al., 1996) and pS2 (Racca et al., 1995). Proliferation markers like Ki67 (reviewed in van Diest et al., 2004) are also used. Other studies have suggested that the assessment of the tumour suppressor gene p53 might be an important prognostic marker for breast carcinomas (Beck et al., 1995). Evaluation of p53 expression has also been investigated as potential predictor of response to chemotherapy, but contradictory results were found (reviewed in Barrett-Lee et al. 2005). In addition to the assessment of these markers prior to endocrine therapy, interestingly, several authors have also monitored variations in their levels with time during anti-hormone treatment and have attempted to establish a correlation between expression levels and response to the treatment (Chang et al., 2000; Kenny et al., 2001; Makris et al., 1998).

In this study, semiquantitative immunocytochemistry was used to investigate the effect of HPMA copolymer conjugates on those cellular markers considered most

relevant to this project. Immunocytochemistry was chosen because it allows a direct visualisation of the expression of the protein under investigation at its precise cellular location and it requires relatively small volumes of reagents, making it more convenient than other techniques such as Western Blotting.

To seek further evidence that free and polymer-bound AGM were able to inhibit aromatase at cellular level, MCF-7 and MCF-7ca cells were first examined for the expression of the ER and the oestrogen-regulated genes PgR and pS2 after incubation with steroid-free, oestradiol-supplemented or androstenedione-supplemented medium. The MCF-7ca cells were then exposed to free and polymer-bound AGM in the presence of the aromatase substrate androstenedione and the expression of PgR was subsequently assessed.

To investigate the mechanism of cytotoxicity of the HPMA copolymer-Dox and HPMA copolymer-AGM-Dox, their effect on the proliferation marker Ki67 was studied in MCF-7 and MCF-7ca cells. Ki67 is a protein expressed by the cells in all phases of cell cycle, but it is not expressed in G0 (reviewed in Scholzen and Gerdes, 2000). This makes Ki67 an ideal marker for investigating whether the conjugates affect proliferation differently.

Finally, experiments were conducted to investigate whether the conjugates induced apoptosis. It is known that free Dox is able to induce apoptosis (reviewed in Gewirtz, 1999). Indeed, some studies have suggested that HPMA copolymer-Dox is also able to induce apoptosis *in vitro* in human ovarian carcinoma cells (Minko et al., 1999). These authors suggest that the HPMA copolymer-Dox is more effective at apoptosis induction than the free Dox (Minko et al., 2001). Other studies, however, showed that HPMA copolymer-Dox exerts its cytotoxic activity primarily by induction of necrosis (Demoy et al., 2000; Musila et al., 2001). Although the mechanism of action of the HPMA copolymer-Dox is still fiercely debated (reviewed in Duncan, 2005), the possibility of apoptosis-induction cannot be disregarded. In the case of the HPMA copolymer-AGM-Dox apoptosis-induction may be more probable as it is known that aromatase inhibitors are able to induce apoptosis (reviewed in Johnston and Dowsett, 2003).

It is important to note that the HPMA copolymer-AGM-Dox might be able to induce apoptosis via two different mechanisms. First, the combination conjugate may act following endocytic uptake and subsequent drugs release, Dox and AGM could exert synergistic effects as free drugs. However, there is also the possibility that the HPMA copolymer conjugates exert their action at the plasma membrane level (Hovorka et al., 2002) (Fig. 6.1). In Chapter 5, a marked membrane binding was seen for both conjugates in MCF-7 and MCF-7ca cells, which might support the hypothesis of membrane interaction.

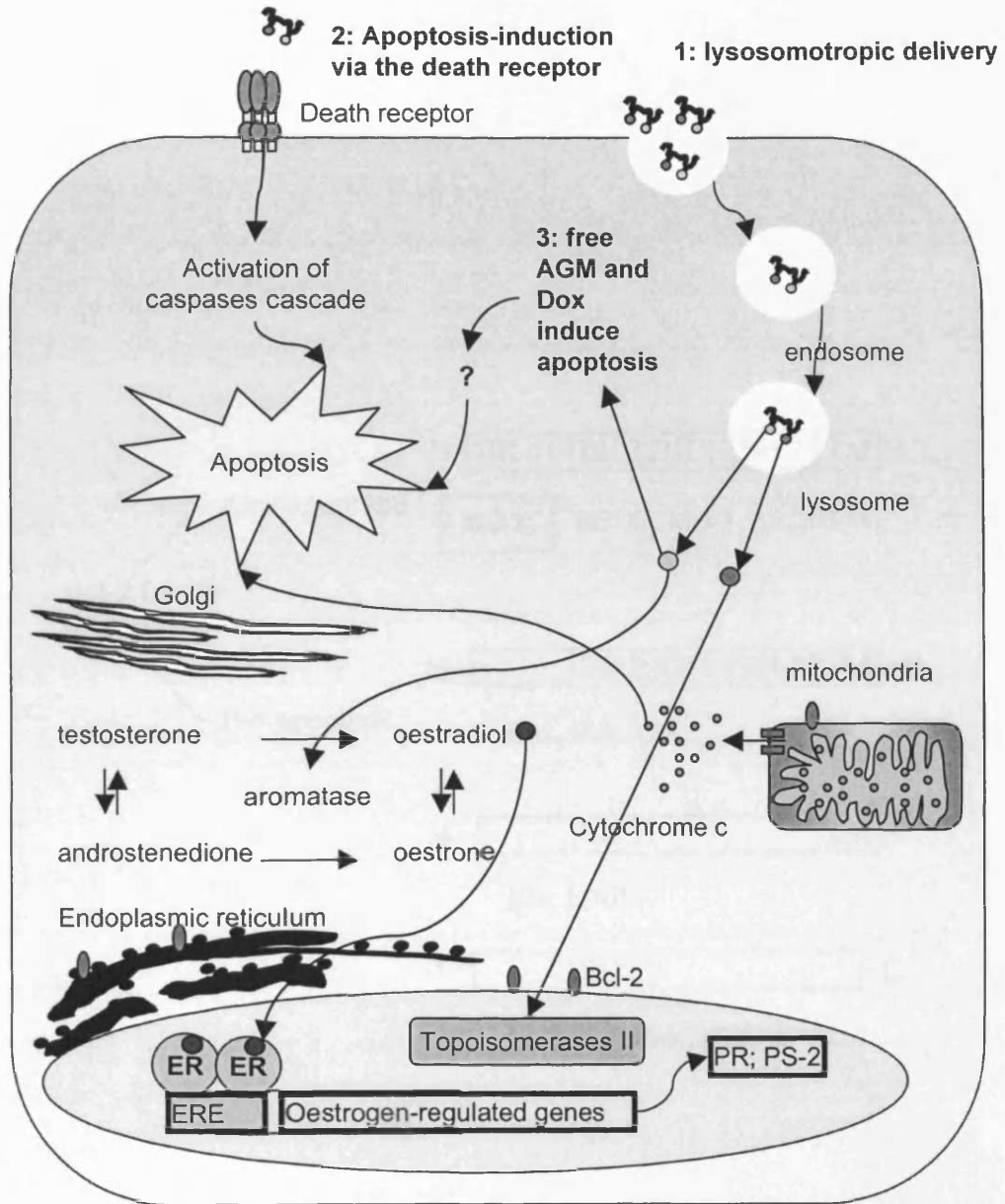
Apoptosis is an extremely complex process involving several proteins. Amongst them, the Bcl-2 family is well known as a key element in apoptosis regulation. Some proteins in this family induce apoptosis while others prevent it (summarised in Fig. 6.2). For example, Bcl-2 (a protein located on the external membrane of the mitochondria, on the nuclear membrane and on the endoplasmic reticulum) has an anti-apoptotic, pro-survival action (reviewed in Burlacu, 2003; Thomenius and Distelhorst, 2003). In this study, Bcl-2 was selected as a marker because it is involved in the cell survival, and also it is an oestrogen-regulated gene (Willsher et al., 2002). Therefore, it was considered an ideal marker for a conjugate carrying both a classical chemotherapeutical agent and an aromatase inhibitor.

In summary, the aim of this study was to use immunocytochemistry to firstly, confirm inhibition of aromatase, and secondly to investigate whether HPMA copolymer-Dox and HPMA copolymer-AGM-Dox displayed different effects on cell proliferation (Ki67) and/or cell-survival (Bcl-2) in MCF-7 and MCF-7ca cells.

6.2. METHODS

6.2.1. Immunocytochemistry

Immunocytochemistry was used to monitor the cellular expression of five markers: ER, PgR, pS2, Bcl-2 and Ki-67. The protocol for immunocytochemistry staining of PgR, pS2, ki67 and Bcl-2 had already been optimised by the technical staff of the Tenovus Centre for Cancer Research (Welsh School of Pharmacy, Cardiff University). The ER staining protocol required optimisation in respect of the concentration of the primary and of the secondary antibody (the goat anti-mouse (GAM)). As the quantity of polymer conjugates was limited it was also necessary to



Legend:

- = Bcl-2
- = cytochrome C
- ▮ = Bax
- = oestradiol
- = AGM
- = Dox

1: lysosomotropic delivery: the conjugate is internalised, trafficked to the lysosomal compartment where the drugs are released. The free drugs act at their target sites.

2: Apoptosis-induction via the death receptor: the conjugate interacts directly with the death receptor (no drug release required).

3: Apoptosis induction by the free drugs: the drugs are released and as free drug induce apoptosis

Fig. 6.1. Schematic representation of the possible mechanisms of action of the HPMA copolymer-Dox-AGM at cellular level

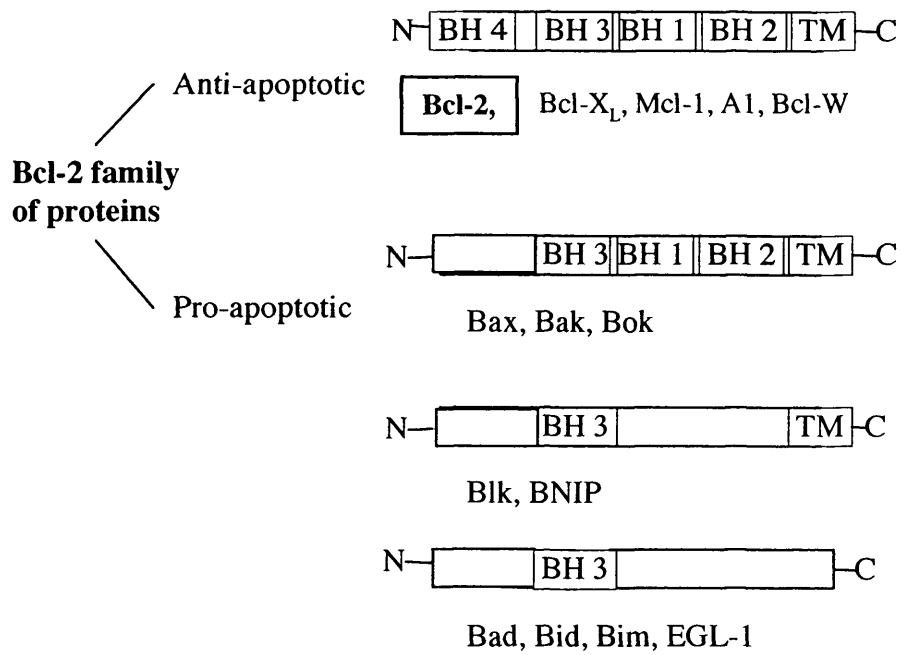


Fig. 6.2. Schematic representation of the protein members of the Bcl-2 family (adapted from Burlacu, 2003)

optimise the experimental technique before experiments could be carried out. Three different systems (each requiring different volumes of medium) for growing MCF-7 and MCF-7ca, cells prior to immunocytochemical staining were compared (Fig. 6.3). These techniques are described below:

- *square tespa coated glass coverslips*. This is the system routinely used in Tenovus Centre for Cancer Research. A square coverslip (22 mm x 22 mm) was placed in a Petri dish (35 mm diameter) prior to the addition of cell suspension (1.5 mL of medium per Petri dish).
- *round tespa coated glass coverslips* (16 mm diameter). The coverslips were placed in a 12-well plate (one coverslip per well), prior to the addition of cell suspension (0.5 mL of medium is required for each well).
- *silicon rubber wall*. In this case, a silicon rubber wall was placed on top of a tespa coated glass slide, creating 12-wells (Fig. 6.3). This system required 0.2 mL of medium per well.

Cells were prepared and added as described below.

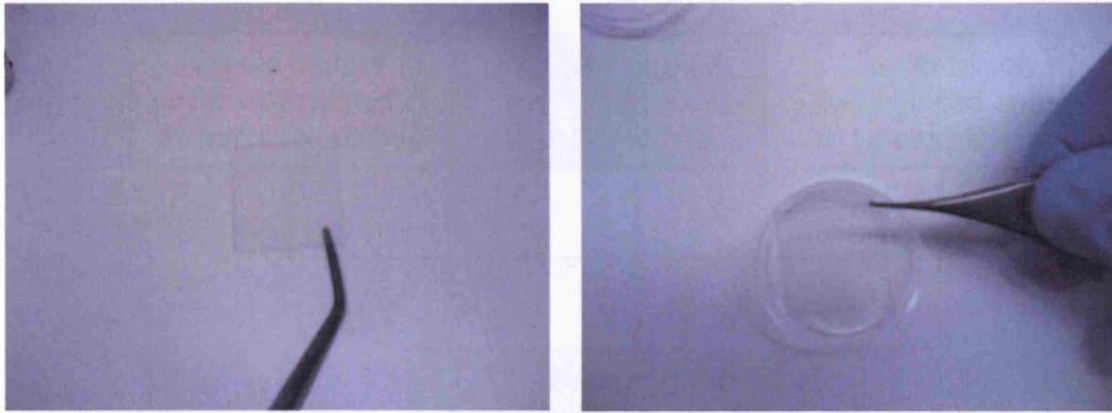
6.2.1.1. Cell preparation for immunocytochemistry

The procedure used to prepare cells prior to immunocytochemical staining is shown schematically in Fig. 6.4. The protocol used for the round coverslips (optimum method) is described in detail below, and differences in procedure for the other two methods are indicated in the scheme (Fig. 6.4). The same protocol was used for MCF-7 and for MCF-7ca cells.

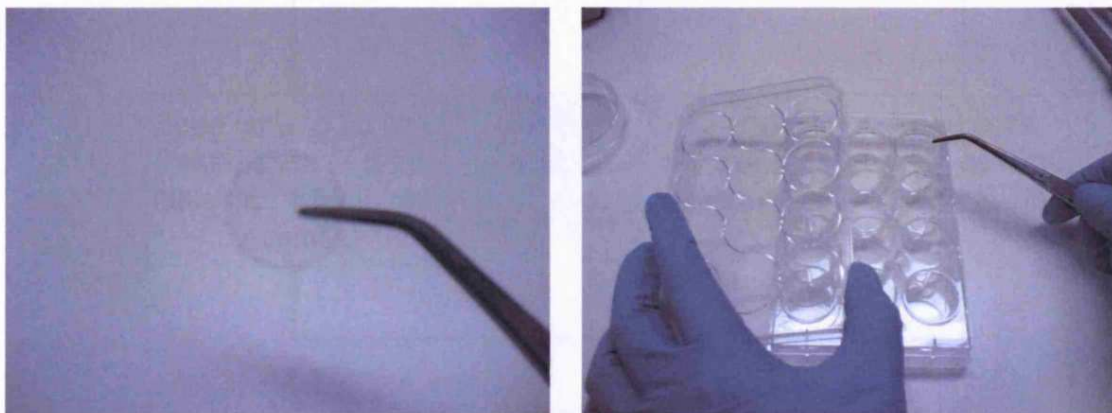
Prior to the cell seeding, sterile glass coverslips (16 mm diameter) were placed into the wells (one coverslip per well) of a 12-well plate. The cells were harvested as previously described (section 2.3.6.2.), seeded at a density of 1.66×10^5 cells/mL (0.5 mL/well) and then allowed to adhere for 24 h.

One of three different protocols was used depending on the experiment being performed (see below for description and Fig. 6.5 for schematic representation).

a) Square coverslip in 35 mm diameter Petri dish (1.5 mL)



b) Round coverslip in 12-well plate (0.5 mL)



c) Silicon rubber placed on a glass slide (0.2 mL)

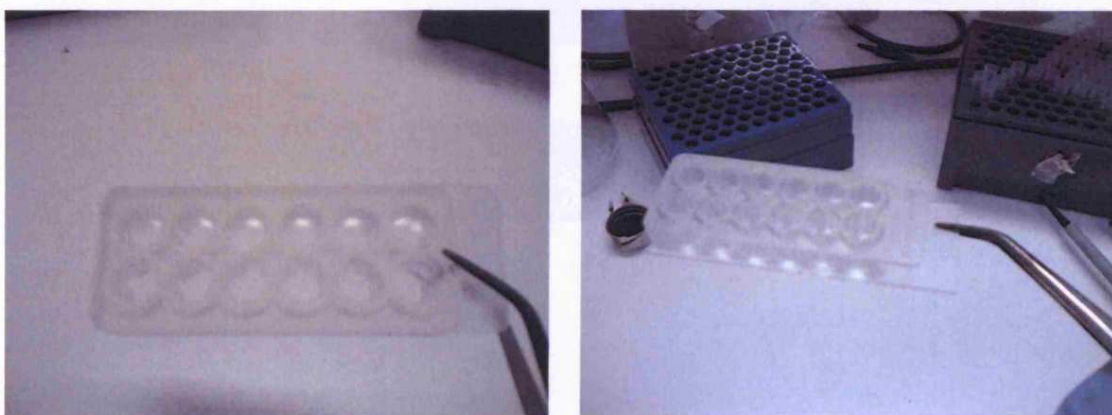


Fig. 6.3. The three systems tested for growing cells prior to ICC staining. Panel (a) shows the square coverslip (22 x 22 mm) placed in a Petri dish (35 mm diameter); panel (b) shows a round coverslip (16 mm) placed in 12-well plate; panel (c) shows the silicon rubber placed on the glass slide

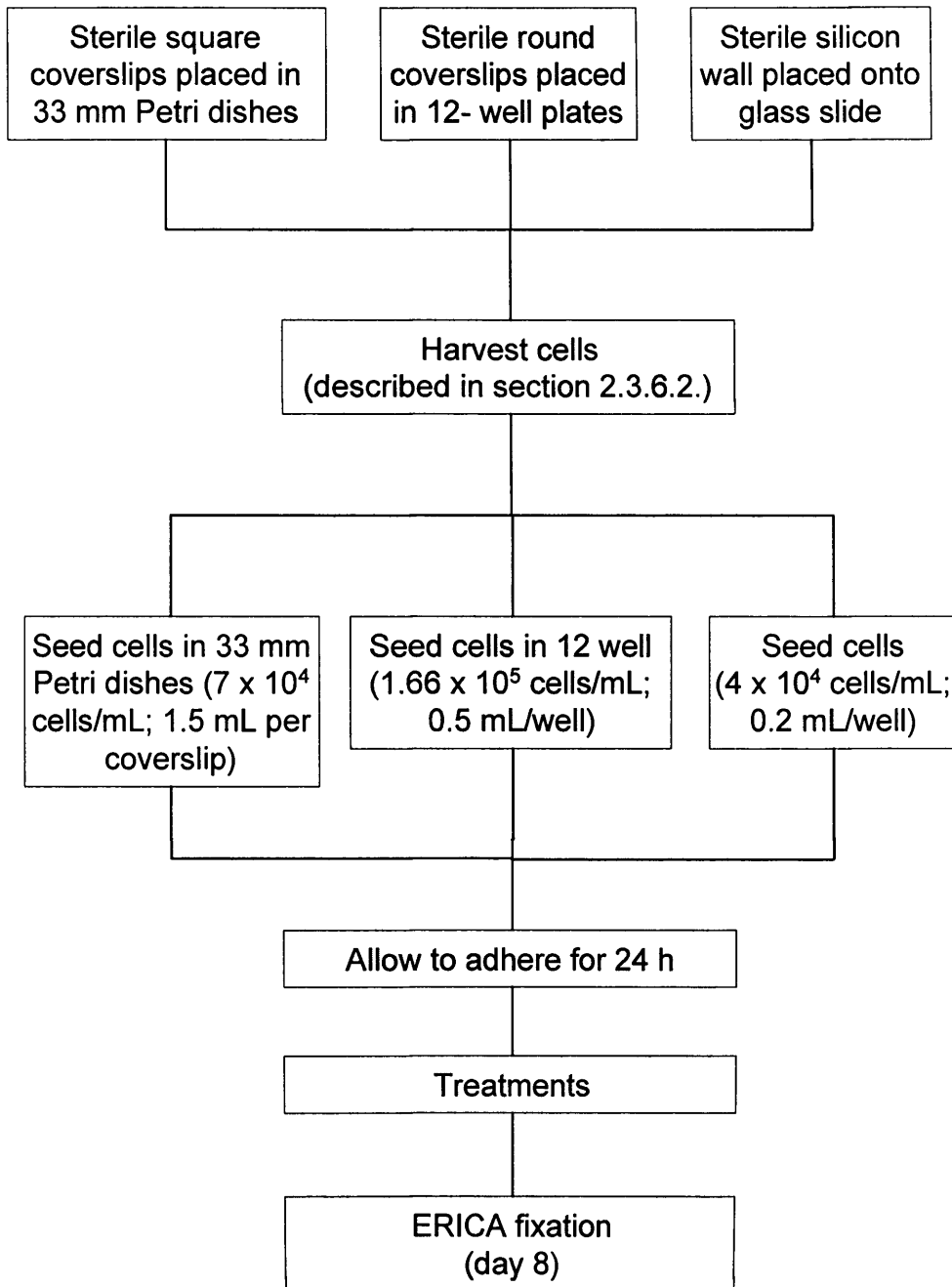
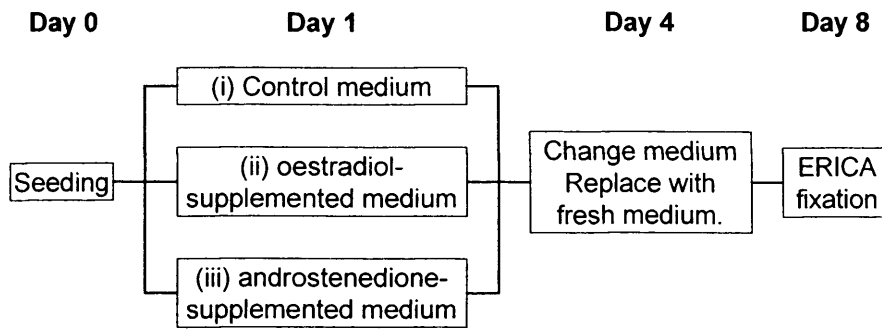
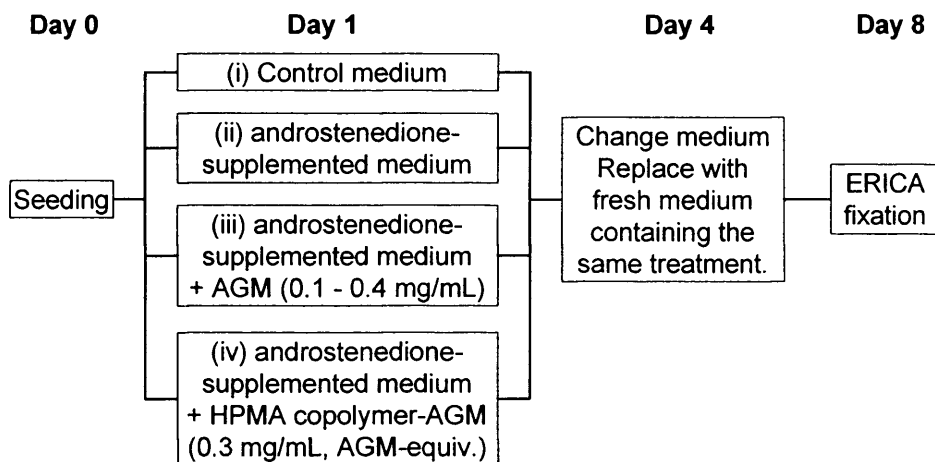


Fig. 6.4. Schematic representation of cell preparation prior to immunocytochemical analysis in the three different systems in exam

Immunocytochemistry ER, PgR and pS2 in MCF- and MCF-7ca cells



Immunocytochemistry of PgR in MCF-7ca cells incubated with androstenedione and free and HPMA copolymer-AGM



Immunocytochemistry of Ki67 and Bcl-2 in MCF-7 and MCF-7ca after incubation with HPMA copolymer-Dox and HPMA copolymer-AGM-Dox.

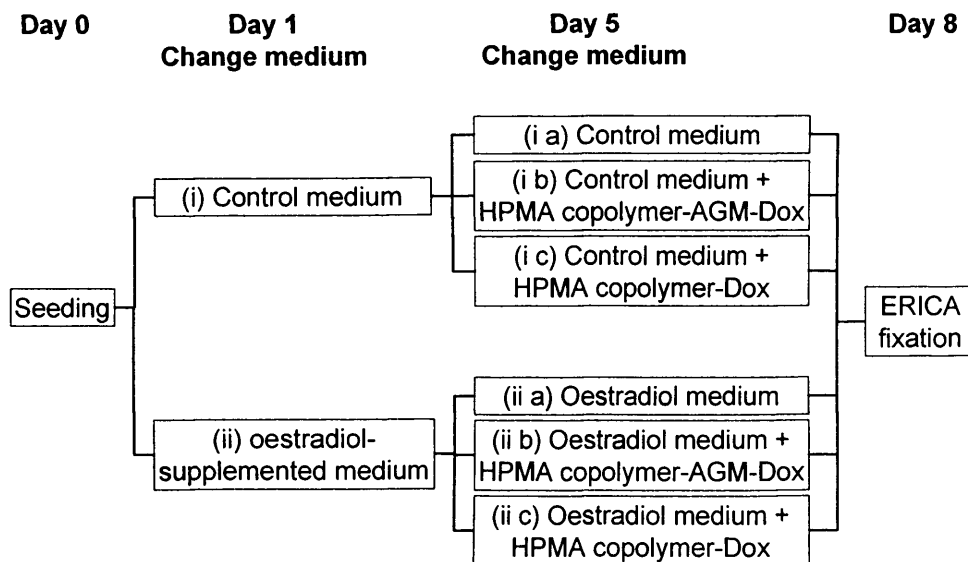


Fig. 6.5. Schematic representation of the different experimental protocols used for MCF-7 and MCF-7ca prior to immunocytochemical analysis

Immunocytochemistry of ER, PgR and pS2 in MCF-7 and MCF-7ca cells

This protocol (and the following protocol) was designed to parallel the experiments previously described investigating aromatase inhibition (sections 2.3.10 – 2.3.13).

After 24 h the medium was replaced with either (i) control medium (WRPMI + 5% SFCS), (ii) medium containing oestradiol (WRPMI + 5% SFCS + 10^{-9} M oestradiol) (iii) medium containing androstenedione (WRPMI + 5% SFCS + 5×10^{-8} M androstenedione). In each case, on day 4 the medium was again replaced with fresh medium and the cells left until day 8 when they were fixed as described below.

Immunocytochemistry of PgR in MCF-7ca cells incubated with androstenedione and free AGM or HPMA copolymer-AGM

After 24 h the medium was replaced with either control medium, (WRPMI + 5% SFCS) or medium containing androstenedione (WRPMI + 5% SFCS + 5×10^{-8} M androstenedione) or medium containing androstenedione, further supplemented with a range of concentrations of free AGM (0.1 mg/mL, 0.2 mg/mL or 0.4 mg/mL) or HPMA copolymer-AGM (0.3 mg/mL AGM-equiv.). In all cases, the medium was replaced on day 4 and the cells were allowed to grow before fixation on day 8 (for method see below).

Immunocytochemistry of Ki67 and Bcl-2 in MCF-7 and MCF-7ca after incubation with HPMA copolymer-Dox and HPMA copolymer-AGM-Dox

The protocol was designed to resemble, as closely as possible, the experimental conditions used for the determination of the IC_{50} values of the conjugates (section 2.3.9 and Chapter 4).

After 24 h the medium was removed and replaced with fresh medium; either control or oestradiol-supplemented medium. On day 5, the medium was again removed and replaced with fresh medium containing the conjugates at a concentration equivalent to the IC_{50} values previously determined for the HPMA copolymer-AGM-Dox i.e.:

- (i) in MCF-7 0.022 mg/mL Dox equiv. (using control medium)
 0.075 mg/mL Dox-equiv. (using oestradiol-containing medium);

- (ii) in MCF7ca 0.012 mg/mL Dox equiv. (using control medium)
 0.0082 mg/mL Dox-equiv. (using oestradiol-containing medium).

The cells were incubated for a further 72 h with the conjugates and then fixed on day 8 as described below.

6.2.1.2. The fixation protocol: "Oestrogen receptor immunocytochemical assay" (ERICA) fixation

The fixation protocol developed by Abbott Laboratories to detect the ER, (ERICA) was used and it is schematically represented in Fig. 6.6. The coverslips were carefully taken from the plate with a pair of tweezers and placed in a rack that was quickly (to prevent drying) put into a bath filled with formaldehyde solution (4 % in PBS) for 15 min at room temperature. The rack was then moved to another bath containing PBS (5 min room temperature) and subsequently to two more baths (methanol 5 min, and acetone 3 min, both placed on dry ice). The temperature of these two baths was monitored to ensure it was constantly kept between - 30 °C and - 10°C. Then the rack was again placed in a PBS bath (5 min, room temperature). Finally, each coverslip was put back in the 12-well plate previously rinsed with ddH₂O and re-filled with a sucrose storage solution (42.8 g sucrose, 0.33 g magnesium chloride anhydrous, 250 mL PBS and 250 mL of glycerol). The coverslips were stored at -20 °C until assayed.

6.2.1.3. Staining of ER, PgR, pS2, Bcl-2 and Ki67

The procedures used to detect ER, PgR, pS2, Bcl-2 and Ki67 were very similar. As an example, a detailed description of ER staining is given. For the other proteins, a schematic representation of the protocol followed is provided in Fig. 6.7.

The coverslips bearing cells were placed on a tray and the storage medium was removed by thorough washings with PBS (2 - 3 washes). Prior to the addition of the primary antibody, the coverslip was washed once with PBS-tween (0.02 %) and the excess solution was removed by gently touching the coverslip edge on a piece of tissue paper. Then, the solution containing the primary antibody (1 : 80, 1 : 120, 1 : 160 or 1 : 200 in PBS) was added to the top face of each coverslip (30 µL per

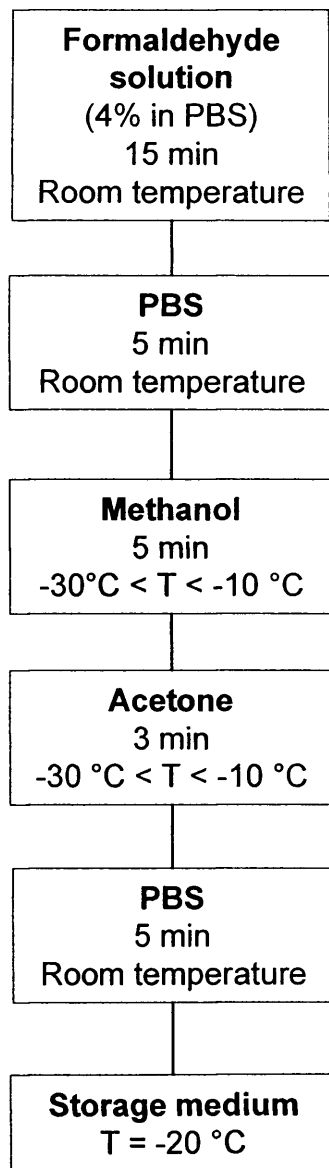
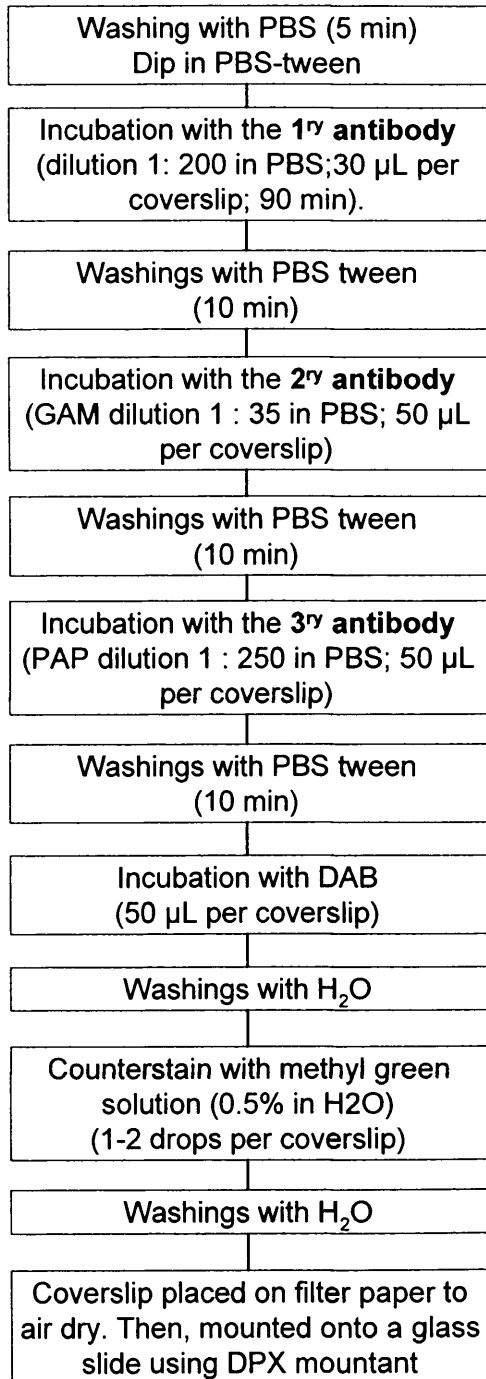


Fig. 6.6. Schematic representation of the fixation procedure followed (ER-ICA, Abbott Laboratories)

a) ER



b) PR

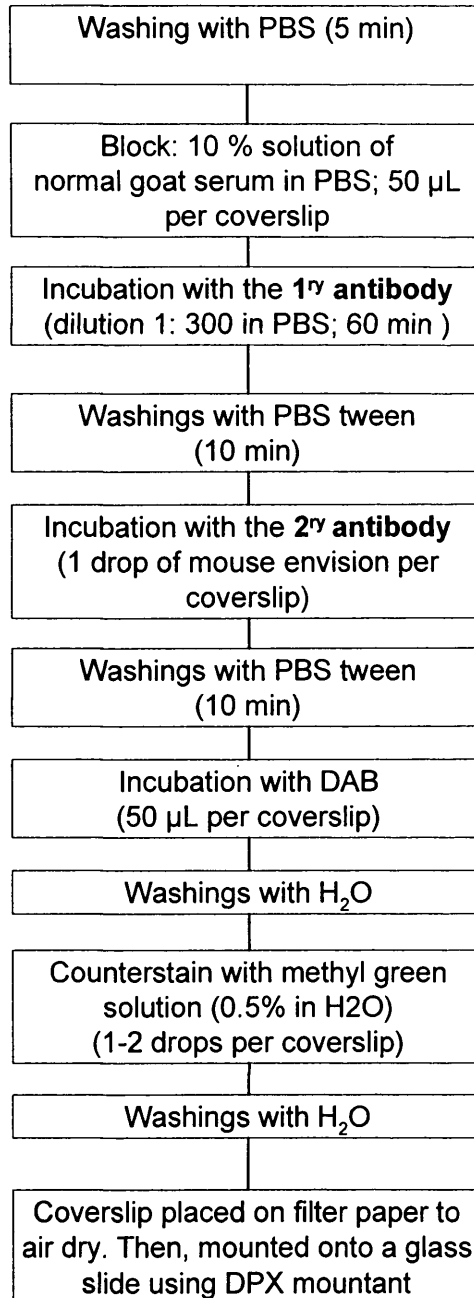
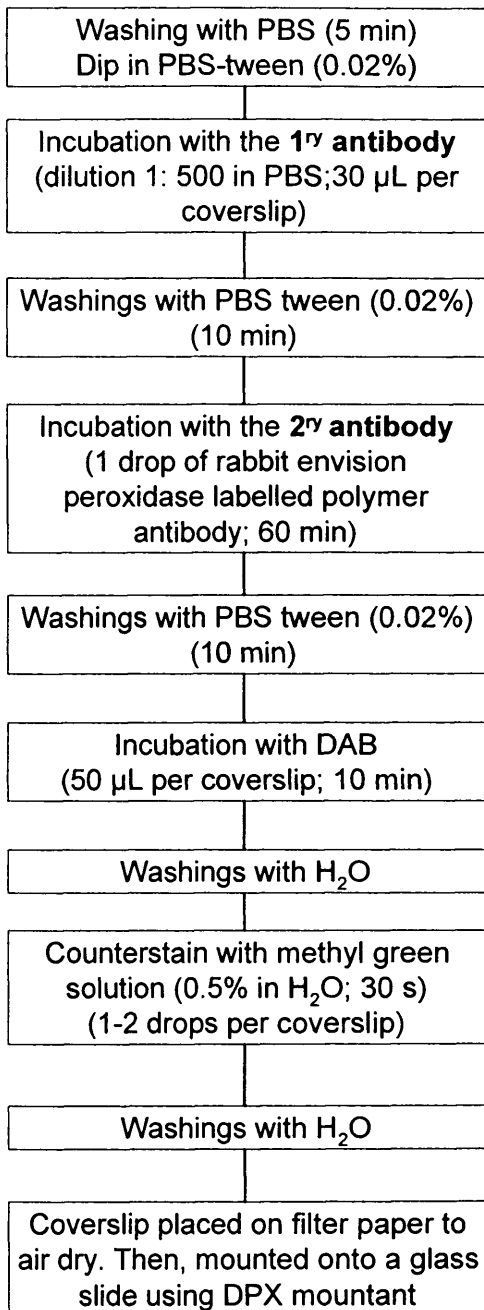


Fig. 6.7. Schematic representation of the ICC staining procedure followed for ER, PgR, pS2, Bcl-2 and Ki67

c) pS2



d) Bcl-2

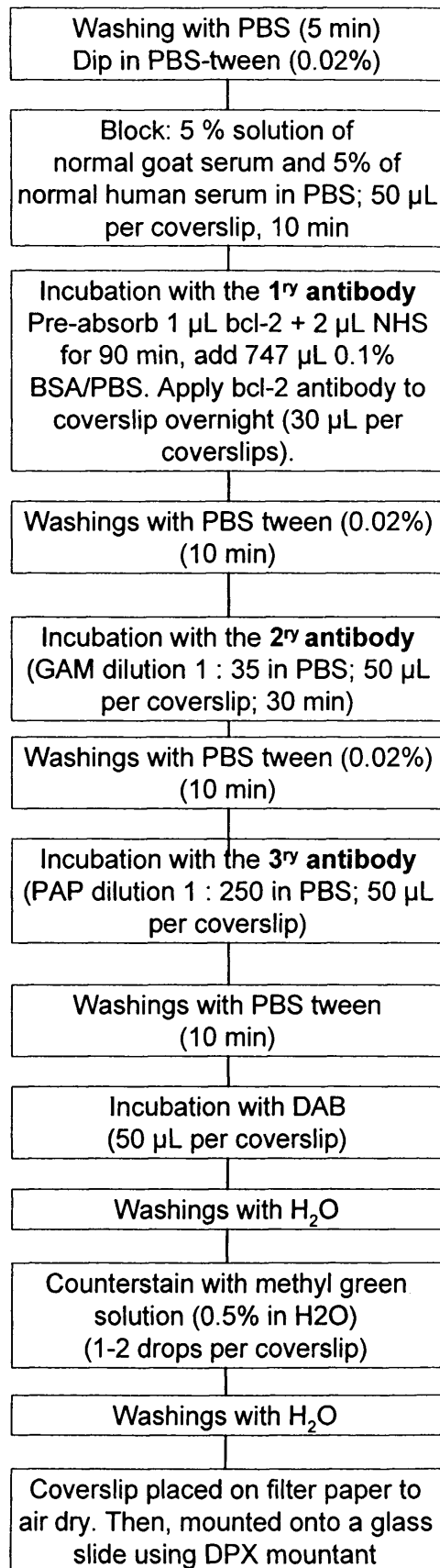


Fig. 6.7. Continued

e) Ki67

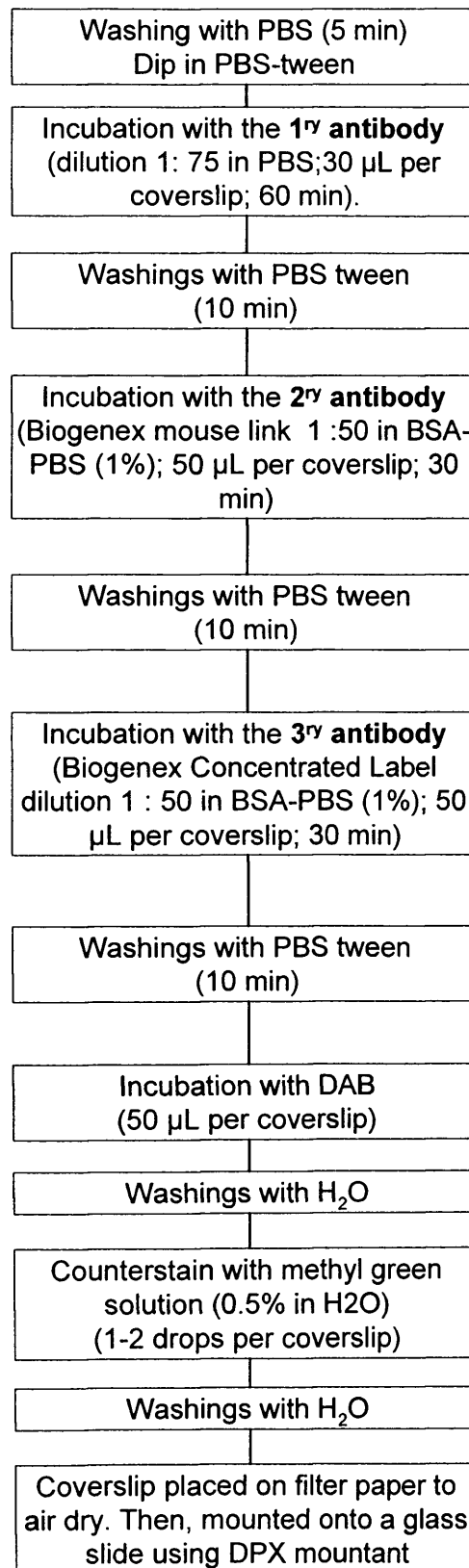


Fig. 6.7. Continued

coverslip), and then it was incubated at room temperature for 90 min. After this time, the solution containing the primary antibody was removed by repeated washing with PBS-tween (5 washes, 1 wash every 2 min) and the solution removed as above. The coverslip was then incubated with a solution of the secondary antibody, GAM (1 : 25 or 1 : 35; 50 μ L) for 30 min at room temperature. After this incubation period, the coverslip was washed as before with PBS-tween and, the excess was again removed. Then, the tertiary antibody (a solution of PAP) in PBS 1 : 250; 50 μ L per coverslip) was added and the coverslip left for 30 min at room temperature. Finally, the coverslip was washed with PBS-tween (five times), and incubated with the peroxidase substrate and DAB for 10 min. The DAB solution was then removed by thorough washing with ddH₂O (3 times), and the cells were counterstained with a solution of methyl green (0.5 % in ddH₂O) for 30 s at room temperature. The coverslip was then washed with ddH₂O, placed on filter paper, and allowed to air dry before being mounted onto a glass slide using DPX mountant.

6.3. RESULTS

6.3.1. Optimisation of the ER staining and experimental set-up

Before undertaking the immunocytochemical characterisation of MCF-7 and MCF-7 ca cells, it was necessary to establish the optimal dilution of primary and secondary (GAM) antibodies for ER staining. When a range of primary antibody dilutions was used, nuclear staining was apparent in all cases (Fig. 6.8). However, at high primary antibody concentrations, cytoplasmic staining was also apparent (Fig. 6.8). As the dilution of 1 : 200 gave a good nuclear staining and a clear background, it was chosen for the subsequent experiments (Fig. 6.8). It is also interesting to note that the cell population showed different staining intensities. Three different sub-populations were present: poorly stained, moderately stained or markedly stained (Fig. 6.8d). An optimisation of the GAM concentration was also necessary. Although nuclear staining was evident at all concentrations tested (Fig. 6.9), a clearer background was seen at a dilution 1 : 35 (Fig. 6.9b), so this concentration was chosen for all subsequent experiments.

Once ER staining had been optimised, it was possible to compare three different experimental systems that might be used for cell incubation with polymer conjugates. The results obtained using the square and the round coverslips produced comparable

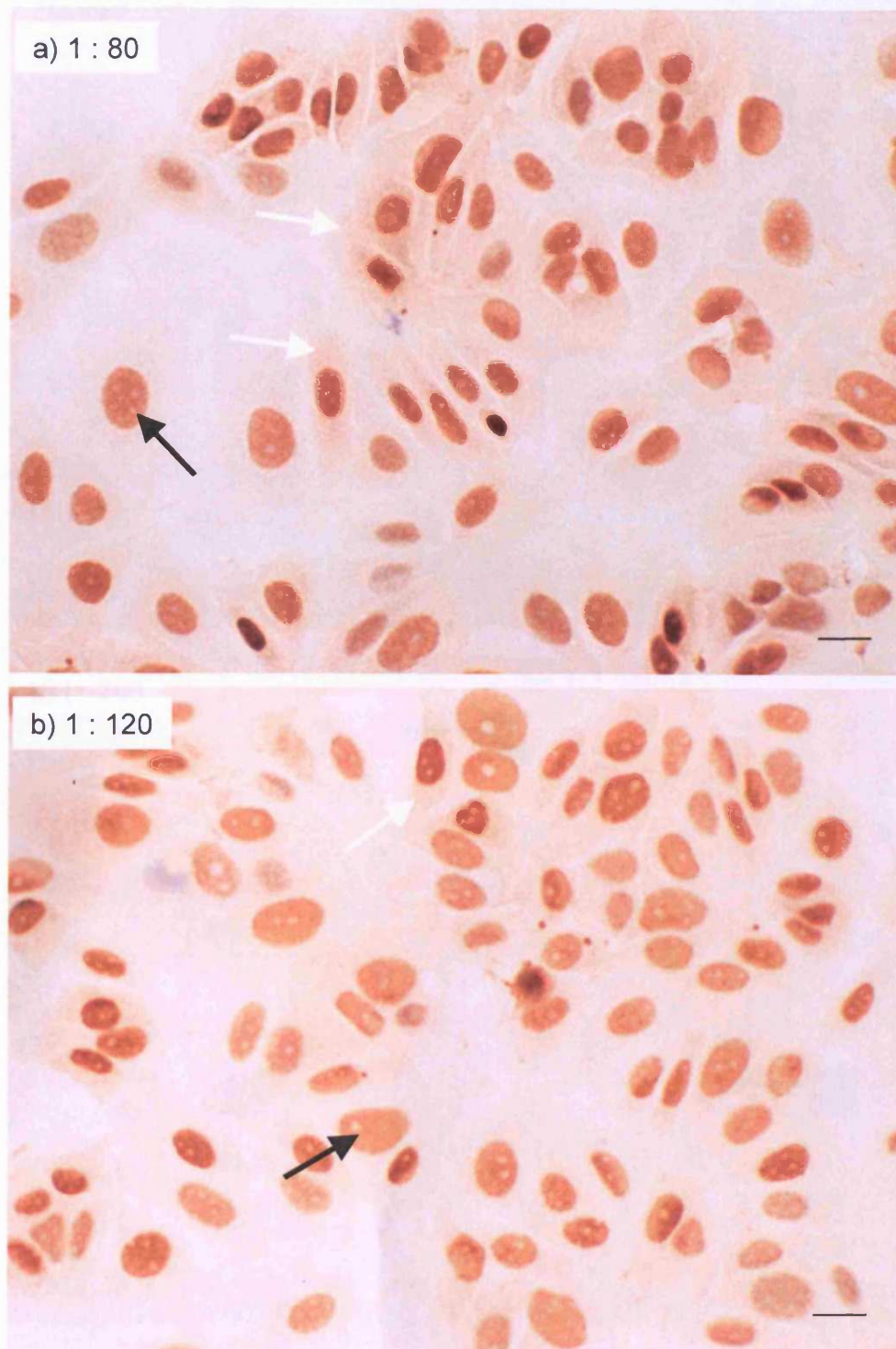


Fig. 6.8. ER staining in MCF-7 cells using the primary antibody at 4 different dilutions (1 : 80, 1 : 120, 1 : 160 and 1 : 200; panel a, b, c and d, respectively). Black arrows indicate nuclear staining; white arrows indicate cytoplasmic staining; blue arrows indicate different degrees of staining: poorly stained (1), moderately stained (2) and markedly stained (3). Size bar = 10 μ m

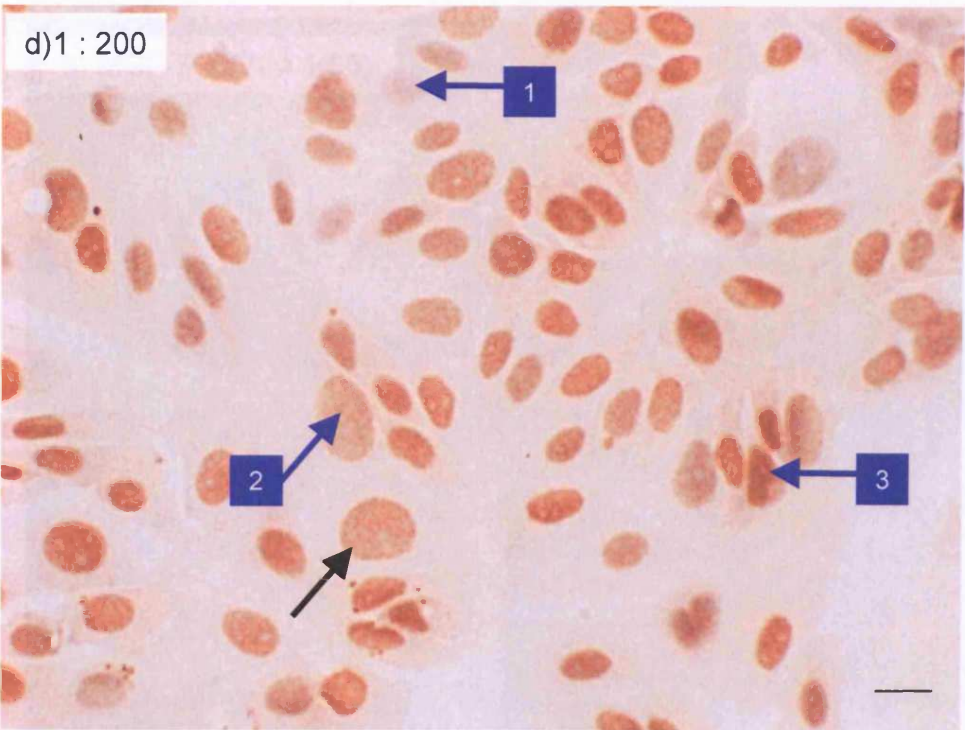
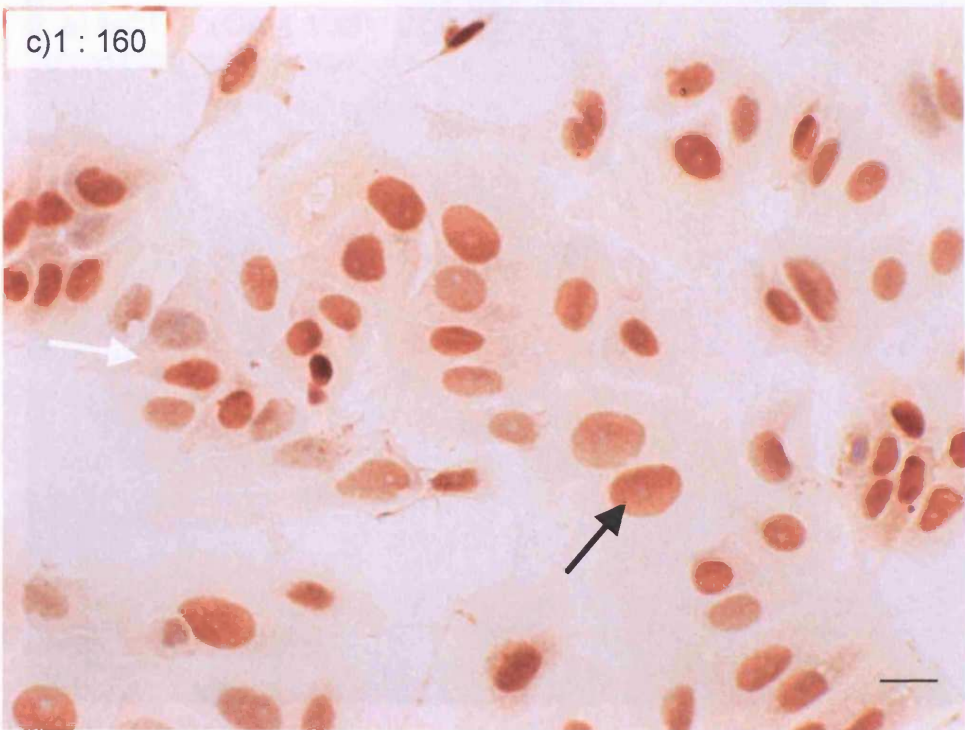


Fig. 6.8. Continued

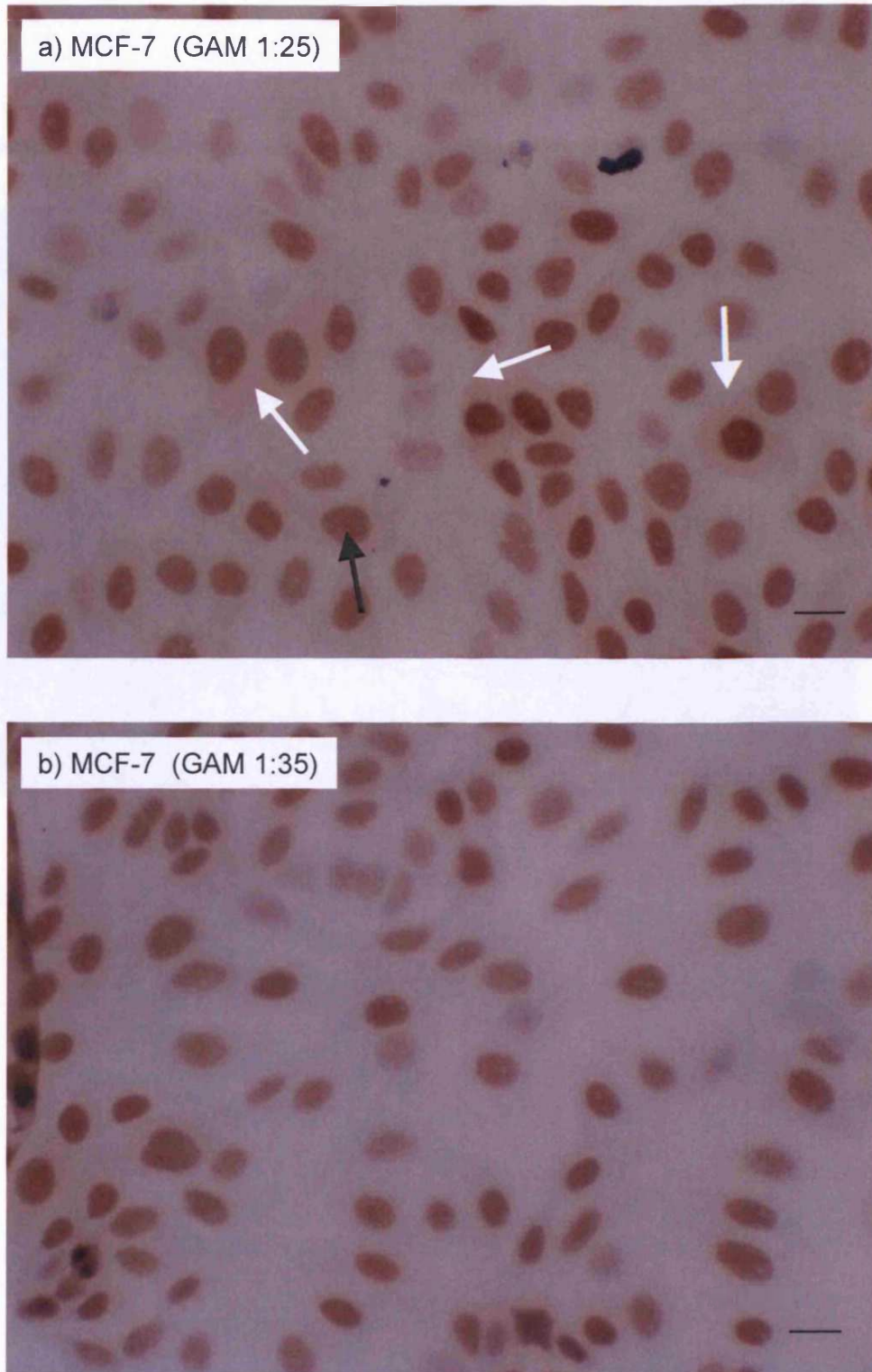


Fig.6.9. ER staining in MCF-7 cells visualised following incubation with different concentrations of GAM. Panels (a) and (b) staining obtained (primary antibody at 1 : 200) using the GAM at 1: 25 or 1 :35, respectively. Panel (c) staining obtained (primary antibody at 1 : 75) using GAM 1 :75. Black arrows indicate nuclear staining; white arrows indicate cytoplasmic staining. Size bar = 10 μ m

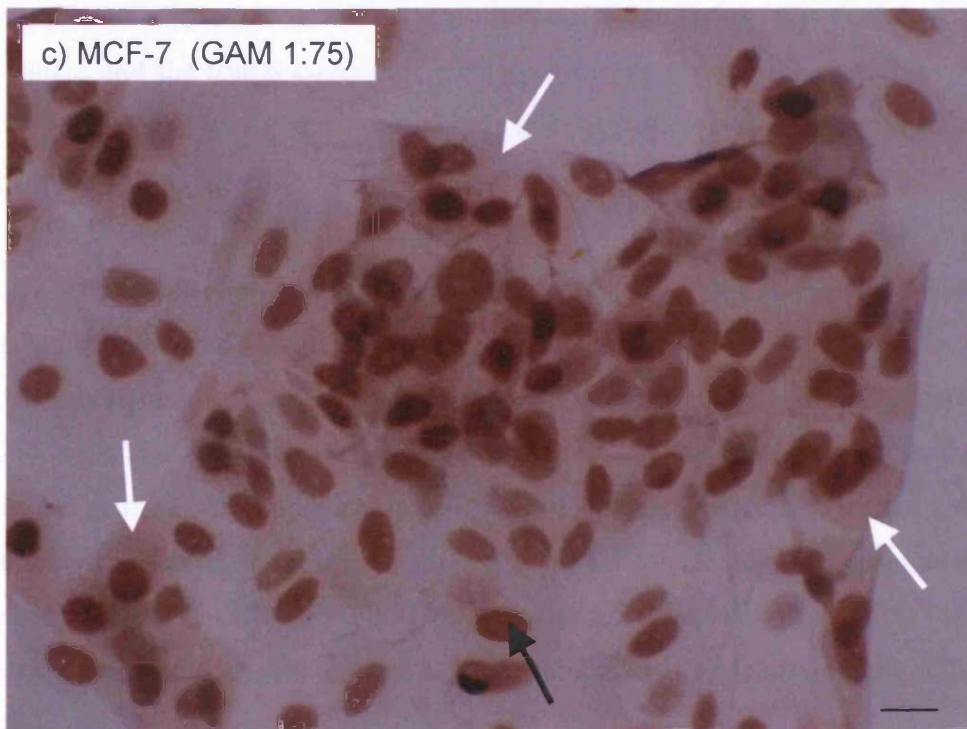


Fig. 6.9. Continued

results. The cells grew in a similar way and reached comparable confluency after 8 days. The ER staining observed was similar between the two systems (Fig. 6.10a and b). However, when the cells were grown on glass slides in the silicon rubber walled system, fewer cells grew and there was also poor ER-staining (Fig. 6.10c). As both the square and the round coverslips gave comparable results, the round coverslips were chosen for subsequent experiments as this incubation system required a smaller reagent volume (0.5 mL).

6.3.2. Characterisation of ER, PgR and pS2 expression in MCF-7 and MCF-7ca cells in presence and absence of AGM

First, both cell lines were characterised for basal expression of ER, PgR and pS2. MCF-7 cells showed good nuclear ER staining in absence of steroids (Fig. 6.11a). When the medium was supplemented with oestradiol (10^{-9} M), cells reached a higher degree of confluency and down-regulation of the ER expression was seen (increased number of negative cells) (Fig. 6.11b). In contrast, ER expression in MCF-7ca cells was not influenced by the presence or the absence of androstenedione although addition did lead to increased confluency (Fig. 6.12).

The expression of PgR and pS2, the two oestrogen-regulated proteins assayed, was markedly induced by oestradiol in MCF-7 cells (Fig. 6.13, 6.15). It is important to note that unlike PgR staining (nuclear), pS2 staining was mainly cytosolic and was more marked in the peri-nuclear region (Fig. 6.15). Whilst the addition of androstenedione did not have any effect on the expression of the PgR in MCF-7 cells (Fig. 6.13c), in MCF-7ca cells androstenedione induced the expression of PgR (Fig. 6.14). Incubation of MCF-7ca with the androstenedione did not, however, have any impact on the expression of pS2 (Fig. 6.16). For this reason, in order to investigate whether free or polymer-bound AGM had an effect on gene expression, it was decided to assess the PgR when MCF-7ca cells were incubated in presence of androstenedione. The presence of free, and polymer-bound AGM decreased androstenedione-induced growth. However, AGM did not inhibit androstenedione-induced PgR expression (Fig. 6.17). In fact, a slight stimulatory effect was seen. Cells incubated with the HPMA copolymer-AGM showed the same pattern of PgR expression as cells incubated with free AGM (Fig. 6.17f).

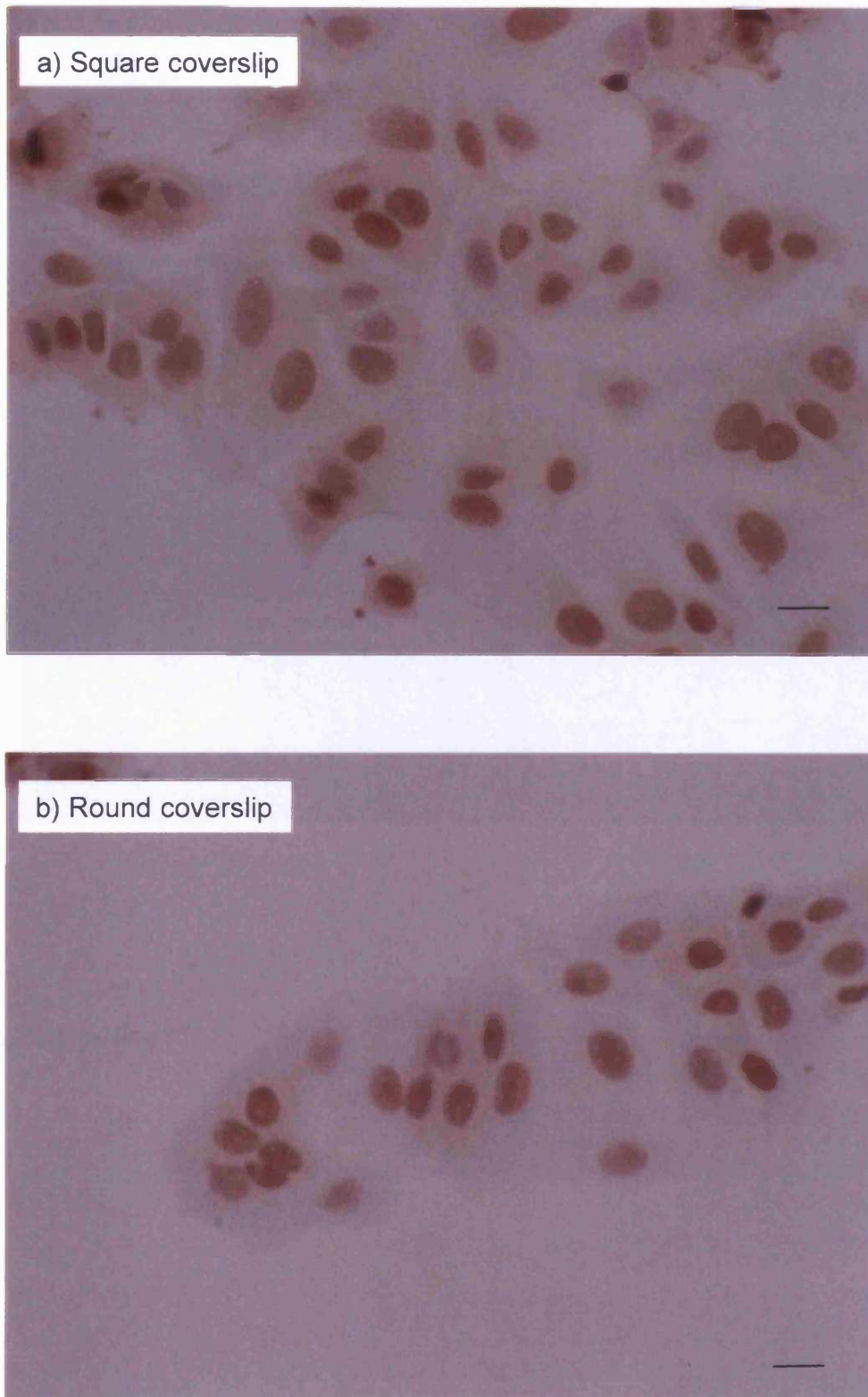


Fig. 6.10. Comparison of ER staining in MCF-7 cells grown using three different techniques. The cells were grown on square coverslips (panel a), on round coverslips (panel b) or on a slide where wells were formed by a silicon rubber (panel c). Size bar = 10 μm

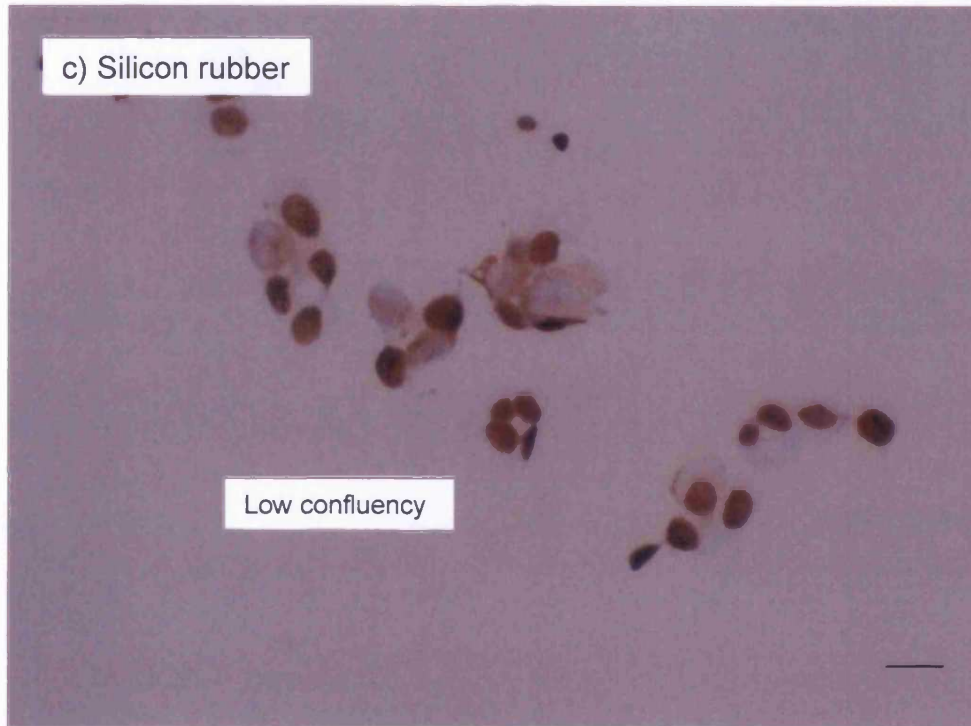
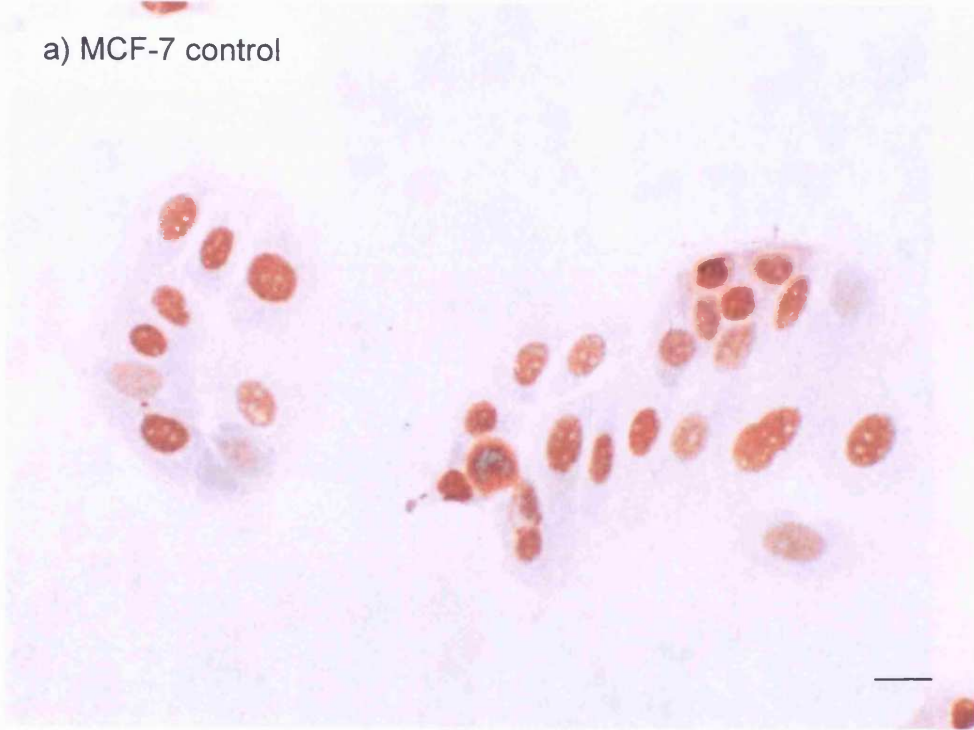


Fig. 6.10. Continued

a) MCF-7 control



b) MCF-7 oestradiol

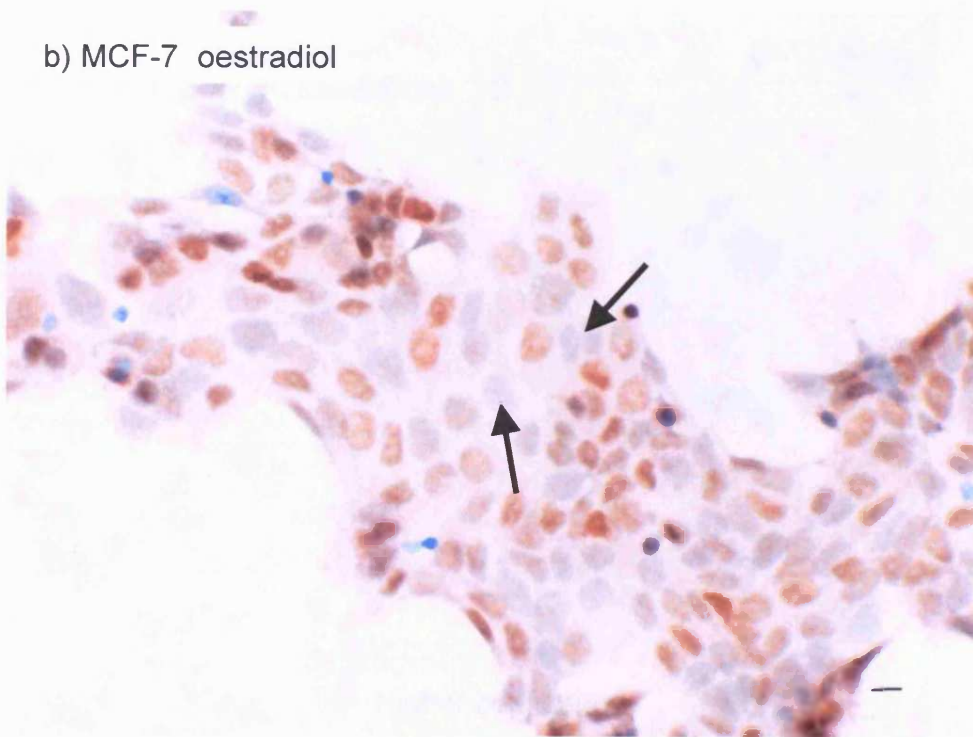


Fig. 6.11. ER expression in MCF-7 in presence of control medium (panel a) or oestradiol-supplemented medium (panel b). Black arrows indicate negative cells. Size bar = 10 μ m

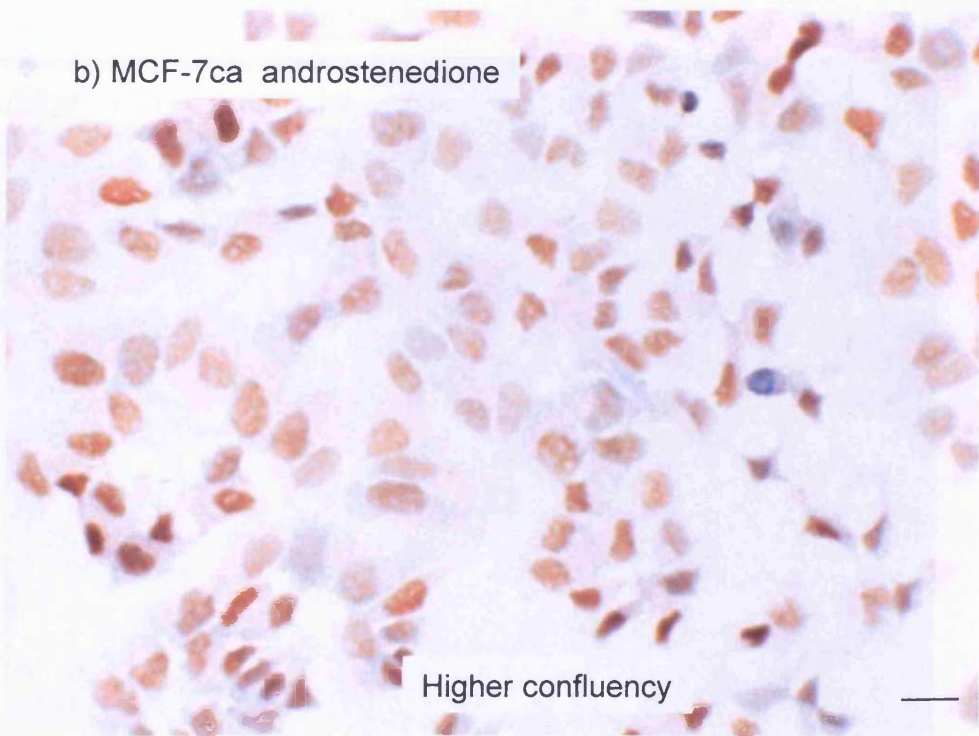
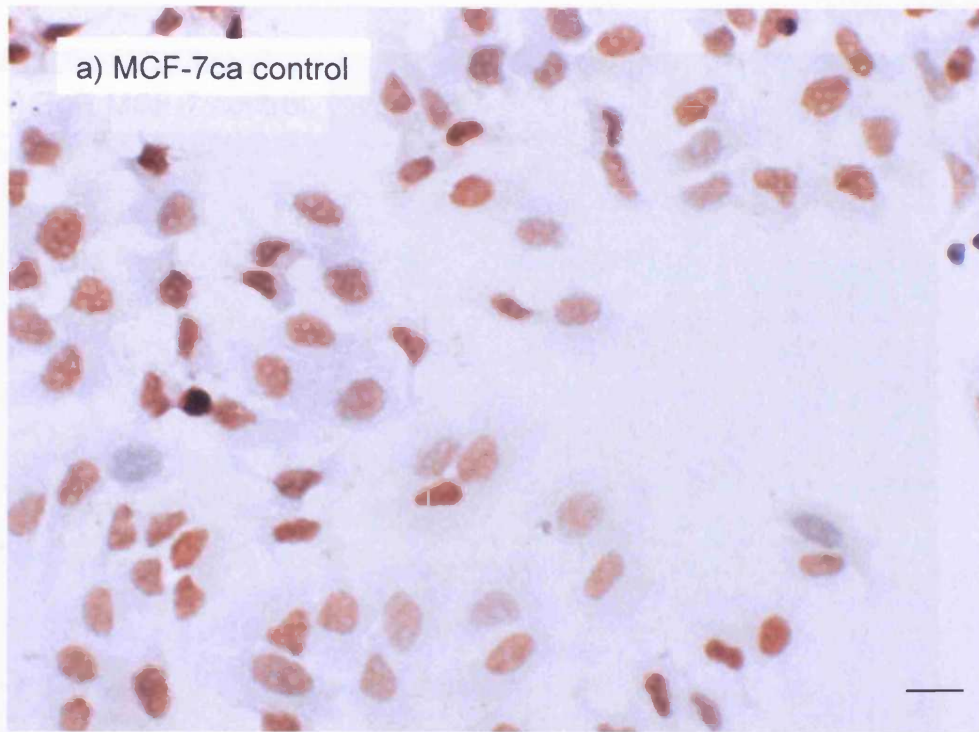


Fig. 6.12. ER expression in MCF-7ca cells grown in control medium (panel a) or androstenedione-supplemented medium (panel b). Size bar = 10 μ m

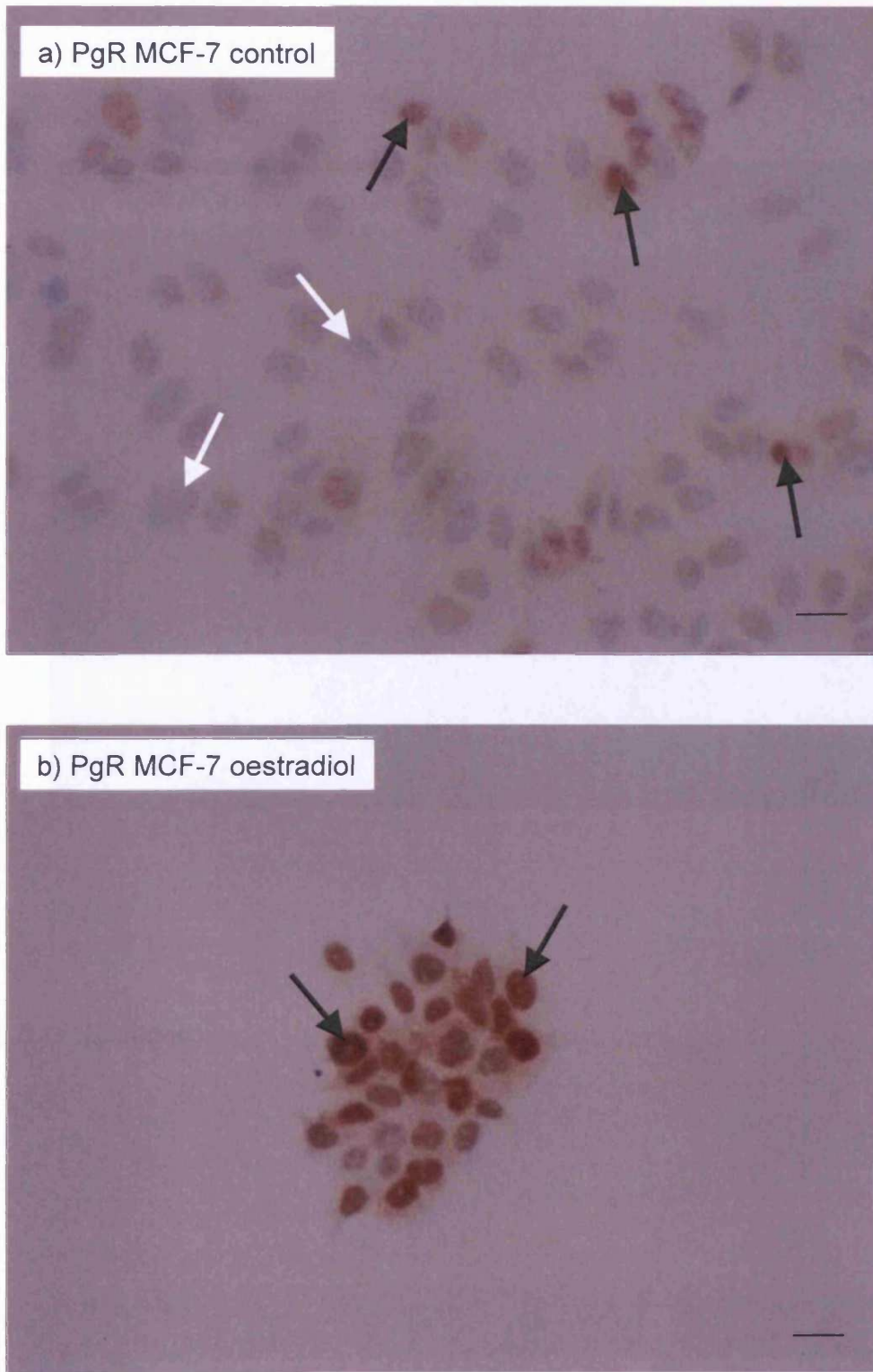


Fig. 6.13. PgR expression in MCF7 cells grown in control medium (panel a), oestradiol-supplemented medium (panel b) or androstenedione-supplemented medium (panel c). Black arrows indicate positively stained cells and white arrows indicate negative or very poorly stained cells. Size bar = 10 μm

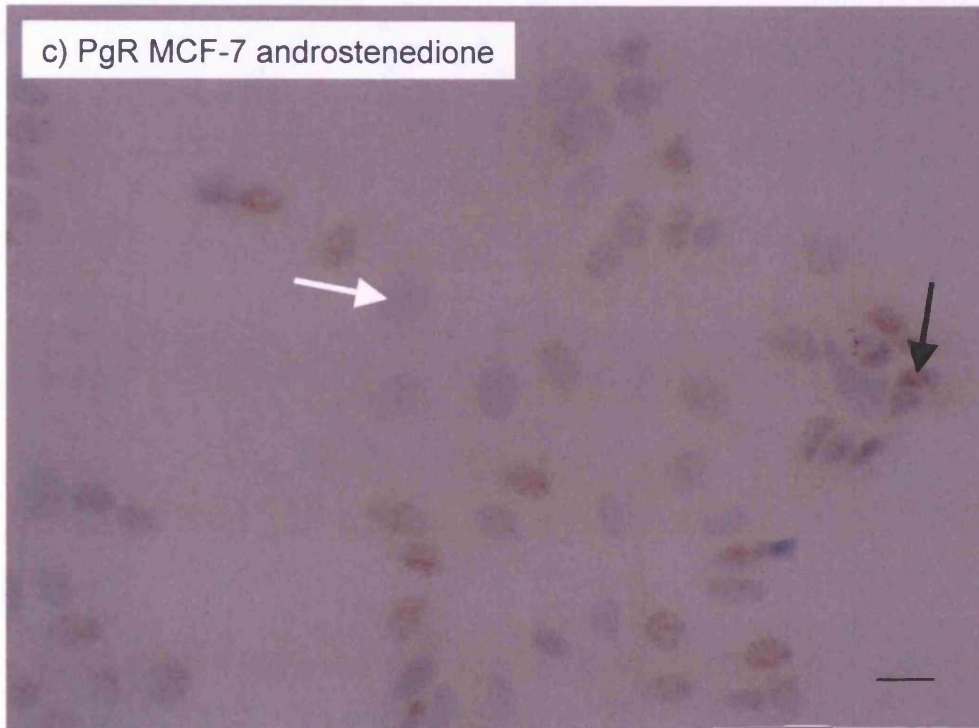


Fig. 6.13. Continued

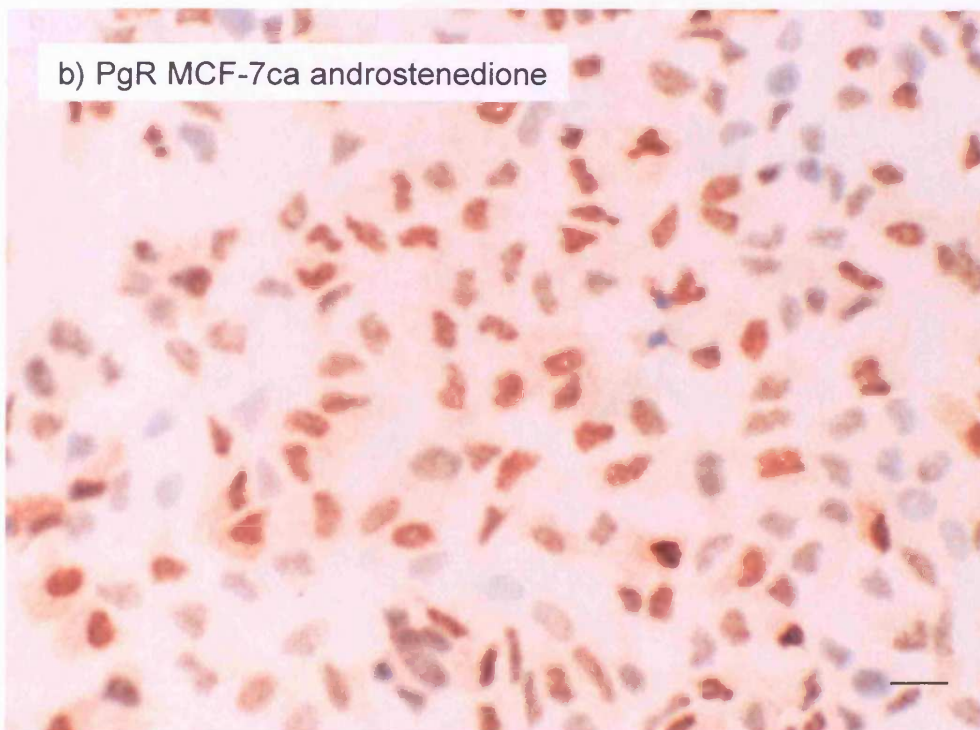


Fig. 6.14. PgR expression in MCF-7ca cells grown in control medium (panel a), or androstenedione-supplemented medium (panel b). Size bar = 10 μ m

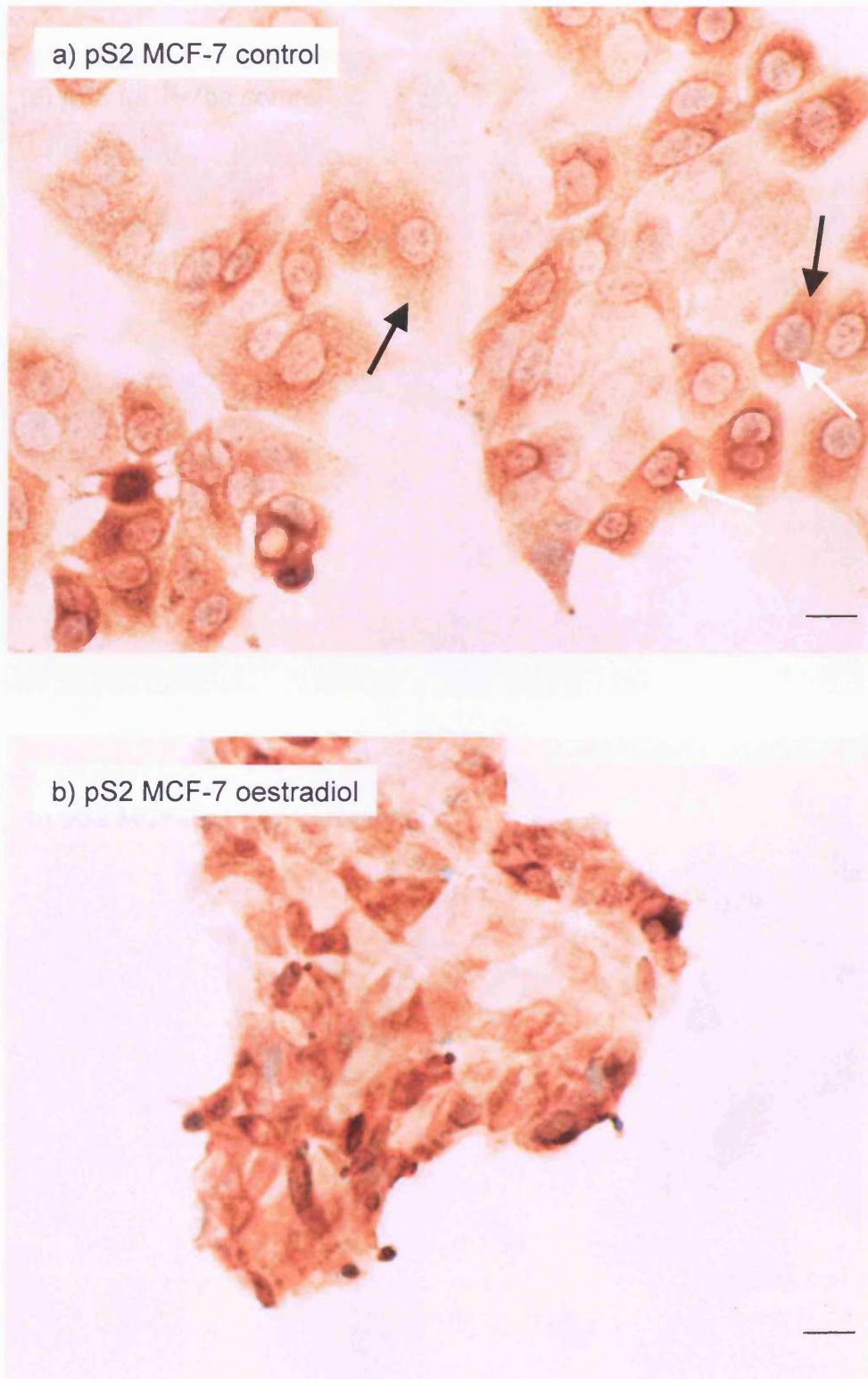


Fig. 6.15. pS2 expression in MCF-7 cells grown in control medium (panel a) or oestradiol-supplemented medium (panel b). Black arrows indicate cytosolic staining; white arrows indicate peri-nuclear staining. Size bar = 10 μm

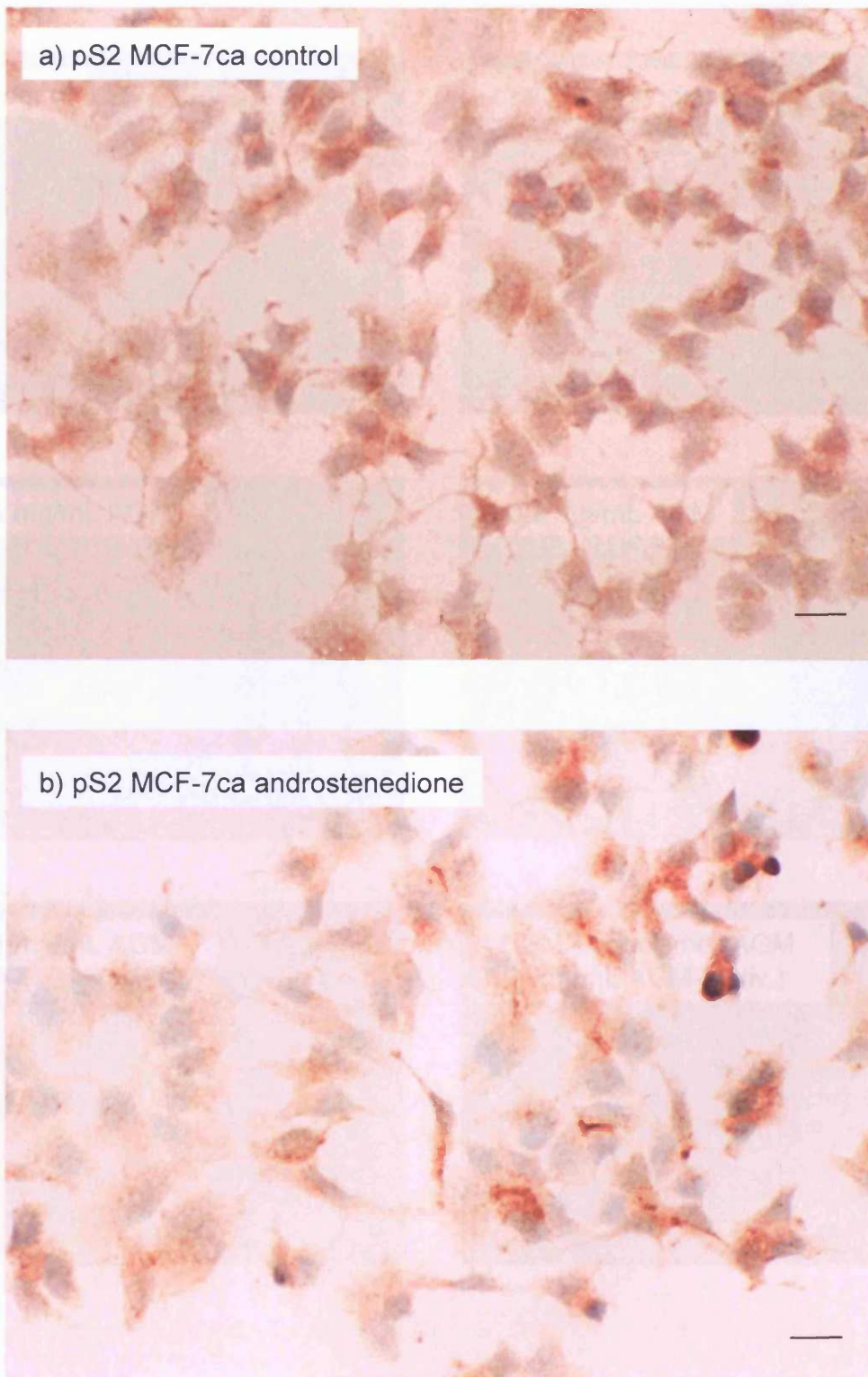


Fig. 6.16. pS2 expression in MCF-7ca cells. Cells were grown in control medium (panel a) or androstenedione-supplemented medium (panel b). Size bar = 10 μ m

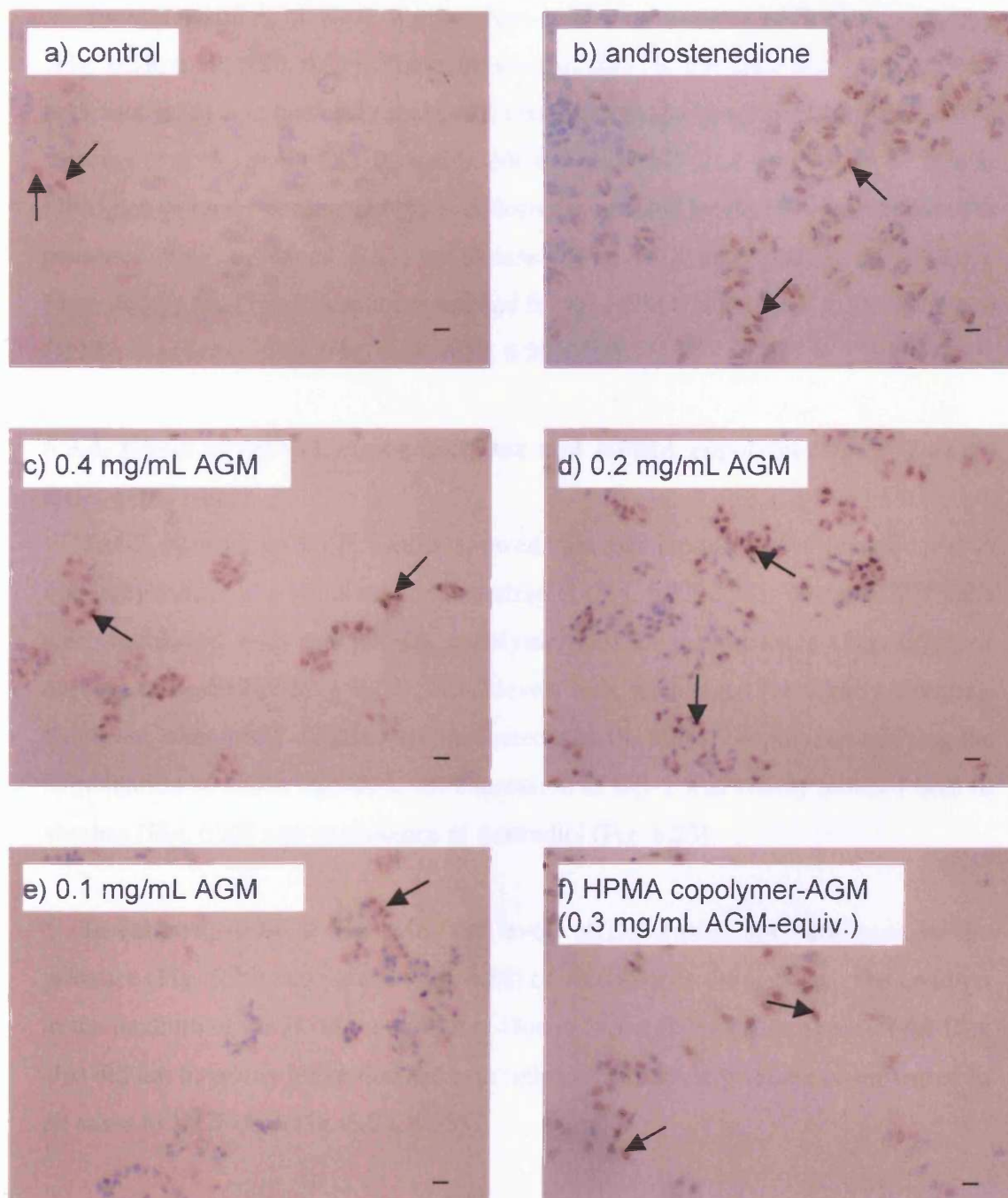


Fig. 6.17. Effect of androstenedione, free AGM and HPMA copolymer-AGM on PgR expression in MCF-7ca cells. Cells were grown in control medium (panel a); androstenedione-supplemented medium (panel b); androstenedione and free AGM supplemented medium (panel c-d-e at the concentration indicated); androstenedione and HPMA copolymer-AGM supplemented medium (panel f). Black arrows indicate positively stained cells. Size bar = 10 μ m

6.3.3. Effect of HPMA copolymer-Dox and HPMA copolymer-AGM-Dox on the expression of the proliferation marker Ki67

Immunostaining of Ki67 was nuclear, with predominant nucleoli localisation (Fig. 6.18, 6.19, 6.20, 6.21). The expression of Ki67 in presence of oestradiol (Fig. 6.19 and 6.21) was markedly increased compared to the basal levels (in absence of steroids (Fig. 6.18 and 6.20)) both in MCF-7 and MCF-7ca. Incubation with both HPMA copolymer conjugates led to a decrease of Ki67 levels in both cell lines (in presence (Fig. 6.19 and 6.21) or absence (Fig. 6.18 and 6.20) of oestradiol). Interestingly, this effect was more marked for the HPMA copolymer-AGM-Dox than HPMA copolymer-Dox (Fig. 6.18, 6.19, 6.20, 6.21).

6.3.4. Effect of HPMA copolymer-Dox and HPMA copolymer-AGM-Dox on Bcl-2 expression

Bcl-2 staining in MCF-7 cells showed that this protein is cytoplasmic and is markedly induced by the presence of oestradiol (Fig. 6.22, 6.23). When MCF-7 cells were incubated with the HPMA copolymer-Dox in the presence (Fig. 6.23) or absence of oestradiol (Fig. 6.22), Bcl-2 levels were unchanged (or slightly induced). However, when MCF-7 cells were incubated with the HPMA copolymer carrying the combination of AGM and Dox, the expression of Bcl-2 was visibly reduced both in absence (Fig. 6.22) and in presence of oestradiol (Fig. 6.23).

In contrast, in MCF-7ca cells, the levels of Bcl-2 were not influenced by the presence (Fig. 6.25) or absence (Fig. 6.24) of oestradiol in the medium. The addition in the medium of the HPMA copolymer-Dox or of the HPMA copolymer-AGM-Dox also did not have any impact on the expression of Bcl-2 which remained un-varied in all cases in MCF-7ca (Fig. 6.24, 6.25).

6.4. DISCUSSION

Investigating the mechanism of action of HPMA copolymer-AGM-Dox is a fascinating, but intrinsically complicated challenge. First of all, the mechanism of action of each drug needs to be considered individually. However, the simultaneous presence of the two drugs provides an opportunity for additive or even synergistic effects. Furthermore, the chemical linkage of the drug to the polymeric carrier also complicates the matter due to the resultant change in the cellular pharmacokinetics

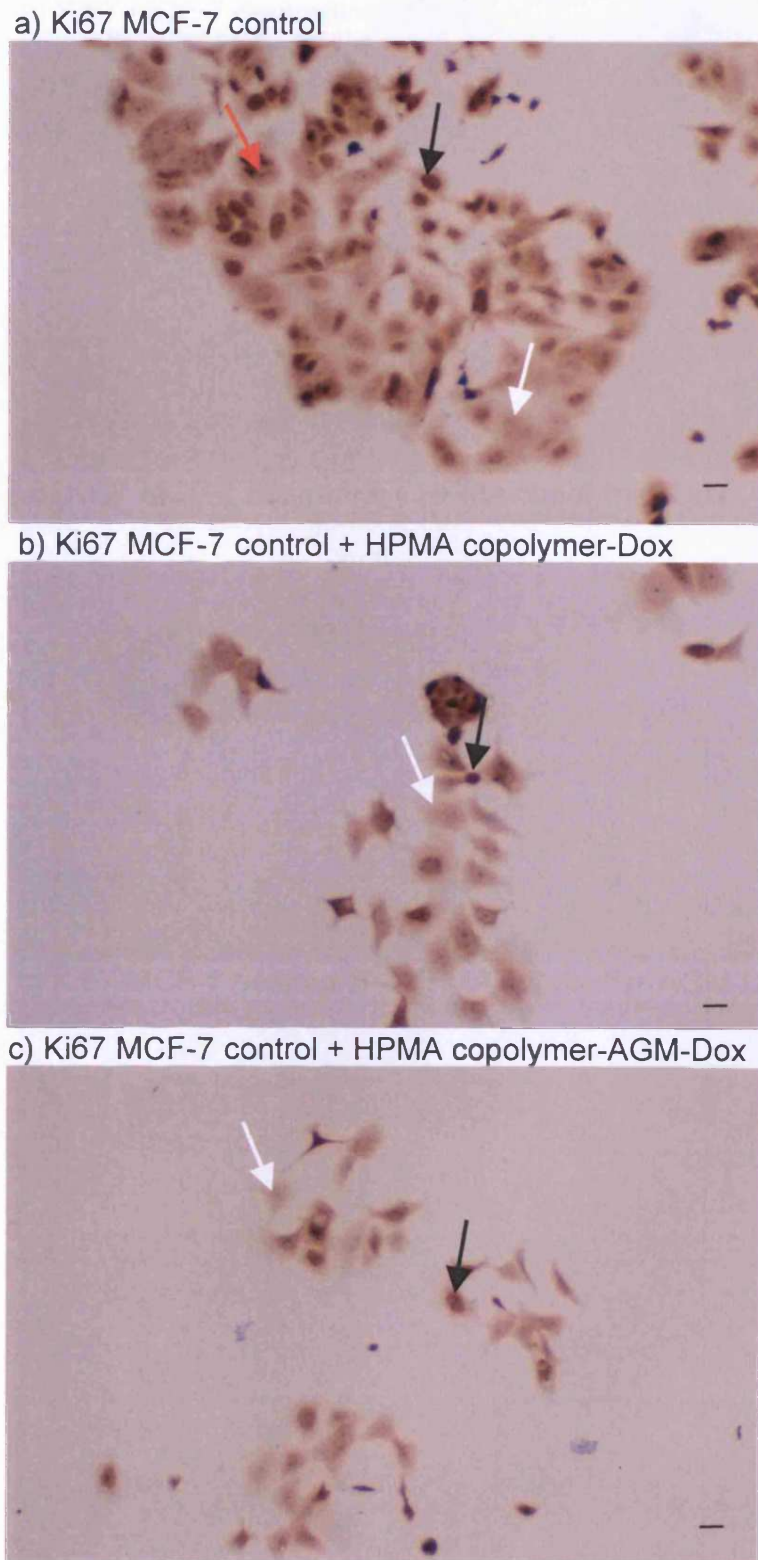


Fig. 6.18. Effect of HPMA copolymer-Dox conjugates on Ki67 expression in absence of steroids in MCF-7 cells. Cells were incubated with control medium (panel a), control medium supplemented with HPMA copolymer-Dox (panel b) or HPMA copolymer-AGM-Dox (panel c). Black arrows indicate nuclear staining; white arrows indicate unstained cells; red arrows indicate nucleoli staining. Size bar = 10 μm

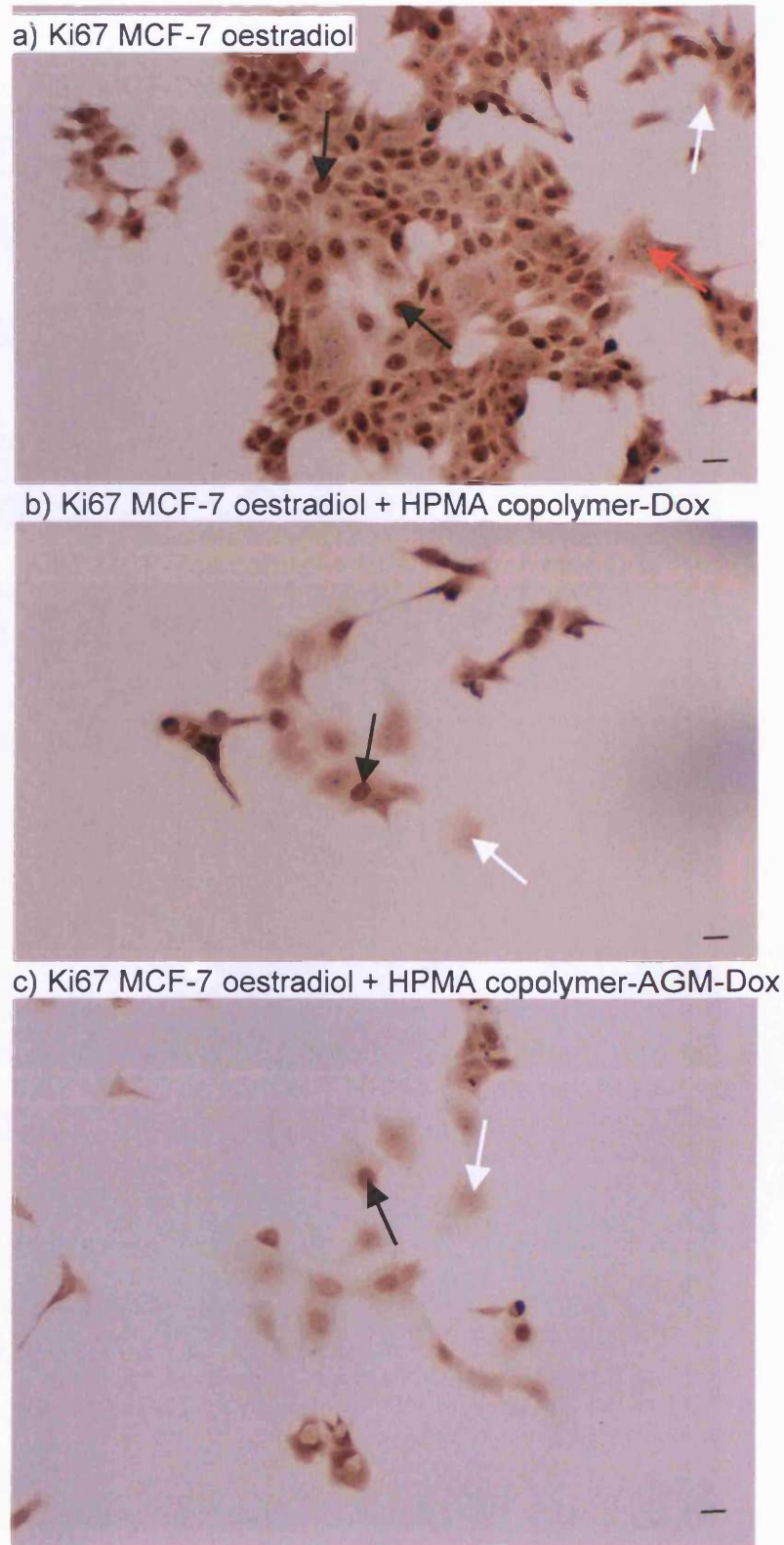
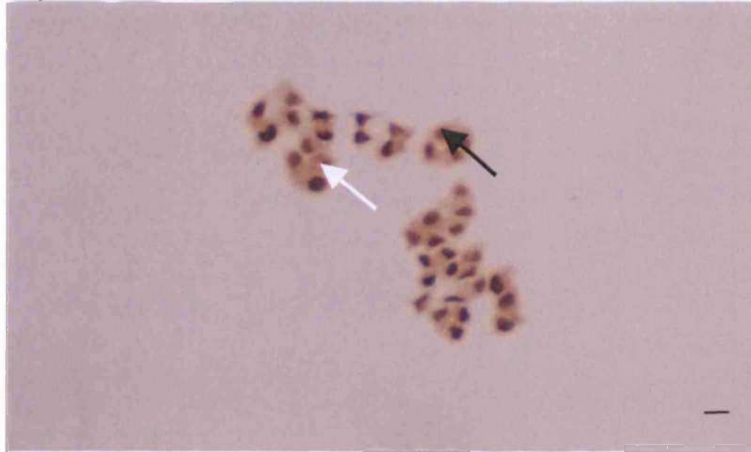
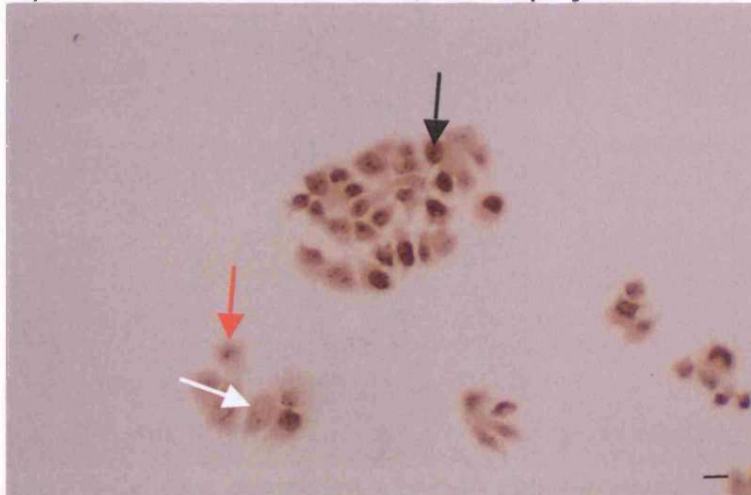


Fig. 6.19. Effect of HPMA copolymer-Dox conjugates on Ki67 expression in presence of oestradiol in MCF-7 cells. Cells were incubated with oestradiol medium (panel a), oestradiol medium supplemented with HPMA copolymer-Dox (panel b) or HPMA copolymer-AGM-Dox. Black arrows indicate nuclear staining; white arrows indicate unstained cells; red arrows indicate nucleoli staining. Size bar = 10 μ m

a) Ki67 MCF-7ca control



b) Ki67 MCF-7ca control + HPMA copolymer-Dox

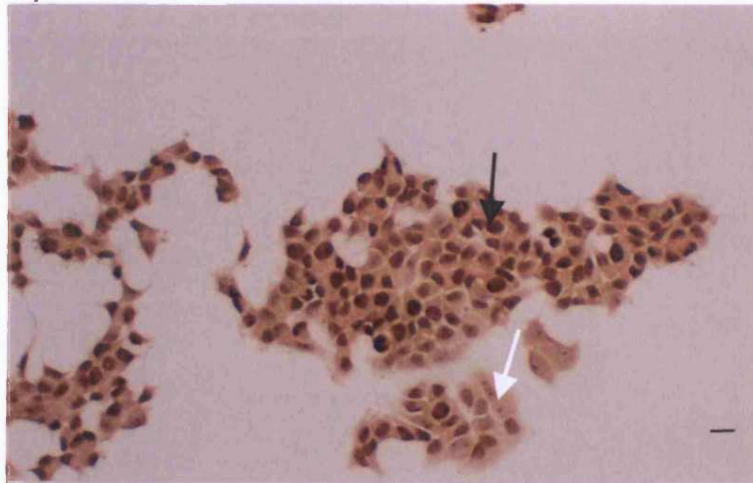


c) Ki67 MCF-7ca control + HPMA copolymer-AGM-Dox



Fig. 6.20. Effect of HPMA copolymer-Dox conjugates on Ki67 expression in absence of steroids in MCF-7ca cells. Cells were incubated with control medium (panel a), control medium supplemented with HPMA copolymer-Dox (panel b) or HPMA copolymer-AGM-Dox (panel c). Black arrows indicate nuclear staining; white arrows indicate unstained cells; red arrows indicate nucleoli staining. Size bar = 10 µm

a) Ki67 MCF-7ca oestradiol



b) Ki67 MCF-7ca oestradiol + HPMA copolymer-Dox



c) Ki67 MCF-7ca oestradiol + HPMA copolymer-AGM-Dox

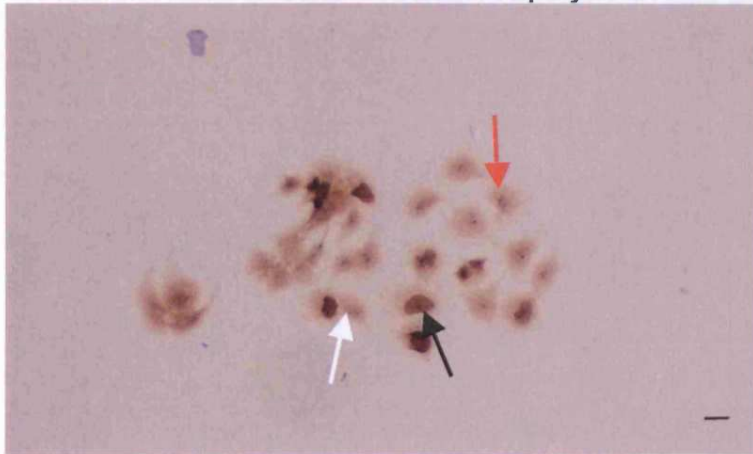
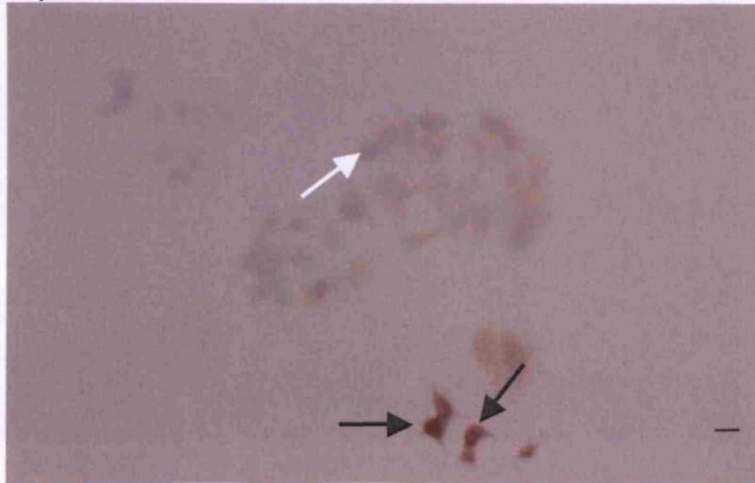


Fig. 6.21. Effect of HPMA copolymer-Dox conjugates on Ki67 expression in presence of oestradiol in MCF-7ca cells. Cells were incubated with oestradiol medium (panel a), oestradiol medium supplemented with HPMA copolymer-Dox (panel b) or HPMA copolymer-AGM-Dox. Black arrows indicate nuclear staining; white arrows indicate unstained cells; red arrows indicate nucleoli staining. Size bar = 10 μm

a) Bcl-2 MCF-7 control



b) Bcl-2 MCF-7 control + HPMA copolymer-Dox



c) Bcl-2 MCF-7 control + HPMA copolymer-AGM-Dox

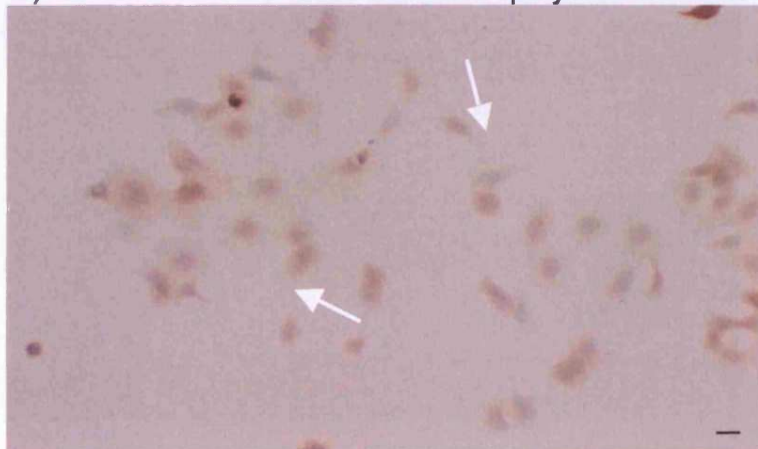
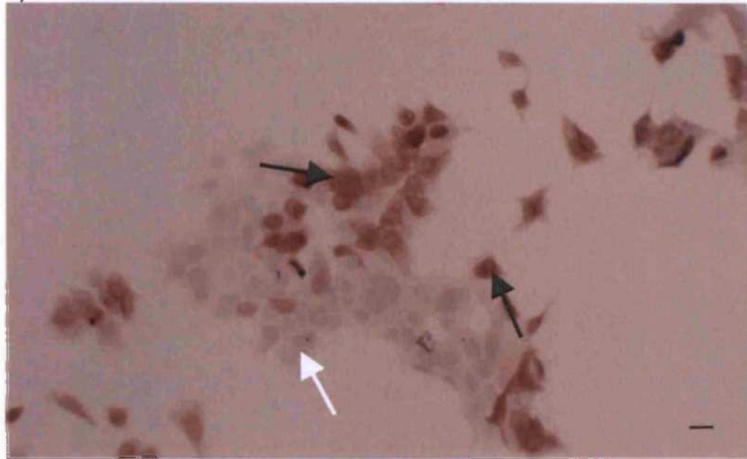
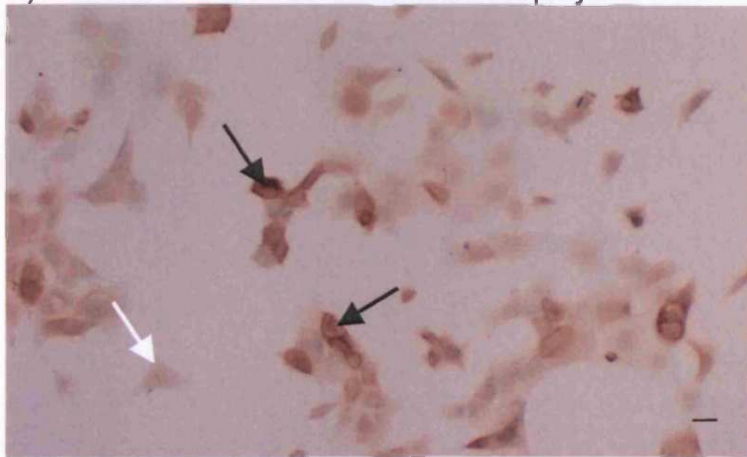


Fig. 6.22. Effect of HPMA copolymer-Dox conjugates on Bcl-2 expression in absence of steroids in MCF-7 cells. Cells were incubated with control medium (panel a), control medium supplemented with HPMA copolymer-Dox (panel b) or HPMA copolymer-AGM-Dox (panel c). Black arrows cytoplasmic staining; white arrows indicate unstained cells; Size bar = 10 μ m

a) Bcl-2 MCF-7 oestradiol



b) Bcl-2 MCF-7 oestradiol + HPMA copolymer-Dox



c) Bcl-2 MCF-7 oestradiol + HPMA copolymer-AGM-Dox

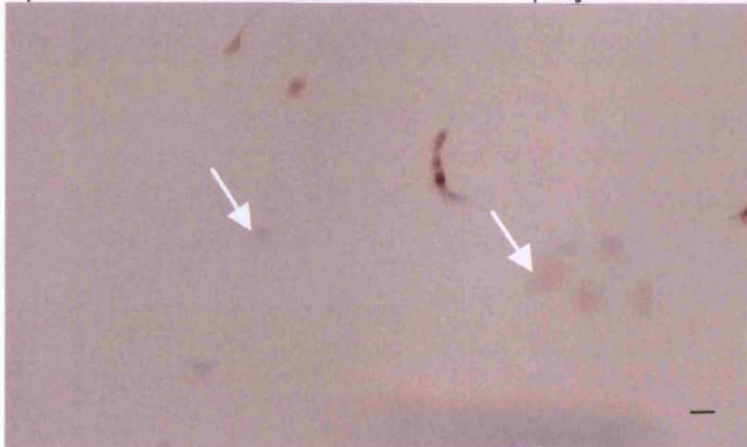


Fig. 6.23. Effect of HPMA copolymer-Dox conjugates on Bcl-2 expression in presence of oestradiol in MCF-7 cells. Cells were incubated with oestradiol medium (panel a), oestradiol medium supplemented with HPMA copolymer-Dox (panel b) or HPMA copolymer-AGM-Dox. Black arrows indicate cytoplasmic staining; white arrows indicate unstained cells; Size bar = 10 μ m

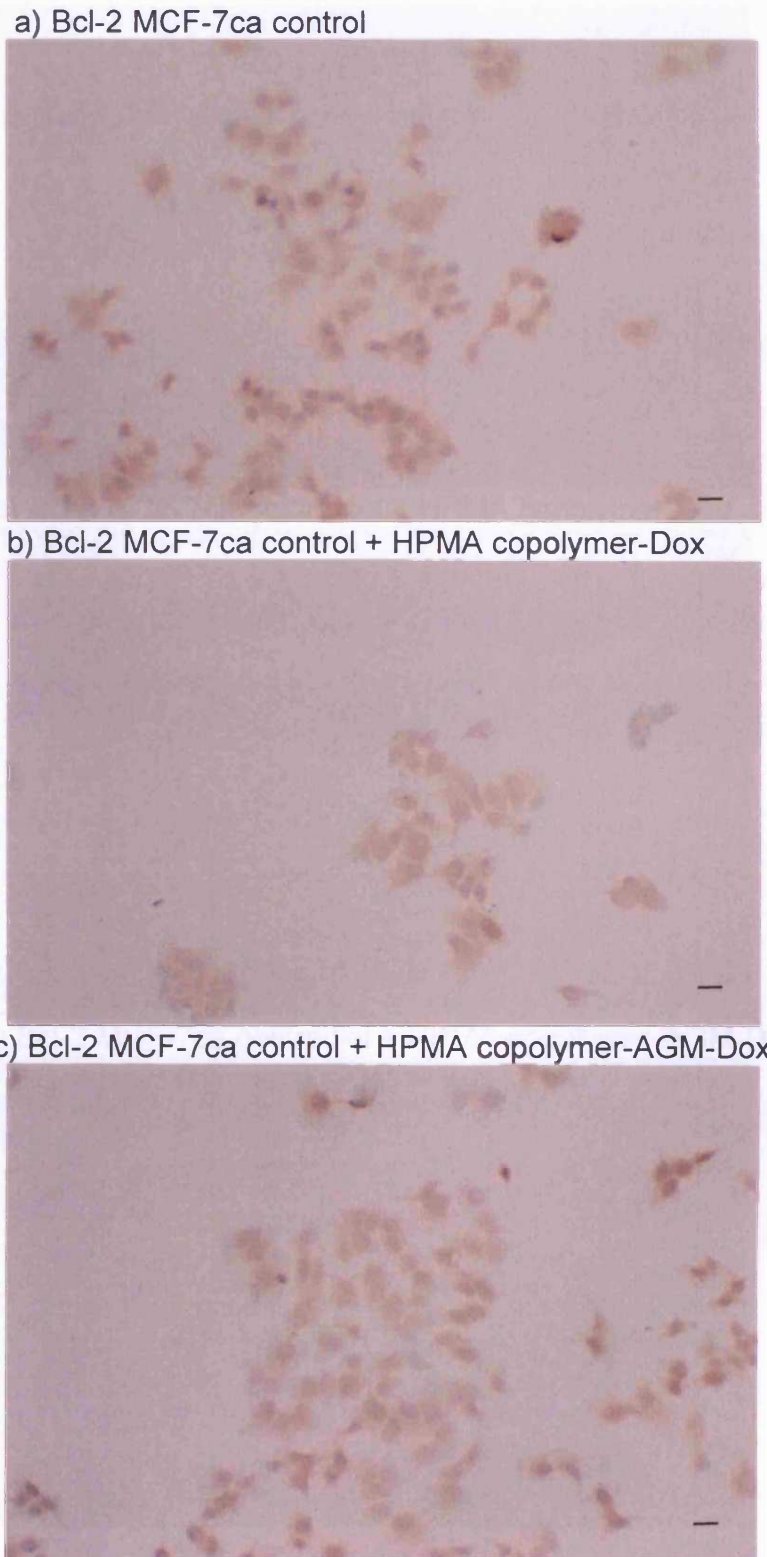
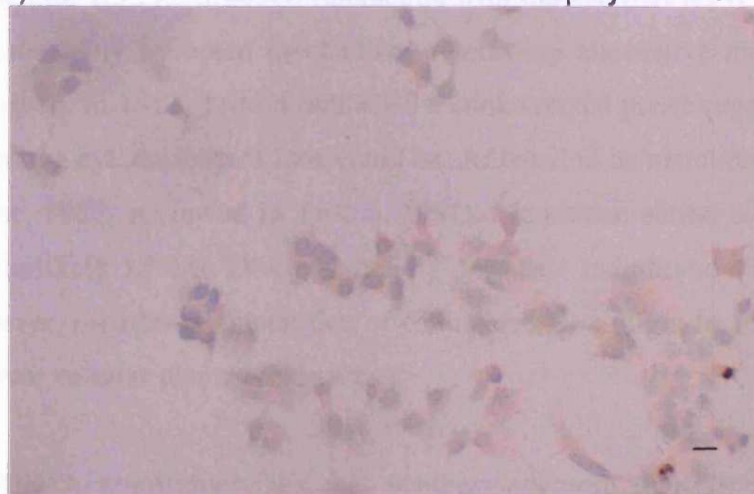


Fig. 6.24. Effect of HPMA copolymer-Dox conjugates on Bcl-2 expression in absence of steroids in MCF-7ca cells. Cells were incubated with control medium (panel a), control medium supplemented with HPMA copolymer-Dox (panel b) or HPMA copolymer-AGM-Dox (panel c). Size bar = 10 μ m

a) Bcl-2 MCF-7ca oestradiol



b) Bcl-2 MCF-7ca oestradiol + HPMA copolymer-Dox



c) Bcl-2 MCF-7ca oestradiol + HPMA copolymer-AGM-Dox

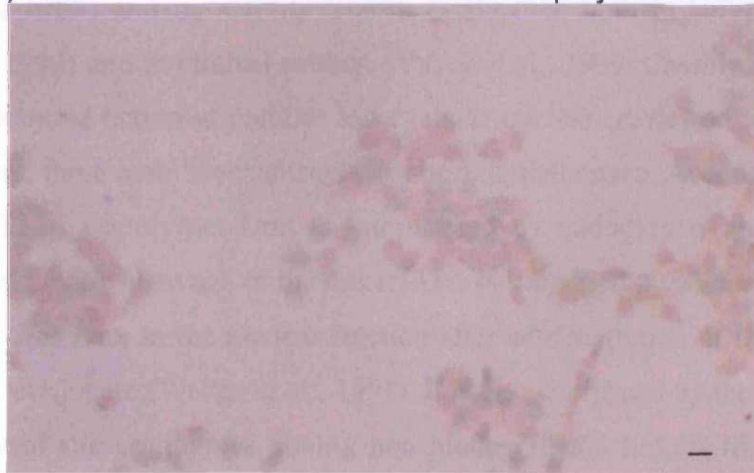


Fig. 6.25. Effect of HPMA copolymer-Dox conjugates on Bcl-2 expression in presence of oestradiol in MCF-7ca cells. Cells were incubated with oestradiol medium (panel a), oestradiol medium supplemented with HPMA copolymer-Dox (panel b) or HPMA copolymer-AGM-Dox. Size bar = 10 µm

compared to the free drug: relatively slow internalisation of the conjugate followed by time-dependent liberation of free Dox and/or AGM depending on conjugate composition. This will expose the drug targets to different drug concentrations (with time) than they would meet if the drug was administered as free compound. Finally, the different intracellular distribution of the polymer conjugate might expose the drug to alternative targets and thus lead to new or additional mechanisms of action compared to the free drug.

The mechanisms of action attributed to free Dox have been discussed previously in Chapter 1 (section 1.3.2). Although interaction with topoisomerases II at nuclear level is the most widely accepted mechanism, interesting alternative mechanisms have been described. In 1982, Tritton published a controversial paper suggesting for the first time that the cytotoxicity of Dox could be attributed to its membrane activity (Tritton and Yee, 1982; reviewed in Tritton, 1991). Membrane-action of free Dox seems at least unlikely as free Dox can rapidly permeate membranes by passive diffusion. However, membrane interaction of conjugated Dox might be more likely due to the different cellular pharmacokinetics.

Although HPMA copolymer-Dox was synthesised more than 20 years ago (Kopecek et al, 1985) and its activity is well established both in animal models (Duncan et al., 1992) and in clinical settings (Vasey et al., 1999; Cassidy, 2000), its precise mechanism of action at cellular level is still unclear (reviewed in Duncan 2005). At present, three main mechanisms have been hypothesised. According to the first model, HPMA copolymer-Dox is internalised by endocytosis and Dox is released after enzymatic cleavage of the linker. This is supported by studies showing the presence of free Dox in the nuclear fraction after administration of the HPMA copolymer-Dox conjugate (Wedge et al., 1991). It is also confirmed by the complete lack of activity of the conjugates having non biodegradable linkers like HPMA copolymer-GG-Dox (Duncan et al.1989) and HPMA copolymer-GG-platinite (Gianasi et al., 1999; reviewed in Duncan, 2005). However, this lack of activity could also be explained by the fact that a dipeptide like the GG could be too short a spacer to allow membrane interaction. The second hypothesis, first proposed by Rihova and colleagues, suggests that HPMA copolymer-Dox causes cell death by interaction with the plasma membrane (Hovorka et al., 2002). The main argument in

favour of this mechanism is that they were not able to detect free Dox in the nucleus even after 72 h incubation with HPMA-Dox, suggesting that the conjugate toxicity was not due to Dox release (Hovorka et al., 2002). Finally, Minko and Kopeček have attributed HPMA copolymer-Dox toxicity to induction of apoptosis (Minko et al., 2001) although in one study they suggested that necrosis was the main mechanism of action of HPMA copolymer-Dox (Demoy et al., 2000).

The combination conjugate contains both Dox and AGM. It could be hypothesised that free AGM, being an aromatase inhibitor, will interfere with oestrogen signalling. Also, aromatase inhibitors have been shown to induce apoptosis (reviewed in Johnston and Dowsett, 2003). Even more interestingly, there are some elements where oestrogen signalling and the apoptosis pathways overlap, possibly involving Bcl-2. In the attempt to dissect the mechanism of action of the HPMA copolymer-AGM-Dox conjugate, the first step was to examine aromatase inhibition in relation to cellular markers of oestrogen action.

The PgR is an oestrogen-regulated protein that has been widely studied in breast cancer tissue from patients treated with anti-hormones (Collett et al., 1996). In the study presented here, androstenedione induced the expression of PgR in MCF-7ca cells. This is consistent with PgR being a marker for oestrogen activity. Interestingly, the lack of stimulatory activity seen in MCF-7 cells also suggests that androstenedione does not act as a ligand for the ER and that the androstenedione induced overexpression of PgR could be attributed to its aromatase-mediated transformation to oestrogens.

Counterintuitively, however, the incubation of the MCF-7ca cells with androstenedione in presence of free or polymer-bound AGM was not able to reverse this effect. The effect of some aromatase inhibitors (letrozole, anastrozole, exemestane) and tamoxifen on the levels of the PgR has been investigated clinically. Miller *et al.* (2005) looked at the levels of PgR after 3 months treatment with these drugs. Interestingly, while tamoxifen did not affect the level of PgR in an obvious way (decreased, increased and unvaried levels were found, with an increase being paradoxically the most likely event). The aromatase inhibitors examined downregulated PgR levels in the vast majority of the cases (46 patients out of 50

showed a decrease). It is important to note, that our study was *in vitro* and was performed with a much shorter incubation time (10 days). As the experimental conditions were markedly different a direct comparison can be difficult. To my knowledge, no studies have been reported assessing PgR levels after treatment with AGM, however there are studies monitoring aromatase activity. AGM was shown to paradoxically increase aromatase activity *in vitro* (Kao et al., 1999; Miller et al., 2003). In this perspective, the PgR levels found after incubation with androstenedione and AGM could be the result of this increased activity. Another possibility is that the presence of AGM creates an environmental pressure by which cells containing a higher level of aromatase are more likely to survive than cells with lower levels of this enzyme. For this project, it was also interesting to observe that once again the behaviour of the HPMA copolymer-AGM was consistent with that of the free drug.

The clinical relevance of the proliferation marker ki67 is well-established. Previous studies showed that patients responding to tamoxifen treatment had a greater decrease in this protein's level (Makris et al., 1998). Also, decreased expression of ki67 after treatment was correlated with a lower risk of relapse (Chang et al., 2000; Geisler et al., 2001; Kenny et al., 2001). In this respect, the decreased levels of ki67 found after treatment with HPMA copolymer-Dox and the even lower levels found with the HPMA copolymer-AGM-Dox indicate an appropriate biological activity of the conjugates used in the present study and confirm previously reported cytotoxicity data (Chapter 4).

The assessment of the Bcl-2 levels in MCF-7 cells led to the most interesting findings. In this study, although HPMA copolymer-Dox and HPMA copolymer-AGM-Dox were administrated at the same concentration (adjusted in Dox-equiv.), decreased levels of bcl-2 were found only with the combination polymer. The lack of activity of the HPMA copolymer-Dox is consistent with previous studies showing that this conjugate did not have any effect on any of the members of the Bcl-2 family except Bax (Kovar et al., 2003). However, this is in contrast with studies from another research group where decreased expression of Bcl-2 after incubation with HPMA copolymer-Dox was reported *in vitro* both at gene (Minko et al., 2001; Kunath et al., 2000;) and protein level (Malugin et al., 2005) and *in vivo* (Minko et

al, 2000). It also suggests that the increased cytotoxicity of the HPMA copolymer-AGM-Dox previously described (Chapter 4), could be attributed to activation of apoptosis pathways. However, to achieve a full picture of the mechanism of action of the HPMA copolymer-Dox-AGM other studies monitoring the levels of other markers involved in apoptosis, for instance bax, are warranted.

The lack of effect on Bcl-2 levels in MCF-7ca cells was initially surprising and disappointing. However, as the expression of Bcl-2 was extremely low in all the experimental conditions tested (presence or absence of oestradiol or androstenedione) it seems that it is not an ideal marker for this specific cell line.

6.5. CONCLUSIONS

In this study the activity of the HPMA copolymer conjugates was investigated at cellular level. Two main results were reported here. Firstly, the HPMA copolymer conjugates were found to decrease cell proliferation (more markedly, for the HPMA copolymer-AGM-Dox), which correlates with the cytotoxicity studies reported previously (Chapter 4). Also, the downregulation of Bcl-2 by the HPMA copolymer-AGM-Dox suggests that this conjugate might induce apoptosis in MCF-7 cells. While investigations of other markers is needed to achieve a full picture of the mechanism of action, these findings suggest that the different impact that the HPMA copolymer-AGM-Dox has on apoptosis could be at least partially responsible for the increased activity of this conjugate.

Chapter 7:

General Discussion

7.1. GENERAL COMMENTS AND HISTORICAL PERSPECTIVE

As this study is finishing, it is interesting to note that 2005 is the 40th anniversary of the death of Hermann Staudinger, the Nobel laureate who proved the existence of polymers “as chain molecules” (Ringsdorf, 2004) and also the 30th anniversary of the publication of the article that gave birth to the field of polymer-anticancer drug conjugates (Ringsdorf, 1975; reviewed in Haag and Kratz, 2006). Collaborative interdisciplinary research started by Duncan and Kopecek (Duncan et al., 1987; Duncan et al., 1992; reviewed in Duncan 2005) gave rise to the first synthetic polymer anticancer conjugate to enter clinical trial in 1994 (Vasey et al., 1999) (Fig. 7.1). A number of preliminary studies were carried out to obtain the optimal polymer molecular weight that would guarantee polymer excretion and to design the linker to be cleaved in the lysosomal compartment (Duncan et al., 1980; Duncan et al., 1983). The *in vitro* and *in vivo* experiments performed in the ‘80s and early ‘90s (Duncan et al., 1989; Duncan et al., 1992), paved the way to the clinical evaluation of HPMa copolymer-Dox (Vasey et al., 1999; Cassidy 2000), soon followed by other HPMa copolymer conjugates that contained platinates, CPT and paclitaxel (Schoemaker et al., 2002; Rademaker-Lakhai et al., 2004).

In the field of breast cancer, endocrine therapy has dramatically progressed since the first oophorectomy was performed, more than a century ago (Beatson, 1896). In 1974, tamoxifen was marketed for the treatment of breast cancer and from a failed potential contraceptive it became the standard first line endocrine treatment for this disease (reviewed in Jordan, 2003a and in Jordan, 2003b). More recently, the development of 2nd and 3rd generation aromatase inhibitors (Brodie, 2002) and the research of new, selective molecular targets leading to the development of novel drugs such as the antibody Herceptin[®] (reviewed in Leyland-Jones, 2002) prove how active breast cancer research is (Fig. 7.1).

Although, the most recent statistics indicate that two thirds of women newly diagnosed with breast cancer are likely to survive at least 20 years (Cancer Research UK) the high incidence of this disease and the mortality rates of advanced metastatic breast cancer, make it a high health priority.

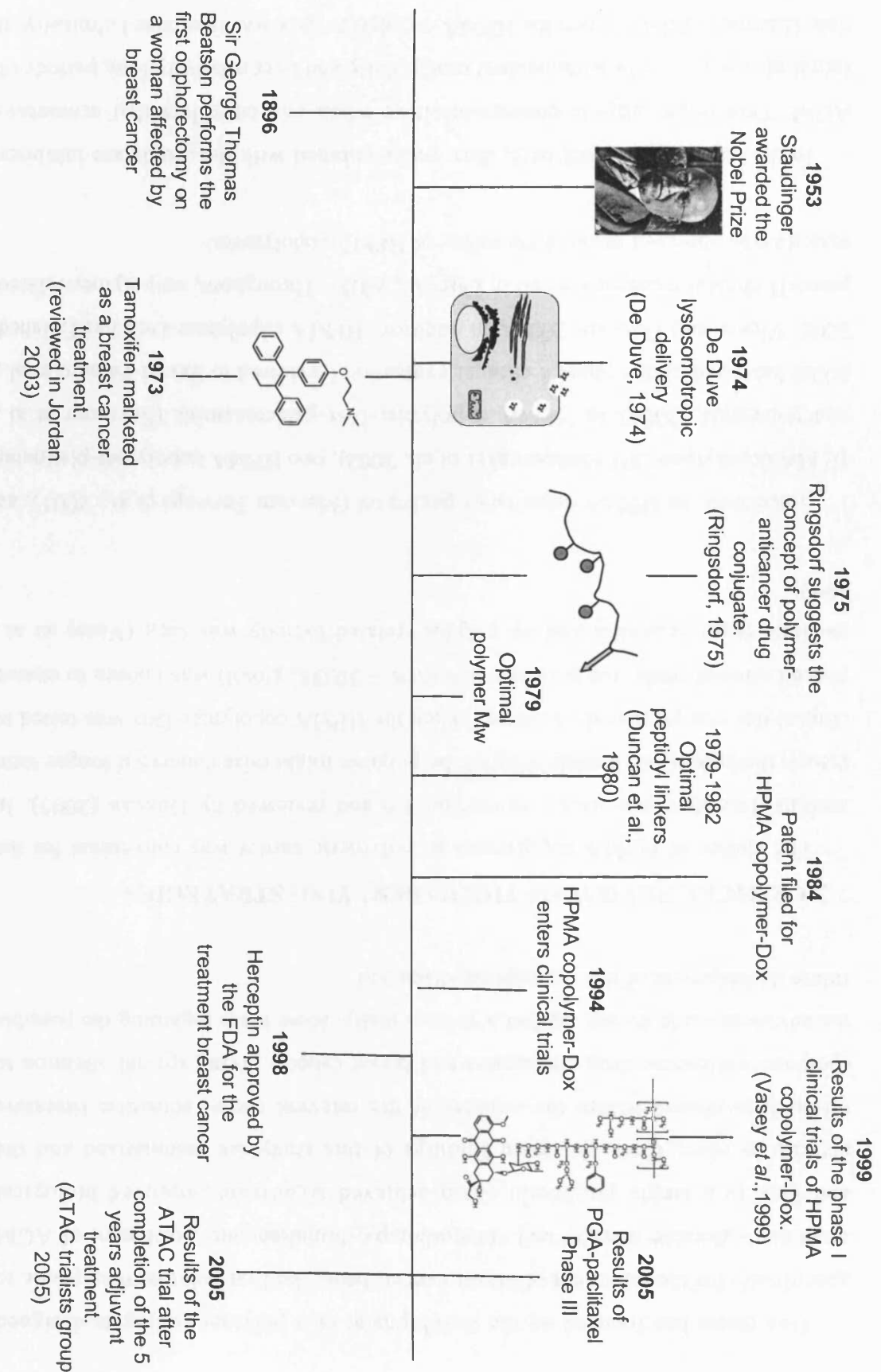


Fig. 7.1. Milestones in the history of polymer anticancer drug conjugates and breast cancer treatment

This thesis has focused on the development of a polymer conjugate designed *specifically* for the treatment of breast cancer, being the first polymer therapeutic to combine endocrine therapy and chemotherapy. Simultaneous attachment of AGM and Dox to a single polymeric chain achieved significant improved biological activity *in vitro*. Here, the main findings of this study are summarised and the research is placed within the context of the relevant recent scientific literature (polymer-anticancer drug conjugates and breast cancer) giving special attention to the advances made during the last 3 years. Finally, some ideas regarding the possible future development of this concept are discussed.

7.2. CRITICAL REVIEW OF THE UNDERLYING STRATEGIES

The choice of HPMA copolymers as polymeric carrier was convenient for the reasons described previously in section 1.6 and reviewed by Duncan (2005). In theory, the lack of biodegradability of the polymer might raise concern if longer-term clinical use was proposed. However, when the HPMA copolymer-Dox was tested in phase I clinical trials, the polymer size ($M_w \sim 30,000$ g/mol) was chosen to ensure eventual renal excretion and no polymer-related toxicity was seen (Vasey et al., 1999).

Since then, an HPMA copolymer-paclitaxel (Meerum Terwogt et al., 2001), an HPMA copolymer-CPT (Schoemaker et al., 2002), two HPMA copolymer-platinates and (Novotnik, 2004) an HPMA copolymer-Dox-galactosamine (Seymour et al., 2002) have undergone phase I clinical evaluation (reviewed in Satchi-Fainaro et al., 2005; Vicent and Duncan, 2006). In addition, HPMA copolymer-Dox has finished phase II clinical trials (reviewed in Duncan, 2005). Throughout, no polymer-related toxicity was observed proving the safety of HPMA copolymers.

In the studies presented here, Dox was combined with the aromatase inhibitor AGM. This might appear counter-intuitive when one considers that aromatase inhibitors are generally administered orally, daily and over relatively long periods of time (Lonning, 2004). When the HPMA copolymer-Dox was first tested clinically, it was administered every 3 weeks (Vasey et al., 1999). The increased activity that the HPMA copolymer-AGM-Dox showed *in vitro* suggests that such a conjugate has at

least the potential of improving the performance of the HPMA copolymer-Dox when administered intravenously, with a similar administration schedule, possibly to patients with resistant metastatic disease.

7.3. RECENT DEVELOPMENTS IN THE FIELD: THIS WORK IN THE CONTEXT OF OTHER POLYMER-DRUG CONJUGATES AND OTHER BREAST CANCER TREATMENTS.

During the three years of this experimental project, some important events in both the field of breast cancer and polymer-drug conjugates have emerged.

In January 2005 the ATAC trial was completed following 5 years adjuvant therapy with either tamoxifen or anastrozole (arimidex[®]) (ATAC Trialists Group, 2005). This study showed the superiority of the aromatase inhibitor anastrozole against tamoxifen (the most well-established drug for breast cancer treatment) in terms of improved disease-free survival, improved time to recurrence, reduction of distant metastasis, and appearance of contralateral breast cancer. The trialists group recommended the use of anastrozole as first line adjuvant treatment in postmenopausal women. Although the improvements in therapy seen may not be applicable to all the aromatase inhibitors (due to differences in potency and mechanism of action), it is however possible to say that the promising results from the ATAC trial put aromatase inhibitors in a key position in the treatment of breast cancer.

As for the field of polymer-anticancer conjugates, in 2003, a phase II clinical study of PGA-paclitaxel in breast cancer patients reported activity for this conjugate (partial responses and stable disease). Phase II clinical trials combining this conjugate with carboplatin for the treatment of ovarian cancer showed a 95 % response rate (Herzog et al., 2005). Also, a Phase III study using again the combination of PGA-paclitaxel and carboplatinum in non small cell lung cancer patients showed comparable activity to the combination of the free drugs but was less toxic (Langer et al., 2005). This conjugate is the most advanced in clinical development (currently in phase III) (Singer et al., 2005) and might be the very first anticancer conjugate to reach the market.

Finally, while the concept of polymer-drug conjugates seemed to have been confined for years to established chemotherapy agents, lately, conjugates containing experimental drugs are emerging. In 2004, the first HPMA copolymer conjugate containing an anti-angiogenic drug was described (Satchi-Fainaro et al., 2004) and in 2001 the first conjugate containing the PI3 kinase inhibitor wortmannin was described (Varticovski et al., 2001). Indeed, the concept of polymer-drug conjugates is expanding beyond the limits of cancer therapy. Recently, a HPMA copolymer conjugate was synthesised that contained an anti-leishmania compound (Nan et al., 2001).

7.4. SUMMARY OF THE MAIN FINDINGS OF THIS WORK AND POSSIBLE FUTURE DEVELOPMENTS.

This project started with the synthesis and the characterisation of a novel family of HPMA copolymer conjugates. After a first attempt to bind AGM to the HPMA copolymer by aminolysis, the synthesis was improved using DCC coupling (Vicent et al., 2005). This led to the preparation of reproducible batches of conjugates with higher drug content.

After the synthesis of the conjugates their biological activity was evaluated (Chapter 4). The combination polymer was more active than the HPMA copolymer-Dox. This exciting finding raised two questions. Why is the combination polymer more active and is this (i.e. AGM-Dox) the best combination therapy or would a rational choice of another pair of drugs provide even better activity? Potential answers to the first question were discussed in Chapters 5 and 6. The main conclusions are summarised below. The second question was addressed below, where possible future experiments to develop this concept further are described.

Chapter 5 examined cellular pharmacokinetics as a possible explanation for the observed superiority of the HPMA copolymer-AGM-Dox over the HPMA copolymer-Dox. No clearout explanations were identified. Neither the uptake rate nor the uptake mechanism seemed to be responsible for the different biological activity found. Although further investigations could be performed these preliminary results suggest that the physico-chemical characteristics of the polymer carrier rather than the drug were the main factor that determined the uptake.

The preliminary studies undertaken in the last part of the project tried to investigate the mechanism of action of the conjugates by analysing changes in cellular markers after exposing MCF-7 and MCF-7ca cells to polymer conjugates (Chapter 6). Even for HPMA copolymer-Dox the precise mechanism of action is currently a hotly debated topic (reviewed in Duncan, 2005). The experiments presented in this thesis suggested that the HPMA copolymer-AGM-Dox decreased the level of Bcl-2 while the HPMA copolymer-Dox did not. However, one limitation of this study is that Bcl-2 was the only marker tested. It would be interesting to monitor changes in other proteins involved in the apoptosis pathway, for instance, Bax. As it has been suggested that the HPMA copolymer-Dox can have an effect on apoptosis that is initiated via the mitochondria (Malugin et al., 2004), other markers involved in this pathway could also be assessed.

A number of the results presented in this thesis underline the advantages of a polymer-based combination therapy. However, some questions still need to be addressed. Here, first, the most important experiments that still need to be undertaken to complete this work are discussed, and then from a broader perspective, some future research areas that might be explored are presented.

The studies performed so far, and the suggested experiments, are summarised in Fig. 7.2. If we consider the HPMA copolymer-AGM-Dox conjugate, several *in vitro* experiments would give a more complete picture of (i) their mechanism of action (ii) their future therapeutic potential. For example, the trafficking of the conjugate (presented in Chapter 5) would benefit from further studies on conjugate exocytosis rate and rate of intracellular drug liberation. Also, the investigation of the cellular mechanisms of their action (Chapter 6) is only in its infancy. The expression of several other markers, such as Bax or caspases, could be investigated to probe further whether apoptosis is induced by these conjugates.

To assess whether the HPMA copolymer-AGM-Dox conjugate has potential for clinical evaluation the most important experiments relate to its *in vivo* testing of its pharmacokinetic properties and antitumour activity. Since both MCF-7 and MCF-7ca

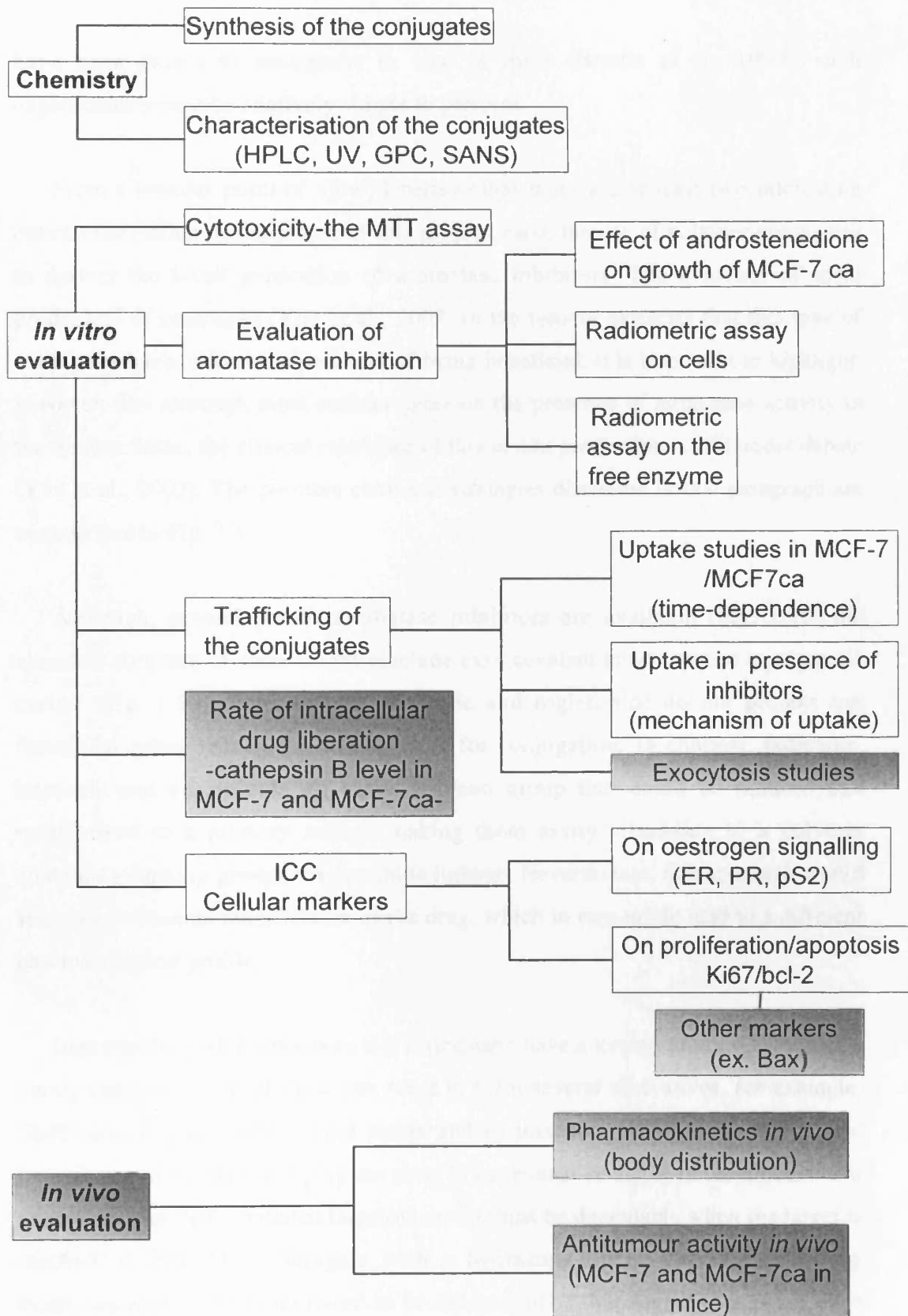


Fig. 7.2. Flowchart representing the assessment of HPMA copolymer-AGM (±Dox) conjugates. White boxes represent studies already performed while grey boxes indicate possible future studies

have been grown as xenografts *in vivo* in mice (Brodie et al., 1999), such experiments would be relatively simple to perform.

From a broader point of view, I believe that there are at least two interesting options for further development of this project. First, the use of polymer conjugates to deliver the latest generation of aromatase inhibitors. The evidence of local production of oestrogen (Yue et al., 2002) in the tumour suggests that this type of conjugates have at least the potential of being beneficial. It is important to highlight, however, that although most authors agree on the presence of aromatase activity in the tumour tissue, the clinical relevance of this *in situ* production is still under debate (Yue et al., 2002). The possible chemical strategies discussed in this paragraph are summarised in Fig. 7.3.

Although, several potent aromatase inhibitors are available (Fig. 1.10) the chemical structure of some might preclude easy covalent attachment to a polymeric carrier (Fig. 1.10). For example, vorozole and rogletimide do not present any functional group that could be exploited for conjugation. In contrast, fadrozole, letrozole and anastrozole all carry a cyano group that could be reduced and transformed to a primary amine, making them easily attachable to a polymer containing carboxy groups via an amide linkage. Nevertheless, this approach would lead to a permanent modification of the drug, which in turn might lead to a different pharmacological profile.

Importantly, both exemestane and formestane have a ketone group which from a purely chemical point of view can react to form several derivatives, for example, Schiff base, oximes, ketals, enol esters and hydrazones (Bundgaard, 1985). It is important to remember that polymer-drug linkage must be stable in the bloodstream to capitalise an EPR-mediated targeting and it must be degradable when the target is reached. A PEG-Dox conjugate with a hydrazone linker was synthesised by Rodrigues et al. (1999) and found to be stable at pH 7, but degraded at pH 5. Also acetals are pH-dependent bonds and have been already suggested for polymer-drug conjugates (Vicent et al., 2004). In this case a polymeric backbone must be chosen that has an hydrazine group, or a diol to give a hydrazone or an acetal, respectively.

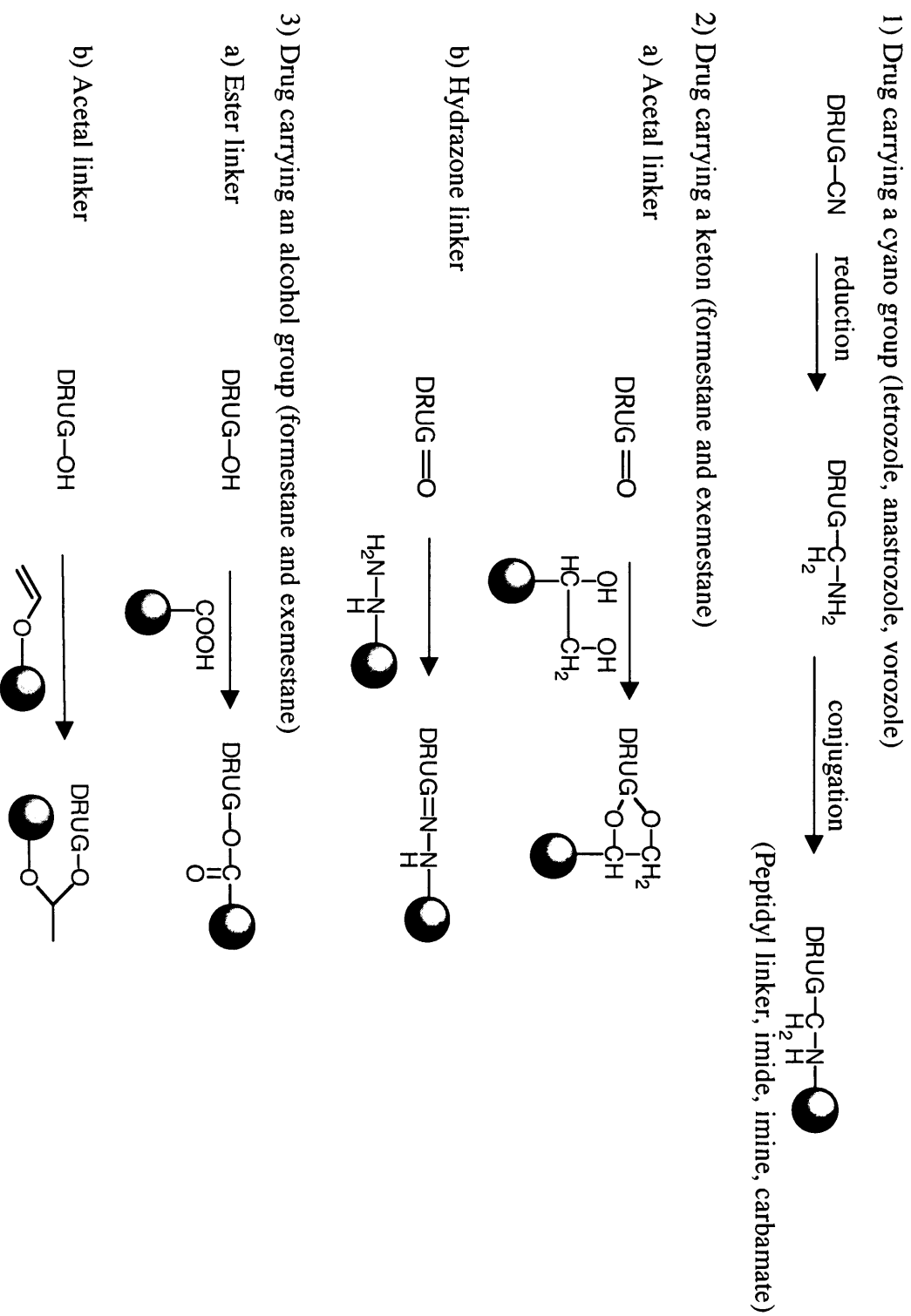


Fig. 7.3. Some of the possible synthetic approaches for novel polymer-aromatase inhibitor conjugates

Significantly, formestane presents also an alcohol that could be easily reacted with a carboxylic acid from the polymeric chain. The ester linkage has been historically unsuccessful for HPMA copolymer conjugates. Indeed, both HPMA copolymer CPT and HPMA copolymer paclitaxel showed toxicity that can, at least partially be correlated to the poor stability of the conjugate linker and to the premature release of the drug (reviewed in Duncan 2003b). However this type of bond was suitable when PGA acid was used as carrier probably due to different conformation of the polymeric chain leading to different accessibility of the linker (Singer et al., 2005).

This project confirmed the possibility of achieving increased antitumour activity by combining two drugs on the same polymeric carrier. The emergence of new drugs against new molecular targets (discussed in section 1.3) provides an amazing opportunity to generate novel polymer-based combination therapy. Although, the need for a chemical linkage that is eventually degraded in the lysosomal compartment restricts the field to molecules that present a chemical group suitable for conjugation.

The advantages of combination therapy for cancer treatment are already well known. For example, the standard chemotherapy protocol is routinely performed with cocktail of drugs (section 1.3) (Bonadonna et al., 1984; Hortobagyi, 2002; Kardinal, 1992). More recently, trastuzumab (Herceptin[®]), the antibody targeting HER-2 has also shown better performance when combined with conventional chemotherapy (Nabholtz and Gligorov, 2005).

However, there are some limiting factors. First of all, combining two different drugs does not necessarily mean that an increased therapeutic effect will be achieved. Although there is a general consensus that appropriate combinations can be beneficial, in some cases, combination therapy may even be counterproductive. For example, 2 years after the start of the ATAC trial, it was recognised that the combination of anastrozole and tamoxifen was significantly worse than anastrozole alone (ATAC Trialists Group, 2002). It is also important to note that if a combination of two drugs is administered as simple mixture, they will reach the tumour tissue independently and according to the pharmacokinetic of each drug. On the contrary,

with the polymer-based combination presented here, the drugs will be delivered to the tumour simultaneously.

The time is ripe for a future development of this concept. A rational choice of the drugs has the potential of generating a promising second-generation of polymer-based combination therapies.

References

A

Aboul-Enein H.Y. (1986). Aminoglutethimide. In *Analytical Profiles of Drug Substances*, Florey K. (ed). Academic press, inc: San Diego, California 92101. pp. 35-69.

Al-Shamkhani A. and Duncan R. (1995). Synthesis, controlled release properties and antitumour activity of alginates-cis-aconityl-daunomycin conjugates. *International Journal of Pharmaceutics*, **122**, 107-119.

Ali S. and Coombes C. (2002). Endocrine-responsive breast cancer and strategies for combating resistance. *Nature Reviews Cancer*, **2**, 101-114.

ATAC Trialists Group. (2005). Results of the ATAC (Arimidex, Tamoxifen Alone or in Combination) trial after completion of 5 years' adjuvant treatment for breast cancer. *Lancet*, **365**, 60-62.

B

Barrett-Lee P.J. (2005). Growth factor signalling in clinical breast cancer and its impact on response to conventional therapies: a review of chemotherapy. *Endocrine-Related Cancer*, **12**, S125-S133.

Beatson G. (1896). On the treatment of inoperable cases of carcinoma of the mamma: Suggestions for a new method of treatment with illustrative cases. *Lancet*, **2**, 104-107 and 162-165.

Beck T., Weller E.E., Weikel W., Brumm C., Wilkens C. and Knapstein G. (1995). Usefulness of immunohistochemical staining for p53 in the prognosis of breast carcinomas: correlations with established prognosis parameters and with the proliferation marker, MIB-1. *Gynecologic Oncology*, **57**, 96-104.

- Bonadonna G., Brambilla C., Rossi A., Bonfante V., Ferrari L., Crippa F. and Villani F. (1984). Epirubicin in advanced breast cancer. The experience of the Milan Cancer Institute. In *Advanced in Anthracycline Chemotherapy: Epirubicin*, Bonadonna, G. (ed). MASSON ITALIA EDITORI: Milano. pp. 63-70.
- Brigger I., Chaminade P., Marsaud V., Appel M., Besnard M., Gurny R., Renoir M. and Couvreur P. (2001). Tamoxifen encapsulation within polyethylene glycol-coated nanospheres. A new antiestrogen formulation. *International Journal of Pharmaceutics*, **214**, 37-42.
- Brocchini S. and Duncan R. (1999). Pendent drugs, release from polymers. In *Encyclopedia of Controlled Drug Delivery*, Mathiowitz E. (ed). John Wiley and Sons: New York. pp. 786-816.
- Brodie A.M., Schwarzel W.C. and Brodie H.J. (1976). Studies on the mechanism of oestrogen biosynthesis in the rat ovary—I. *Journal of Steroid Biochemistry*, **7**, 787-793.
- Brodie A.M. and Longcope C. (1980). Inhibition of peripheral aromatization by aromatase inhibitors, 4-hydroxy- and 4-acetoxy-androstene-3,17-dione. *Endocrinology*, **106**, 19-21.
- Brodie A., Lu Q. and Long B. (1999). Aromatase inhibitors and their antitumour effects in model system. *Endocrine-Related Cancer*, **6**, 205-210.
- Brodie A.M.H. and Njar V.C.O. (2000). Aromatase inhibitors and their application in breast cancer treatment. *Steroids*, **65**, 171-179.
- Brodie A. (2002). Aromatase inhibitors in breast cancer. *Trends in Endocrinology and Metabolism*, **13**, 61-65.
- Burak Jr W.E., Quinn A.L., Farrar W.B. and Brueggemeier R.W. (1997). Androgens influence estrogen-induced responses in human breast carcinoma cells

through cytochrome P450 aromatase. *Breast Cancer Research and Treatment*, **44**, 57-64.

Bundgaard, H. (1985). Design of prodrugs: bioreversible derivatives for various functional groups and chemical entities. In *Design of Prodrugs*, Bundgaard, H. (ed). Elsevier Science Publishers Biomedical Division: Amsterdam. pp. 1-92.

Burlacu A. (2003). Regulation of apoptosis by Bcl-2 family proteins. *Journal of Cellular and Molecular Medicine*, **7**, 249-257.

C

Calabresi P. and Chabner B.A. (1996). Chemotherapy of neoplastic diseases. In *Goodman and Gilman's The Pharmacological Basis of Therapeutics*, Molinoff, P.B. and Ruddon R.W. (eds). The McGraw-Hill Companies, Inc.: New York. pp. 1225-1287.

Camplo M., Charvet-Faury A.S., Borel C., Turin F., Hantz O., Trabaud C., Niddam V., Mourier N., Graciet J.C., Chermann J.C. and Kraus J.L. (1996). Synthesis and antiviral activity of N-4'-dihydropyridinyl and dihydroquinolinylcarbonyl-2-hydroxymethyl-5-[cytosine-1'-yl]-1,3-oxathiolane derivatives against human immunodeficiency virus and duck hepatitis B virus. *European Journal of Medicinal Chemistry*, **31**, 539-546.

Cassidy J. (2000). PK1: Results of phase I studies. *Proceedings of the Fifth International Symposium on Polymer Therapeutics: From Laboratory to Clinical Practice*, 20.

Cavallaro G., Maniscalco L., Licciardi M. and Giammona G. (2004). Tamoxifen-loaded polymeric micelles: preparation, physico-chemical characterization and in vitro evaluation studies. *Macromolecular Biosciences*, **4**, 1028-1038.

- Cera C., Palumbo M., Stefanelli S., Rassa M. and Palu G. (1992). Water-soluble polysaccharide-anthracycline conjugates: biological activity. *Anticancer Drug Design*, **7**, 143-151.
- Chang, J., Powles T.J., Allred D.C., Ashley S.E., Makris A., Gregory R.K., Osborne C.K. and Dowsett M. (2000). Prediction of clinical outcome from primary tamoxifen by expression of biological markers in breast cancer patients. *Clinical Cancer Research*, **6**, 616-621.
- Chang J. and Elledge R.M. (2002). Pharmacology, biology and clinical use of triphenylethylenes. In *Endocrine Therapy of Breast Cancer*, Robertson J.F.R., Nicholson R.I. and Hayes D.F. (eds). Martin Dunitz: London. pp.33-44.
- Claing A., Perry S.J., Achirioloaie M., Walker J.K.L. Albanesi J.P., Lefkowitz and Premont R.T. (1999). Multiple endocytic pathways of G protein-coupled receptors delineated by GIT1 sensitivity. *Proceedings of the National Academy of Sciences of the United States of America*, **97**, 1119-1124.
- Collett K., Hartveit F., Skjærven R. and Mæhle B.O. (1996). Prognostic role of oestrogen and progesterone receptors in patients with breast cancer: relation to age and lymph node status. *Journal of Clinical Pathology*, **49**, 920-925.
- Configliacchi E., Razzano G., Rizzo V. and Vigevani A. (1996). HPLC methods for determination of bound and free doxorubicin, and of bound and free galactosamine, in methacrylamide polymer-drug conjugates. *Journal of Pharmaceutical and Biomedical Analysis*, **15**, 123-129.
- Conner S.D. and Schmid, S.L. (2003). Regulated portals of entry into the cells. *Nature*, **422**, 37-44.
- Crivellato E., Candussio L., Rosati A.M., Decorti G., Klugmann F.B. and Mallardi F. (1999). Kinetics of doxorubicin handling in the LLC-PK1 kidney epithelial cell line is mediated by both vesicle formation and P-glycoprotein drug transport. *The Histochemical Journal*, **31**, 635-643.

Crown J., Dieras V., Kaufmann M., von Minckwitz G., Kaye S.B., Leonard R., Marty M., Misset J.-L., Osterwalder B. and Piccard M. (2002). Chemotherapy for metastatic breast cancer-report of a European expert panel. *The Lancet Oncology*, **3**, 719-727.

D

Dancey J., Sausville E.A. (2003). Issues and progress with protein kinase inhibitors for cancer treatment. *Nature Reviews Drug Discovery*, **2**, 296-313.

Danesi R., Fogli S., Gennari A., Conte P. and Del Tacca, M. (2002). Pharmacokinetic-pharmacodynamic relationship of the anthracycline anticancer drug. *Clinical Pharmacokinetics*, **41**, 431-444.

Darnell J.E.J. (2002). Transcription factors as targets for cancer therapy. *Nature Reviews Cancer*, **2**, 740-749.

De Duve C., De Barse T., Poole B., Trouet A., Tulkens P. and Van Hoof F. (1974). Lysosomotropic agents. *Biochemical Pharmacology*, **23**, 2495-2531.

Demoy M., Minko T., Kopeckova P. and Kopecek J. (2000). Time- and concentration-dependent apoptosis and necrosis induced by free and HPMA copolymer-bound doxorubicin in human ovarian carcinoma cells. *Journal of Controlled Release*, **69**, 185-196.

Denizot F. and Lang R. (1986). Rapid colorimetric assay for cell growth and survival. Modifications to the tetrazolium dye procedure giving improved sensitivity and reliability. *Journal of Immunological Methods*, **89**, 271-277.

Devleeschouwer N., Body J.J., Legros N., Muquardt C., Donnay I., Wouters P. and Leclercq G. (1992). Growth factor-like activity of phenol red preparations in the MCF-7 breast cancer cell line. *Anticancer Research*, **12**, 789-794.

- Dordal M.S., Ho A.C., Jackson-Stone M., Fu Y.F., Goolsby C.L. and Winter J.N. (1995). Flow cytometric assessment of the cellular pharmacokinetics of fluorescent drugs. *Cytometry*, **20**, 307-314.
- Dorssers L.C.J., van der Flier S., Brinkman A., van Agthoven T., Veldscholte J., Berns E.M.J.J., Klijn J.G.M., Beex L.V.A.M., and Foekens J.A. (2001). Tamoxifen resistance in breast cancer. *Drugs*, **61**, 1721-1733.
- Downward J. (2003). Targeting RAS signalling pathways in cancer therapy. *Nature Reviews Cancer*, **3**, 11-22.
- Duncan R., Lloyd J.B. and Kopecek J. (1980). Degradation of side chains of N-(2-hydroxypropyl) methacrylamide copolymers by lysosomal enzymes. *Biochemical and Biophysical Research Communications*, **94**, 284-290.
- Duncan R., Rejmanova P., Kopecek J. and Lloyd J.B. (1981). Pinocytic uptake and intracellular degradation of N-(2-hydroxypropyl) methacrylamide copolymers. *Biochimica et Biophysica Acta*, **678**, 143-150.
- Duncan R., Cable H.C., Lloyd J.B., Rejmanova P. and Kopecek J. (1983). Polymers containing enzymatically degradable bonds, 7. Design of oligopeptide side chains in poly[N-(2-hydroxypropyl)methacrylamide] copolymers to promote efficient degradation by lysosomal enzymes. *Makromolekulare Chemie*, **84**, 1997-2008.
- Duncan R. and Kopecek J. (1984). Soluble synthetic polymers as potential drug carriers. *Advances in Polymer Science*, **57**, 51-101.
- Duncan R., Cable H.C., Strohmalm J. and Kopecek (1986). Pinocytic capture and endocytosis of rat immunoglobulin IgG-N-(2-hydroxypropyl)methacrylamide copolymer conjugates by rat visceral yolk sacs cultured in vitro. *Bioscience Reports*, **6**, 869-877.

- Duncan R., Kopeckova-Rejmanova P., Strohalm J., Hume I., Cable H.C., Pohl J., Lloyd J.B. and Kopecek J. (1987). Anticancer agents coupled to N-(2-hydroxypropyl)methacrylamide copolymers. I. Evaluation of daunomycin and puromycin conjugates in vitro. *British Journal of Cancer*, **55**, 165-174.
- Duncan R., Kopeckova P., Strohalm J., Hume I., Lloyd J.B. and Kopecek J. (1988). Anticancer agents coupled to N-(2-hydroxypropyl)methacrylamide copolymers. II. Evaluation of daunomycin conjugates in vivo against L1210 leukaemia. *British Journal of Cancer*, **57**, 147-156.
- Duncan R., Hume I.C., Kopeckova P., Ulbrich K., Strohalm J. and Kopecek J. (1989). Anticancer agents coupled to N-(2-hydroxypropyl)methacrylamide copolymers. 3. Evaluation of adriamycin conjugates against mouse leukaemia L1210 in vivo. *Journal of Controlled Release*, **10**, 51-63.
- Duncan R., Seymour L.W., O'Hare K.B., P.A.F., Wedge S., Hume I.C., Ulbrich K., Strohalm J., Subr V., Spreafico F., Grandi M., Ripamonti M., Farao M. and Suarato A. (1992). Preclinical evaluation of polymer-bound doxorubicin. *Journal of Controlled Release*, **19**, 331-346.
- Duncan R., Coatsworth J.K. and Burtles S. (1998). Preclinical toxicology of a novel polymeric antitumour agent: HPMMA copolymer-doxorubicin (PK1). *Human and Experimental Toxicology*, **17**, 93-104.
- Duncan R. (1999). Polymer conjugates for tumour targeting and intracytoplasmic delivery. The EPR effect as a common gateway? *Pharmaceutical Science Technology Today*, **2**, 441-449.
- Duncan R. (2002). Polymer-drug conjugates: targeting cancer. In *Biomedical aspects of drug targeting*, Muzykantov V. and Torchilin V. (eds). Kluwer Academic Publishers. pp. 193-209.
- Duncan R., (2003a). The dawning era of polymer therapeutics. *Nature Reviews Drug Discovery*, **2**, 347-362.

Duncan, R., (2003b). Polymer-anticancer drug conjugates. In *Handbook of Anticancer Drug Development*, Budman, D., Calvert, H. and Rowinsky, E. (eds) Lippincott Williams & Wilkins: Baltimore, MD, USA. pp. 239-260.

Duncan R. (2004). Nanomedicines in action. *The Pharmaceutical Journal*, **273**, 485-488.

Duncan R. (2005). N-(2-Hydroxypropyl) methacrylamide copolymer conjugates. In *Polymeric Drug Delivery System*, Kwon, G.S. (ed). Marcel Dekker, Inc.: New York. pp. 1-92.

E

Ellis I.O., Dowsett M., Bartlett J., Walker R., Cooke T., Gullick W., Gusterson B., Mallon E. and Barrett-Lee P. (2000a). Recommendations for HER testing in the UK. *Journal of Clinical Pathology*, **53**, 890-892.

Ellis M.J., Hayes D.F. and Lippman M.E. (2000). Treatment of metastatic breast cancer. In *Diseases of the Breast*, Harris J.R. (ed). Lippincott Williams and Wilkins: Philadelphia. pp. 749-797.

Etrych T., Jelinkova M., Rihova B. and Ulbrich K. (2001). New HPMA copolymers containing doxorubicin bound via pH-sensitive linkage: synthesis and preliminary in vitro and in vivo biological properties. *Journal of Controlled Release*, **73**, 89-102.

F

Fiucci G., Ravid D., Reich R. and Liscovitch M. (2002). Caveolin-1 inhibits anchorage-independent growth, anoikis and invasiveness in MCF-7 human breast cancer cells. *Oncogene*, **21**, 2365-2375.

Flanagan P.A., Kopeckova P., Kopecek J. and Duncan R. (1989). Evaluation of protein-N-(2-hydroxypropyl)methacrylamide copolymer conjugates as targetable drug carriers. 1. Binding, pinocytic uptake and intracellular distribution of transferrin and anti-transferrin receptor antibody conjugates. *Biochemica et Biophysica Acta*, **993**, 83-91.

Flanagan P.A., Duncan R., Subr V., Ulbrich K., Kopeckova P., Kopecek J. (1992). Evaluation of protein-N-(2-hydroxypropyl)methacrylamide copolymer conjugates as targetable drug carriers. 2. Body distribution of conjugates containing transferrin, antitransferrin receptor antibody or anti-Thy 1.2 antibody and effectiveness of transferrin-containing daunomycin conjugates against mouse L1210 leukaemia in vivo. *Journal of Controlled Release*, **18**, 25-38.

Folkman J. and Shing Y. (1992). Angiogenesis. *The Journal of Biological Chemistry*, **267**, 10931-10934.

Fontana G., Maniscalco L., Schillaci D., Cavallaro G. and Giammona G. (2005). Solid lipid nanoparticles containing tamoxifen characterisation and *in vitro* antitumoral activity. *Drug Delivery*, **12**, 385-392.

Friedrichs K., Holzel F. and Janicke F. (2002). Combination of taxanes and anthracyclines in first-line chemotherapy of metastatic breast cancer: an interim report. *European Journal of Cancer*, **38**, 1730-1738.

G

Gee J.M.W., Madden T.-A., Robertson J.F.R. (2002). Clinical response and resistance to SERMs. In *Endocrine Therapy of Breast Cancer*, Robertson J.F.R., Nicholson R.I. and Hayes D.F. (eds) Dunitz: London. pp. 154-189.

Gee J.M.W., Howell A., Gullick W.J., Benz C.C., Sutherland R.L., Santen R.J., Martin L-A., Ciardiello F., Miller W.R., Dowsett M., Barrett-Lee P., Robertson J.F.R., Johnston S.R., Jones H.E., Wakeling A.E., Duncan R. and

Nicholson R.I. (2005). Consensus statement. *Endocrine-Related Cancer*, **12**, S1-S7.

Geisler J., Detre S., Berntsen H., Ottestad L., Lindtjorn B., Dowsett M. and Lonning P.E. (2001). Influence of neoadjuvant anastrozole (Arimidex) on intratumoral oestrogen levels and proliferation markers in patients with locally advanced breast cancer. *Clinical Cancer Research*, **7**, 1230-1236.

Gewirtz D.A. (1999). A critical evaluation of the mechanism of action proposed for the antitumour effects of the anthracycline antibiotics adriamycin and daunorubicin. *Biochemical Pharmacology*, **57**, 727-741.

Gianasi E., Wasil M., Evagorou E.G., Kedde A., Wilson G. and Duncan R. (1999). HEMA copolymer platins as novel antitumour agents: in vitro properties, pharmacokinetics and antitumour activity *in vivo*. *European Journal of Cancer*, **35**, 994-1002.

Goss P.E. and Strasser K. (2002). Tamoxifen resistant and refractory breast cancer the value of aromatase inhibitors. *Drugs*, **62**, 957-966.

Gross J.M. and Yee D. (2002). How does the oestrogen receptor work? *Breast Cancer Research*, **4**, 62-64.

Guo J.A., Hsiue G.H and Juang T.M. (2002). Synthesis and biological properties of antitumor-active conjugates of ADR with dextran. *Journal of Biomaterials Science Polymer Edition*, **13**, 1135-1151.

H

Haag R. and Kratz F. (2006). Polymer therapeutics: concepts and applications. *Angewandte Chemie International Edition*, **45**, 1198-1215.

- Hackstein H., Taner T., Logar A.J. Thomson A.W. (2002). Rapamycin inhibits macropinocytosis and mannose receptor-mediated endocytosis by bone marrow-derived dendritic cells. *Blood*, **1**, 1084-1087.
- Hailstones D., Slier L.S., Parton R.G. and Stanley K.K. (1998). Regulation of caveolin and caveolae by cholesterol in MDCK cells. *Journal of Lipid Research*, **39**, 369-379.
- Hayes D.F. and Robertson J.F.R. (2002). Overview and concept of endocrine therapy. In *Endocrine Therapy of Breast Cancer*, Robertson J.F.R., Nicholson R.I. and Hayes D.F. (eds). Martin Dunitz: London. pp. 3-10.
- Hermanson G.T. (1996). *Bioconjugate Techniques*. Academic Press, INC.: San Diego. pp. 177-180.
- Herzog T., Barret R.J., Edwards R. and Oldham F.B. (2005). Phase II study of paclitaxel polyglumex (PPX)/carboplatin (C) for 1st line induction and maintenance therapy of stage III/IV ovarian or primary peritoneal carcinoma. *Proceedings of the American Society of Clinical Oncology*, 5012.
- Hortobagyi G.N. (2002). The status of breast cancer management: challenges and opportunities. *Breast Cancer Research and Treatment*, **75**, S61-S65.
- Hovorka O., St'astny M., Etrych T., Subr V., Strohalm J., Ulbrich K. and Rihova B. (2002). Differences in the intracellular fate of free and polymer-bound doxorubicin. *Journal of Controlled Release*, **80**, 101-117.
- Howell A. (2000). Faslodex (ICI 182780): an oestrogen receptor downregulator. *European Journal of Cancer*, **36**, S87-S88.
- Howell A. and Johnston S.R.D. (2002). Selective oestrogen receptor modulators (SERMs). In *Endocrine Therapy of Breast Cancer*, Robertson J.F.R., Nicholson R.I. and Hayes D.F. (eds). Martin Dunitz: London. pp. 45-62

Ilangumaran S. and Hoessli D.C. (1998). Effects of cholesterol depletion by cyclodextrin on the sphingolipid microdomains of the plasma membrane. *Biochemical Journal*, **335**, 433-440

I

Ivanov A.I., Nusrat A. and Parkos C.A. (2004). Endocytosis of epithelial apical junctional proteins by a clathrin-mediated pathway into a unique storage compartment. *Molecular Biology of the Cell*, **15**, 176-188.

J

Jakacka M., Ito M., Weiss J., Chien P., Gehm B.D. and Jameson J.L. (2001). Oestrogen receptor binding to DNA is not required for its activity through nonclassical AP1 pathway. *Journal of Biological Chemistry*, **276**, 13615-13621.

Johannes L. and Lamaze C. (2002). Clathrin-dependent or not: is it still the question? *Traffic*, **3**, 443-451.

Johnston J.O., Wright C.L. and Metcalf B.W. (1984). Time-dependent inhibition of aromatase in trophoblastic tumor cells in tissue culture. *Journal of Steroid Biochemistry*, **20**, 1221-1226.

Johnston S.R.D. and Dowsett M. (2003). Aromatase inhibitors for breast cancer: lessons from the laboratory. *Nature Reviews Cancer*, **3**, 821-831.

Jones A.T., Gumbleton M. and Duncan R. (2003). Understanding endocytic pathways and intracellular trafficking: a prerequisite for effective design of advanced drug delivery systems. *Advanced Drug Delivery Reviews*, **55**, 1353-1357.

Jordan V.C. (2003a). Tamoxifen: a most unlikely pioneering medicine. *Nature Reviews Drug Discovery*, **2**, 205-213.

Jordan V.C. (2003b). Is tamoxifen the Rosetta stone for breast cancer? *Journal of the National Cancer Institute*, **95**, 338-340.

Julyan P.J., Seymour L.W., Ferry D.R., Daryani S., Boivin C.M., Doran J., David M., Anderson A., Christodoulou C., Young A.M., Hessewood S. and Kerr D.J. (1999). Preliminary clinical study of the distribution of HPMA copolymers bearing doxorubicin and galactosamine. *Journal of Controlled Release*, **57**, 281-290.

K

Kardinal C.G. (1992). Chemotherapy of breast cancer. In *The Chemotherapy Source Book*, Perry, M.C. (ed). Williams and Wilkins: Baltimore. pp. 948-988.

Kee S.H., Cho E.-J., Song J.-W., Park K.S., Baek L.J. and Song K.-J. (2004). Effects of endocytosis inhibitory drugs on rubella virus entry into VeroE6 cells. *Microbiology and Immunology*, **48**, 823-829.

Kenny F.S., Willsher P.C., Gee J.M.W., Nicholson R.I., Pinder S.E., Ellis I.O. and Robertson J.F.R. (2001). Change in the expression of ER, bcl-2 and MIB1 on primary tamoxifen and relation to response in ER positive breast cancer. *Breast Cancer Research and Treatment*, **65**, 135-144.

Ketelaar J.A.A. and Hellingman J.E. (1951). Chemical studies on insecticides. Determination of parathion and dimethylparathion. *Analytical Chemistry*, **23**, 645-650.

Kitawaki J., Kim T., Kanno H., Noguchi T., Yamamoto T. and Okada H. (1993). Growth suppression of MCF-7 human breast cancer cells by aromatase inhibitors: a new system for aromatase inhibitor screening. *Journal of Steroids Biochemistry and Molecular Biology*, **44**, 667-670.

Kopecek J., Cifkova I., Rejmanova P., Strohalm J., Obereigner B. and Ulbrich K. (1981). Polymers containing enzymatic degradable bonds. Preliminary experiments in vivo. *Macromolecular Chemistry*, **182**, 2941-2949.

Kopecek J., Rejmanova P., Strohalm J., Ulbrich K., Rihova B., Chytrý V., Duncan R. and Lloyd J.B. (1985). Synthetic polymeric drugs Czech. Patent Application: 0097-85, British Patent Application 85 00209.

Kovar L., Ulbrich K., Kovar M., Strohalm J., Stastny T., Etrych T. and Rihova B. (2003). The effect of HPMA-copolymer-bound doxorubicin conjugates on the expression of genes involved in apoptosis signalling. *Journal of Controlled Release*, **91**, 247-248.

Kovar M., Kovar L., Subr V., Etrych T., Ulbrich K., Mrkvan T., Loucka J. and Rihova B. (2004). HPMA copolymers containing doxorubicin bound by a proteolytically or hydrolytically cleavable bond: comparison of biological properties in vitro. *Journal of Controlled Release*, **99**, 301-314.

Kuiper G.G.J.M., Enmark E., Pelto-Huikko M., Nilsson S. and Gustafsson J.-A. (1996). *Proceedings of the National Academy of Sciences of the United States of America*, **93**, 5925-5930.

Kunath K., Kopeckova P., Minko T. and Kopecek J. (2000). HPMA copolymer-anticancer drug-OV-TL16 antibody conjugates. 3. The effect of free and polymer-bound Adriamycin on the expression of some genes in the OVCAR-3 human ovarian carcinoma cell line. *European Journal of Pharmaceutics and Biopharmaceutics*, **49**, 11-15.

L

Langer C.J., Socinski M.A., Ross H. and O'Byrne K.J. (2005). Paclitaxel poliglumex (PPX)/carboplatin vs paclitaxel/carboplatin for the treatment of PS2 patients with chemotherapy-naïve advanced non small cell lung cancer (NSCLC): A

- phase III study. *Proceedings of the American Society of Clinical Oncology*, 7011.
- Leyland-Jones B. (2002). Trastuzumab: hopes and realities. *The Lancet Oncology*, **3**, 137-144.
- Liem A., Appleyard M., O'Neill M., Hupp T., Chamberlain M. and Thompson A. (2003). Doxorubicin and vinorelbine act independently via p53 expression and p38 activation respectively in breast cancer cell lines. *British Journal of Cancer*, **88**, 1281-1284.
- Lloyd J.B. (2000). Lysosome membrane permeability: implications for drug delivery. *Advanced Drug Delivery Reviews*, **41**, 189-200.
- Long B.J., Tilghman S.L., Yue W., Thiantanawat A., Grigoriev D.N. and Brodie A.M.H. (1998). The steroidal antiestrogen ICI 182,780 is an inhibitor of cellular aromatase activity. *Journal of Steroids Biochemistry and Molecular Biology*, **67**, 293-304.
- Long B.J., Jelovac D., Thiantanawat A. and Brodie A.M. (2002). The effect of second-line antiestrogen therapy on breast tumor growth after first-line treatment with aromatase inhibitor letrozole: long-term studies using the intratumoral aromatase postmenopausal breast cancer model. *Clinical Cancer Research*, **8**, 2378-2388.
- Longcope C., Femino A. and Johnston J.O. (1988). Inhibition of peripheral aromatization in baboons by an enzyme-activated aromatase inhibitor (MDL 18,962). *Endocrinology*, **122**, 2007-2011.
- Lonning P.E. (2000). Clinico-pharmacological aspects of different hormone treatments. *European Journal of Cancer*, **36**, S81-S82.
- Lonning P.E. (2004). Aromatase inhibitors in breast cancer. *Endocrine-Related Cancer*, **11**, 179-189.

M

- Macaulay V.M., Nicholls J.E., Gledhill J., Rowlands M.G., Dowsett M. and Ashworth A. (1994). Biological effects of stable overexpression of aromatase in human hormone-dependent breast cancer cells. *British Journal of Cancer*, **69**, 77-83.
- Maeda H. (1994). Polymer conjugated macromolecular drugs for tumor-specific targeting. In *Polymer site-specific Pharmacotherapy*, Domb A.J. (ed). John Wiley and Sons Ltd: New York. pp.95-116.
- Maeda H., Sawa T. and Konno T. (2001). Mechanism of tumor-targeted delivery of macromolecular drugs, including the EPR effect in solid tumor and clinical overview of the prototype polymeric drug SMANCS. *Journal of Controlled Release*, **74**, 47-71.
- Makris A., Powles T.J., Allred D.C., Ashley S., Ormerod M.G., Titley J.C. and Dowsett M. (1998). Changes in hormone receptors and proliferation markers in tamoxifen treated breast cancer patients and the relationship with response. *Breast Cancer Research and Treatment*, **48**, 11-20.
- Malugin A., Kopeckova P. and Kopecek J. (2004). HEMA copolymer-bound doxorubicin induces apoptosis in human ovarian carcinoma cells by a Fas-independent pathway. *Molecular Pharmaceutics*, **1**, 174-182.
- Malugin A., Kopeckova P. and Kopecek J. (2005). Apoptosis induced in ovarian cancer cells by HEMA copolymer-bound doxorubicin is mediated by bcl-2 family proteins. *Proceedings of the 32nd International Symposium for Controlled Release of Bioactive Materials*, 246.
- Manunta M., Tan P.H., Sagoo P., Kashefi K. and George A.J.T. (2004). Gene delivery by dendrimers operates via a cholesterol-dependent pathway. *Nucleic Acid Research*, **32**, 2730-2739.

- Maxfield F.R. and McGraw T.E. (2004). Endocytic recycling. *Nature Reviews Molecular Cell Biology*, **5**, 121-132.
- Mazue' G., Iatropoulos M., Imondi A., Castellino S., Brughera M., Podesta' A., Della Torre P. and Moneta D. (1995). Anthracyclines: A review of general and special toxicity studies. *International Journal of Oncology*, **7**, 713-726.
- Meerum Terwogt J.M., ten Bokkel Huinink W.W., Schellens J.H.M., Schot M., Mandjes I., Zurlo M., Rocchetti M., Rosing H., Koopman F. and Beijnen J.H. (2001). Phase I clinical trial and pharmacokinetic study of PNU166945, a novel water soluble polymer-conjugated prodrug of paclitaxel. *Anti-Cancer Drugs*, **12**, 315-323.
- Mendichi R., Rizzo V., Gigli M. and Schieronni A.G. (2002). *Bioconjugate Chemistry*, **13**, 1253-1258.
- Miller W.R. and Dixon J.M. (2000). Antiaromatase agents: preclinical data and neoadjuvant therapy. *Clinical Breast Cancer*, **1**, S9-14.
- Miller W.R. and Dixon J.M. (2002). Endocrine and clinical endpoints of examestane as neoadjuvant therapy. *Cancer Control*, **9**, 9-15.
- Miller W.R., Anderson T.J., Evans D.B., Krause A., Hampton G. and Dixon J.M. (2003). An integrated view of aromatase and its inhibition. *Journal of Steroid Biochemistry and Molecular Biology*, **86**, 413-421.
- Miller W.R., Anderson T.J., White S., Larionov A., Murray J., Evans D., Krause A. and Dixon J.M. (2005). Aromatase inhibitors cellular and molecular effects. *Journal of Steroid Biochemistry and Molecular Biology*, **95**, 83-89.
- Minko T., Kopeckova P. and Kopecek J. (1999). Comparison of the anticancer effect of free and HPMA copolymer-bound adriamycin in human ovarian carcinoma cells. *Pharmaceutical Research*, **16**, 986-996.

- Minko T., Kopeckova P. and Kopecek J. (2000). Efficacy of the chemotherapeutic action of HPMA copolymer-bound doxorubicin in a solid tumour model of ovarian carcinoma. *International Journal of Cancer*, **86**, 108-117.
- Minko T., Kopeckova P. and Kopecek J. (2001). Preliminary evaluation of caspases-dependent apoptosis signalling pathways of free and HPMA copolymer-bound doxorubicin in human ovarian carcinoma cells. *Journal of Controlled Release*, **71**, 227-237.
- Moghimi S.M., Hunter A.C. and Murray J.C. (2005). Nanomedicine: current status and future prospects. *The FASEB Journal*, **19**, 311-330.
- Monneret C. (2001). Recent developments in the field of antitumour anthracyclines. *European Journal of Medicinal Chemistry*, **6**, 483-493.
- Mosmann T. (1983). Rapid colorimetric assay for cellular growth and survival: application to proliferation and cytotoxicity assays. *Journal of Immunological Methods*, **65**, 55-63.
- Mouridsen H.T. and Robert N.J. (2005). The role of aromatase inhibitors as adjuvant therapy for early breast cancer in postmenopausal women. *European Journal of Cancer*, **41**, 1678-1689.
- Musila R., Quarcoo N., Kortenkamp A. and Duncan R. (2001). In vivo assessment of time-dependent DNA damage induced by HPMA copolymer-doxorubicin (PK1) using the alkaline single cell electrophoresis (Comet) assay. *Proceedings of the International Symposium for Controlled Release of Bioactive Materials*, **28**, 1307-1308.

N

Nabholtz J.M. and Gligorov J. (2005). Docetaxel/trastuzumab combination therapy for the treatment of breast cancer. *Expert Opinion on Pharmacotherapy*, **6**, 1555-1564.

Nan A., Nanayakkara N.P.D., Walker L.A., Yardeley V., Croft S.L. and Gandehari H. (2001). N-(2-Hydroxypropyl)methacrylamide (HPMA) copolymers for targeted delivery of 8-aminoquinoline antileishmanial drugs. *Journal of Controlled Release*, **77**, 233-243.

Nichols B. (2003). Caveosomes and endocytosis of lipid rafts. *Journal of Cell Science*, **116**, 4707-4714.

Nicholson R.I. and Gee J.M.W. (2000). Oestrogen and growth factor cross-talk and endocrine insensitivity and acquired resistance in breast cancer. *British Journal of Cancer*, **82**, 501-513.

Nicholson R.I., Hutcheson I.R., Harper M.E., Knowlden J.M., Barrow D., McClelland R.A., Jones H.E., Wakeling A.E. and Gee J.M.W. (2001). Modulation of epidermal growth factor receptor in endocrine-resistant, oestrogen receptor-positive breast cancer. *Endocrine-Related Cancer*, **8**, 175-182.

Nicholson E.I., Hutcheson I.R., Hiscox S.E., Knowlden J.M., Giles M., Barrow D. and Gee J.M.W. (2005). Growth factor signalling and resistance to selective oestrogen receptor modulators and pure anti-oestrogens: the use of anti-growth factor therapies to treat or delay endocrine resistance in breast cancer. *Endocrine-Related Cancer*, **12**, S29-S36.

Njar V.C.O., Brodie A.M.H. (1999). Comprehensive pharmacology and clinical efficacy of aromatase inhibitors. *Drugs*, **58**, 233-255.

Nowotnik D.P. (2004). Preclinical development and Phase I results with HPMA copolymer platinates. *Proceedings of the 6th International Conference on Polymer Therapeutics: From Laboratory to Clinical Practice*, 25.

O

O'Hare K.B., Duncan R., Strohalm J., Ulbrich K. and Kopeckova P. (1993). Polymeric drug-carriers containing doxorubicin and melanocyte-stimulating hormone: *in vitro* and *in vivo* evaluation against murine melanoma. *Journal of Drug Targeting*, **1**, 217-229.

Omelyanenko V., Kopeckova P., Gentry C. and Kopecek J. (1998). Targetable HPMA copolymer-adriamycin conjugates. Recognition, internalization, and subcellular fate. *Journal of Controlled Release*, **53**, 25-37.

Orlandi P.A. and Fishman P.H. (1998). Filipin-dependent inhibition of cholera toxin: evidence for toxin internalisation and activation through caveolae-like domains. *Journal of Cell Biology*, **141**, 905-915.

Osborne C.K. and Fuqua S.A.W. (1994). Mechanisms of tamoxifen resistance. *Breast Cancer Research and Treatment*, **32**, 49-55.

P

Paech K., Webb P., Kuiper G.G.J.M., Nilsson S., Gustafsson J.-A., Kushner P.J. and Scanlan T.S. (1997). Differential ligand activation of oestrogen receptors ER α and ER β at AP1 sites. *Science*, **277**, 1508-1510.

Pettersson K., Delaunay F. and Gustafsson J.-A. (2000). Oestrogen receptor β acts as a dominant regulator of oestrogen signalling. *Oncogene*, **19**, 4970-4978.

Pettersson K. and Gustafsson J.-A. (2001). Role of oestrogen receptor beta in oestrogen action. *Annual Review in Physiology*, **63**, 165-192.

Pinciroli V., Rizzo V., Angelucci F., Tato M. and Vigevani A. (1997). ¹H NMR characterisation of methacrylamide polymer conjugates with the anticancer drug doxorubicin. *Magnetic Resonance in Chemistry*, **35**, 2-8.

R

Racca S., Conti G., Pietribiasi F., Stramignoni D., Tampellini M., Valetto M., Ghezzi F. and Di Carlo F. (1995). Correlation between pS2 protein positivity, steroid receptor status and other prognostic factors in breast cancer. *International Journal of Biological Markers*, **10**, 87-93.

Rademaker-Lakhai J.M., Terret C., Howell S.B., Baud C.M., de Boer R.F., Pluim D., Beijnen J.H., Schellens J.H.M. and Droz J.-P. (2004). A phase I and pharmacological study of the platinum polymer AP5280 given as an intravenous infusion once every 3 weeks in patients with solid tumours. *Clinical Cancer Research*, **10**, 3386-3395.

Rejman J., Oberle V., Zuhorn I.S. and Hoekstra D. (2004). Size-dependent internalization of particles via the pathways of clathrin and caveolae-mediated endocytosis. *Biochemical Journal*, **377**, 159-169.

Rejmanova P., Labsky J. and Kopecek J. (1977). Aminolysis of monomeric and polymeric p-nitrophenyl esters of methacryloylated amino acids. *Macromolecular Chemistry*, **178**, 2159-2168.

Rice JR, Howell SB. (2004). AP-5346 Polymer-delivered platinum complex. *Drug Future* **29**: 561-5.

Rihova B., Etrych T., Pechar M., Jelinkova M., Stastny M., Horvorka O., Kovar M. and Ulbrich K. (2001). Doxorubicin bound to a HPMA copolymer carrier through hydrazone bond is effective also in a cancer cell line with a limited content of lysosomes. *Journal of Controlled Release*, **74**, 225-232.

Ringsdorf H. (1975). Structure and properties of pharmacologically active polymers. *Journal of Polymer Science: Polymer Symposium*, **51**, 35-53.

Ringsdorf H. (2004). Hermann Staudinger and the future of polymer research jubilees-beloved occasions for cultural piety. *Angewandte Chemie International Edition*, **43**, 1064-1076.

Rodal S.K., Skretting G., Garred O., Vilhardt F., van Deurs B. and Sandvig K. (1999). Extraction of cholesterol with methyl- β -cyclodextrin perturbs formation of clathrin-coated endocytic vesicles. *Molecular Biology of the Cells*, **10**, 961-974.

Rodrigues P.C.A., Beyer U., Schumacher P., Roth T., Fiebig H.H., Unger C., Messori L., Orioli P., Paper D.H., Mulhaupt R. and Kratz F. (1999). Acid-sensitive polyethylene glycol conjugates of doxorubicin: preparation, in vitro efficacy and intracellular distribution. *Bioorganic and Medicinal Chemistry*, **7**, 2517-2524.

Ryan K. (1959). Metabolism of C-16-oxygenated steroids by human placenta: the formation of estriol. *The Journal of Biological Chemistry*, **234**, 2006-2008.

S

Sakamoto T., Eguchi H., Omoto Y., Ayabe T., Mori H. and Hayashi S.-i. (2002). Oestrogen receptor-mediated effects of tamoxifen on human endometrial cancer cells. *Molecular and Cellular Endocrinology*, **192**, 93-104.

Santner S.J., Chen S., Zhou D., Korsunsky Z., Martel J. and Santen R.J. (1993). Effect of androstenedione on growth of untransfected and aromatase-transfected MCF-7 cells in culture. *Journal of Steroid Biochemistry and Molecular Biology*, **44**, 611-616.

- Satchi-Fainaro R., Puder M., Davies, J.W., Tran, H.T., Sampson, D.A., Greene, A., Corfas, G. and Folkman J. (2004). Targeting angiogenesis with a conjugate of HPMA copolymer and TNP-470. *Nature medicine*, **10**, 255-261.
- Satchi-Fainaro R., Duncan R. and Barnes C.M. (2005). Polymer therapeutics for cancer: Current status and future challenges. *Advances in Polymer Sciences*, **193**, 1-65.
- Schoemaker N.E., van Kesteren C., Rosing H., Jansen S., Swart M., Lieverst J., Fraier D., Breda M., Pellizzoni C., Spinelli R., Porro M.G., Beijnen J.H., Schellens J.H.M. and ten Bokkel Huinink W.W. (2002). A phase I pharmacokinetic study of MAG-CPT, a water-soluble polymer conjugate of camptothecin. *British Journal of Cancer*, **87**, 608-614.
- Scholzen T. and Gerdes J. (2000). The Ki-67 protein: from the known to the unknown. *Journal of Cellular Physiology*, **182**, 311-322.
- Schwarzenbach R.P., Stierli R., Folsom B.R. and Zeyer J. (1988). Compound properties relevant for assessing the environmental partitioning of nitrophenols. *Environmental Science and Technology*, **22**, 83-92.
- Searle F., Gac Breton S., Keane R., Dimitrijevic S., Brocchini S. and Duncan R. (2001). N-(2-hydroxypropyl)methacrylamide copolymer-6-(3-aminopropyl)-ellipticine conjugates synthesis characterisation preliminary in vitro and in vivo studies. *Bioconjugate Chemistry*, **12**, 711-718.
- Seib F.P. (2005). Endocytosis and trafficking of polymer therapeutics in melanoma cells. *PhD Thesis Cardiff University*.
- Seymour L.W. and Duncan R. (1987). Effect of molecular weight (Mw) of N-(2-hydroxypropyl) methacrylamide copolymers on body distribution and rate of excretion after subcutaneous, intraperitoneal and intravenous administration to rats. *Journal of Biomedical Materials Research*, **21**, 1341-1358.

- Seymour L.W., Ulbrich K., Steyger P.S., Brereton M., Subr V., Strohal J. and Duncan R. (1994). Tumour tropism and anti-cancer efficacy of polymer-based doxorubicin prodrugs in the treatment of subcutaneous murine B16F10 melanoma. *British Journal of Cancer*, **70**, 636-641.
- Seymour L.W., Ferry D., Anderson D., Julyan P., Poyner R., Doran J., Young A., Burtles S. and Kerr D. (2002). Hepatic drug targeting: phase I evaluation of polymer-bound doxorubicin. *Journal of Clinical Oncology*, **20**, 1668-1676.
- Sgouras D. and Duncan R. (1990). Methods for the evaluation of biocompatibility of soluble synthetic polymers which have potential for biomedical use: 1-Use of the tetrazolium-based colorimetric assay (MTT) as a preliminary screen for evaluation of in vitro cytotoxicity. *Journal of Materials Science: Materials in Medicine*, **1**, 61-68.
- Shenoy D.B. and Amiji M.M. (2005). Poly(ethylene oxide)-modified poly (ϵ -caprolactone) nanoparticles for targeted delivery of tamoxifen in breast cancer. *International Journal of Pharmaceutics*, **293**, 261-270.
- Shiah J.G., Sun Y., Kopeckova P., Peterson C.M., Straight R.C. and Kopecek J. (2001). Combination chemotherapy and photodynamic therapy of targetable N-(2-hydroxypropyl) methacrylamide copolymer-doxorubicin/mesochlorin e6 –OV-TL16 antibody immunoconjugates. *Journal of Controlled Release*, **74**, 249-253.
- Singer J.W., Schaffer S., Baker B., Bernareggi A., Stromatt S., Nienstedt D. and Besman M. (2005). Paclitaxel poliglumex (XYOTAX; CT-2103): an intracellularly targeted taxane. *Anti-Cancer Drugs*, **16**, 243-254.
- Sorkin A. (2000). The endocytosis machinery. *Journal of Cell Science*, **113**, 4375-4376.

Sun X., Yau V.K., Briggs B.J. and Whittaker G.R. (2005). Role of clathrin-mediated endocytosis during vesicular stomatitis virus entry into host cells. *Virology*, **338**, 53-60.

Swanson J.A. and Watts C. (1995). Macropinocytosis. *Trends in Cell Biology*, **5**, 424-427.

T

Thanou M. and Duncan R. (2003). Polymer-protein and polymer conjugates in cancer therapy. *Current Opinion in Investigational Drugs*, **4**, 701-709.

Thomenius M.J. and Distelhorst C.W. (2003). Bcl-2 on the endoplasmic reticulum: protecting the mitochondria from a distance. *Journal of Cell Science*, **116**, 4493-4499.

Tomlinson R. (2003). Degradable polyacetals for the development of polymer therapeutics. *PhD thesis University of London*.

Tritton T.R. and Yee G. (1982). The anticancer agent adriamycin can be actively cytotoxic without entering. *Science*, **217**, 248-250

Tritton T.R. (1991). Cell surface actions of adriamycin. *Pharmacology and Therapeutics*, **49**, 293-309.

Tulkens P. and Trouet A. (1978). The uptake and intracellular accumulation of aminoglycoside antibiotics in lysosomes of cultured rat fibroblasts. *Biochemical Pharmacology*, **27**, 415-424.

Turner K.J., Macpherson S., Millar M.R., McNeilly A.S., Williams K., Cranfield M., Groome N.P., Sharpe R.M., Fraser H.M. and Saunders P.T.K. (2002). Development and validation of a new monoclonal antibody to mammalian aromatase. *Journal of Endocrinology*, **172**, 21-30.

Twentyman P.R. and Luscombe M. (1987). A study of some variables in tetrazolium dye (MTT) based assay for cell growth and chemosensitivity. *British Journal of Cancer*, **56**, 279-285.

U

UCCCR. (2000). UKCCCR guidelines for the use of cell lines in cancer research. *British Journal of Cancer*, **82**, 1495-1509.

Uchegbu I.F, Ringsdorf H. and Duncan R. (1996). The lower critical solution temperature of doxorubicin polymer conjugates. *Proceedings of the International Symposium for Controlled Release of Bioactive Materials*, **23**, 791-792.

Ulbrich K., Varticovski L., Lu Z.R., Mitchell K., De Aos I. and Kopeček J. (2001). Water-soluble HPMA copolymer-wortmannin conjugate retains phosphoinositide 3-kinase inhibitory activity in vitro and in vivo. *Journal of Controlled Release*, **74**, 275-281.

V

Van Diest P.J., van der Wall E. and Baak J.P.A. (2004). Prognostic value of proliferation in invasive breast cancer: a review. *Journal of Clinical Pathology*, **57**, 675-681.

Varticovski L., Lu Z.R., Mitchell K., De Aos I. and Kopeček J. (2001). Water-soluble HPMA copolymer-wortmannin conjugate retains phosphoinositide 3-kinase inhibitory activity in vitro and in vivo. *Journal of Controlled Release*, **74**, 275-281.

Vasey, P.A., Kaye, S.B., Morrison, R., Twelves, C., Wilson, P., Duncan, R., Thomson, A.H., Murray, L.S., Hilditch, T.E., Murray, T., Burtles, S., Fraier, D., Frigerio, E., and Cassidy, J. (1999). Phase I clinical and pharmacokinetic study of PK1 [N-(2-hydroxypropyl)methacrylamide copolymer doxorubicin]:

first member of a new class of chemotherapeutic agents-drug-polymer conjugates. *Clinical Cancer Research*, **5**, 83-94.

Vergote I., Neven P., van Dam P., Serreyn R., De Prins F., De Sutter P. and Albertyn G. (2000). The oestrogen receptor and its selective modulators in gynaecological and breast cancer. *European Journal of Cancer*, **36**, S1-S9.

Veronese F.M., Schiavon O., Pasut G., Mendichi R., Andersson L., Tsirk A., Ford J., Wu G., Kneller S., Davies J. and Duncan R. (2005). PEG-doxorubicin conjugates: influence of polymer structure on drug release, in vitro cytotoxicity, biodistribution, and antitumor activity. *Bioconjugate Chemistry*, **16**, 775-784.

Vicent M.J., Tomlinson R., Brocchini S. and Duncan R. (2004). Polyacetal-diethylstilboestrol: a polymeric drug designed for pH-triggered activation. *Journal of Drug Targeting*, **12**, 491-501.

Vicent M.J., Greco F., Nicholson R.I., Paul A., Griffiths P.C. and Duncan R. (2005). Polymer therapeutics designed for a combination therapy of hormone-dependent cancer. *Angewandte Chemie International Edition*, **44**, 2-6.

Vicent M.J. and Duncan R. (2006). Polymer conjugates: nanosized medicines for treating cancer. *Trends in Biotechnology*, **24**, 39-47.

Vistica D.T., Skehan P., Scudiero D., Monks A., Pittman A. and Boyd M.R. (1991). Tetrazolium-based assays for cellular viability: a critical examination of selected parameters affecting formazan production. *Cancer Research*, **51**, 2515-2520.

W

Wan K.W., Malgesini B., Verpili I., Ferruti P., Griffiths P.C., Paul A., Hann A.C. and Duncan R. (2004). Poly(amidoamine) salt form: effect on pH-dependent

membrane activity and polymer conformation in solution. *Biomacromolecules*, **5**, 1102-1109.

Wedge S.R. (1991). Mechanism of action of polymer-anthracyclines: potential to overcome multidrug resistance. *PhD Thesis Keele University*.

Wedge S.R., Duncan R. and Kopeckova P. (1991). Comparison of the liver subcellular distribution of free daunomycin and that bound to galactosamine targeted N-(2-hydroxypropyl) methacrylamide copolymers following intravenous administration in the rat. *British Journal of Cancer*, **63**, 546-549.

Willsher P.C., Kenny F.S., Gee J.M.W., Nicholson R.I. and Robertson J.F.R. (2002). Biological changes in preliminary breast cancer during antiestrogen therapies. In *Endocrine Therapy of Breast Cancer*, Robertson J.F.R., Nicholson R.I. and Hayes D.F. (eds). Martin Dunitz: London. pp.209-231

Y

Yue W., Wang J., Savinov A. and Brodie A. (1995). Effects of aromatase inhibitors on growth of mammary tumors in a nude mouse model. *Cancer Research*, **55**, 3073-3077.

Yue W., Wang J. and Hamilton C. (1998). In situ aromatisation enhances breast tumour estradiol levels and cellular proliferation. *Cancer Research*, **58**, 927-932.

Yue W., Mor G., Naftolin F., Pauley R., Shim W.-S., Harvey H.A. and Santen R.J. (2002). Aromatase inhibitors in breast cancer. In *Endocrine Therapy of Breast Cancer*, Robertson J.F.R., Nicholson R.I. and Hayes D.F. (eds). Martin Dunitz: London. pp. 75-106.

Z

Zhou D., Pompon D. and Chen S. (1990). Stable expression of human aromatase complementary DNA in mammalian cells: a useful system for aromatase inhibitor screening. *Cancer Research*, **50**, 6949-6954.

Zuhorn I.S., Kalicharan R. and Hoekstra D. (2002). Lipoplex-mediated transfection of mammalian cells occurs through the cholesterol dependent clathrin mediated pathway of endocytosis. *Journal of Biological Chemistry*, **277**, 18021-18028.

Zunino F., Savi G., Giuliani F., Gambetta R., Supino R., Tinelli S and Pezzoni G. (1984). Comparison of antitumor effects of daunorubicin covalently linked to poly-L-amino acid carriers. *European Journal of Cancer and Clinical Oncology*, **20**, 421-425.

Websites

American Cancer Society

www.cancer.org

American Society of Clinical Oncology

www.asco.org

Cancer Research UK

www.cancerresearchuk.org

National Cancer Institute

www.cancer.gov

Appendix I

List of Publications

Review

- Duncan, R., Vicent M.J., Greco, F., Nicholson et al., (2005). Polymer-drug conjugates: towards a novel approach for the treatment of endocrine-related cancer. *Endocrine-Related Cancer*, **12**, S189-S199.

Primary Papers

- Vicent, M.J., Greco, F., Nicholson, R.I., Paul, A., Griffiths, P.C. & Duncan, R. (2005). Polymer Therapeutics Designed for a Combination Therapy of Hormone-Dependent Cancer. *Angewandte Chemie International Edition*, **44**, 2-6.
- Greco F., Vicent M.J., Penning N., Nicholson R.I. and Duncan R. (2005). HPMA copolymer-aminoglutethimide conjugates inhibit aromatase in MCF-7 cell lines. *Journal of Drug Targeting*, **13**, 459-470.
- Greco F., Vicent M.J., Gee S., Jones A., Gee J., Nicholson R.I. and Duncan R. (2006). Investigating the mechanism of action of HPMA copolymer conjugates carrying a combination of endocrine and chemotherapy. *Journal of Controlled Release*. (manuscript in preparation).
- Bettio F., Canevari M., Veronese F., Bordin F., Marzano C., Guiotto A., Greco F., Duncan R. (2006). Synthesis and biological evaluation of novel furocoumarin PEG conjugates. *Journal of Controlled Release*. (manuscript in preparation).

Abstracts

- M.J. Vicent, F. Greco, D. Barrow, R. Nicholson and R. Duncan (2003). Using Polymer Conjugates to Optimise Combination Therapy For Treatment Of Hormone-Dependent Cancer. *Proceedings of the International Symposium of Controlled Release of Bioactive Materials*, **30**, # 487.
- F. Greco, M.J. Vicent, D. Barrow, R. Nicholson and R. Duncan (2004). *In vitro* evaluation of HPMA copolymer-Dox –AGM conjugates. *Proceedings of 6th International Symposium on Polymer Therapeutics*, 77.

- **F. Greco**, M.J. Vicent, D. Barrow, R. Nicholson and R. Duncan (2004) Evaluation of HEMA copolymer-Dox-AGM conjugates in vitro: a novel polymer combination for the treatment of breast cancer. *Journal of Pharmacy and Pharmacology*, S-17.
- Duncan R., Vicent M.J., **Greco F.**, Nicholson R., Wan K., Paul, A., Griffiths, P., (2004). Polymer therapeutics as novel anticancer agents: current status and future prospects. *Proceedings 35th International Symposium Princess Takamatsu Cancer Research Fund*, 38-39.
- **Greco F.**, Vicent M.J., Nicholson R.I. and Duncan R. (2005). Mechanism of action of a novel polymer combination therapy for breast cancer. *Proceedings of the International Symposium of Controlled Release of Bioactive Materials*, **32**, 257.
- Duncan R., Vicent M.J., **Greco F.** and Nicholson R. (2005). Polymer therapeutics designed to treat breast and prostate cancer. *Proceedings of 229th American Chemical Society National meeting*, 54.

Appendix II

Drug Design

**Polymer Therapeutics Designed for a
Combination Therapy of Hormone-Dependent
Cancer****


María J. Vicent, Francesca Greco, Robert I. Nicholson,
Alison Paul, Peter C Griffiths, and Ruth Duncan**

Over the last decade, polymer therapeutics have emerged as first-generation nanomedicines.^[1] The term polymer therapeutics was coined to include water-soluble polymers that are polymeric drugs,^[2] hybrid polymer–drug^[1,3] and polymer–protein conjugates,^[4] polymeric micelles that contain covalently bound drugs.

[*] Dr. M. J. Vicent,* F. Greco, Prof. Dr. R. Duncan
Centre for Polymer Therapeutics
Welsh School of Pharmacy, Cardiff University
King Edward VII Avenue, Redwood Building, CF103XF Cardiff (UK)
Fax: (+44) 292-087-4536
E-mail: mjvicent@ochoa.fib.es
Prof. Dr. R. I. Nicholson
Tenovus Centre for Cancer Research
Welsh School of Pharmacy, Cardiff University
King Edward VII Avenue, Redwood Building, CF103XF Cardiff (UK)
Dr. A. Paul, Dr. P. C. Griffiths
School of Chemistry, Cardiff University
Cardiff CF103TB (UK)

[†] Present address:
Centro de Investigación Principe Felipe, FVIB
Medicinal Chemistry Unit
Av. Autopista del Saler 16, E-46013 Valencia (Spain)

[**] We thank the Marie Curie Individual Fellowship, Contract No. HPMF-CT-2002-01555 (M.J.V.), the Tenovus Research Centre, and the Centre for Polymer Therapeutics, Cardiff University (F.G.) for financial support. We also thank Richard K. Heenan and Stephen M. King from the ISIS facility, Rutherford Appleton Laboratories, Chilton, Didcot, Oxfordshire (UK) for their help in the SANS data interpretation and the CCLRC and EPSRC for allocation of neutron-beam time.

 Supporting information for this article is available on the WWW under <http://www.angewandte.org> or from the author.

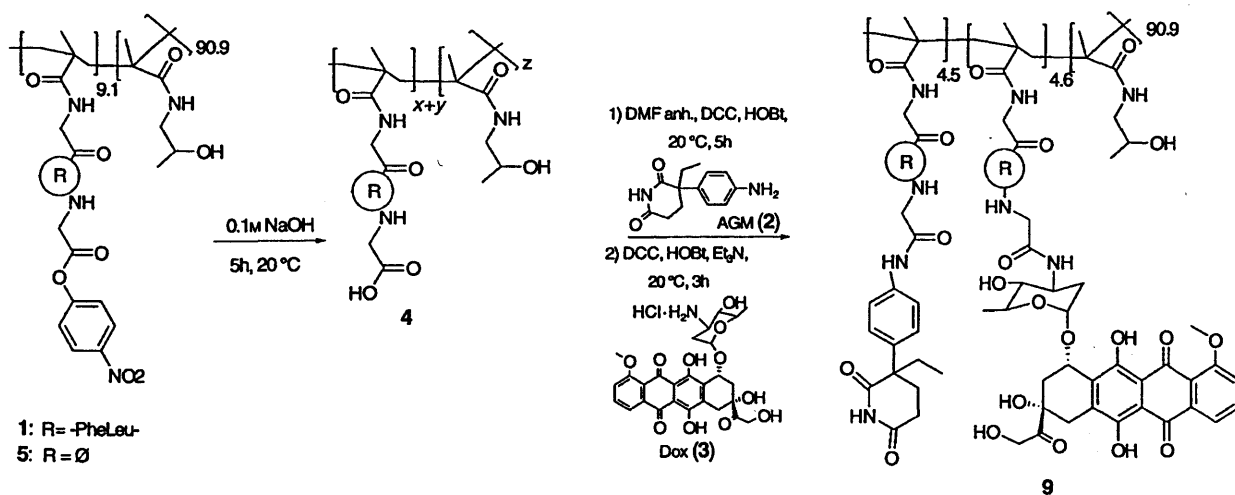
lently bound drug,^[5] and multicomponent polyplexes used as nonviral vectors^[6] to deliver genes and proteins into the cytosolic compartment of the cell. Of particular relevance to this study are those polymer–drug conjugates now finding acceptance as a new class of antitumor agents.^[1,3,6] Polymer conjugates have distinct advantages over conventional chemotherapy. These include 1) passive tumor targeting owing to the enhanced permeability and retention (EPR) effect, a phenomenon that arises from the hyperpermeability of angiogenic tumor blood vessels,^[7] 2) lower toxicity of bound drug,^[8] and 3) after cellular uptake by the endocytic route, the potential to bypass mechanisms of drug resistance, including p-glycoprotein-mediated multidrug resistance (MDR).^[9] So far, only conjugates derived from polyethyleneglycol (PEG),^[10] polyglutamic acid (PGA),^[11] polysaccharides,^[12] and *N*-(2-hydroxypropyl)methacrylamide (HPMA) copolymer conjugates^[13] have progressed to clinical trials. The HPMA copolymer–doxorubicin (Dox) conjugate PK1 (also named FCE28068) was the first synthetic polymer conjugate to enter Phase I trials in 1994.^[8] Since then, HPMA copolymer conjugates with established chemotherapy drugs (such as taxol, platinates, or camptothecins)^[6,13] and two gamma-camera imaging agents derived from HPMA copolymer have also progressed to clinical testing. Conjugates are now being synthesized to contain experimental drugs^[14] and drugs directed towards new therapeutic targets (e.g. antiangiogenic HPMA copolymer–TNP470^[15]). Further developments in this field include chemotherapy with two-step polymer–drug combinations (e.g. polymer-directed enzyme prodrug therapy (PDEPT)^[16]).

The aim of this study was to design a polymer conjugate that would for the first time combine endocrine therapy and chemotherapy with the hope of eliciting improved antitumor activity in breast cancer. Arrival of the selective oestrogen receptor antagonist tamoxifen led to a 28% reduction in mortality of breast cancer patients at 5 years.^[17] Even so, the prognosis for patients with metastatic breast cancer is still poor, the survival rate at 5 years being <20%. The mixed antagonist/agonist activity of tamoxifen and the acquired

resistance that can develop over time limit its therapeutic potential.^[18] To circumvent this problem, there has been growing interest in the use of aromatase inhibitors. They prevent estrogen biosynthesis by inhibiting P450 aromatase present in normal tissue and in breast-cancer cells of postmenopausal women (77% of the new cases of breast cancer diagnosed each year).^[19] Recent clinical trials in these patients showed that the aromatase inhibitors letrozole and anastrozole were more effective in treating estrogen receptor positive breast cancer than tamoxifen.^[20]

In our case, we hypothesized that the combination of endocrine therapy and chemotherapy by simultaneous attachment to the same polymer would bring significant advantages. The combination could be administered as a single dose; benefits would be the manufacture of a single conjugate and improved patient compliance. After EPR-mediated targeting, the arrival of both pendant drugs within the tumor cells at the same time is guaranteed. It also provides the opportunity to tailor polymer–drug linkers to impart different rates of drug release for each compound, thus allowing agents to act synergistically. As HPMA copolymer–Dox has already shown activity in chemotherapy refractory breast-cancer patients^[8] and this polymer has proven clinical safety, HPMA was chosen as the polymeric carrier (1 and 5), and the anthracycline antibiotic Dox (3) (widely used as a first-line treatment for breast cancer) was selected as the model chemotherapeutic. The first-generation aromatase inhibitor, aminoglutethimide (AGM; 2), was chosen as the endocrine model.

A library of conjugates 6–11 was synthesized to contain Dox, AGM, or both drugs attached to the same polymeric chain (Scheme 1, Table 1, Supporting Information). HPMA copolymer intermediates ($M_w \approx 20\,000$ – $25\,000\text{ gmol}^{-1}$; $M_w/M_n = 1.3$ – 1.5) were used that contained either the tetrapeptide linker Gly–Phe–Leu–Gly (known to be cleaved by lysosomal thiol-dependent protease cathepsin B to release Dox)^[6,13] or a Gly–Gly linker (known to be nondegradable and as such to provide a reference control for biological experiments). First, conjugates were prepared by aminolysis of polymeric intermediates in which the C-terminus of the



Scheme 1. Synthesis of HPMA copolymer-AGM-Dox conjugate (9) using DCC coupling reactions. DMF = *N,N*-dimethylformamide, DCC = 1,3-dicyclohexylcarbodiimide, HOBT = 1-hydroxybenzotriazole.

Table 1: Characteristics of the HPMA copolymer conjugates.

	Conjugate	Side-chain content [mol %]	Total drug [% w/w] ^[a]		Free drug [% total drug] ^[a]		Rg (± 0.3) [nm] ^[d]
			AGM	DOX	AGM	DOX	
6 ^[b]	HPMA copolymer–GFLG–AGM	5	6.2	–	0.75	–	ND
6 ^[c]	HPMA copolymer–GFLG–AGM	5	6.0	–	0.58	–	7.9
7 ^[b]	HPMA copolymer–GFLG–AGM	10	5.1	–	0.25	–	ND
7 ^[c]	HPMA copolymer–GFLG–AGM	10	10.4	–	0.59	–	16.5
8 ^[b]	HPMA copolymer–GG–AGM	5	3.4	–	1.17	–	ND
8 ^[c]	HPMA copolymer–GG–AGM	5	5.4	–	0.61	–	4.1
9 ^[b]	HPMA copolymer–GFLG–AGM–Dox	10	3.1	4.2	0.60	0.10	ND
9 ^[c]	HPMA copolymer–GFLG–AGM–Dox	10	5.4	7.2	0.73	0.23	12.8
10 ^[b]	HPMA copolymer–GFLG–Dox	5	–	6.6	–	0.39	7.7
11 ^[b]	HPMA copolymer–GFLG–Dox	10	–	14.1	–	0.78	12.4

[a] Total drug and free drug content determined by HPLC. Free drug content expressed as a percentage of total drug. [b] Conjugates synthesized by aminolysis (see supporting information). [c] Conjugates synthesized by DCC coupling (see Supporting Information). [d] Determined by SANS. Fit to a Gaussian coil with Schultz polydispersity. Polydispersity considered 1.3 in all cases. ND = not determined.

peptide side-chains were esterified with *p*-nitrophenol.^[21] The lower reactivity of the aromatic amine of AGM, however, favored the use of DCC-mediated coupling. The improved yield of conjugation was particularly noticeable when AGM was bound to the polymeric precursor containing pendant side chains (10 mol %) (Table 1). FTIR and NMR spectroscopy confirmed the identity of the product, and NOE measurements verified the covalent binding of AGM (see Supporting Information). These observations were consistent with previous NOESY and TOCSY experiments, which established the structure of HPMA copolymer–Dox.^[22]

Accurate characterization of the bioactive content of any polymer–drug conjugate destined for biological or clinical testing is essential. It is well known that the extinction coefficient of a bound drug can change significantly upon conjugation.^[23] In this instance, measurement of the total and free Dox was straightforward, and a validated HPLC method was used.^[24] For example, the Dox content of conjugate **9** was 7.2% w/w (free Dox < 0.8% w/w total drug) (Table 1). The AGM content was more difficult to determine. Values were obtained either by UV/Vis spectroscopy with an *N*-Gly-AGM (**13**) derivative as standard or by an indirect HPLC method established to quantify residual AGM left after reaction (Table 1 and Supporting Information). Overall, the AGM content of the conjugates was in the range 3.1–10.4% w/w (free AGM content < 1.2% w/w total AGM) and in conjugate **9** it was 5.4% w/w (Table 1). The molecular weight of the conjugates was in the range $M_w \approx 25\,000$ – $30\,000\text{ g mol}^{-1}$.

It has been postulated that polymer–drug conjugates exist in solution as unimolecular micelles and that conformation is influenced by drug loading. At present, however, there is almost no direct physical evidence to support this hypothesis.^[25] We have recently demonstrated the value of small-angle neutron scattering (SANS) in providing insight into the solution conformation of polymer therapeutics, particularly in relation to the pH-triggered conformational change of endosomolytic polymers.^[26] SANS was used in this case for the first time to define conjugate structure in solution (Table 1 and Supporting Information). The Gaussian coil model for polymer conformation showed the best fit to the raw

scattering data. Whereas HPMA copolymer–GFLG–Dox (**10**) and HPMA copolymer–GFLG–AGM (5 mol %) (**6**) conjugates prepared from the same polymeric intermediate had similar Rg (radius of gyration) values (7.7 and 7.9 nm, respectively; truly nano-sized medicines), an increase in the side-chain content to 10 mol % led to an increase in Rg to 16.5 nm for the AGM conjugate **7**, but only to 12.5 nm for the Dox conjugate (**11**). Interestingly the HPMA copolymer–GFLG–AGM–Dox conjugate **9** also displayed an Rg value of 12.8 nm. This might be explained by the tendency of Dox to display π – π stacking, thus leading to the formation of more-compact unimolecular micelles. It is clear that polymer–drug conjugate conformation is affected by both the drug loading and chemical nature of the drug.

Effective functioning of polymer–drug conjugates relies on 1) the stability of the polymer–drug linker in the circulatory system and, after arrival in the tumor tissue and cellular uptake by endocytosis, 2) lysosomal enzyme cleavage of the linker to release the active drug. All the HPMA copolymer conjugates were completely stable in buffer alone, as was the HPMA copolymer–GG–AGM (**8**) in the presence of isolated rat liver lysosomal enzymes (Figure 1c and Supporting Information). However, in the presence of lysosomal enzymes, Dox and AGM were released from conjugates containing the Gly–Phe–Leu–Gly linker. The drug-release profile displayed marked differences depending on conjugate composition. For conjugates **10** and **11**, Dox release began immediately after addition of enzyme (Figure 1b) and was linear with time; it was apparent that the lower the Dox loading (cf. **10** and **11**) the greater the drug release after 5 h (see Supporting Information). This is in agreement with the solution conformation predicted by SANS (Table 1). Enzyme accessibility would be limited by a more compact coil structure. AGM release (conjugates **6** and **7**) also showed dependence on drug loading with a lower initial release for the highest loading (**7**) (Figure 1a). After 30 min, however, AGM liberation from **7** accelerated and release from **6** started to plateau (see supplementary information for comparison at 5 h).

When incubated with lysosomal enzymes, the conjugate containing both AGM and Dox as the combination (**9**)

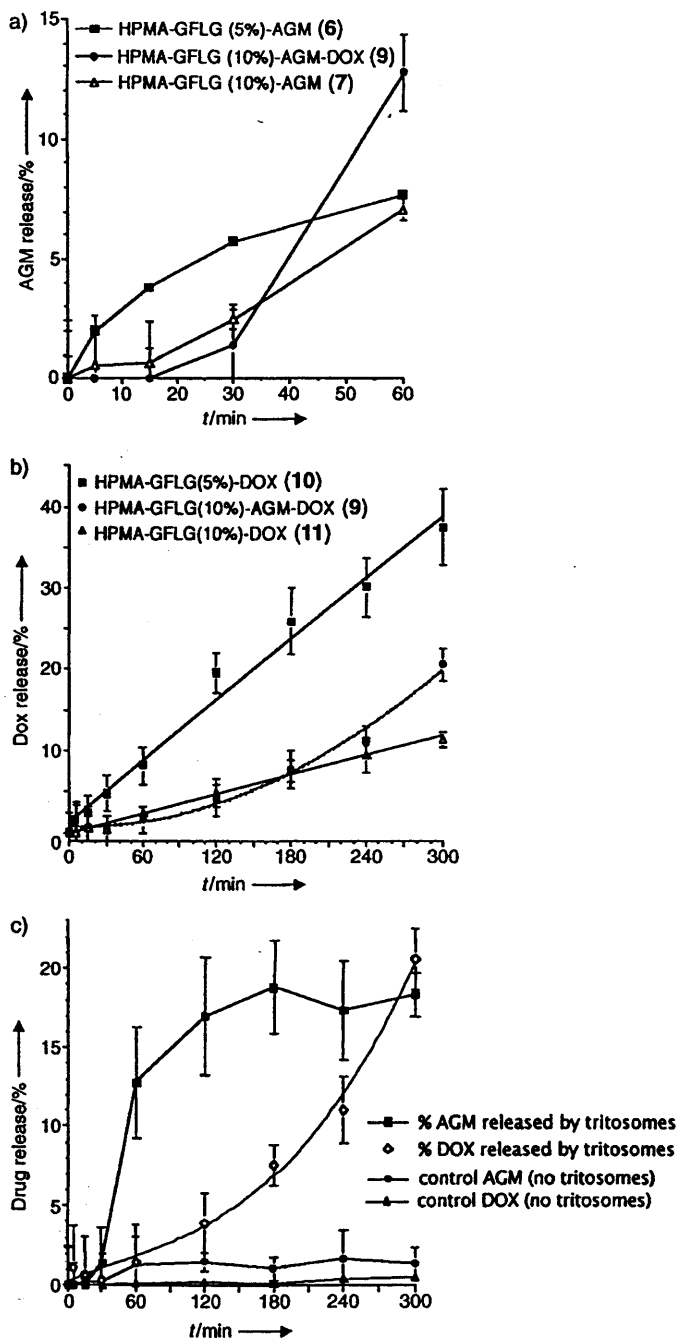


Figure 1. Liberation of Dox or AGM from HPMA copolymer conjugates during incubation with rat liver lysosomal enzymes (tritosomes). Release of a) AGM, b) Dox, and c) Dox and AGM from the HPMA copolymer-GFLG-AGM-DOX conjugate (9). In all cases, drug release is expressed as a percentage of the total drug bound, and data represent the mean \pm SEM ($n=4$). In specific cases, the release of drug in the absence of enzymes (control) is also shown.

displayed different profiles of drug liberation (Figure 1c) in comparison with that seen for the single-drug-pendant conjugates (at both 5 and 10 mol % loading). Both Dox and AGM release show a marked lag phase with little release over the first 30 min. However, after this time, AGM release was enhanced relative to 6 and 7, and the Dox release rate was

initially slower but then returned to that seen for 10. The dynamic and complex geometry of this unimolecular micelle structure determines enzyme access leading to these complex release kinetics. To investigate how the release profile would translate into cytotoxicity, a human estrogen-dependent breast-cancer cell line MCF-7 and the aromatase-transfected derivative MCF-7ca were used (Figure 2 and Supporting Information). As expected, as a result of its slow rate of cellular uptake by endocytosis and the relatively prolonged duration needed for drug liberation, HPMA copolymer-GFLG-DOX (10) was much less active than free Dox (3). For example, their IC_{50} values against the MCF-7 cell line were $>150 \mu\text{M}$ and $0.74 \mu\text{M}$ Dox-equivalents, respectively. Neither the HPMA copolymer-GFLG-AGM (6), nor individual mixtures of drug conjugates bearing AGM (6) or Dox (10) caused an elevation in cytotoxicity in either cell line MCF-7 or MCF-7ca (see Supporting Information).

In contrast, when AGM and DOX were covalently linked to the same polymeric backbone, that is, in conjugate 9, the *in vitro* cytotoxicity was significantly greater than seen for 10, 3, or 6 against MCF-7 cells. The enhanced cytotoxicity of 9 was even more evident for the aromatase expressing MCF-7ca cells (see Figure 2 and Supporting Information). The IC_{50} values obtained for MCF-7ca cells incubated with 3, 6, or 9 were $5238 \mu\text{M}$, $>1377 \mu\text{M}$, and $40.9 \mu\text{M}$ AGM-equivalents, respectively. Conjugate 9 displayed approximately tenfold enhancement in cytotoxicity in the aromatase cell line, irrespective of whether the data are expressed in terms of Dox- or AGM-equivalents. Although it is necessary to understand the precise molecular mechanism of action of these novel conjugates better, it has been reported that aromatase inhibitors can also promote apoptosis, so they may potentiate Dox cytotoxicity in this way.^[19]

To conclude, the HPMA copolymer-GFLG-AGM-DOX conjugate (9) is the first polymer therapeutic to combine chemotherapy and endocrine therapy. The fact that AGM and Dox can act synergistically to produce markedly enhanced cytotoxicity *in vitro* relative to that of the HPMA copolymer-GFLG-DOX conjugate (10) (PK1), which has already shown activity in breast-cancer patients clinically, underlines the potential importance of this polymer-drug combination. It should be emphasized that mixtures of polymer conjugates containing only AGM or only Dox did not show synergistic benefit. The studies reported confirm cellular uptake of conjugate by endocytosis (verified by flow cytometry as shown in Figure 2b and in the Supporting Information), and also demonstrate the requirement of lysosomal thiol-dependent protease degradation of the polymer-drug linker to liberate drug and thus promote cytotoxicity. All the components (HPMA copolymers, Dox and AGM) are well established clinically, so further preclinical studies are warranted to establish the antitumor potential of this novel anticancer strategy *in vivo*. The observation that HPMA copolymer conjugates displayed lower hemolytic activity (10% release at 1 h; $p < 0.001$) than Dox (3) (92% hemoglobin release at 1 h) (see Supporting Information) establishes the suitability for intravenous administration. Tailoring of the linker structure and drug loading within this novel nano-sized medicine (Rg in solution of 12.8 nm) may further optimize the drug-release

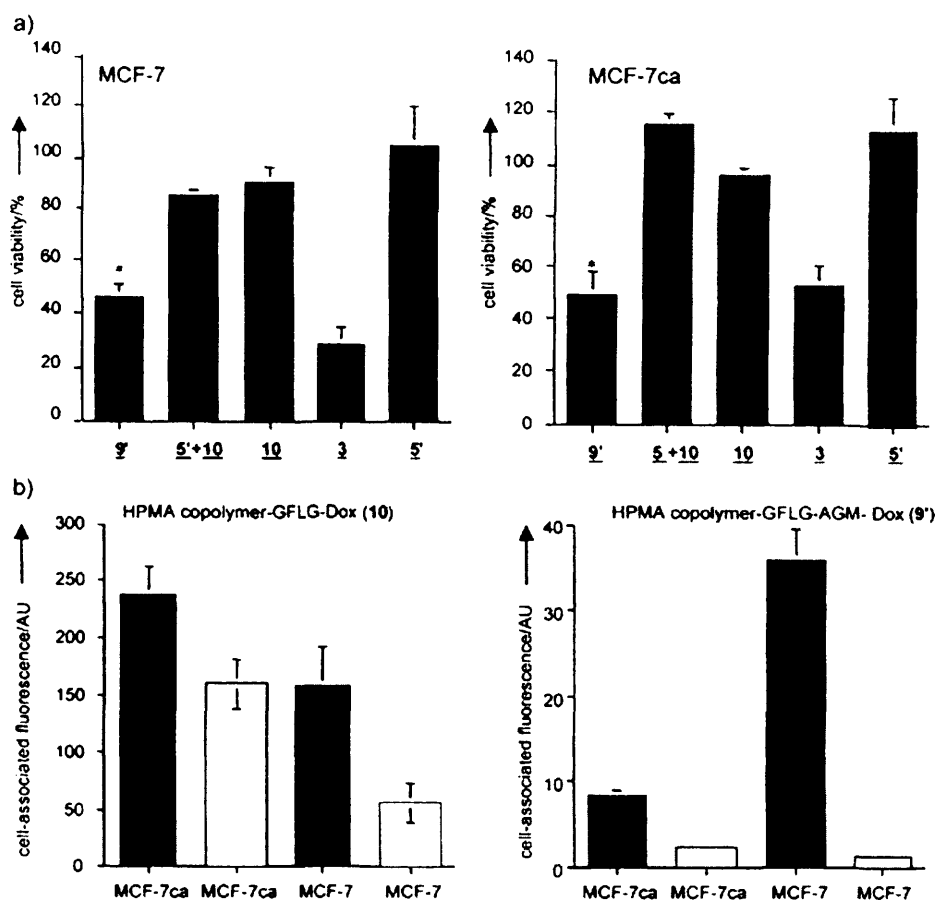


Figure 2. a) Cytotoxicity of Dox and HPMA copolymer conjugates against MCF-7 and MCF-7ca cell lines at the IC_{50} value (0.08 mg mL^{-1} and 0.009 mg mL^{-1} Dox-equivalents, respectively) in the presence of 10^{-9} M estradiol. Measured by MTT assay after 72 h incubation. Data are expressed as mean \pm SEM ($n=3$). The asterisk* indicates statistical significance ($P < 0.05$). b) Cell-associated fluorescence at 37°C (total association, ■) and 4°C (external binding, □) of PK1 and HPMA copolymer-AGM-Dox conjugate in MCF-7 and MCF-7ca cells after 1 h. Data are expressed as mean \pm SEM ($n=6$).

profile and cytotoxicity. Ongoing studies to define the precise molecular mechanisms of conjugate action will be used to steer the choice of chemistry used to achieve optimal release kinetics.

Received: December 16, 2004

Revised: March 15, 2005

Published online: May 24, 2005

Keywords: antitumor agents · drug delivery · drug design · polymers · tumor targeting

[1] R. Duncan, *Nat. Rev. Drug Discovery* **2003**, *2*, 347–360.

[2] W. H. Mandeville, D. I. Goldberg, *Curr. Pharm. Des.* **1997**, *3*, 15–28.

[3] a) H. Ringsdorf, *J. Polym. Sci. Polym. Symp.* **1975**, *51*, 35–53;

b) R. Duncan, J. Kopecek, *Adv. Polym. Sci.* **1984**, *57*, 51–101.

[4] J. M. Harris, R. B. Chess, *Nat. Rev. Drug Discovery* **2003**, *2*, 214–221.

[5] a) M. Yokoyama, M. Miyauchi, N. Yamada, T. Okano, Y. Sakurai, K. Kataoka, S. Inoue, *J. Controlled Release* **1990**, *11*, 269–278; b) Y. Bae, S. Fukushima, A. Harada, K. Kataoka,

Angew. Chem. **2003**, *115*, 4788–4791; *Angew. Chem. Int. Ed.* **2003**, *42*, 4641–4643.

[6] a) R. Duncan, *Handbook of Anticancer Drug Development* (Eds.: D. Budman, H. Calvert, E. Rowinsky), Lippincott Williams & Wilkins, Baltimore, **2003**, pp. 239–260; b) J. W. Singer, B. Baker, P. de Vries, A. Kumar, S. Shaffer, E. Vawter, *Adv. Exp. Med. Biol.* **2003**, *519*, 81–99; c) J. W. Singer, B. Baker, P. de Vries, A. Kumar, S. Shaffer, E. Vawter, M. Bolton, P. Garzone, *Polymer Drugs in the Clinical Stage, Advantages and Prospects* (Eds.: H. Maeda, A. Kabanov, K. Kataoka, T. Okano), Kluwer/Plenum, New York, **2003**, pp. 81–95.

[7] a) Y. Matsamura, H. Maeda, *Cancer Res.* **1986**, *46*, 6387–6392; b) L. W. Seymour, K. Ulbrich, P. S. Steyger, M. Brenton, V. Subr, J. Strohal, R. Duncan, *Br. J. Cancer* **1994**, *70*, 636–641; c) F. M. Muggia, *Clin. Cancer Res.* **1999**, *5*, 7–8; d) H. Maeda, J. Wu, T. Sawa, Y. Matsumura, K. Hori, *J. Controlled Release* **2000**, *65*, 271–284.

[8] P. A. Vasey, S. B. Kaye, R. Morrison, C. Twelves, P. Wilson, R. Duncan, A. H. Thomson, L. S. Murray, T. E. Hilditch, T. Murray, S. Burtles, D. Fraier, E. Frigerio, J. Cassidy, *Clin. Cancer Res.* **1999**, *5*, 83–94.

[9] T. Minko, P. Kopeckova, V. Pozharov, J. Kopecek, *J. Controlled Release* **1998**, *54*, 223–233.

[10] R. B. Greenwald, Y. H. Chloe, McGuire, C. D. Conover, *Adv. Drug Delivery Rev.* **2003**, *55*, 217–250.

[11] C. Li, D-F. Yu, R. A. Newman, F. Cabral, C. Stephens, N. R. Hunter, L. Milas, S. Wallace, *Cancer Res.* **1998**, *58*, 2404–2409.

[12] D. Hreczuk-Hirst, D. Chicco, L. German, R. Duncan, *Int. J. Pharm.* **2001**, *230*, 57–66.

[13] R. Duncan in *Polymeric Drug Delivery Systems* (Ed.: G. S. Kwon), Marcel Dekker, New York, **2005**, pp. 1–92.

[14] a) F. Searle, S. Gac-Breton, R. Keane, S. Dimitrijevic, S. Brocchini, R. Duncan, *Bioconjugate Chem.* **2001**, *12*, 711–718; b) Y. Kasuya, Z-R. Lu, P. Kopeckova, S. E. Tabiji, J. Kopecek, *Pharm. Res.* **2002**, *19*, 115–123; c) L. Varticovski, Z. R. Lu, K. Mitchell, I. De Aos, J. Kopecek, *J. Controlled Release* **2001**, *74*, 275–281; d) M. J. Vicent, S. Manzanaro, J. A. De la Fuente, R. Duncan, *J. Drug Targeting* **2004**, *12*, 503–515.

[15] R. Satchi-Fainaro, M. Puder, J. W. Davies, H. T. Tran, D. A. Sampson, A. K. Greene, G. Corfas, J. Folkman, *Nat. Med.* **2004**, *10*, 225–261.

[16] a) R. Satchi-Fainaro, T. A. Connors, R. Duncan, *Br. J. Cancer* **2001**, *85*, 1070–1076; b) R. Satchi-Fainaro, H. Hailu, J. W. Davies, C. Summerford, R. Duncan, *Bioconjugate Chem.* **2003**, *14*, 797–804.

[17] V. C. Jordan, *Nat. Rev. Drug Discovery* **2003**, *2*, 206–213; Early Breast Cancer Trialist Group: *Lancet* **1998**, *351*, 1451–1467.

- [18] a) M. P. Coleman, *Breast Cancer Res.* **1999**, *1*, 22–26; b) F. Cummings, *Clin. Ther.* **2002**, *24*, Suppl. C: C3–25.
- [19] S. R. D. Johnston, M. Dowsett, *Nat. Rev. Cancer* **2003**, *3*, 821–831.
- [20] P. E. Goss, K. Strasser, *Drugs* **2002**, *62*, 957–966.
- [21] a) P. Rejmanova, J. Labsky, J. Kopeček, *Makromol. Chem.* **1977**, *178*, 2159–2168; b) J. Kopeček, P. Rejmavova, J. Strohalm, K. Ulbrich, B. Rihova, V. Chytrý, R. Duncan, J. B. Lloyd, British Patent Appl. 8500209 (4.1.85), **1985**.
- [22] V. Pincioli, V. Rizzo, F. Angelucci, M. Tato, A. Vigevani, *Magn. Reson. Chem.* **1997**, *35*, 2–8.
- [23] E. Configliacchi, G. Razzano, V. Rizzo, A. Vigevani, *J. Pharm. Biomed. Anal.* **1996**, *15*, 123–129.
- [24] L. W. Seymour, K. Ulbrich, S. R. Wedge, I. C. Hume, J. Strohalm, R. Duncan, *Br. J. Cancer* **1991**, *63*, 859–866.
- [25] R. Mendichi, V. Rizzo, M. Gigli, A. G. Schieronì, *Bioconjugate Chem.* **2002**, *13*, 1253–1258.
- [26] K.-W. Wan, B. Malgesini, I. Verpili, P. Ferruti, P. C. Griffiths, A. Paul, A. C. Hann, R. Duncan, *Biomacromolecules* **2004**, *5*, 1102–1109.

HPMA copolymer–aminoglutethimide conjugates inhibit aromatase in MCF-7 cell lines

FRANCESCA GRECO^{1,2,†}, MARÍA J. VICENT³, NEAL A. PENNING¹,
ROBERT I. NICHOLSON², & RUTH DUNCAN¹

¹Centre for Polymer Therapeutics, Welsh School of Pharmacy, Redwood Building, Cardiff University, King Edward VII Avenue, Cardiff CF10 3XF, UK, ²Tenovus Centre for Cancer Research, Welsh School of Pharmacy, Redwood Building, Cardiff University, King Edward VII Avenue, Cardiff CF10 3XF, UK, and ³Centro de Investigación Príncipe Felipe-FVIB, Av. Autopista del Saler 16, E-46013 Valencia, Spain

Abstract

N-(2-Hydroxypropyl)methacrylamide (HPMA) copolymer–doxorubicin (Dox) has already shown clinical activity in breast cancer patients. Moreover, we have recently found that an HPMA conjugate containing a combination of both Dox and the aromatase inhibitor aminoglutethimide (AGM) shows significantly increased anti-tumour activity *in vitro*[†]. To better understand the mechanism of action of HPMA copolymer–AGM conjugates several models were used here to investigate their effect on cell growth and aromatase inhibition. Cytotoxicity of HPMA copolymer conjugates containing AGM, Dox and also the combination AGM–Dox was determined by MTT assay in MCF-7 and MCF-7ca cells. Androstenedione (5×10^{-8} M) stimulates the growth of MCF-7ca cells. Both free AGM and polymer-bound AGM (0.2–0.4 mg/ml) were shown to block this mitogenic activity. When MCF-7ca cells were incubated [³H]androstenedione both AGM and HPMA copolymer–GFLG–AGM (0.2 mg/ml AGM-equiv.) showed the ability to inhibit aromatase. Although, free AGM was able to inhibit isolated human placental microsomal aromatase in a concentration dependent manner, polymer-bound AGM was not, suggesting that drug release is essential for activity of the conjugate. HPMA copolymer conjugates containing aromatase inhibitors have potential for the treatment of hormone-dependant cancers, and it would be particularly interesting to explore further as potential therapies in post-menopausal women as components of combination therapy.

Keywords: Breast cancer, aromatase inhibitors, HPMA copolymer–drug conjugates, polymer therapeutics

Introduction

The use of polymer anticancer-drug conjugates to deliver cytotoxic drugs more selectively to tumour tissue is becoming well established (Duncan 2003a,b). All conjugates in clinical development carry well-known cytotoxic drugs including doxorubicin (Dox) (Vasey et al. 1999), platinates (Rademaker-Lakhai et al. 2004; Rice and Howell 2004) and paclitaxel (Singer et al. 2005). Polymer conjugation provides the advantages of: (i) passive targeting of the tumour tissue due to the hyperpermeability of tumour vasculature

(Matsumura and Maeda 1986; Seymour et al. 1994); (ii) decreased drug toxicity (Duncan et al. 1992; Vasey et al. 1999) and (iii) the ability to bypass some resistance mechanisms e.g. P-gp mediated-resistance (Minko et al. 1998; Vasey et al. 1999). However, use of polymeric carriers to deliver endocrine therapy is largely unexplored. Like other solid tumours, the hormone-dependent cancers, including breast and prostate cancer, are treated by surgical removal, radiotherapy and chemotherapy. In this case hormone therapy is also widely used as first line therapy, or in both neoadjuvant

Correspondence: R. Duncan, Centre for Polymer Therapeutics, Welsh School of Pharmacy, Redwood Building, Cardiff University, King Edward VII Avenue, Cardiff CF10 3XF, UK. Tel: 44 2920874180. Fax: 44 2920874536. E-mail: duncanr@cf.ac.uk

[†]It should be noted that the synthesis of this compound and its preliminary biological evaluation was recently described in: Vicent MJ, Greco F, Nicholson RI, Paul A, Griffiths PC, Duncan R, 2005. Polymer Therapeutics Designed for a Combination Therapy of Hormone-Dependent Cancer. *Angewandte Chemie International Edition* 44: 2–6.

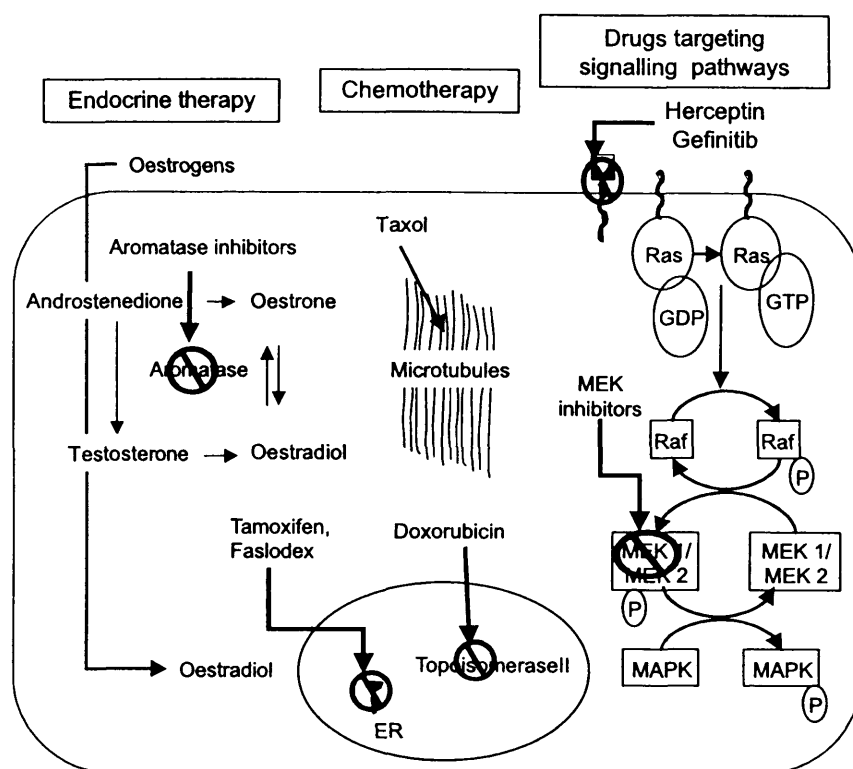


Figure 1. Schematic representation of current treatments for breast cancer and their mechanisms of action.

and adjuvant settings (Hayes and Robertson 2002, Figure 1).

Introduction of the selective oestrogen receptor modulator (SERM) tamoxifen led to a 28% reduction in mortality of breast cancer patients at 5 years (Jordan 2003). Nevertheless its mixed antagonist/agonist effect, the development of acquired resistance, and side effects including increased risk of endometrial cancer limit the therapeutic potential of tamoxifen. Consequently, the prognosis for metastatic breast cancer patients is still poor with <20% survival at 5 years (Jordan 2003). For this reason there has been renewed interest in the use of inhibitors, which block the p450 enzyme aromatase, and thus the pathway responsible for the biosynthesis of oestrogens (Johnston and Dowsett 2003). Recent clinical trials showed that the aromatase inhibitor anastrozole was superior to tamoxifen in terms of efficacy, time to recurrence and had less side effects (ATAC Trialists Group 2005).

N-(2-Hydroxypropyl)methacrylamide (HPMA) copolymers have already been used to prepare six anticancer drug conjugates that have progressed into clinical development (Duncan 2003b, 2005). In Phase I trials (Vasey et al. 1999), HPMA copolymer–Dox (PK1, FCE 28068) displayed a 5-fold reduced clinical toxicity (maximum tolerated dose (MTD) = 320 mg/m² Dox equiv.) compared to free Dox (MTD ~ 80 mg/m²), and anticancer activity in chemotherapy-resistant breast

cancer patients. Thus HPMA copolymers were used to prepare a combination of endocrine therapy, in the form of the aromatase inhibitor aminoglutethimide (AGM), and chemotherapy Dox. This recently described conjugate (Vicent et al. 2005) was the first polymer-bound endocrine therapy. Moreover, the HPMA copolymer–Dox–AGM conjugate displayed remarkably enhanced cytotoxicity in MCF-7 (a breast cancer cell line), and MCF-7ca (an aromatase transfected cell line) compared to FCE28068, the conjugate that has already shown clinical activity. The reasons for this behaviour are not yet understood.

The aim of this study was to investigate the mechanism of action of HPMA copolymer–GFLG–AGM. Several different approaches were used. First, MCF-7 and MCF-7ca were grown in the presence of androstenedione and testosterone. These compounds enhance aromatase-mediated cell growth and thus the model can be used to investigate aromatase inhibition by free and polymer-bound AGM. To obtain a direct measure of cell-associated aromatase inhibition, MCF-7 and MCF-7ca cells were incubated with the aromatase substrate [³H]androstenedione in the presence and absence of free and bound AGM. Finally, to explore the possibility that polymer-bound AGM could inhibit aromatase directly, experiments were conducted with isolated human placental aromatase *in vitro*.

Materials and methods

Materials

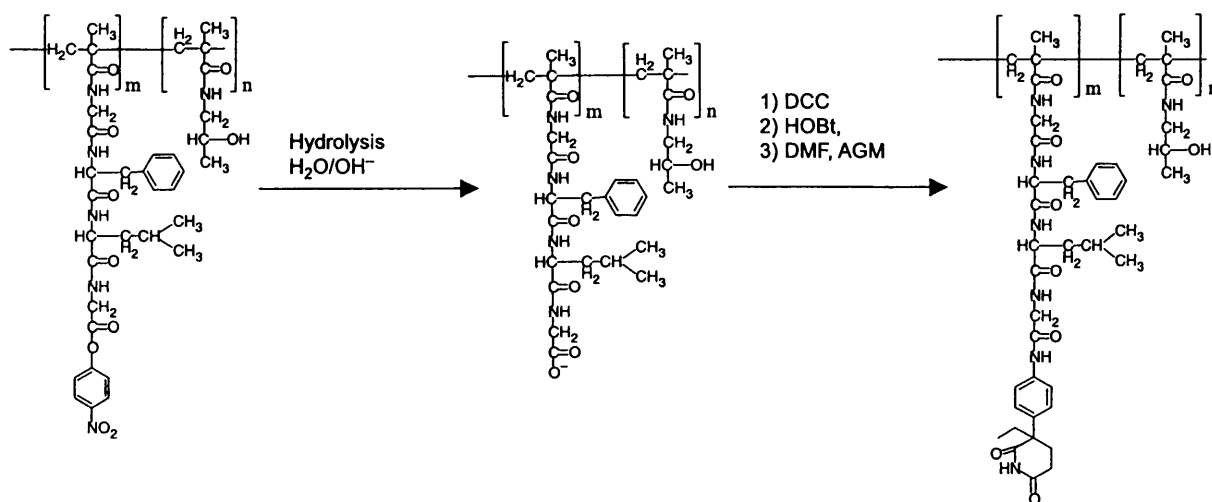
Synthesis and characterisation. HPMA copolymer-GFLG-(5 mol%)-ONp ($M_w \sim 25,000$ g/mol) was supplied by Polymer Laboratories Inc. (UK). Anhydrous dimethylformamide (DMF), 1,3-dicyclohexylcarbodiimide (DCC), 1-hydroxybenzotriazol (OHBT), AGM and sodium hydroxide pellets were supplied by Sigma-Aldrich (UK). Dox hydrochloride and HPMA copolymer-GFLG-Dox were kindly donated by Pharmacia (Italy). Sephadex™ LH20 was supplied by Amersham Biosciences AB (Sweden). HPLC grade dichloromethane, diethyl ether, acetone, MeOH and isopropanol were from Fisher Scientific (UK).

Biological assays. 3-(4,5-Dimethylthiazol-2-yl)-2,5-diphenyl-2H-tetrazoliumbromide (MTT), NADPH, optical grade DMSO were from Sigma (UK). Oestradiol, androstenedione and testosterone, were also from Sigma (UK), and they were dissolved in absolute EtOH at a concentration of 10^{-2} M and stored at -20°C . Before experiments, solutions in culture medium were prepared starting from the ethanolic stock solutions. Foetal calf serum (FCS), RPMI 1640, with L-glutamine and RPMI 1640 without phenol red, with L-glutamine were from Gibco BRL Life Technologies (UK). Geneticin (G418) solution (50 mg/ml) was from Invitrogen (UK). [1,2,6,7- ^3H]androst-4-ene-3,17dione ([^3H]androstenedione) was supplied by Amersham Biosciences (UK). Formic acid was purchased from Aldrich (UK). Liquid scintillation cocktail, OptiPhase 'HiSafe' 3 was from Perkin Elmer (UK). Mercuric chloride was purchased from BDH Chemicals (UK).

Synthesis and characterisation of HPMA copolymer-GFLG-AGM

Synthesis. HPMA copolymer-GFLG-AGM conjugates were synthesised as described in Vicent et al. (2005) and the procedure is shown in Scheme 1. Briefly, HPMA copolymer-GFLG(5 mol%)-ONp (150 mg, 0.044 mmol ONp groups) was dissolved in double distilled water (ddH₂O) (~ 5 ml) and a 0.1 M NaOH solution (1.32 ml) was added. The reaction was allowed to proceed for 4 h at RT and monitored by measuring ONp displacement by UV spectroscopy at 400 nm. The reaction mixture was then purified by dialysis against water for approximately 2 days (membrane: M_w cut-off ~ 2000) and freeze dried, to obtain a white solid (yield $\sim 85\%$). HPMA copolymer-GFLG (5 mol%)-COOH (150 mg; 0.046 mmol in respect of the -COOH) was dissolved in anhydrous DMF (1 ml), under nitrogen atmosphere, then DCC (19 mg, 0.092 mmol) was added as a solid. After 10 min OHBT (12.5 mg, 0.092 mmol) was added, also as a solid, and the reaction was allowed to proceed for 30 min. AGM (10.7 mg, 0.046 mmol) was dissolved in a minimal amount of anhydrous DMF and added to the reaction mixture. The reaction was allowed to proceed under a nitrogen atmosphere for approximately 5 h and was monitored by TLC (mobile phase CHCl₃-MeOH 95:5 (v/v); R_f free AGM 0.53, R_f conjugate 0).

The precipitated urea was filtered-off, and DMF was partially evaporated under reduced pressure. The product was first purified by precipitation in a mixture of acetone: ether (4:1 (v/v); ~ 250 ml). To further purify the product was dissolved in methanol (~ 0.5 ml) and applied to a Sephadex LH20 column (5×50 cm, eluent MeOH). The purified compound was then dissolved in a minimal amount of water and freeze-dried. The overall yields based on polymer



Scheme 1. Synthesis of HPMA copolymer-GFLG-AGM conjugate.

weight were 70–80%. The filtration residues and also the impure fractions from the chromatographic column were kept and evaporated in order to analyse the total content of AGM in conjugates by indirect analysis, described below.

Determination of total AGM content by HPLC. The dried residue obtained from the conjugation reactions was dissolved in HPLC grade CH_2Cl_2 and all remaining precipitate was filtered off. AGM is completely soluble in CH_2Cl_2 . The solvent was evaporated under reduced pressure and MeOH (5 ml) was added to make the stock solution. Aliquots ($3 \times 100 \mu\text{l}$) were placed into polypropylene tubes, the pH of the samples was adjusted to 8.5 with ammonium formate buffer (100 μl , 1 M, pH 8.5) and Dnm was added as internal reference standard (100 μl of a 1 $\mu\text{g}/\text{ml}$ stock aqueous solution), then the volume was made up to 1 ml with ddH₂O. A mixture of chloroform–propan-2-ol at a ratio of 4:1 (5 ml) was added. Samples were then thoroughly extracted by vortexing ($3 \times 10 \text{ s}$). The upper aqueous layer was carefully removed and the organic phase was evaporated under N₂. The dry residue was dissolved in 100 μl of HPLC grade methanol.

In parallel, the same procedure was carried out for the free AGM (using 100 μl of a 1 mg/ml stock aqueous solution). Addition of 1 ml of methanol to re-dissolve the product gave a 100 $\mu\text{g}/\text{ml}$ stock from which a range of concentrations were prepared (2–60 $\mu\text{g}/\text{ml}$). AGM was quantified by HPLC using a Bondapak C18 (150 \times 3.9 mm) column. Flow rate 1 ml/min and a gradient elution was used (solvent A: isopropanol–H₂O 12:88 (v/v), solvent B: isopropanol–H₂O 29:71 (v/v) adjusted to at pH 3.2 with *o*-phosphoric acid. Total run time was 20 min and the gradient profile was: $t = 5 \text{ min A } 100\%$, $t = 9 \text{ min A } 0\%$, $t = 14 \text{ min A } 0\%$, $t = 16 \text{ min A } 50\%$, $t = 18 \text{ min A } 100\%$ and $t = 20 \text{ min A } 100\%$). The retention time was equal to 5.18 min for AGM. To monitor AGM an UV detector (Spectroflow 783 Kratos analytical) with a fixed-wavelength filter (254 nm) was used and a Fluoromonitor III fitted with interference filters at 485 nm for excitation and 560 nm for emission was used to monitor the Dnm standard.

Determination of free AGM content by HPLC. Aqueous solutions of HPMA copolymer–AGM conjugates (1 mg/ml) were prepared. Aliquots ($3 \times 100 \mu\text{l}$) were then taken and extracted as described above. The AGM content was assessed by HPLC as previously described for total AGM content.

Preparation of SFCS. Five hundred millilitres of FCS was adjusted to a pH of 4.2 adding HCl 5 M and equilibrated to a temperature of 4°C. A charcoal

solution was prepared adding 18 ml of ddH₂O, 0.2 g of Norit A charcoal and 0.01 g of dextran T-70. Twenty-five millilitres of the charcoal solution were added to the acidic FCS and the suspension was stirred for 16 h at 4°C. Then, the suspension was centrifuged (40 min at 12,000g) and coarsely filtrated with celite to remove the charcoal. The pH was adjusted to 7.2 with NaOH 5 M, the suspension was filtered with millipore filters 0.2 μm and stored in appropriate containers at -20°C

Cytotoxicity of HPMA copolymer conjugates

Cytotoxicity was evaluated using the MTT assay (72 h incubation) against MCF-7 and MCF-7ca cells as described by Sgouras and Duncan (1990) with modifications. The protocol for this experiment is shown in Figure 2a. Cells were seeded in sterile 96-well microtitre plates at a seeding density 4×10^4 cells/ml in WRPMI 1640 with 5.0 mM L-glutamine and 5% (v/v) charcoal-stripped (steroid-depleted) foetal calf serum plus additional geneticin (1 mM) in MCF-7ca cell line. After 24 h the medium was replaced by media with or without oestradiol (10^{-9} M), and the plates were then incubated for 4 days. On day 5, compounds (0.2 μm filter sterilised) were added at the given concentrations. After 67 h of incubation (day 8), MTT (20 μl of a sterile-filtered 5 mg/ml solution in PBS) was added to each well, and the cells were incubated for a further 5 h. After removal of the medium, the precipitated formazan crystals were dissolved in optical grade DMSO (100 μl , 30 min at 37°C), and the plates were read spectrophotometrically at 550 nm using a microtitre plate reader. Cell viability was expressed as a percentage of the viability of untreated control cells.

Effect of AGM and HPMA copolymer–AGM on the growth of MCF-7 and MCF-7ca cells in the presence of androstenedione

The protocol for this experiment is shown in Figure 2b. To establish the assay, MCF-7 and MCF-7ca were seeded in 96-well plates ($\sim 4 \times 10^4$ cells/ml). As phenol red is mitogenic in these cell-lines (Devleeschouwer et al. 1992), RPMI phenol red-free (WRPMI) supplemented with 5% of charcoal-stripped FCS was used. After 24 h the medium was removed, then replaced with fresh medium containing androstenedione (10^{-11} – 10^{-6} M) or testosterone (10^{-11} – 10^{-4} M). The final concentration of EtOH in all the samples was 0.01%. The medium was also changed on day 4 and 8. The number of cells present was estimated at day 11 using an MTT-assay (Sgouras and Duncan 1990). Briefly, 20 μl of sterile-filtered MTT solution (5 mg/ml in PBS) were added to each well. After 5 h the medium was removed and the blue-formazan crystals were dissolved in 100 μl of DMSO per well. Absorbance at 550 nm was read on a

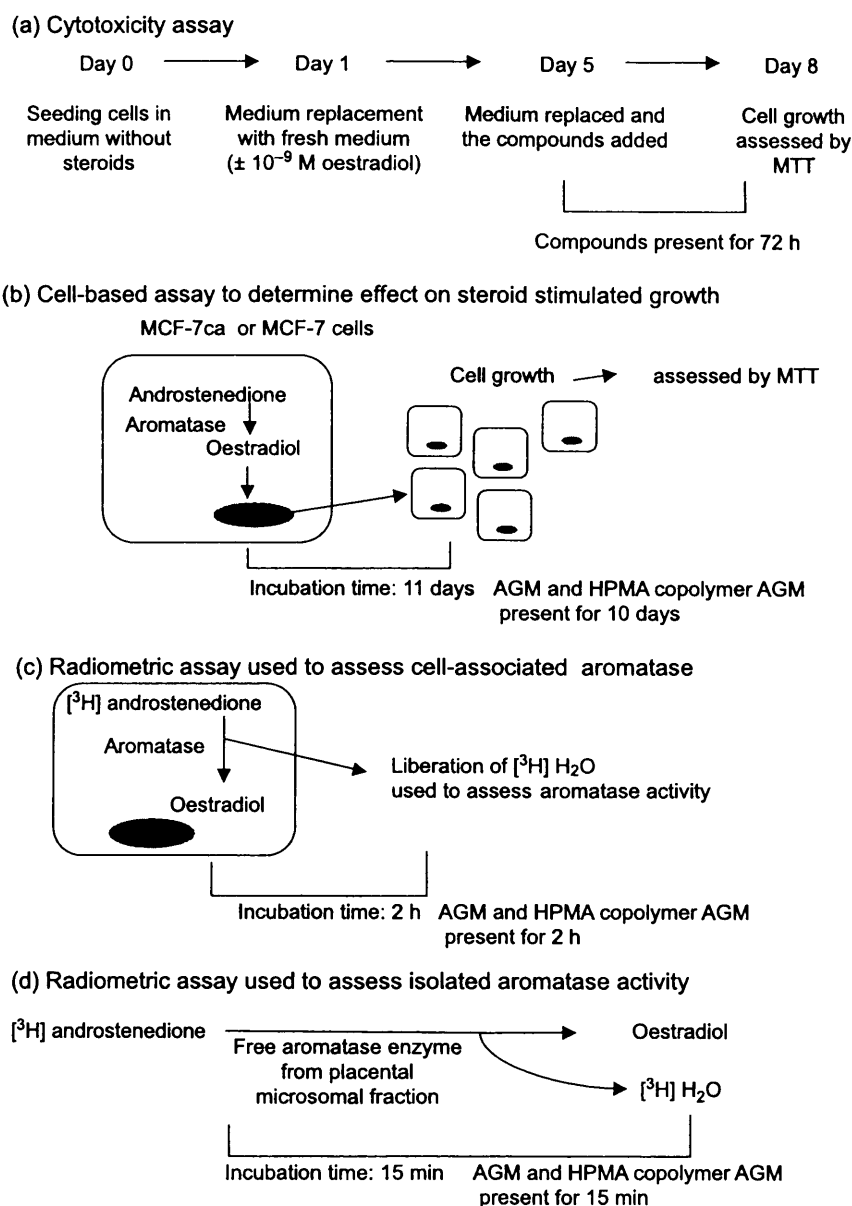


Figure 2. Schematic representation of the *in vitro* methods used showing the duration of exposure of the compounds to: Panels (a–c) MCF-7 or MCF-7ca cells and panel (d) enzyme.

microtiter plate reader. Both androstenedione and testosterone stimulated cell growth, but androstenedione had a more pronounced effect over a broader range of concentration. Therefore, MCF-7ca cells exposed to androstenedione (5×10^{-8} M) were chosen as the best model to explore further aromatase inhibition. MCF-7ca cells were seeded in 96-well plates as described above. After 24 h the medium was removed and replaced with medium containing androstenedione (5×10^{-8} M) and the test compounds; AGM (0.8, 0.4, 0.2, 0.1 mg/ml), or HPMA copolymer-GFLG-AGM (0.8, 0.4, 0.2 mg/ml AGM-equiv.). Medium containing 0.01% EtOH (\pm androstenedione) were used as controls. The medium was changed on days 4 and 8 and cell

numbers were measured at day 11 using the MTT assay as described above.

Effect of AGM and HPMA copolymer-AGM on aromatase activity assessed using $[^3\text{H}]$ androstenedione

The method of Long et al. (2002) was adapted for this experiment and the protocol is shown in Figure 2c. MCF-7 and MCF-7ca were cultured in steroid-free medium for 3 days prior to the beginning of the experiment. The $[^3\text{H}]$ androstenedione solution was prepared as follows; 50 μl of 0.5 mM androstenedione in EtOH was diluted to 1 ml with isopropanol-EtOH (1:1 v/v) to give 0.025 mM stock solution. To 1 ml of this solution 35 μl of $[^3\text{H}]$ androstenedione (1 mCi/ml)

were added, leading to the working solution. Both cell lines were seeded in 6-well plates ($\sim 3 \times 10^5$ cells/ml) in WRPMI supplemented with 5% of charcoal-stripped serum and left to attach for 24 h. Then, cells were incubated with fresh medium containing [^3H]androstenedione (15 μl of the working solution; 0.5 μCi) and free AGM or HPMA copolymer-AGM conjugate for 2 h. The medium was collected in a glass tube and formic acid (300 μl) was added. Excess [^3H]androstenedione was first removed by extraction into chloroform (2 ml) with thorough mixing. The aqueous phase (1 ml) was transferred to another glass tube and aqueous charcoal suspension (1%; 1 ml) was then added before thoroughly vortexing again. This mixture was centrifuged for 15 min at 1638g. The aromatase activity in test samples, and in MCF-7 cells (used as a control) was expressed as a percentage of the activity of the MCF-7ca cells incubated with [^3H]androstenedione in the absence of inhibitors. After centrifugation 1 ml of the supernatant was added to scintillation vials containing 4 ml of liquid scintillation cocktail and thoroughly vortexed. The [^3H]H₂O content was quantified using a β counter.

Evaluation of aromatase activity using isolated human placental microsomes

The protocol is outlined in Figure 2d. Frozen human placental microsomes were thawed under cold running water and kept on ice until use. An aliquot (10 μl) of the working solution of [^3H]androstenedione (described in the previous paragraph) was placed in a glass tube and phosphate buffer (400 μl) was added. Then, an ethanolic solution containing AGM (just ethanol for the control) was also added (10 μl). Finally, the enzyme (30 μl) and NADPH solution in PBS (50 μl , 0.16 mmol/L) were added to start the reaction and the incubation was carried out in a shaking water bath at 37°C. For practical reasons, the polymer was dissolved directly in the phosphate buffer (10 μl of EtOH were added for consistency with the free AGM sample). The reaction was terminated after 15 min by addition of a solution of mercuric chloride (0.1 mM, 300 μl). Activated charcoal (1%) was added to each tube to remove excess [^3H]androstenedione, and it was separated by centrifugation (as described above) to leave [^3H]H₂O in the supernatant. An aliquot (1 ml) of the supernatant was processed for β counting as described above and the enzyme activity determined by measuring the liberation of the [^3H]H₂O. Results are expressed as a percentage of the control, i.e. aromatase activity without addition of inhibitor.

Statistical analysis

Statistical significance was estimated using ANOVA single factor followed by Bonferroni *post hoc* test. The α value was set at 0.05.

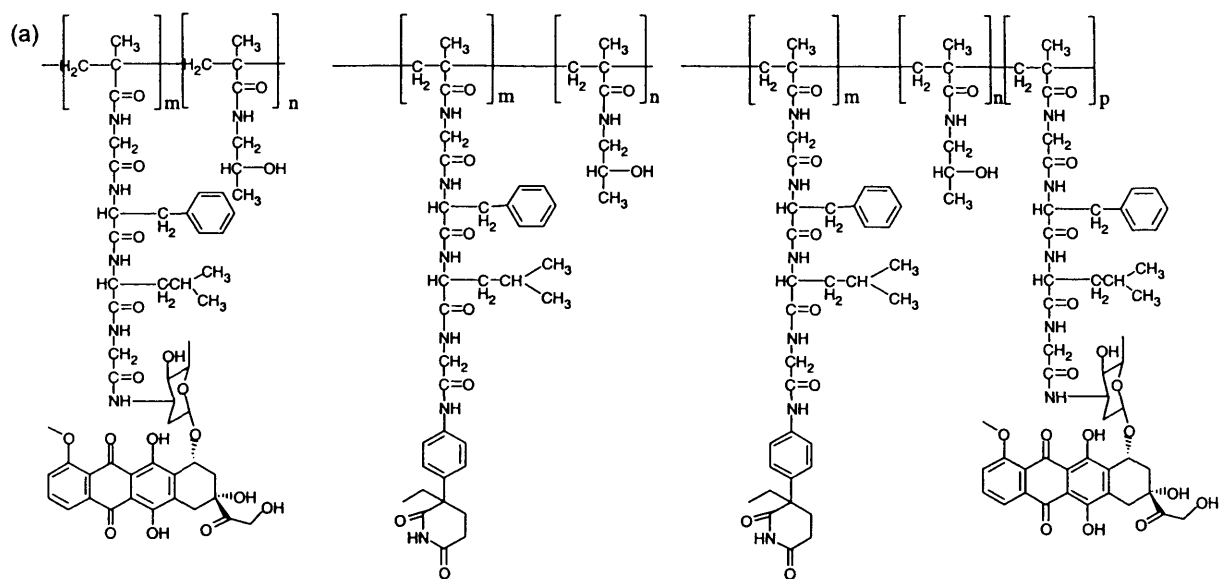
Results

A series of HPMA copolymer-AGM conjugates were synthesised (Figure 3). Three batches of HPMA copolymer-GFLG-AGM were prepared and the synthesis showed good batch-to-batch reproducibility. The total and free drug content in the conjugate was carefully determined by HPLC (Figure 3b). The total AGM loading was ~ 6 wt%, and the free AGM content was always < 1.2 (% total drug bound). One-dimensional nuclear Overhauser effect (NOE) $^1\text{H-NMR}$ spectroscopy confirmed covalent linkage of AGM to the polymer (Figure 3c). Experiments investigating the cytotoxicity of conjugates in MCF-7 and MCF-7ca cells both in the presence and the absence of oestradiol showed that HPMA copolymer-AGM was not cytotoxic. Even when HPMA copolymer-AGM was added as a combination with HPMA copolymer-Dox little toxicity was observed. In contrast, addition of a polymer bearing both AGM and Dox caused greater cytotoxicity which in the case of MCF-7ca cells was equivalent to that observed for free Dox. The cytotoxicity of this conjugate was observed in both the presence and absence of oestradiol (Figure 4).

To establish a cell-based model cell growth was purposely stimulated by addition of the aromatase substrates testosterone and androstenedione. Testosterone showed mitogenic activity in MCF-7ca cells at a concentration of 10^{-6} – 10^{-7} M, while lower concentrations had no effect. Neither testosterone (data not shown) nor androstenedione had an effect on the growth of MCF-7 cells (Figure 5a). Androstenedione also had a mitogenic effect on MCF-7ca cells, but this was more marked than what seen for testosterone and occurred across a broader range of concentrations (10^{-8} – 10^{-6} M). Therefore, an androstenedione concentration of 5×10^{-8} M was chosen for further experiments. A time-dependant study showed that growth stimulation was only seen after day 8, and began to plateau at day 11 (Figure 5d). Therefore, MCF-7ca cells and an incubation time of 11 days were selected for further studies.

Addition of AGM to the MCF-7ca cells incubated in the presence of androstenedione showed concentration-dependant reduction in growth (Figure 6a), and at 0.2 mg/ml AGM completely inhibited the androstenedione-mediated growth stimulation. Similarly, HPMA copolymer-GFLG-AGM caused concentration-dependant growth inhibition (Figure 6b). At higher concentrations, both free and polymer-bound AGM decreased cell viability to a level that was lower than seen for the controls with or without androstenedione (Figure 6).

When the MCF-7ca aromatase activity was further investigated using a radiometric assay, free AGM (Figure 7a) decreased enzyme activity to give a maximum inhibition of ($\sim 25\%$) and HPMA copolymer-AGM showed similar results at 0.2–0.4 mg/ml AGM-equiv. However, surprisingly at the highest

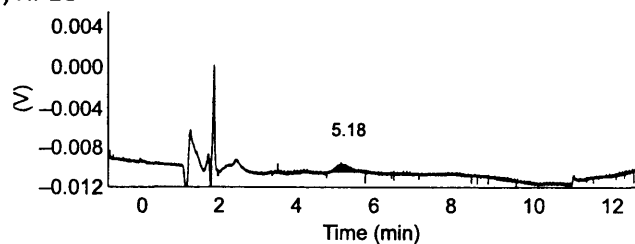


Sample	batch	total AGM*	free AGM#	total Dox*	free Dox#
HPMA GFLG AGM	1	6.0	0.6	N/A	N/A
HPMA GFLG AGM	2	6.4	1.2	N/A	N/A
HPMA GFLG AGM	3	5.9	0.2	N/A	N/A
HPMA GFLG Dox		N/A	N/A	6.6	0.4
HPMA GFLG Dox AGM		5.4	0.7	7.2	0.2

* expressed as % w/w

free drug content expressed as percentage of total drug

(b) HPLC



(c) NOE

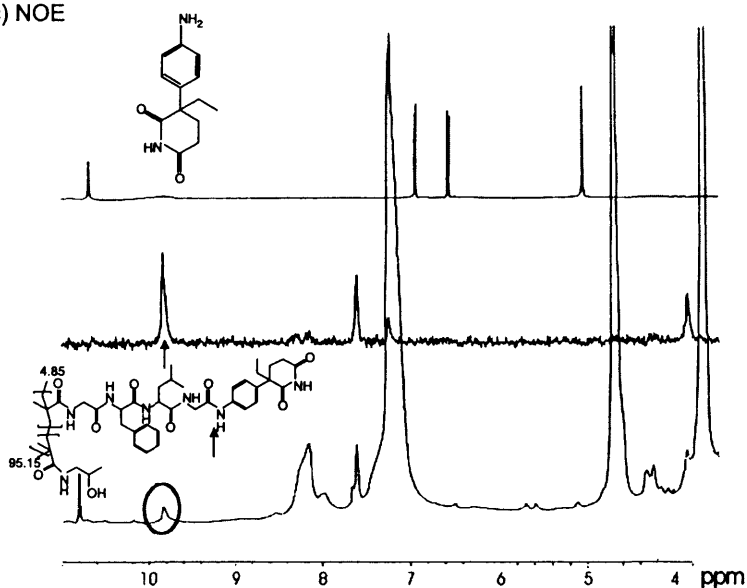


Figure 3. Structures and characteristics of the HPMA copolymer conjugates studied. Panel (a) shows the structure and drug content; panel (b) shows a typical HPLC chromatogram of free AGM after extraction from HPMA copolymer-GFLG-AGM conjugate; and panel (c) the NOE spectrum of HPMA copolymer-GFLG-AGM.

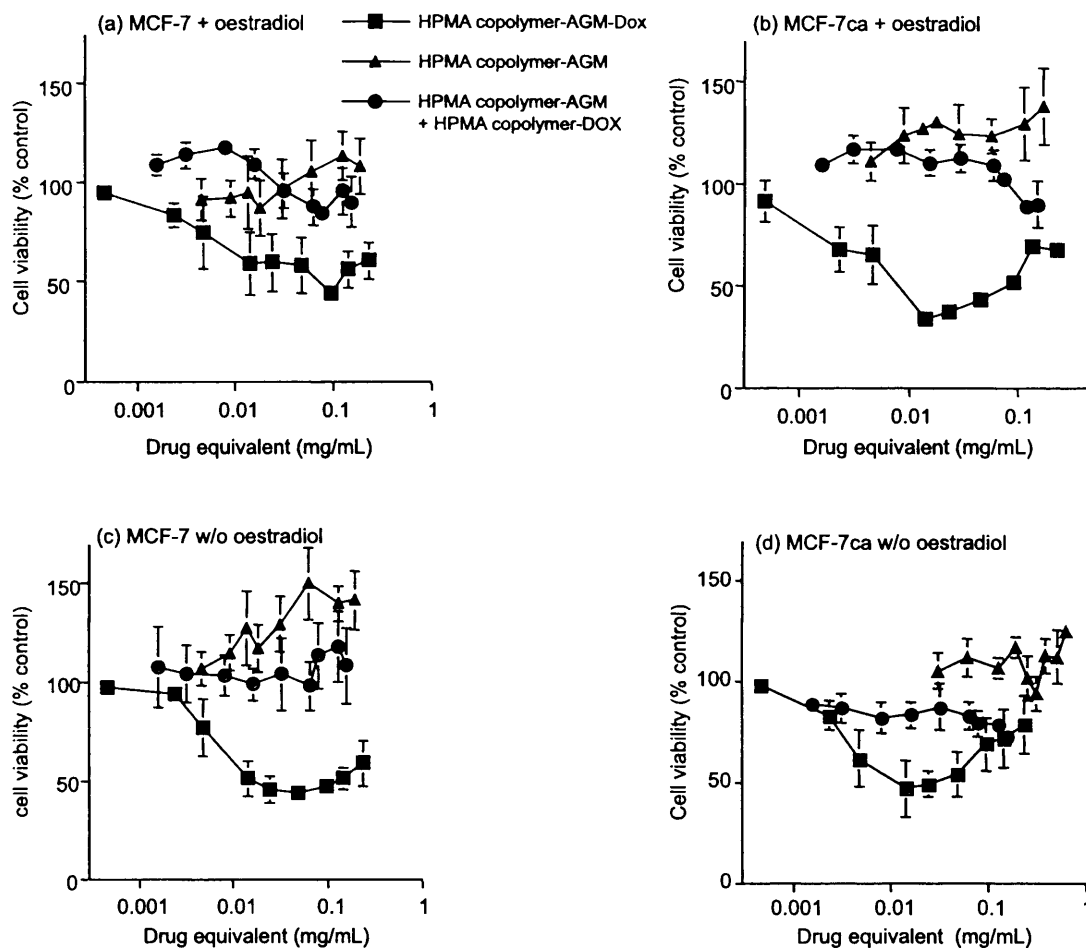


Figure 4. *In vitro* cytotoxicity of HPMA copolymer conjugates in MCF-7 and MCF-7ca cells in the presence and absence of oestradiol. Panel (a) MCF-7 with oestradiol; panel (b) MCF-7ca with oestradiol; and panel (c) MCF-7 without addition and panel (d) MCF-7ca without addition. Data shown represent mean \pm SEM; where $n = 3$.

HPMA copolymer-AGM concentrations (0.8 mg/ml AGM-equiv.) aromatase inhibition was lost. Interestingly, the maximum inhibition caused by AGM and HPMA-AGM was equivalent to the baseline activity seen in MCF-7 cells. Whilst, free AGM inhibited isolated microsomal aromatase in a dose-dependent manner (Figure 8a), the HPMA copolymer-AGM conjugate did not. Indeed no inhibition occurred even at 10-fold higher concentration used for free AGM (Figure 8b).

Discussion

Aromatase inhibitors such as anastrozole and letrozole are becoming a preferred treatment for certain breast cancers. These agents are usually taken orally and sometimes over relatively long periods. Thus the rationale for synthesis polymer conjugates proposed here requires some justification. Perceived disadvantages would be the fact that macromolecular conjugates require intravenous administration,

aromatase inhibitors are relatively non-cytotoxic, and oestrogen production can occur at many sites throughout the body. However, two important observations suggest the design of the HPMA copolymer-bound aromatase inhibitor conjugates will be worthwhile (Vicent et al. 2005). First, there is evidence that local production of oestrogens in the breast tumour tissue, particularly in post-menopausal women, plays an important role in tumour growth (Goss and Strasser 2002). This suggests that tumour targeting by the EPR effect should be beneficial. Furthermore, aromatase inhibitors are also able to induce apoptosis, and they can potentiate the anti-tumour effects of chemotherapy (Johnston and Dowsett 2003). Therefore, here it was hoped to build on past experience HPMA copolymer conjugates containing a lysosomally degradable -GFLG-linker and Dox which have already shown activity clinically in breast cancer patients (Duncan 2005; Greco et al. 2005). Whilst aminolysis of HPMA copolymer-ONp intermediates is routinely used for

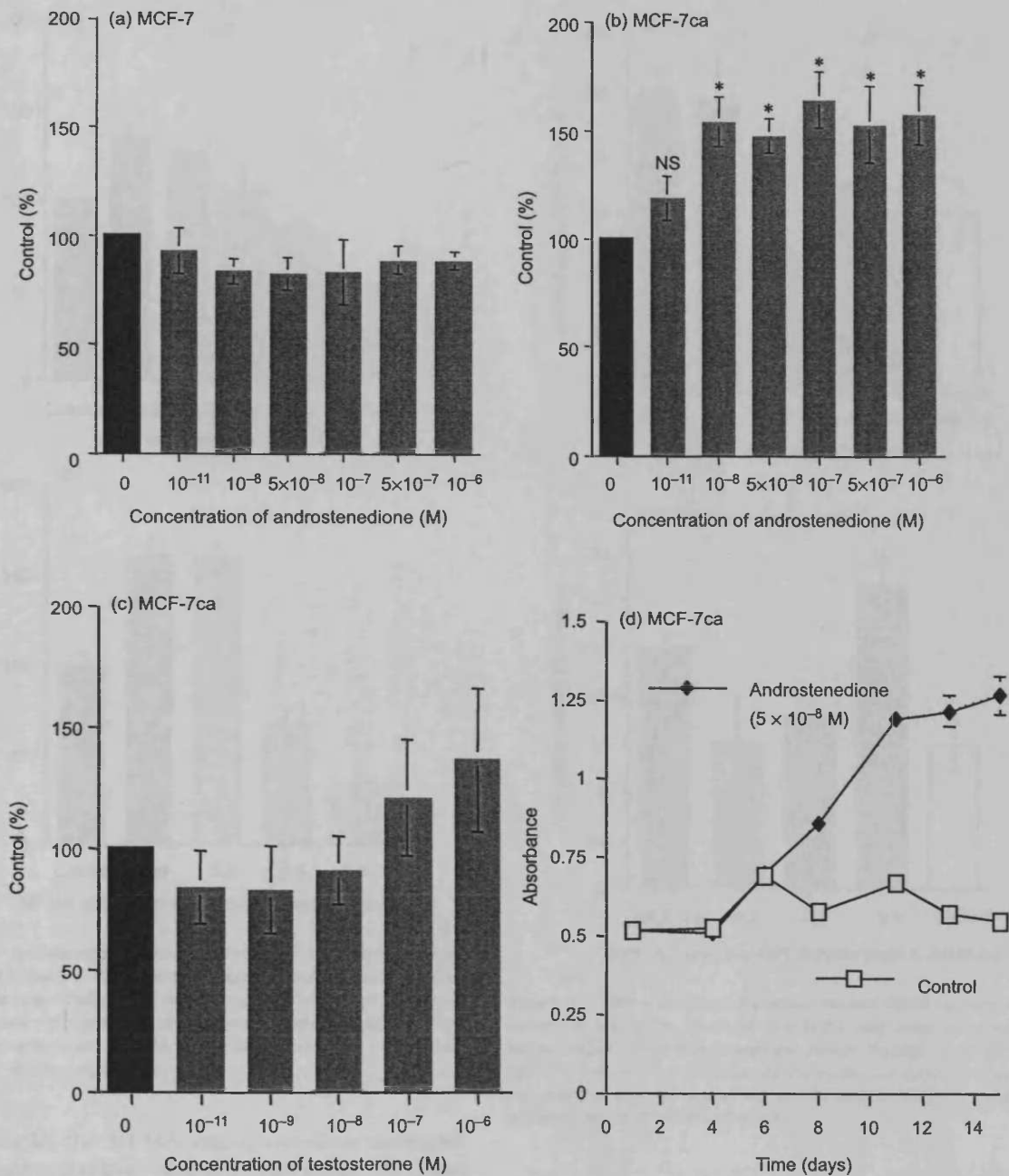


Figure 5. Effect of testosterone and androstenedione on MCF-7 and MCF-7ca cell growth. In panels (a-c) the growth of cells in the presence of these steroids (at the concentrations shown) was measured on day 11 using the MTT assay. The results are expressed as percentage of the control with no addition. For panel (d) cell growth was measured every 2-3 days until day 15 using the MTT assay. The values represent mean \pm SEM; $n = 3$ (at least).

drug conjugation (Rejmanova et al. 1977; Duncan et al. 1988; Searle et al. 2001), here the DCC-mediated coupling gave improved AGM loading (~ 6 wt%). Aminolysis is poorly efficient in this case (~ 3 wt% AGM) due to the lower reactivity of the aromatic amine (Vicent et al. 2005).

Use of *in vitro* cell based assays to compare the activity of polymer conjugates containing potent chemotherapy and free drug is not helpful as the screening system for

in vivo candidate selection. This is due to the profoundly different cellular pharmacokinetics of the low molecular weight and macromolecular compounds (Duncan et al. 1992, 2003b). Drugs such as Dox and AGM rapidly enter all cells by passive diffusion, hence their poor tumour selectivity. In contrast, macromolecular conjugates are internalised via the endocytic pathways at a much slower rate, and subsequent drug liberation (i.e. conjugate activation) can take hours or days.

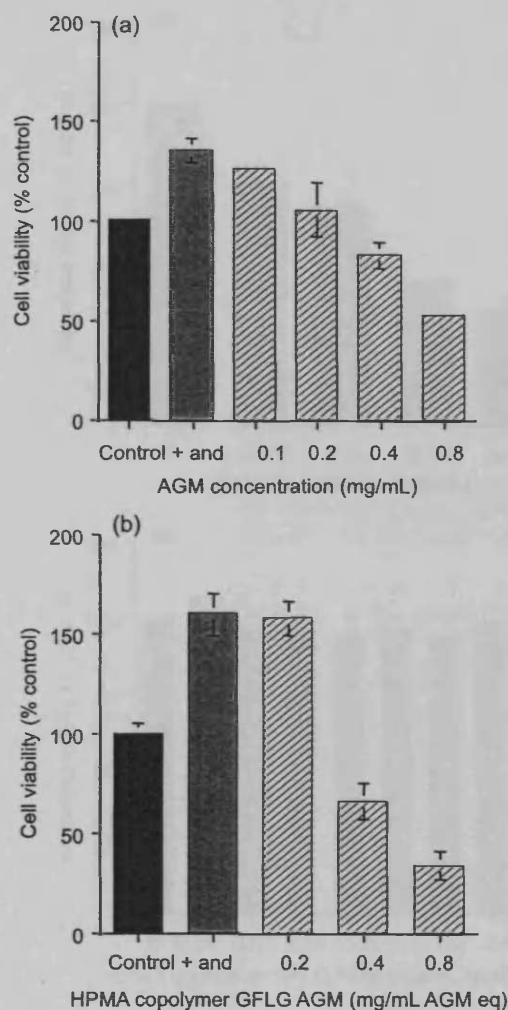


Figure 6. Inhibition of the mitogenic effect of androstenedione by free AGM (panel a) or HPMA copolymer-AGM (panel b). Cell growth was measured after 11 days using MTT assay and the results are expressed as percentage of the control without addition. The values represent mean \pm SEM; $n = 3$ for AGM and $n = 6$ HPMA copolymer AGM, respectively.

For example, the HPMA copolymer-Dox conjugate which displayed activity clinically (Vasey et al. 1999) and enhanced anti-tumour activity compared to free Dox in many tumour models *in vivo* (Duncan et al. 1992, 2005) is almost completely inactive *in vitro* (~100-fold less active than free Dox) (Seymour et al. 1990; Duncan et al. 1992). Only chemotherapy-containing polymer conjugates that are unstable in tissue culture medium, i.e. liberate free drug extracellularly, (Gianasi et al. 1999), contain free drug (all batches include at least trace amounts), act via interaction with the plasma membrane, or contain ligands known to promote rapid internalisation by receptor-mediated endocytic uptake show significant cytotoxicity *in vitro*.

It was therefore particularly surprising to find that an HPMA copolymer-Dox-AGM conjugate was significantly more toxic than HPMA copolymer-Dox

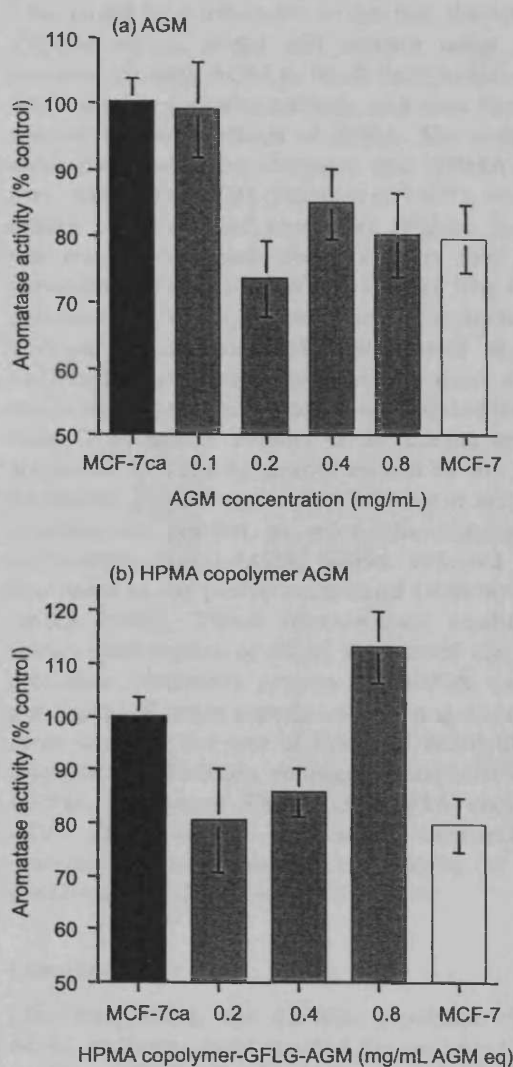


Figure 7. Effect of free and polymer-bound AGM on aromatase activity in MCF-7ca. Panel (a) free AGM, and panel (b) polymer-bound AGM at the concentrations shown. Results obtained with MCF-7 cells with no addition are shown for comparison. Data are expressed as a percentage of the activity seen in MCF-7ca without addition, mean \pm SEM and $n \geq 12$.

or indeed a mixture of the conjugates (HPMA copolymer-Dox + HPMA copolymer-AGM) *in vitro* (Figure 4, Vicent et al. 2005). As a simple mixture of the conjugates did not show enhanced cytotoxicity it would suggest that the mechanism of action of the combination therapy requires simultaneous delivery of both agents from the same polymeric platform. Recently, when studying the endocytic uptake of these conjugates by MCF-7 and MCF-7ca cells, we have shown that HPMA copolymer-AGM-Dox shows neither a greater the rate of, nor different pathway of, internalisation than the individual conjugates. Indeed HPMA copolymer-Dox displays greater membrane binding (Greco et al. 2005). As the cytotoxicity of Dox precludes evaluation

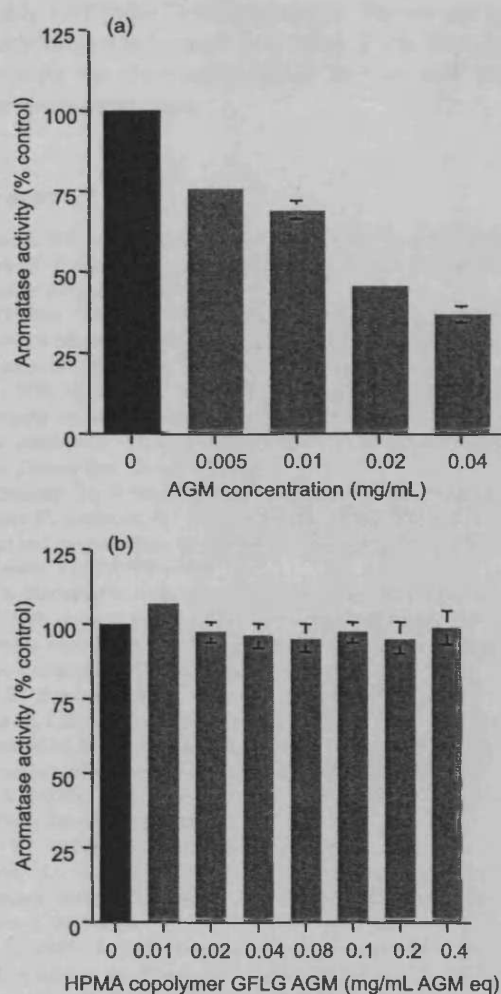


Figure 8. Effect of free and polymer-bound AGM on aromatase activity in isolated human placental microsomal extract. Panel (a) free AGM, and panel (b) polymer-bound AGM at the concentrations shown. Data are expressed as a percentage of the activity without addition; mean \pm SEM and $n \geq 4$.

of aromatase inhibition by the combination conjugate, this study was designed to examine the mechanism of action of HPMA copolymer-AGM using a variety of models and incubation times (Figure 2).

Oestrogens play an important role in the growth of breast cancers, and oestradiol is known to promote the growth of both MCF-7 and MCF-7ca cells. Consistent with the observations of Santner et al. (1993), results presented here showed that addition of the aromatase substrates androstenedione and testosterone stimulated growth of MCF-7ca cells, but not MCF-7 (Figure 5). The latter suggests that testosterone and androstenedione, which have a similar structure to oestradiol, do not act as direct oestrogen receptor agonists. Both free AGM and HPMA copolymer-AGM were able to reverse the mitogenic activity of androstenedione, and indeed at higher AGM concentration (0.4 and 0.8 mg/ml) cell growth was even lower than seen in the control (Figure 6).

This could be attributable to the fact that charcoal-stripped serum might still contain some residual steroids, allowing AGM to block their transformation into oestrogens, or alternatively, and most likely, non-specific cytotoxic effects of AGM. The radiometric assay provided direct evidence that HPMA copolymer-AGM, like AGM (Burak et al. 1997), was able to inhibit cell-associated aromatase (Figure 7). Whilst the results described above suggest that HPMA copolymer-GFLG-AGM can act like free AGM in cell-based systems, experiments conducted with isolated human placental microsomal aromatase showed that polymer-bound-AGM cannot itself act as an enzyme inhibitor, whereas as expected free AGM does. This lack of activity of the conjugate can be attributed to steric hindrance caused by the polymer backbone. Furthermore, this decrease in activity was possible to predict as even the simple AGM metabolite, acetyl-AGM, shows reduced activity compared to the parent compound (<50%) (Aboul-Enen 1986). These observations confirm that intracellular release of AGM is a critical step for the aromatase inhibitory activity of HPMA copolymer conjugates. Further experiments are ongoing to define more carefully the rate of Dox and AGM liberation from the combination conjugate compared with the HPMA copolymer-Dox and HPMA copolymer-AGM alone as this step seems instrumental in determining the enhanced cytotoxicity of HPMA copolymer-AGM-Dox.

Conclusions

Like free AGM, the HPMA copolymer-GFLG-AGM conjugate demonstrated the capacity to inhibit androstenedione-stimulated growth of MCF-7ca cells, and a radiometric assay also confirmed its ability to inhibit cell-associated aromatase. Inability of conjugate to inhibit isolated aromatase enzyme shows that release of free AGM is essential for activity. It is important to note that while AGM in the μ M range is active against the free enzyme, the more modern third generation aromatase inhibitors (e.g. anastrozole or letrozole) are more potent and demonstrate activity at nM concentrations (Long et al. 1998). This suggests that polymer conjugation of such compounds could lead to even more marked anti-tumour activity. We conclude that polymer therapeutics containing aromatase inhibitors, either using conjugates as single agents or drug combinations are worthy of further *in vivo* exploration with a view to identifying candidates suitable for clinical evaluation.

Acknowledgments

F. Greco is supported by the Centre for Polymer Therapeutics and by Tenovus Centre for Cancer Research. M. J. Vicent is supported by a Marie Curie

Fellowship (HPMF-CT-2002-01555). We would like to acknowledge Dr Simons and Miss Sook Wah Yee for providing the placental enzymes and for their help with the aromatase assay.

References

- Aboul-Enein HY. 1986. Aminoglutethimide. In: Florey K, editor. Analytical Profiles of Drug Substances. 15. San Diego, CA: Academic press. p 35–69.
- ATAC Trialists Group 2005. Results of the ATAC (Arimidex, Tamoxifen Alone or in Combination) trial after completion of 5 years adjuvant treatment for breast cancer. *Lancet* 365:60–62.
- Burak Jr, WE, Quinn AL, Farrar WB, Brueggemeier RW. 1997. Androgens influence estrogen-induced responses in human breast carcinoma cells through cytochrome P450 aromatase. *Breast Cancer Res Treat* 44:57–64.
- Devleeschouwer N, Body JJ, Legros N, Muquardt C, Donnay I, Wouters P, Leclercq G. 1992. Growth factor-like activity of phenol red preparations in the MCF-7 breast cancer cell line. *Anticancer Res* 12:789–794.
- Duncan R, Kopeckova P, Strohalm J, Hume I, Lloyd JB, Kopecek J. 1988. Anticancer agents coupled to *N*-(2-hydroxypropyl)methacrylamide copolymers. II. Evaluation of daunomycin conjugates *in vivo* against L1210 leukaemia. *Br J Cancer* 57:147–156.
- Duncan R, Seymour LW, O'Hare KB, Flanagan PA, Wedge S, Hume IC, Ulbrich K, Strohalm J, Subr V, Spreafico F, Grandi M, Ripamonti M, Farao M, Suarato A. 1992. Preclinical evaluation of polymer-bound doxorubicin. *J Control Release* 19:331–346.
- Duncan R. 2003a. The dawning era of polymer therapeutics. *Nat Rev Drug Discov* 2:347–362.
- Duncan R. 2003b. Polymer-anticancer drug conjugates. In: Budman D, Calvert H, Rowinsky E, editors. Handbook of anticancer drug development. Baltimore, MD: Williams & Wilkins. p 239–260.
- Duncan R. 2005. *N*-(2-Hydroxypropyl) methacrylamide Copolymer Conjugates. In: Kwon GS, editor. Polymeric drug delivery systems. New York, NY: Marcel Dekker Inc. p 1–92.
- Gianasi E, Wasil M, Evagorou EG, Kedde A, Wilson G, Duncan R. 1999. HEMA copolymer platinate as novel antitumor agents: *In-vitro* properties, pharmacokinetics and antitumor activity *in vivo*. *Eur J Cancer* 35:994–1002.
- Goss PE, Strasser K. 2002. Tamoxifen resistant and refractory breast cancer the value of aromatase inhibitors. *Drugs* 62:957–966.
- Greco F, Vicent MJ, Nicholson RI, Duncan R. 2005. Mechanism of action of a novel polymer combination therapy for breast cancer. *Proc Int Symp Control Release Bioact Mater* 32:257.
- Hayes DF, Robertson JFR. 2002. Overview and concepts of endocrine therapy. In: Robertson JFR, Nicholson RI, Hayes DF, editors. Endocrine therapy of breast cancer. London: Martin Dunitz. p 3–10.
- Johnston SRD, Dowsett M. 2003. Aromatase inhibitors for breast cancer: Lessons from the laboratory. *Nat Rev Cancer* 3:821–831.
- Jordan VC. 2003. Tamoxifen: A most unlikely pioneering medicine. *Nat Rev Drug Discov* 2:205–213.
- Long BJ, Tilghman SL, Yue W, Thiantanawat A, Grigoriev DN, Brodie AMH. 1998. The steroidal antiestrogen ICI 182,780 is an inhibitor of cellular aromatase activity. *J Steroid Biochem Mol Biol* 67:293–304.
- Long BJ, Jelovac D, Thiantanawat A, Brodie AM. 2002. The effect of second-line antiestrogen therapy on breast tumour growth after first-line treatment with the aromatase inhibitor letrozole: Long term studies using the intratumoral aromatase postmenopausal breast cancer model. *Clin Cancer Res* 8:2378–2388.
- Matsumura Y, Maeda H. 1986. A new concept for macromolecular therapeutics in cancer chemotherapy; Mechanism of tumorigenic accumulation of proteins and the antitumor agent SMANCS. *Cancer Res* 6:6387–6392.
- Minko T, Kopeckova P, Pozharov V, Kopecek J. 1998. HEMA copolymer bound adriamycin overcomes MDR1 gene encoded resistance in a human ovarian carcinoma cell line. *J Control Release* 54:223–233.
- Rademaker-Lakhai JM, Terret C, Howell SB, Baud CM, de Boer RF, Plum D, Beijnen JH, Schellens JHM, Droz JP. 2004. A Phase I and pharmacological study of the platinum polymer AP5280 given as an intravenous infusion once every 3 weeks in patients with solid tumors. *Clin Cancer Res* 10:3386–3395.
- Rejmanova P, Labsky J, Kopecek J. 1977. Aminolysis of monomeric and polymeric *p*-nitrophenyl esters of methacryloylated amino acids. *Makromol Chem* 178:2159–2168.
- Rice JR, Howell SB. 2004. AP-5346 polymer-delivered platinum complex. *Drug Future* 29:561–565.
- Santner SJ, Chen S, Zhou D, Korsunsky Z, Martel J, Santen RJ. 1993. Effect of androstenedione on growth of untransfected and aromatase-transfected MCF-7 cells in culture. *J Steroid Biochem Mol Biol* 44:611–616.
- Searle F, Gac-Breton S, Keane R, Dimitrijevic S, Brocchini S, Duncan R. 2001. *N*-(2-hydroxypropyl)methacrylamide copolymer-6-(3-aminopropyl)-ellipticine conjugates, synthesis, characterisation and preliminary *in vitro* and *in vivo* studies. *Bioconjugate Chem* 12:711–718.
- Seymour LW, Ulbrich K, Strohalm J, Kopecek J, Duncan R. 1990. The pharmacokinetics of polymer-bound adriamycin. *Biochem Pharmacol* 39:1125–1131.
- Seymour LW, Ulbrich K, Styger PS, Brereton M, Subr V, Strohalm J, Duncan R. 1994. Tumouritropism and anticancer efficacy of polymer-based doxorubicin prodrugs in the treatment of subcutaneous murine B16F10 melanoma. *Br J Cancer* 70:636–641.
- Sgouras D, Duncan R. 1990. Methods for the evaluation of biocompatibility of soluble synthetic polymers which have potential for biomedical use: 1-Use of the tetrazolium-based colorimetric assay (MTT) as a preliminary screen for evaluation of *in vitro* cytotoxicity. *J Mater Sci Mater Med* 1:61–68.
- Singer JW, Schaffer S, Baker B, Bernareggi A, Stromatt S, Nienstedt D, Besman M. 2005. Paclitaxel polyglumex (XYOTAX; CT-2103): An intracellularly targeted taxane. *Anti-Cancer Drugs* 16:243–254.
- Vasey PA, Kaye SB, Morrison R, Twelves C, Wilson P, Duncan R, Thomson AH, Murray LS, Hilditch TE, Murray T, Burtles S, Fraier D, Frigerio E, Cassidy J. 1999. Phase I Clinical and Pharmacokinetic study of PK1 [*N*-(2-Hydroxypropyl)methacrylamide Copolymer Doxorubicin]: First member of a new class of chemotherapeutic agents-drug-polymer conjugates. *Clin Cancer Res* 5:83–94.
- Vicent MJ, Greco F, Nicholson RI, Paul A, Griffiths PC, Duncan R. 2005. Polymer therapeutics designed for a combination therapy of hormone-dependent cancer. *Angew Chem- Int Edit* 44:2–6.

Polymer–drug conjugates: towards a novel approach for the treatment of endocrine-related cancer

R Duncan¹, M J Vicent^{*1}, F Greco^{1,2} and R I Nicholson²

¹Centre for Polymer Therapeutics and ²Tenovus Centre for Cancer Research, Welsh School of Pharmacy, Cardiff University, Redwood Building, King Edward VII Avenue, Cardiff CF10 3XF, UK

(Requests for offprints should be addressed to R Duncan; Email: DuncanR@cf.ac.uk)

^{*}(M J Vicent is now at Centro de Investigación Príncipe Felipe, FVIB, Medicinal Chemistry Unit, Av Autopista del Saler 16, E-46013 Valencia, Spain)

Abstract

The last decade has seen successful clinical application of polymer–protein conjugates (e.g. Oncaspar, Neulasta) and promising results in clinical trials with polymer–anticancer drug conjugates. This, together with the realisation that nanomedicines may play an important future role in cancer diagnosis and treatment, has increased interest in this emerging field. More than 10 anticancer conjugates have now entered clinical development. Phase I/II clinical trials involving *N*-(2-hydroxypropyl)methacrylamide (HPMA) copolymer–doxorubicin (PK1; FCE28068) showed a four- to fivefold reduction in anthracycline-related toxicity, and, despite cumulative doses up to 1680 mg/m² (doxorubicin equivalent), no cardiotoxicity was observed. Antitumour activity in chemotherapy-resistant/refractory patients (including breast cancer) was also seen at doxorubicin doses of 80–320 mg/m², consistent with tumour targeting by the enhanced permeability (EPR) effect. Hints, preclinical and clinical, that polymer anthracycline conjugation can bypass multidrug resistance (MDR) reinforce our hope that polymer drugs will prove useful in improving treatment of endocrine-related cancers. These promising early clinical results open the possibility of using the water-soluble polymers as platforms for delivery of a cocktail of pendant drugs. In particular, we have recently described the first conjugates to combine endocrine therapy and chemotherapy. Their markedly enhanced *in vitro* activity encourages further development of such novel, polymer-based combination therapies. This review briefly describes the current status of polymer therapeutics as anticancer agents, and discusses the opportunities for design of second-generation, polymer-based combination therapy, including the cocktail of agents that will be needed to treat resistant metastatic cancer.

Endocrine-Related Cancer (2005) 12 S189–S199

Introduction

The search continues for more selective therapies that will destroy either tumour cells or angiogenic tumour vasculature without harming normal tissue. Although the last two decades have seen successes, including introduction of new chemotherapy (e.g. taxanes

(Jordan & Wilson 2004), tamoxifen (Jordan 2003) second- and third-generation aromatase inhibitors (Brodie & Njar 2000), Herceptin (Harries & Smith 2002), Gleevec (Atkins & Gershell 2002) and Avastin (Ferrara *et al.* 2004)), improvement in terms of tumour response or increased patient survival has largely relied on a combination of these new agents with existing chemotherapy, leading to incremental benefit in survival. Emergence of drug resistance remains a significant problem in the treatment of breast and prostate cancer. In the case of breast cancer, arrival of the selective oestrogen receptor (ER) antagonist

This paper was presented at the 1st Tenovus/AstraZeneca Workshop, Cardiff (2005). AstraZeneca has supported the publication of these proceedings.

tamoxifen contributed to a 28% reduction in mortality at 5 years (Jordan 2003). Even so, the prognosis for patients with metastatic breast cancer is still poor, the survival rate at 5 years being under 20%. The mixed antagonist/agonist activity of tamoxifen and the acquired resistance that can develop in the long term limit its therapeutic potential (Coleman 1999, Cummings 2002). To circumvent this problem, there has been growing interest in the use of aromatase inhibitors (Brodie & Njar 2000, Lønning 2004), and recent clinical trials indicate that letrozole and anastrozole are more effective in treating ER-positive breast cancer than tamoxifen (Goss & Strasser 2002, Howell *et al.* 2005). The challenge of finding 'breakthrough' therapeutics able significantly to prolong the survival of patients with resistant metastatic breast and prostate cancer remains.

Two distinct research approaches are being pursued in the hunt for improved therapy. First, and by far the largest area reviewed in the literature (Chabner & Roberts 2005), is the use of low-molecular-weight chemotherapy and the search for novel, tumour-specific molecular targets. Of particular interest in relation to endocrine-related cancer are agents designed to interrupt the signal transduction pathways and/or stimulate apoptosis, such as epidermal growth factor receptor inhibitors (Atalay *et al.* 2003, Haran 2004), tyrosine kinase inhibitors (Daub *et al.* 2004, Singer *et al.* 2004) and modulators of apoptosis (Igney & Krammer 2002). In theory, new targets should allow design of 'perfect' drug molecules with exquisite therapeutic activity and no side effects. In reality, with the exception of Gleevec, which is used for the treatment of chronic myelogenous leukaemia and gastrointestinal tumours, this has proved difficult to achieve, and even in this case acquired resistance is a problem. With the explosion of molecular mechanism information from genomics and proteomics research, global oncology research is largely focusing on the search for the 'perfect', low-molecular-weight anti-cancer agent. Approaches include screening of natural product molecules, and modelling-driven synthesis of synthetic low-molecular-weight drugs. Recent successes with monoclonal antibodies have also popularised the search for natural macromolecules, including antibodies, proteins and oligonucleotides, that might have the required antitumour biological activity. Evolving in parallel, and, indeed, as a complementary approach, is the design of novel drug delivery systems (DDS) as cancer treatments (recently reviewed in Duncan 2005b). DDS have been designed for controlled release of endocrine therapy, such as Zoladex and Leupron depot, formulations which have proved so important in the

treatment of endocrine-related cancers, for local delivery of chemotherapy (e.g. Gliadel for treatment of glioblastoma multiforme), and to improve tumour drug targeting (e.g. the antibody conjugate Mylotarg and the polymer conjugate Xyotax). In the context of cancer therapeutics, the current and potential contribution of DDS is often overlooked (Chabner & Roberts 2005). Over the last 10–15 years, systemically administered DDS and monoclonal antibody therapeutics have come of age. Entry of a growing number of products into routine clinical use is giving credibility to this field (reviewed in Duncan 2003b, 2005b) (Table 1). These nanosized hybrid systems often combine a drug, protein or antibody with a polymer or polymer-coated liposome and they can rightly be viewed as the first 'nanomedicines' (Fig. 1) (Allen 2002, Duncan 2003a, Torchillin 2005). Although the contribution of DDS as cancer therapeutics is still overlooked by many, there is a growing realisation that nanotechnology, as applied to medicine, has the potential to bring significant advances in the diagnosis and treatment of cancer (Ferrari 2005). See also the following reports for an introduction to this field: Editorial 2003 'Nanomedicine: grounds for optimism'. *Lancet*, 362; 673; NIH Roadmap for Nanomedicines, May 2004 <http://nihroadmap.nih.gov/>; Commission of the European Communities Communication: *Towards a European Strategy for Nanotechnology*, Brussels, COM 338, May 2004; UK; the European Science Foundation's 'Forward Look on Nanomedicines', February 2005 (<http://www.esf.org/newsrelease/83/SPB23Nanomedicine.pdf>) and the NIH/NCI 'Cancer Nanotechnology Plan' July 2004 (http://nano.cancer.gov/alliance_cancer_nanotechnology_plan.pdf). In 2003, an amazing milestone was reached when the US Federal Drug Administration approved more biotech products (defined in the broadest sense and including DDS) as new medicines than more conventional, low-molecular-weight drugs.

Polymer conjugates: rationale for design

Although many are aware of the emergence of liposomal and antibody-based products, there is still little appreciation of the growing list of polymer therapeutics used as medicines. Commercialisation of polymer–protein conjugates (such as polyethyleneglycol (PEG)-Lasparaginase (Oncaspar) and PEGylated-recombinant methionyl human granulocyte colony stimulating factor (G-CSF) (Neulasta) in the USA (Harris & Chess 2003), coupled with the transfer of the *N*-(2-hydroxypropyl)methacrylamide (HPMA)

Table 1 Examples of antibodies and drug delivery systems used in cancer therapy

Product	Status	Payload	Indication
Therapeutic antibodies			
Rituxan [®]	Market	–	Non-Hodgkin's Lymphoma CD20 +ve
Herceptin [®]	Market	–	HER2 +ve breast cancer
Campath	Market	–	B-cell Chronic Lymphocytic
Avastin	Market	–	Leukaemia
Antibody-drug conjugates			
Mylotarg [®]	Market	calicheamicin	Acute Myeloid Leukaemia CD33 +ve
Radioimmunotherapeutics			
Tositumomab [®] CD20	Market	[¹³¹ I]iodide	Non-Hodgkin's Lymphoma
Zevalin [®] CD20	Market	[⁹⁰ Y]ttrium	Non-Hodgkin's Lymphoma
Liposomes			
Daunoxome [®]	Market	daunorubicin	Kaposi's Sarcoma
Doxil [®] /Caelyx [®]	Market	doxorubicin	Kaposi's Sarcoma, Ovarian cancer
Depocyt-lipidic formulation	Market	cytarabine	Intrathecal therapy of lymphomatous meningitis
Polymer-protein conjugates			
Zinostatin Stimalmer [®] (SMANCS)	Market	neocarzinostatin	Local administration – hepatocellular carcinoma
Oncaspar [®] PEG-L-asparaginase	Market	asparaginase	Acute Lymphoblastic Leukaemia
PEG-intron [™]	Market	α-interferon 2b	Hepatitis C, also in clinical development
PEG-α-interferon 2b			in cancer, multiple sclerosis, HIV/AIDS
Neulasta [™]	Market	G-CSF	Neutropenia associated with
PEG-G-CSF			cancer chemotherapy
Polymer-drug conjugates			
CT-2103, XYOTAX [™]	Phase II/III	paclitaxel	Particularly lung and ovarian cancer
Polyglutamate-paclitaxel PK1; FCE28068	Phase II	doxorubicin	Particularly lung and breast cancer
HPMA copolymer-doxorubicin PK2; FCE28069	Phase I/II	doxorubicin	Hepatocellular carcinoma
HPMA copolymer- doxorubicin-galactosamine AP5280	Phase II	platinite	Cancer
HPMA copolymer platinite AP5346	Phase I	platinite	Cancer
HPMA copolymer platinite CT-2106 Polyglutamate- camptothecin	Phase I	camptothecin	Cancer
PROTHECAN [™]	Phase II	camptothecin	Cancer
PEG-camptothecin			
Polymeric micelles			
NK911 PEG-aspartic acid-doxorubicin micelle	Phase I	doxorubicin	Cancer

copolymer–doxorubicin conjugate (PK1, FCE28068) into clinical trials in Europe in 1994 (Duncan 2003b, 2005a), has been the breakthrough that led to the exponential growth of interest in this field. The term 'polymer therapeutics' describes several distinct classes of agent, including polymeric drugs, polymer–drug conjugates, polymer–protein conjugates, polymeric micelles to which drug is covalently bound, and the multicomponent polyplexes that are now being developed as non-viral vectors (reviewed in Duncan

2003a). They are all considered 'new chemical entities' by regulatory authorities, more like therapeutic antibodies and their conjugates than DDS, which simply non-covalently entrap their drug payload. Over the last decade, more than 10 water-soluble polymer-drug conjugates (sometimes best visualised as macromolecular prodrugs) have entered phase I/II clinical trials as i.v. administered anticancer agents. These include six conjugates based on *N*-(2-hydroxypropyl)methacrylamide (HPMA) copolymers and, more recently, a

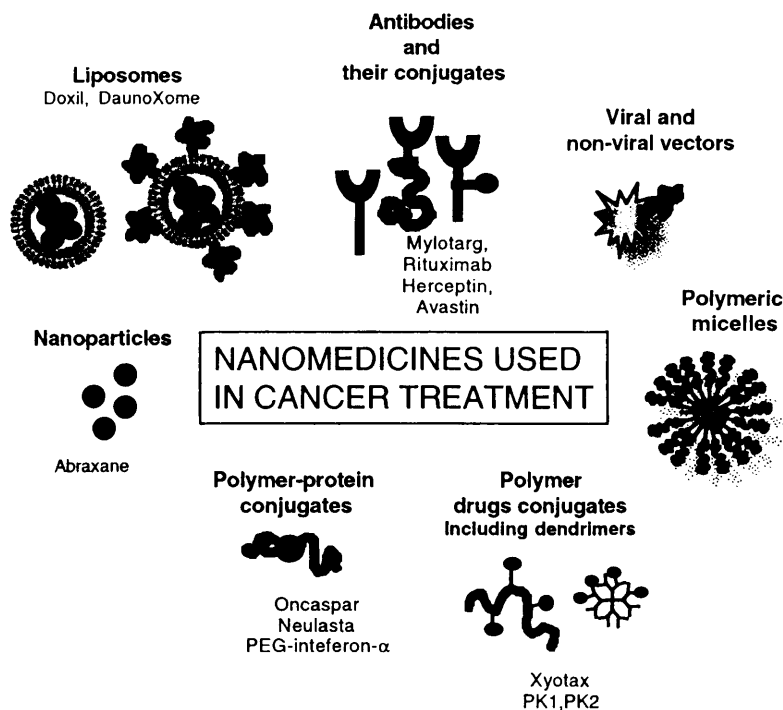


Figure 1 Schematic illustration of the therapeutics and technologies in clinical development and/or on the market as treatment for cancer that can be viewed as nanomedicines.

series of PEG and polyglutamic acid conjugates (Table 1). The evolution of this field has been reviewed in Duncan (2003a,b, 2005a,b).

Polymer–drug conjugates: rationale for design

The concept of polymer–anticancer conjugates was first proposed in 1975 (Ringsdorf 1975), and the biological rationale for their design (Duncan & Kopecek 1984, Duncan 1992) and current understanding of the mechanism of action is well documented (Duncan 2003b, 2005a). Briefly, these macromolecular prodrugs comprise a minimum of three components, as shown schematically in Fig. 2a): a natural or synthetic, water-soluble polymeric carrier (usually of 10 000–100 000 Da), a biodegradable polymer–drug linkage (often a peptidyl or ester linkage) and a bioactive antitumour agent. Not surprisingly, the first conjugates synthesised in the 1970s and early 1980s incorporated the most important anticancer agents of that era, particularly anthracycline antibiotics (daunorubicin and doxorubicin), alkylating agents (cyclophosphamide and melphalan) and antimetabolites (methotrexate and 5-fluorouracil).

Normally polymer–drug conjugates achieve tumour-specific targeting by the enhanced permeability and retention (EPR) effect (Matsumura & Maeda 1986). Hyperpermeable angiogenic tumour vessels allow preferential extravasation of circulating macromolecules and liposomes, and once in the interstitium they are retained there by lack of intratumoural lymphatic drainage. This leads to significant tumour targeting (>10–100-fold compared to free drug) and levels up to 20% dose/g have been reported for HEMA copolymer–doxorubicin conjugates, depending on tumour size. Both polymer- and tumour-related characteristics govern the extent of EPR-mediated targeting. Smaller tumours exhibit the highest concentration of polymer–drug. Using HEMA copolymer fractions in the range 10 000–800 000 Da as probes (Seymour *et al.* 1995, Noguchi *et al.* 1998), we found that tumour uptake of polymers (usual molecular diameter 5–20 nm) had broad size tolerance and good intratumoural penetration compared with that reported for liposomes and nanoparticles. Conjugates have also been synthesised to contain ligands that might promote receptor-mediated targeting (including antibodies, peptides and saccharides) (reviewed in Duncan 2005a,b). Although this is an attractive possibility, and proof of concept can easily be verified

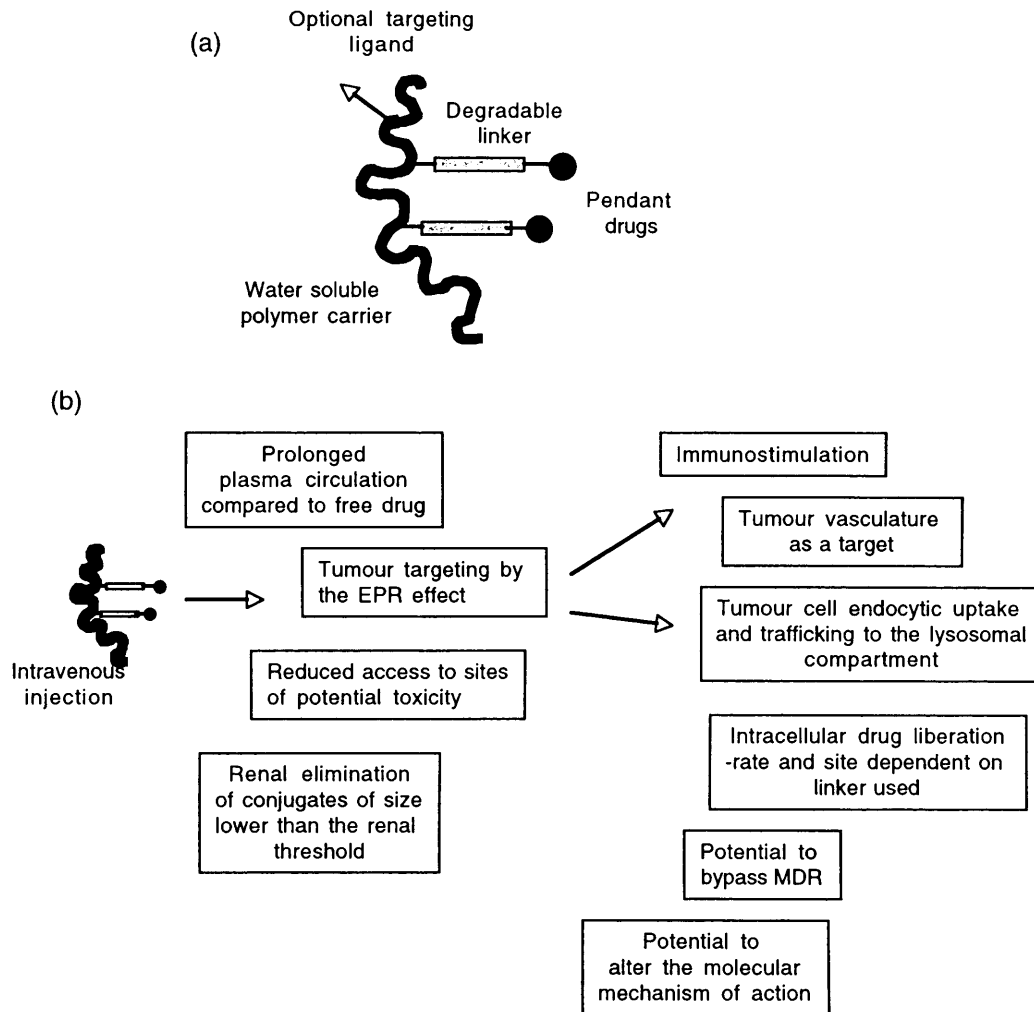


Figure 2 Schematic diagram showing the structure of polymer–drug conjugates (panel a) and the mechanisms of action of polymer conjugates (panel b).

in vitro, so far only one such conjugate has progressed into phase I trial, and this was HPMA copolymer-doxorubicin-galactosamine, which was designed as a treatment for hepatocellular carcinoma or secondary liver disease (PK2, FCE28069) (Seymour *et al.* 2002).

The growing database of *in vitro*, *in vivo* and clinical data allows reappraisal of our current understanding of the mechanism of action of HPMA copolymer-anticancer conjugates (Duncan 2005a). The mechanism of action is complex, and it is clear that many factors act in concert to produce the antitumour effect observed *in vivo* (Fig. 2b). Drug pharmacokinetics are profoundly changed after polymer conjugation. After i.v. administration, the conjugate is initially retained in the vascular compartment, so that drug $t_{1/2\alpha}$ is increased and the levels of free drug detected in plasma are very

low (>100–1000 times less than seen for the conjugated drug). Preclinical rodent pharmacokinetic studies and clinical pharmacokinetics correlate well (reviewed in Duncan 2003b, 2005a). The plasma half-life of HPMA copolymer anticancer conjugates is typically 1–6 h, and elimination occurs predominantly via the kidney; over 50% of conjugated drug is excreted within 24 h. Only in the case of the hepatocyte-targeted conjugate PK2 does hepatobiliary elimination play a major role after liver targeting. This altered biodistribution reduces drug access to potential sites of toxicity, including the heart and bone marrow. This, together with the enhanced elimination of inactive, conjugated drug via the kidney (when the polymer–drug linker is stable), explains the significant reduction in toxicity of anticancer conjugates such as PK1 and PK2 in man (Vasey

et al. 1999, Seymour *et al.* 2002). Gamma camera imaging has shown some evidence to support EPR174-mediated tumour localisation in patients (Vasey *et al.* 1999). However, when colorectal cancer patients were given HPMA copolymer–camptothecin (MAG-CPT) 24 h before surgical removal of the tumour, the levels of conjugate measured in tumour tissue did not show preferential localisation compared to normal tissue (Sarapa *et al.* 2003). Further studies are needed in the clinical setting to clarify the clinical significance of the EPR effect in human tumours of different tissue origin and the extent of targeting at different stages of tumour development (primary, metastatic, postsurgery, etc.). Not least, we need to understand more about the effect of different dosing protocols and combinations with drug and/or radiotherapy on clinically related, EPR-mediated targeting.

Observations made in preclinical and clinical studies underline the need for careful design of the polymer drug linker so that it is stable in transit and degraded at a suitable rate intratumourally (reviewed in Duncan 2003b, 2005a). With HPMA copolymer conjugates, the lysosomally degradable peptidyl linkers (activated by thiol-dependant proteases) have shown the most promise. Hydrolytically labile terminal ester bonds have also been used to prepare conjugates of paclitaxel and camptothecin, and pH-sensitive hydrazone or *cis*-aconityl linkers are also currently being explored preclinically. A variety of terminal ligands have been used to synthesise HPMA copolymer–platinates with cisplatin-‘like’ (Gianasi *et al.* 1999), carboplatin-‘like’ (Gianasi *et al.* 2002) and oxaliplatin-‘like’ structure. Whichever linking chemistry is used, it is important to note that there is a clear influence of drug loading on conjugate conformation in solution. This in turn governs drug release rate and consequently therapeutic index. High loading with hydrophobic drugs can reduce the rate of prodrug activation, and solution conformation determines rates of both hydrolytic and enzymatic degradation.

Not only does drug conjugation affect whole-body pharmacokinetics, but it also changes fate at the cellular level. While many low-molecular-weight compounds enter tumour cells rapidly (within minutes) by passage across the plasma membrane, polymer conjugates are taken into cells much more slowly by endocytosis (reviewed in Duncan 2005a,b). This frequently makes comparative *in vitro* screening of activity almost meaningless. Conjugates containing free drug as a contaminant or that rapidly off-load drug in the tissue culture medium appear most potent. These conjugates, however, are often the least likely to exhibit a good therapeutic index *in vivo*. Endocytic

internalisation of conjugates has been verified with a variety of cell lines, using ¹²⁵I-labelled probes, HPLC assay of drug, and both epifluorescence and confocal microscopy. This route of cellular entry appears to enable agents to bypass efflux pump-mediated MDR.

There is growing evidence to support an immunostimulatory action of HPMA copolymer anticancer conjugates (reviewed in Duncan 2005a). Rihova has postulated that the early antitumour activity *in vivo* occurs via cytotoxic or cytostatic action, but that secondary immunostimulatory action of circulating low levels of conjugate supplement this effect (Rihova *et al.* 2003). This hypothesis is supported by the following evidence:

- 1 It is observed that pretreatment of animals with immunosuppressive agents (such as doxorubicin and cyclosporine A) accelerates the growth of subsequently implanted tumour, whereas pretreatment with HPMA copolymer–doxorubicin does not.
- 2 An increase in circulating natural killer (NK) cell numbers and anticancer antibodies is seen in animals treated with conjugate.
- 3 Increased NK and lymphokine activated killer (LAK) cells have been seen in breast cancer patients treated with HPMA copolymer–Dox-IgG (Rihova *et al.* 2003).

Clinical status of polymer–drug conjugates as single agents

In 1994, the first synthetic polymer – anticancer conjugate entered clinical trial. This was HPMA copolymer–Gly-Phe-Leu-Gly-doxorubicin (PK1, FCE28068). It has a molecular mass of ~30 000 Da and a doxorubicin content of ~8.5 wt% (Vasey *et al.* 1999). This peptidyl linker was designed to be hydrolysed by thiol-dependent proteases (particularly cathepsin B) after lysosomotropic delivery. In phase I trials, PK1 was administered as a short infusion every 3 weeks, and it had a maximum tolerated dose of 320 mg/m² (doxorubicin equivalent) (Vasey *et al.* 1999). This is approximately fourfold higher than the normal safe clinical dose of doxorubicin, and a much higher anthracycline dose than can be safely given in liposomal form. The FCE28068 dose-limiting toxicities were typical of the anthracyclines, including febrile neutropenia and mucositis. Despite cumulative doses up to 1680 mg/m² (doxorubicin equivalent), no cardiotoxicity was observed. Antitumour activity was seen in patients considered chemotherapy resistant/refractory (including breast cancer) and at lower doxorubicin doses

(80–180 mg/m²). Activity at the lower dose was consistent with EPR-mediated targeting.

Despite a large number of research studies exploring ligand-targeted polymer conjugates (reviewed in Duncan 2005a), PK2 (FCE28069) is still the only targeted conjugate to be tested clinically (Seymour *et al.* 2002). It was designed to recognise the hepatocyte asialoglycoprotein receptor and has been explored as a treatment for hepatocellular carcinoma. In phase I/II, the maximum tolerated dose of FCE28069 was 160 mg/m² (doxorubicin equivalent). Gamma camera imaging confirmed that most of the conjugate localised to liver. The majority of conjugate was present in normal liver (after 24 h, 16.9% dose) with lower accumulations within hepatic tumour (3.2% dose). However, it was estimated that this hepatoma-associated drug was still 12–50 fold higher than could be achieved with administration of free doxorubicin. Antitumour activity was seen in patients with primary hepatocellular carcinoma in this study.

Clinical studies with an HPMA copolymer-paclitaxel conjugate (PNU166945) and HPMA copolymer-camptothecin (MAG-CPT; PNU 166148) were disappointing. In both cases, this was probably due to lack of ester linker stability during transport in the circulation and/or renal elimination. HPMA copolymer-paclitaxel showed toxicity consistent with commonly observed paclitaxel toxicities: flu-like symptoms, mild nausea and vomiting, mild haematological toxicity and neuropathy (Meerum Terwogt *et al.* 2001). Neurotoxicity grade 2 occurred in two patients at a dose of 140 mg/m² (although grade 1 was pre-existing on their entry), and one patient at 196 mg/m² had grade 3 neuropathy after the fourth cycle. Although no dose limiting toxicities (DLTs) were reported, dose escalation was discontinued prematurely due to concerns of potential clinical neurotoxicity. In this small patient cohort, antitumour activity was also observed. A paclitaxel-refractory breast cancer patient showed remission of skin metastasis after two courses at 100 mg/m² (paclitaxel equivalent). Two other patients had stable disease at a dose of 140 mg/m². PNU166148 (MAG-CPT) containing Gly-C6-Glycamptothecin showed severe and unpredictable cystitis in phase I clinical trials, and cumulative bladder toxicity was dose limiting. No objective clinical responses were seen; however, one patient with renal cell carcinoma had tumour shrinkage and a colon patient had stable disease (Schoemaker *et al.* 2002).

HPMA copolymer platinates (Rademaker-Lakhai *et al.* 2004), polymeric micelles containing doxorubicin and paclitaxel (Nakanishi *et al.* 2001), and PEG-camptothecin and paclitaxel conjugates (Greenwald

et al. 2003) are also undergoing early clinical evaluation. However, the polymer conjugate most advanced in clinical development is a polyglutamate-paclitaxel conjugate (Li *et al.* 1998, Auzenne *et al.* 2002) called Xyotax, which is being developed by Cell Therapeutics (Seattle, WA, USA). An extensive phase II/III evaluation is under way, focusing on non small cell lung cancer (NSCLC) patients being treated with Xyotax as either a single agent (compared with paclitaxel, gemcitabine or vinorelbine) or in combination with carboplatin. Earlier phase I/II studies have reported very interesting activity in NSCLC and also relapsed ovarian cancer. Several phase III clinical trials are currently concluding (see latest abstracts at American Society for Clinical Oncology 2005, www.asco.org), and the Gynecologic Oncology Group (GOG) in the USA has recently initiated a phase III clinical trial involving Xyotax in ovarian cancer patients.

Novel polymeric anticancer agents and polymer–drug combinations

Conjugates tested clinically so far have incorporated only established chemotherapeutic agents, including doxorubicin, paclitaxel, camptothecins and platinates. Clinical proof of the concept is now paving the way for synthesis of second-generation conjugates containing experimental chemotherapy and novel polymer-based combinations. The approaches under investigation are shown schematically in Fig. 3, and all are based on the premise that the EPR effect will promote tumour selective delivery of polymeric anticancer conjugates to tumour tissue in humans (acting as a gateway for both passive and, in future, receptor-mediated targeting). Recently synthesised conjugates designed for lysosomal delivery contain novel antitumour agents, such as compounds that have failed in early clinical development due to unacceptable toxicity (e.g. ellipticines (Searle *et al.* 2001) and TNP-470 (Satchi-Fainaro *et al.* 2004)), or interesting novel natural product antitumour agents (e.g. geldanamycin derivatives (Nishiyama *et al.* 2003), 1,5-diazaanthraquinones (Vicent *et al.* 2004a) and wortmannin (Varticovski *et al.* 2001)). In all cases, HPMA copolymers of traditional structure (molecular weight characteristics and a Gly-Phe-Leu Gly linker) have been used as a platform, with the terminal linker dependent on compound chemistry. HPMA copolymer-TNP470 (Satchi-Fainaro *et al.* 2004) is the first polymer-based antiangiogenic agent, and it shows considerable promise *in vivo*.

While many are beginning to explore novel polymer architectures, including dendrimers as carriers of

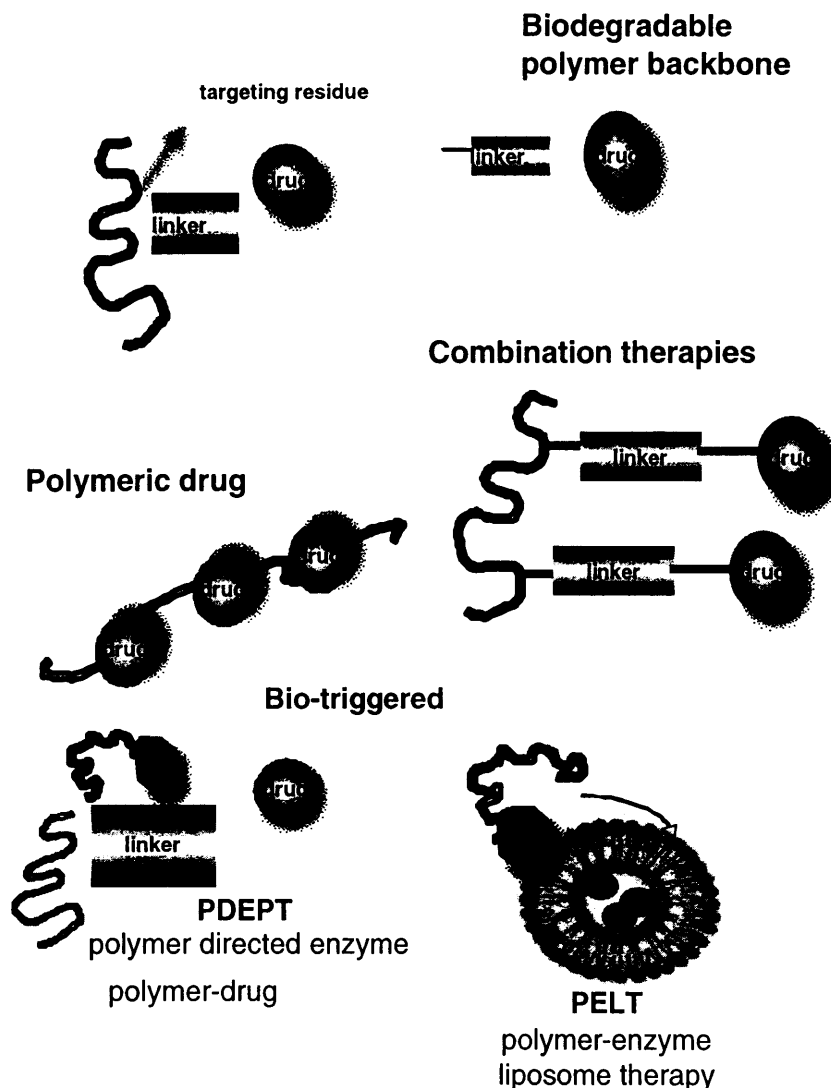


Figure 3 Schematic diagram showing the polymer anticancer drugs, polymer–drug conjugates and polymer–drug combinations currently under study.

anticancer agents (Malik *et al.* 1999), the most pressing need is design of new biodegradable polymeric carriers that can be used at relatively high molecular weight to promote greater EPR-mediated targeting and then safely eliminated. Our recent studies have explored dextrin, a natural polymer degraded by amylase (Hreczuk-Hirst *et al.* 2001), and pendant chain functionalised polyacetals that display pH-dependent degradation after internalisation into the endosomal or lysosomal compartment (Tomlinson *et al.* 2002, 2003). These polymers can incorporate the drug (e.g. doxorubicin) via pendant linkage or as a component of the polymer main chain (Vicent *et al.* 2004b).

In the context of endocrine-related cancer, we have recently described diethylstilboestrol (DES) conjugate with DES as a component of the polymer backbone. Although this relatively old agent was used as a model compound, a new concept of anticancer drug delivery was established (Vicent *et al.* 2004b). These polymeric prodrugs incorporate DES into the polymer main chain in such a way that after endocytic internalisation the conjugates undergo pH-dependent degradation (much faster rates of DES release are seen at acidic pH) to liberate principally the bioactive *trans*-DES form. Polyacetal DES showed enhanced *in vitro* cytotoxicity compared to free DES, indicating potential for

further evaluation *in vivo* where EPR-mediated targeting can be exploited to deliver higher tumour DES concentrations selectively.

Two-step anticancer treatments, such as polymer enzyme polymer prodrug therapy (PDEPT), have also been developed with the advantage of a burst of drug release in the tumour interstitium. In this case, a polymer–enzyme conjugate is prepared (PEGylated enzymes are already in routine clinical use (Table 1)) that will hydrolyse selectively a polymer drug linker within the tumour interstitium. The concept of PDEPT was exemplified first by an HPMA copolymer cathepsin B–PK1 combination (Satchi *et al.* 2001), and subsequently a non-mammalian enzyme linker combination HPMA copolymer- β -lactamase combined with HPMA-copolymer-glycine-glycine-cephalosporin-doxorubicin (Satchi-Fainaro *et al.* 2003). We have also shown that HPMA copolymer-bound phospholipases can also be used to modulate drug liberation from liposomes (Duncan *et al.* 2001). This strategy has been called polymer-enzyme liposome therapy (PELT).

Polymer conjugates containing endocrine and chemotherapy combinations

The polymeric carrier provides an ideal platform for delivery of a cocktail of drugs simultaneously. We have recently reported the first endocrine-chemotherapy combination in the form of the model compound HPMA-copolymer-aminoglutethimide-doxorubicin (Vicent *et al.* 2005). Here it was hypothesised that combination of endocrine therapy and chemotherapy by simultaneous attachment to the same polymer would bring significant advantages. The combination can be administered as a single dose, leading to the benefits of manufacture of a single conjugate and improved patient compliance. After EPR-mediated targeting, arrival of both pendant drugs within the tumour cells at the same time is guaranteed. It also provides the opportunity to tailor polymer–drug linkers to impart different rates of drug release for each compound, allowing agents to act synergistically. In *in vitro* experiments using MCF-7 cells and an aromatase-transfected cell line MCF-7Ca, it was found that conjugates containing both drugs (aminoglutethimide and doxorubicin) showed markedly enhanced cytotoxicity compared to PK1 (the conjugate that has already shown activity in breast cancer patients clinically), while mixtures of polymer conjugates containing only aminoglutethimide or only doxorubicin did not show synergistic benefit. These observations

underline the possibility of designing polymer–drug combinations for improved treatment of breast and prostate cancer.

Conclusions

Enormous progress is being made in understanding the molecular basis of endocrine-related cancer, and this brings great potential to design improved therapeutic strategies (Sledge & Miller 2003). Although the pharmaceutical industry prefers to develop small-molecule anticancer agents that can be administered to patients orally (very convenient to use), macromolecular drugs and delivery systems, including antibodies, proteins and polymer conjugates, are establishing their niche in modern chemotherapy. It is now universally agreed that combination approaches, perhaps involving small molecules (endocrine and chemotherapy), macromolecular drugs such as antibodies, and DDS, including polymer therapeutics, will probably be required to increase therapeutic index and circumvent all routes to resistance.

Acknowledgements

There is no conflict of interest that would prejudice the impartiality of this review. It should be noted that R D's group at Keele University (UK) has been involved in the design and clinical development of FCE28068 and FCE28069. She was employed by Pharmacia, Milan while PNU166945 and PNU166148 were being designed. Her group at the London School of Pharmacy designed the HPMA copolymer platinates that were licensed to Access Pharmaceuticals, Inc., and have subsequently entered clinical testing. Many thanks to Wendy Meeson for editorial assistance with the manuscript.

References

- Allen TM 2002 Ligand-targeted therapeutics in anticancer therapy. *Nature Reviews. Drug Discovery* **2** 750–763.
- Atalay G, Cardoso F, Awada A & Piccart MJ 2003 Novel therapeutic strategies targeting the epidermal growth factor receptor (EGFR) family and its downstream effectors in breast cancer. *Annals of Oncology* **14** 1346–1363.
- Atkins JH & Gershell LJ 2002 Selective anticancer drugs. *Nature Reviews. Cancer* **1** 645–646.
- Auzenne E, Donato NJ, Leroux E, Price RE, Farquhar D & Klostergaard J 2002 Superior therapeutic profile of poly-L-glutamic acid-paclitaxel copolymer compared with taxol in xenogeneic compartmental models of

- human ovarian carcinoma. *Clinical Cancer Research* **8** 573–581.
- Brekke O & Sandlie I 2003 Therapeutic antibodies for human diseases at the dawn of the twenty-first century. *Nature Reviews. Drug Discovery* **2** 52–62.
- Brodie AMH & Njar VCO 2000 Aromatase inhibitors and their application in breast cancer treatment. *Steroids* **65** 171–179.
- Chabner BA & Roberts TG 2005 Timeline – chemotherapy and the war on cancer. *Nature Reviews. Cancer* **5** 65–72.
- Coleman MP 1999 Opinion: why the variation in breast cancer survival in Europe? *Breast Cancer Research* **1** 22–26.
- Cummings F 2002 Evolving uses of hormonal agents for breast cancer therapy. *Clinical Therapeutics* **24** C3–25.
- Daub H, Specht K & Ullrich A 2004 Strategies to overcome resistance to targeted protein kinase inhibitors. *Nature Reviews. Drug Discovery* **3** 1001–1010.
- Duncan R 1992 Drug-polymer conjugates: potential for improved chemotherapy. *Anti-Cancer Drugs* **3** 175–210.
- Duncan R 2003a The dawning era of polymer therapeutics. *Nature Reviews. Drug Discovery* **2** 347–360.
- Duncan R 2003b Polymer-drug conjugates. In *Handbook of Anticancer Drug Development*, pp 239–260. Eds D Budman, H Calvert & E Rowinsky. Philadelphia, USA: Lippincott, Williams & Wilkins.
- Duncan R 2005a *N*-(2-Hydroxypropyl)methacrylamide copolymer conjugates. In *Polymeric Drug Delivery Systems*, pp 1–92. Ed. GS Kwon. New York: Marcel Dekker.
- Duncan R 2005b Targeting and intracellular delivery of drugs. In *Encyclopedia of Molecular Cell Biology and Molecular Medicine*, in press. Ed. RA Meyers. Weinheim, Germany: Wiley-VCH Verlag.
- Duncan R & Kopecek J 1984 Soluble synthetic polymers as potential drug carriers. *Advances in Polymer Science* **57** 51–101.
- Duncan R, Gac-Breton S, Keane R, Musila R, Sat YN, Satchi R & Searle F 2001 Polymer-drug conjugates, PDEPT and PELT: basic principles for design and transfer from the laboratory to the clinic. *Journal of Controlled Release* **74** 135–146.
- Ferrara N, Hillan KJ, Gerber H-P & Novotny W 2004 Case history: discovery and development of bevacizumab, an anti-VEGF antibody for treating cancer. *Nature Reviews. Drug Discovery* **3** 391–400.
- Ferrari M 2005 Cancer nanotechnology: opportunities and challenges. *Nature Reviews. Cancer* **5** 161–171.
- Gianasi E, Wasil M, Evagorou EG, Kedde A, Wilson G & Duncan R 1999 HEMA copolymer platinates as novel antitumor agents: *in vitro* properties, pharmacokinetics and antitumour activity *in vivo*. *European Journal of Cancer* **35** 994–1002.
- Gianasi E, Buckley RG, Latigo J, Wasil M & Duncan R 2002 HEMA copolymers platinates containing dicarboxylate ligands. Preparation, characterisation and *in vitro* and *in vivo* evaluation. *Journal of Drug Targeting* **10** 549–556.
- Goss PE & Strasser K 2002 Tamoxifen resistant and refractory breast cancer: the value of aromatase inhibitors. *Drugs* **62** 957–966.
- Greenwald RB, Choe YH, McGuire J & Conover CD 2003 Effective drug delivery by PEGylated drug conjugates. *Advanced Drug Delivery Reviews* **55** 217–250.
- Haran PM 2004 Epidermal growth factor receptor inhibition strategies in oncology. *Endocrine-Related Cancer* **11** 689–708.
- Harries M & Smith I 2002 The development and clinical use of trastuzumab (Herceptin). *Endocrine-Related Cancer* **9** 75–85.
- Harris JM & Chess RB 2003 Effect of pegylation on pharmaceuticals. *Nature Reviews. Drug Discovery* **2** 214–221.
- Howell A, Cuzick J, Baum M, Buzdar A, Dowsett M, Forbes JF, Hochtin-Boes G, Houghton I, Locker GY & Tobias JS 2005 Results of the ATAC (arimidex, tamoxifen, alone or in combination) trial after completion of 5 years' adjuvant treatment for breast cancer. *Lancet* **365** 60–62.
- Hreczuk-Hirst D, Chicco D, German L & Duncan R 2001 Dextrins as potential carriers for drug targeting: tailored rates of dextrin degradation by introduction of pendant groups. *International Journal of Pharmaceutics* **230** 57–66.
- Igney FK & Krammer PH 2002 Death and anti-death: tumour resistance to apoptosis. *Nature Reviews Cancer* **2** 277–288.
- Jordan MA & Wilson L 2004 Microtubules as a target for anticancer drugs. *Nature Reviews. Cancer* **4** 253–265.
- Jordan VC 2003 Tamoxifen: a most unlikely pioneering medicine. *Nature Reviews. Drug Discovery* **2** 206–213.
- Li C, Yu D, Newman R, Cabral F, Stephens LC, Hunter N, Milas L & Wallace S 1998 Complete regression well-established tumors using a novel water-soluble poly(L-glutamic acid)-paclitaxel conjugate. *Cancer Research* **58** 2404–2409.
- Lønning PE 2004 Aromatase inhibitors in breast cancer. *Endocrine-Related Cancer* **11** 179–189.
- Malik N, Evagorou EG & Duncan R 1999 Dendrimer-platinate: a novel approach to cancer chemotherapy. *Anti-Cancer Drugs* **10** 767–776.
- Matsumura Y & Maeda H 1986 A new concept for macromolecular therapeutics in cancer chemotherapy; mechanism of tumortropic accumulation of proteins and the antitumour agent SMANCS. *Cancer Research* **6** 6387–6392.
- Meerum Terwogt JM, ten Bokkel Huinink WW, Schellens JHM, Schot M, Mandjes IAM, Zurlo MG, Rocchetti M, Rosing H, Koopman FJ & Beijnen JH 2001 Phase I clinical and pharmacokinetic study of PNU166945, a novel water soluble polymer-conjugated prodrug of paclitaxel. *Anti-Cancer Drugs* **12** 315–323.
- Nakanishi T, Fukushima S, Okamoto K, Suzuki M., Matsumura Y, Yokoyama M, Okano T, Sakurai Y & Kataoka K 2001 Development of the polymer micelle

- carrier system for doxorubicin, *Journal of Controlled Release* 74 295–302.
- Nishiyama N, Nori A, Malugin A, Kasuya Y, Kopeckova P & Kopecek J 2003 Free and *N*-(2-hydroxypropyl)-methacrylamide copolymer-bound geldanamycin derivative induce different stress responses in A2780 human ovarian carcinoma cells. *Cancer Research* 63 7876–7882.
- Noguchi Y, Wu J, Duncan R, Strohal J, Ulbrich K, Akaike T & Maeda H 1998 Early phase tumor accumulation of macromolecules: a great difference in clearance rate between tumor and normal tissues. *Japanese Journal of Cancer Research* 89 307–314.
- Rademaker-Lakhai JM, Terret C, Howell SB, Baud CM, de Boer RF, Pluim D, Beijnen JH, Schellens JH & Droz J-P 2004 A phase I and pharmacological study of the platinum polymer AP5280 given as an intravenous infusion once every 3 weeks in patients with solid tumors. *Clinical Cancer Research* 10 3386–3395.
- Rihova B, Strohal J, Prausova J, Kubackova K, Jelinkova M, Rozprimova L, Sirova M, Plocova D, Etrych T, Subr V, Mrkvan T, Kovar M & Ulbrich K 2003 Cytostatic and immunomobilizing activities of polymer-bound drugs: experimental and first clinical data. *Journal of Controlled Release* 91 1–16.
- Ringsdorf H 1975 Structure and properties of pharmacologically active polymers. *Journal of Polymer Science Polymer Symposium* 51 135–153.
- Sarapa N, Britto MR, Speed W, Jannuzzo MG, Breda M, James C, Porro MG, Rocchetti M & Nygren P 2003 Targeted delivery and preferential uptake in solid cancer of MAG-CPT, a polymer bound prodrug of camptothecin – a trial in patients undergoing surgery for colorectal carcinoma. *Cancer Chemotherapy Pharmacology* 52 424–430.
- Satchi R, Connors TA & Duncan R 2001 PDEPT: polymer directed enzyme prodrug therapy. I. HPMA copolymer-cathepsin B and PK1 as a model combination. *British Journal of Cancer* 85 1070–1076.
- Satchi-Fainaro R, Hailu H, Davies JW, Summerford C & Duncan R 2003 PDEPT: polymer directed enzyme prodrug therapy. II. HPMA copolymer- β -lactamase and HPMA copolymer-C-Dox as a model combination. *Bioconjugate Chemistry* 14 797–804.
- Satchi-Fainaro R, Puder M, Davies JW, Tran HT, Sampson DA, Greene AK, Corfas G & Folkman J 2004 Targeting angiogenesis with a conjugate of HPMA copolymer and TNP-470. *Nature Medicine* 10 225–261.
- Schoemaker NE, van Kesteren C, Rosing H, Jansen, Swart M, Lieverst J, Fraier D, Breda M, Pellizzoni C, Spinelli R, Grazia PM, Beijnen JH, Schellens JH & Bokkel Huinink WW 2002 A phase I clinical and pharmacokinetic study of MAG-CPT, a water soluble polymer conjugate of camptothecin. *British Journal of Cancer* 87 608–614.
- Searle F, Gac-Breton S, Keane R, Dimitrijevic S, Brocchini S & Duncan R 2001 *N*-(2-Hydroxypropyl)methacrylamide copolymer-6-(3-aminopropyl)-ellipticine conjugates, synthesis, characterisation and preliminary *in vitro* and *in vivo* studies. *Bioconjugate Chemistry* 12 711–718.
- Seymour LW, Miyamoto Y, Brereton M, Subr V, Strohal J & Duncan R 1995 Influence of molecular size on passive tumour-accumulation of soluble macromolecular drug carriers. *European Journal of Cancer* 5 766–770.
- Seymour LW, Ferry DR, Anderson D, Hesslewood S, Julyan PJ, Payner R, Doran J, Young AM, Burtles S & Kerr DJ 2002 Hepatic drug targeting: phase I evaluation of polymer bound doxorubicin. *Journal of Clinical Oncology* 20 1668–1676.
- Singer CF, Hudelist G, Lamm W, Mueller R, Czerwenka K & Kubista E 2004 Expression of tyrosine kinases in human malignancies as potential targets for kinase-specific inhibitors. *Endocrine-Related Cancer* 11 861–869.
- Sledge GW Jr & Miller KD 2003 Exploiting the hallmarks of cancer: the future conquest of breast cancer. *European Journal of Cancer* 39 1668–1675.
- Tomlinson R, Klee M, Garrett S, Heller J, Duncan R & Brocchini S 2002 Pendant chain functionalised polyacetals that display pH-dependent degradation: a platform for the development of novel polymer therapeutics. *Macromolecules* 35 473–480.
- Tomlinson R, Heller J, Brocchini S & Duncan R 2003 Polyacetal-doxorubicin conjugates designed for pH-dependent degradation. *Bioconjugate Chemistry* 14 1098–1106.
- Torchilin VP 2005 Recent advances with liposomes as pharmaceutical carriers. *Nature Reviews. Drug Discovery* 4 145–160.
- Varticovski L, Lu Z-R, Mitchell K, de Aos I & Kopecek J 2001 Water-soluble HPMA copolymer wortmannin conjugate retains phosphoinositide 3-kinase inhibitory activity *in vitro* and *in vivo*. *Journal of Controlled Release* 74 275–281.
- Vasey P, Kaye SB, Morrison R, Twelves C, Wilson P, Duncan R, Thomson AH, Murray LS, Hilditch TE, Murray T, Burtles S, Fraier D, Frigerio E & Cassidy J 1999 Phase I clinical and pharmacokinetic study of PK1 [*N*-(2-hydroxypropyl)methacrylamide copolymer doxorubicin]: first member of a new class of chemotherapeutic agents – drug-polymer conjugates. *Clinical Cancer Research* 5 83–94.
- Vicent MJ, Manzanaro S, de la Fuente JA, Pérez C & Duncan R 2004a HPMA copolymer-1,5-diazaanthraquinone conjugates as promising anticancer therapeutics. *Journal of Drug Targeting* 12 503–515.
- Vicent MJ, Tomlinson R, Brocchini S & Duncan R 2004b Polyacetal-diethylstilboestrol: a polymeric drug designed for pH-triggered activation. *Journal of Drug Targeting* 12 491–501.
- Vicent MJ, Greco F, Nicholson RI & Duncan R 2005 Polymer-drug conjugates as a novel combination therapy for the treatment of hormone-dependent cancers. *Angewante Chemie* (in press).